University of Alberta
Department of Civil Engineering

Structural Engineering Report 156

MASONRY VENEER WALL SYSTEMS

by

WILLIAM M. McGINLEY

J. WARWARUK

J. LONGWORTH

M. HATZINIKOLAS

JANUARY 1988

STRUCTURAL ENGINEERING REPORT NO. 156

MASONRY VENEER WALL SYSTEMS

by

William M. McGinley[1]

J. Warwaruk[2]

J. Longworth[3]

M. Hatzinikolas[4]

January 1988

Department of Civil Engineering

University of Alberta

Edmonton, Alberta

Canada T6G 2G7

---

1 Former Graduate Student, Department of Civil Engineering and currently Assistant Professor, North Carolina Agricultural and Technical State University, Greensboro, N.C., U.S.A.
2 Professor of Civil Engineering, University of Alberta, Edmonton
3 Professor Emeritus of Civil Engineering, University of Alberta, Edmonton
4 Executive Director, Prairie Masonry Research Institute, Edmonton, Alberta

ABSTRACT

Masonry veneer wall systems are a very durable and asthetically pleasing building envelope. However, recent wall failures have indicated that the methods used for the design of this wall system are inaccurate.

This investigation developed limit states design procedures for masonry veneer wall systems. The limits states of the wall system were identified and a total of 44 full-sized wall tests were used to evaluate the adequacy of these methods.

Two and three dimensional frame models were developed to predict the load-deflection behaviour of the masonry and were found have sufficient accuracy for design purposes.

The in-plane movements of masonry veneer wall systems can greatly affect the performance of the wall system. These effects are discussed and construction details required to account for these movements are presented.

Finally, the effects of partial shear connection between veneer and steel stud backing walls were evaluated.

ACKNOWLEDGEMENTS

This investigation was made possible by financial assistance and material donations provided by the Natural Sciences and Engineering Research Council of Canada, the Prairie Masonry Research Institute, IXL Brick Ltd., and Genstar Concrete Ltd.

The authors would like to thank the Department of Civil Engineering for providing facilities for this research and for its financial support. Financial assistance by the Government of Alberta in the form of a Provincial Fellowship is also acknowledged.

Appreciation should also be expressed to Mr. L. Burden and Mr. R. Helfrich whose assistance during the testing program proved invaluable.

Table of Contents

List of Tables

List of Figures

List of Plates

LIST OF SYMBOLS

A - net area in mm^2

A_e - effective area calculated from load-deflection tests in mm^2

A_p - Net masonry push-out resisting area in mm^2

E - modulus of elasticity in MPa

F_y - yield stress of material in MPa

F_s - shear resistance of the masonry in N

F_r - nominal masonry push-out resistance in N

H - ratio of stud web depth to thickness of the stud metal

I - net moment of inertia in mm^4

I_e - effective stiffness of shear bracket tie systems in mm^4

L - length of member in mm

M - moment resistance in kNm

M_f - applied factored moment in kNm

M - nominal veneer moment resistance in kNm

M_r - factored stud moment resistance in kNm

N - ratio of tie bearing length to the thickness of the stud metal

P_f - applied factored tie load at maximum stud moment in N

P_r - factored crippling resistance of the stud in N

Prob - probability of occurance of an event

R - nominal member resistance

$\bar{R}$ - average member resistance

R_c - ratio of stud cross-sectional bend radius and the stud metal thickness

S - nominal load effect

$\bar{S}$ - average load effect

S_x - net section modulus of the stud in mm^3

T - applied tie load in N

T_n - nominal resistance of the ties in N

V - shear load in N

V_r - resistance coefficient of variation

V_r - load effects coefficient of variation

Y - (R - S)

h - height of stud web in mm

n - bearing length in mm

r - bend radius in stud cross-section in mm

t - thickness of stud metal in mm

y - distance from the neutral axis to the extreme cross-sectional fibre in mm

β - safety index

λ - load factor

ϕ - member resistance performance factor

ϕ_m - veneer moment resistance performance factor

ϕ_{sh} - masonry shear resistance performance factor

ϕ_t - tie resistance performance factor

σ - standard deviation

σ_r - masonry modulus of rupture in MPa

σ_r - masonry modulus of rupture in MPa

σ_s - masonry shear strength in MPa

1. INTRODUCTION

1.1 General

The use of masonry veneer as an exterior finish has been popular for many years. Recently, however, there has been a growing use of masonry veneers in conjunction with non-load-bearing backing walls to form a durable, asthetically pleasing, and effective building envelope. This type of wall system has become particulary attractive in highrise construction.

Figure 1.1 shows a typical masonry veneer wall consisting of an exterior wythe of clay brick, an airspace, and a backing wall. The veneer is connected to the backing wall by corrosion resistant metal ties and the airspace, over which the ties span, ranges from 25 mm to 75 mm. To improve thermal efficiency, the airspace between the veneer and back-up can be partially filled with insulation.

There are two types of backing walls commonly used to back the masonry veneer - hollow concrete block walls and metal stud walls. The two types of backing walls are similar in that they both provide support to the masonry veneer when it is subjected to out-of-plane loading.

Each storey height unit of veneer is supported vertically by a shelf angle which is attached to the building frame at floor level. The veneer and backing wall span vertically between adjacent floor levels with each span acting independently.

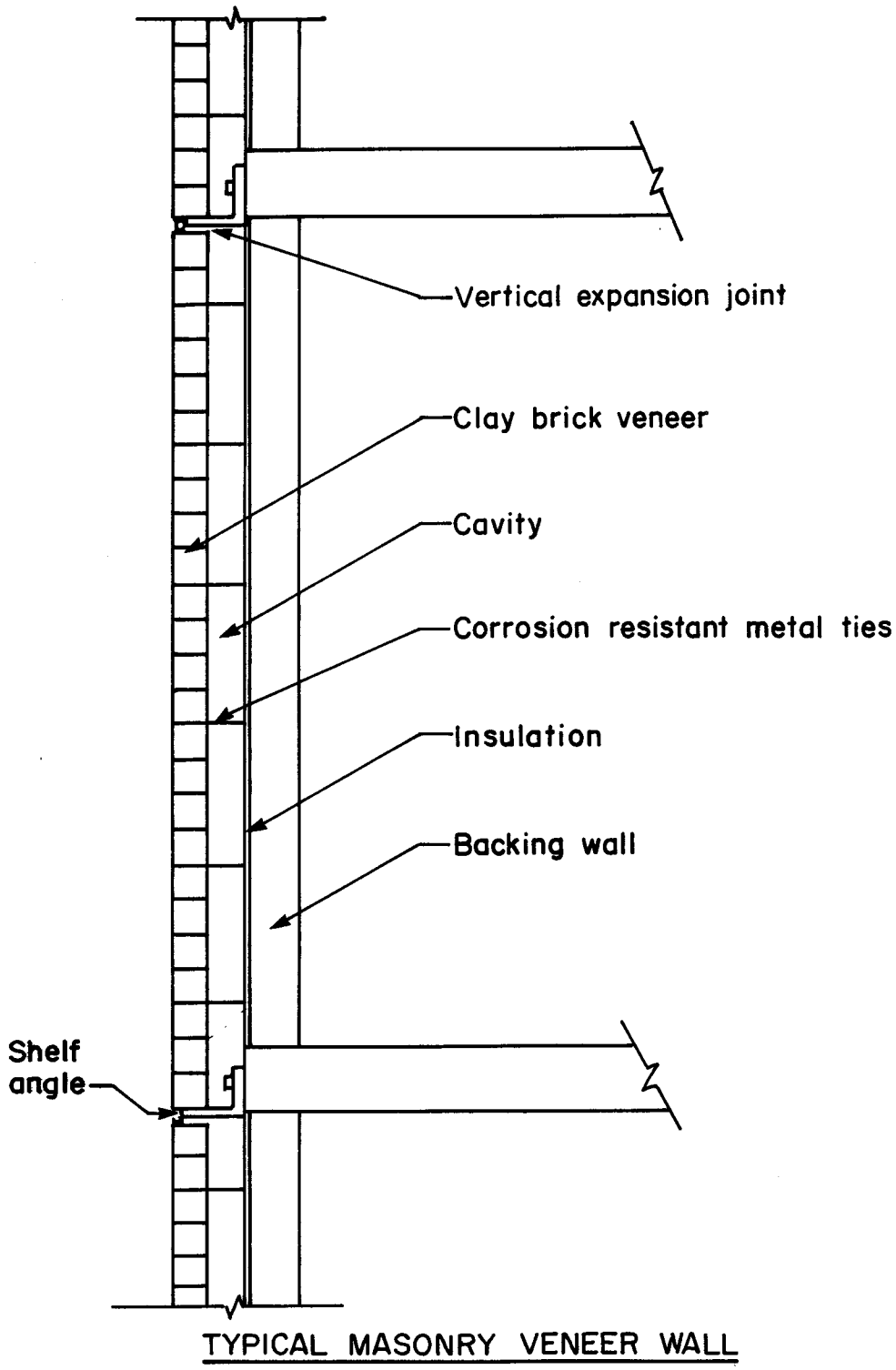

Figure 1.1 Typical Masonry Veneer Wall

Recent wall assembly failures and experimental investigations have indicated that currently accepted methods of design do not adequately account for the actual behaviour of the wall system and are, therefore, inadequate[1,2,3]. An accurate rational design procedure for masonry veneer wall systems is needed if this wall system is to be used successfully.

1.2 Object and Scope

The goals of this investigation are threefold:

1. To review current design procedures and pertinent studies of the behaviour of masonry veneer wall systems.
2. To develop rational design procedures and guidelines for out-of-plane loading that are both simple, accurate and sufficiently versatile to encompass the diverse masonry wall system configurations present in the field.
3. To evaluate the adequacy of these procedures against measured wall system performance.

2. A REVIEW OF CURRENT DESIGN PROCEDURES AND PREVIOUS INVESTIGATIONS

2.1 Introduction

The following section presents a review of current design procedures for and pertinent investigations of masonry veneer wall systems subjected to out-of-plane loading.

Relative in-plane movements between the veneer, backing wall and building frame produced by thermal expansion, moisture expansion, frame movements and shrinkage can cause severe damage to the masonry veneer and must be accounted for in the design of masonry veneer wall systems systems[4,5,6,7]. However, the stresses produced by these movements can be controlled through expansion joints, both horizontal and vertical, and careful planning of the details for corner connections and tie fasteners. Guidelines for wall detailing that compensate for relative wall movements are contained in Chapter 3.

2.2 Current Design Methods

There are two methods used for the design of masonry veneer wall systems for out-of-plane loads. Masonry veneers supported by backing walls constructed with metal studs are generally designed using one method and masonry veneers supported by walls constructed with hollow concrete block are generally designed using the other.

Masonry veneer and metal stud walls are currently designed almost exclusively using loading tables provided by various steel stud manufacturers. These tables ignore the strength of the brick veneer and simply assume that the steel studs will resist the entire uniformly distributed out-of-plane load by simple one way action. Some of the manufacturers assume partial compostite action between studs and gypsum sheathing. The maximum deflection of the steel studs is limited to L/360 although recently this limit has been decreased to L/600[8,9]. This low limit on stud deflection is expected to preclude veneer cracking although the adequacy of this limit is suspect[10].

Spacing of the ties, tie type, minimum veneer thickness and maximum cavity size recommended for use in masonry veneer walls are governed by empirically derived limits specified in the applicable building code. In Canada, CSA Standard CAN3-S304-M86[11] governs the design and construction of masonry buildings. This standard limits the total height of clay brick veneer in each lift of wall to 3.6 m. CSA Standard CAN3-A370-M84, Connectors for Masonry[12], essentially supercedes the S304 code with respect to design of tie systems for masonry veneers. This code recommends spacing limits for corrugated ties of 400 mm horizontal for a 600 mm vertical spacing, and 600 mm horizontal for a 400 mm vertical spacing. The minimum gauge of corrugated ties is limited to 22. This Code also requires that non standard ties be tested using a typical tie and stud assembly. The

total deflection of such an assembly must not cause cracking of the brick veneer.

Masonry veneer walls backed by hollow concrete block walls are designed taking into account the strength of the exterior veneer. The uniformly distributed wind (out-of-plane) load is applied separately to the two wythes in proportion to their relative flexural stiffness[13,14]. The two wythes are then designed so that the maximum allowable stresses specified in the applicable codes are not exceeded. Tie spacing, tie size, and cavity size follow similar limits to those for metal stud backed masonry veneer curtain wall systems.

The Brick Institute of America[15] postulates that if the ties are arranged so that the studs and brick deflect equally then the out-of-plane load can also be distributed to the two walls in stud backed veneer wall systems according to their relative stiffness. The brick veneer is usually stiffer than the stud backing wall and, therefore, will be required to resist a large portion of the wind load. Because of this large veneer loading, the Brick Institute of America suggests that the present deflection limits are not adequate to prevent veneer cracking and, accordingly, recommends a deflection limit of L/600 to L/720. It also recommends that corrugated ties not be used for this type of wall system.

2.3 Prevous Investigations

The unsatisfactory performance of a number of in situ masonry veneer and steel stud wall systems prompted investigations of the behaviour of such wall systems subjected to out-of-plane loads. These investigations are separated into two categories, those related to metal stud backed masonry veneer walls and those related to concrete block backed masonry veneer walls.

2.3.1 Metal Stud Backed Walls

2.3.1.1 Arumala and Brown Investigation

Arumala and Brown[2] at Clemson University, conducted six full sized tests on steel stud backed masonry veneer wall assemblies. All of the wall specimens consisted of a nominal 100 mm brick veneer, 90 mm deep 20 gauge steel studs and adjustable wire ties. The brick veneer spanned 2845 mm and the steel studs spanned 2400 mm on 600 mm centres. These studs were sheathed both sides by 12 mm gypsum wallboard. Three of the wall specimens were loaded to failure under a single application of positive pressure and three were loaded to failure under a single application of negative pressure. The behaviour of the flexible metal ties was also studied during this investigation.

From these tests a wall model was developed and used in a computer analysis of the wall system. It was concluded that distributing the out-of-plane load

according to the relative stiffness of the veneer and backing wall is not an accurate method for predicting wall behaviour. Furthermore, it was concluded that the end conditions, the difference in the span of the two wythes, and the tie stiffness affect the distribution of lateral load as much as the relative stiffnesses of the brick and the studs. Thus, while the behaviour of the wall system is greatly affected by the interaction of the veneer and the metal studs, there are other factors which also have a significant effect on the system behaviour.

Analysis by Arumala and Brown of the results of their full sized wall tests indicated that there is little or no reliable interaction between the studs and gyproc sheathings in the backing wall. This conclusion was confirmed by later cyclic testing of stud wall specimens[4]. Their analysis also indicated that the compressible filler in the top horizontal expansion joint provided negligible restraint to the movement of the wall. As the top of the veneer was essentially free to move, the flexural stress in the brick was reduced and the brick walls were able to reach their design load. The safety factors for the walls ranged from 1.2 to 3.0 for veneer cracking.

In the Arumala and Brown study, the load-deflection behaviour of the ties was studied in isolation from the rest of the backing wall. The ties were tested between a

brick prism and a steel plate and a stiffness factor was derived from the slope of the load-deflection plot for each of the ties. This stiffness factor was then used as a spring constant in a mathematical model of the frame action of the walls. The model and testing ignored the interaction between the flange of the steel stud, tie and exterior gypsum sheathing. The deflection of the stud supports was also neglected in the analysis.

2.3.1.2 University of Alberta Investigations

Two experimental investigations into the behaviour of metal stud backed masonry veneer walls were conducted at the University of Alberta[1,17]. During these investigations a total of 32, 3200 mm high and 1220 mm wide full-sized wall specimens were tested under a positive pressure loading. The effects of wall cavity size, tie type, tie pattern, stud type, exterior sheathing type and tie location were studied. The interaction of the ties, sheathing and studs was also investigated. The thirty-two wall specimens were fabricated and tested in the same manner as presented in Chapter 4 for wall specimens subjected to a positive pressure loading except that strain gauges were not applied to the ties and each wall specimen was taken to failure by a single application of positive pressure after being preloaded to 0.3 kPa. Table 2.1 and Figure 2.1 summarize the important characteristics of each wall specimen.

Table 2.1 A Summary of Full-Sized Wall Specimens

Specimen	Metal Stud		Tie Type	Ext. Sheathing	Cavity (mm)	Tie Pattern
	Thickness (ga.)	Depth (mm)				
MS1W1	18	90	22 C	12 mm Gyp	50	A
MS1W2	18	90	22 C	12 mm Gyp	50	A
MS1W3	18	90	22 C	12 mm Gyp	25	A
MS1W4	18	90	22 C	12 mm Gyp	25	A
MS2W1	18	90	22 C	12 mm Gyp	50	C
MS2W2	18	90	22 C	12 mm Gyp	50	B
MS2W3	18	90	T	12 mm Gyp	50	B
MS2W4	18	90	T	12 mm Gyp	50	C
MS3W1	20	150	22 C	12 mm Gyp	50	C
MS3W2	20	150	22 C	12 mm Gyp	50	B
MS3W3	20	150	T	12 mm Gyp	50	B
MS3W4	20	150	T	12 mm Gyp	50	C
MS4W1	20	150	24 C	12 mm Gyp	50	B
MS4W2	20	150	16 C	12 mm Gyp	50	B
MS4W3	20	150	Ladder	12 mm Gyp	50	D
MS4W4	20	150	V	12 mm Gyp	50	B
DS1W1	18	90	22 C*	25 mm RI	25	B
DS1W2	18	90	22 C	25 mm RI	25	B
DS1W3	18	90	16 C*	25 mm RI	25	B
DS1W4	16	90	16 C*	25 mm RI	25	B
DS2W1	20	90	22 C*	50 mm RI	25	B
DS2W2	20	150	22 C*	50 mm RI	25	B
DS2W3	18	150	16 C*	50 mm RI	25	B
DS2W4	16	90	16 C*	50 mm RI	25	A
DS2W5	16	150	16 C*	50 mm RI	25	B
DS2W6	14	90	16 C*	50 mm RI	25	B
DS3W1	20	90	16 C	none	25	B
DS3W2	20	150	16 C	none	50	B
DS3W3	20	150	16 C*	50 mm RI	25	B
DS3W4	18	150	16 C	none	25	B
DS3W5	16	90	16 C	none	25	B
DS3W6	14	90	16 C	none	25	B

S1W1 - Series 1 Wall 1 from test program 1[1], DS1W1 - Series 1 Wall 1 from test program 2[1]
C - 16, 22, or 24 ga. corrugated strip ties, T - 4.76 mm dia adjustable rod tie (BL319)
Ladder - 3.16 mm dia ladder tie with cross pieces at 400 mm O. C.
V - Adjustable 4.67 mm dia "V" rod tie and platform, RI - Rigid insulation, 25 and 50 mm thick
Note: * - 16 gauge tie platforms in conjunction with ties

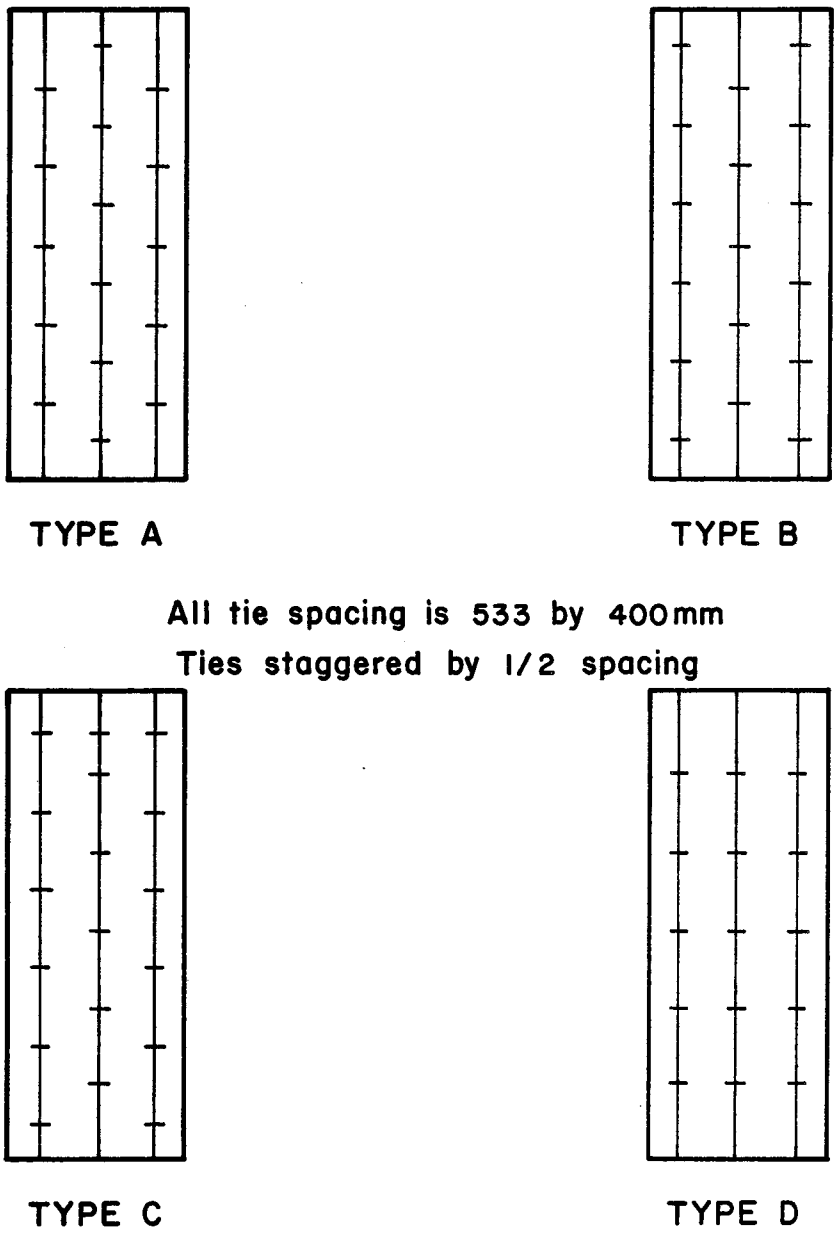

Figure 2.1 A Summary of Tie Patterns

Each wall specimen exhibited deflections proportional to the load until the veneer cracked. After veneer cracking there was an increase in wall deflections until the ultimate wall pressure was reached. For two of the wall specimens the ultimate load was reached before sufficient pressure was applied to the veneer to crack it. Three modes of ultimate failure were observed:

1. The ties failed, either by buckling or by crushing of the exterior sheathing behind the tie.
2. The studs failed by a combined flange bending and flexural buckling at or near one of the tie connections.
3. The web of the studs buckled at one of the top track support.

Due to capacity limits on the loading apparatus, it was not possible to load seven of the wall specimens to complete failure.

Table 2.2 summarises the cracking pressure, location of crack, veneer deflection at cracking, ultimate pressure and modes of ultimate failure for each of the wall specimens tested. These results are used in the evaluation of the proposed design methods, carried out in Chapter 5.

Based the test results from the full sized wall tests and tests of the wall component interactions, these investigations concluded the following:

Table 2.2 A Summary of Wall Test Results

Specimen	Veneer Cracking			Wall System		
	Press. (kPa)	Defl.(mm)	Elev. (mm)	Ult. Press. (kPa)	Failure Mode	Max. Press. (kPa)
MS1W1	--	--	--	1.50	T	1.53*
MS1W2	--	--	--	1.52	T	1.75*
MS1W3	0.71	2.7	1340	4.10	T¢	4.83&
MS1W4	1.06	3.8	1735	2.64	T¢	4.83&
MS2W1	1.46	4.6	1935	2.62	T	3.35*
MS2W2	0.60	2.2	1610	2.96	T	3.46
MS2W3	2.07	6.4	1550	--	--	4.83&
MS2W4	1.40	11.8	1930	--	--	4.83&
MS3W1	--	--	--	2.97	T	3.16*
MS3W2	--	--	--	2.20	T	2.32*
MS3W3	2.05	4.1	1540	3.10	SW	4.83&
MS3W4	2.60	5.9	1265	3.10	SW	4.83&
MS4W1	--	--	--	0.93	T	1.35*
MS4W2	2.50	7.0	1065	3.0, 3.45	T, SW#	4.83
MS4W3	1.33	3.3	1270	2.5, 4.83	SW, T	4.83&
MS4W4	2.07	3.6	0935	2.60	SW, T	4.83&
DS1W1	1.45	4.3	1660	3.01	T	4.16*
DS1W2	1.60	7.8	1530	2.35	T	3.41*
DS1W3	1.20	2.4	1790	6.18	SB	6.18
DS1W4	1.35	2.5	1660	--	--	7.02&
DS2W1	2.26	4.0	1130	3.71	T	5.63&
DS2W2	2.86	3.7	1260	4.42	T	6.88*
DS2W3	2.75	2.5	1790	--	--	8.63&
DS2W4	1.76	6.6	1660	7.70	T	9.52&
DS2W5	--	--	--	9.20	T	10.52&
DS2W6	3.20	5.0	1930	--	--	11.11&
DS3W1	2.01**	3.9	1390	5.37	SB	5.37
DS3W2	2.17**	2.6	1260	7.86	SB	9.35
DS3W3	3.30	3.0	2085	10.26	SB	11.42
DS3W4	2.64**	2.8	1790	13.45	T, SB	13.45
DS3W5	1.35**	1.4	1790	13.89	SB	13.89
DS3W6	2.24	1.8	1790	--	--	12.31&

T - Buckling of some of the wall ties observed, SW - Stud web failure at support
SB - Combined bearing and flexural failure of stud at tie location
Note * - Test stopped when veneer came in contact with stud wall.
& - Test stopped due to capicity limitations of loading air bag, or excessive deflections.
¢ - Collapse of the ties not observed but deflections show nonlinear deflection of ties.
- The stud web at the top support failed, then the bottom stud support web failed.
** - The veneer cracked in more than one location (only first cracking shown).

1. There is significant deformation of the stud cross-section at the tie location and this deformation significantly affects the wall system behaviour.
2. Tie location on the stud flange, compressibilty and restraint of the exterior sheathing, lateral stiffness of the ties and dimensions of the backing stud cross-section are the major factors affecting the interaction of tie and stud.
3. Tie type has little effect on the behaviour of the wall system before veneer cracking, if tie buckling is precluded.
4. Tie type and spacing greatly affects the mode of ultimate wall failure.
5. The track connections at stud supports deflect significantly and can greatly affect the wall system behaviour.
6. Stud type has an effect on the wall behaviour, including not only flexural rigidity but also cross-section deformation.
7. Wall ties are not uniformly loaded over the wall height.
8. Cavity size affects the ultimate failure of the wall system, with larger cavities increasing the probability of tie collapse as the ultimate failure mode.
9. The gypsum sheathing on the stud backing does not

provide significant composite action with the steel stud.

10. The gypsum sheathing provides significant bracing restraint to the compression flange of the steel studs.
11. Rigid insulation, used as an exterior sheathing, provides a less effective bracing restraint when compared to the gypsum sheathing.
12. The wall system exhibits significant reserve strength after veneer cracking.
13. The present methods of design do not accurately predict the wall system behaviour and are, therefore, inadequate.

A plane-frame wall model was developed as part of the investigation and analysed using a direct stiffness frame analysis. The analysis, which accounted for stud and tie interaction and stud support deformation, was found to predict the wall behaviour quite well up to veneer cracking. A detailed development of the wall model and analysis technique is presented in Chapter 6.

2.3.1.3 Bell and Gerpertz Investigation

Bell and Gerpertz conducted a literature review and finite element analysis of brick veneer and steel stud wall systems[3]. Their literature review covered the relevant design documents mentioned earlier and tests conducted by the National Concrete Masonry Association[18], the United States Gypsum Company[19] and

Armula and Brown[2]. Their findings confirmed many of the conclusions of the University of Alberta investigation. In addition their report recommended the following:

1. Distributing lateral load to the veneer and back-up wall in proportion to their relative stiffnesses is not an adequate analysis technique. A rational analysis should be carried out on the wall system and limits established for prevention of veneer cracking.
2. Composite action between the gypsum sheathing and the steel studs should be ignored.
3. Only adjustable ties should be used in the wall system.
4. The ties at each floor level should be designed as each storey height of veneer takes all the load and the ties form the veneer supports.
5. The ties in the middle height of the wall and the stud connections should be designed as if the wind load is applied uniformily to the backing system, or for the loads from the rational analysis.
6. Provide both vertical and horizontal expansion joints to provide for veneer expansion. Frame shorting and racking must also be allowed for in the design of these joints.

In their analysis Bell and Gerpetz modelled the ties as infinitely stiff, but recognized that the actual flexibilty of the ties could have a great effect on the

wall behaviour. They also found that wall end conditions, including stud support deformation, had a great affect on wall behaviour. They further suggested that, because veneer cracking does not necessarily cause the wall system to collapse, veneer cracking should be considered a serviceablity limit.

It is generally recognized that present methods of design for masonry veneer/steel stud wall systems are inadequate. Altough rational methods of analysis have been used for this type of wall system, no definitive procedures for design have been proposed. There is a need for a simple and flexible design procedure for masonry veneer wall systems.

2.3.2 Walls Backed by Hollow Concrete Block

The concrete block backed masonry veneer wall system has generally performed adequately in situ when adequate expansion joints are provided. However, the findings of investigations of stud backed wall behaviour has prompted re-evaluation of the behaviour of concrete block backed masonry wall systems under out-of-plane loads.

2.3.2.1 Brown and Elling Investigation

An analytical investigation by Brown and Elling[20] found that the present methods of design, which distribute lateral load to the backup and veneer in proportion to their relative stiffnesses, do not adequately model the wall system behaviour. Support

conditions, different span lengths and tie flexibilty greatly affect the distribution of the lateral load within the wall system. They also found that tie loads can be far from uniform and tie spacing limits derived based on uniform loading are unconservative. These results were confirmed by Hamid and Carruolo[9] using a three dimensional, isotropic, finite element analysis for cavity wall systems subjected to only out-of-plane loading.

It can be seen that although cavity walls have generally performed adequately, present cavity wall design methods do not accurately model the behaviour of non load-bearing concrete block backed masonry veneers. A more rational and accurate method of design for this type of masonry veneer system is needed.

3. DESIGN OF MASONRY VENEER WALL SYSTEMS

3.1 Introduction

In recent years there has been a trend in structural design codes to shift from working stress design to limit states design. It is generally accepted that limit states design procedures provide for a more uniform safety against failure than working stress design procedures. At present, the Canadian design code for masonry uses a working stress design approach[1]. However, a limit states design code is under development. Furthermore the masonry codes of many countries have adopted, at least in part, limit state design procedures. For these reasons, the limit states design philosophy was used to develop the design methods in this investigation.

This chapter presents limit states design procedures for masonry veneer wall systems subjected to out-of-plane loading. Also presented are guidelines for wall detailing to compensate for relative in-plane wall movements of this wall system.

3.2 Limit States Design

The limit states design philosophy is based on designing structural systems to preclude unacceptable types of system behaviour (limit states). There are two types of limit states; ultimate limit states and serviceability limit states. Ultimate limit states are those limit states where

the system no longer performs its function or endangers lives, such as collapse of a member or structure. Serviceability limit states are those limit states associated with acceptable performance under most conditions, such as maximum deflection of a beam.

For any given structural system there are three basic steps in a limit states design approach:

1. Identify the failure modes (limit states) of the system.
2. Develop relationships between the loads, material properties of the system and each limit state.
3. Establish an adequate safety margin for the occurrence of each limit state using probability theory and consideration for the consequences of each limit state.

3.2.1 Probability of Failure

Adequate levels of safety are derived in limit states design based on probability theory. Both the loading effects (S) and the resistance of the structural system (R) are assumed to be randomly distributed. Figure 3.1 shows typical distributions of the each of these variables. If the loading effects are greater than the system resistance, then failure occurs. Failure is possible in the region where the distributions of R and S overlap (the shaded region in Figure 3.1). The probability that the resistance is less than the loading effects is then[21]:

$$\text{Prob} = P\{(R - S) < 0\} \qquad [3.1]$$

or

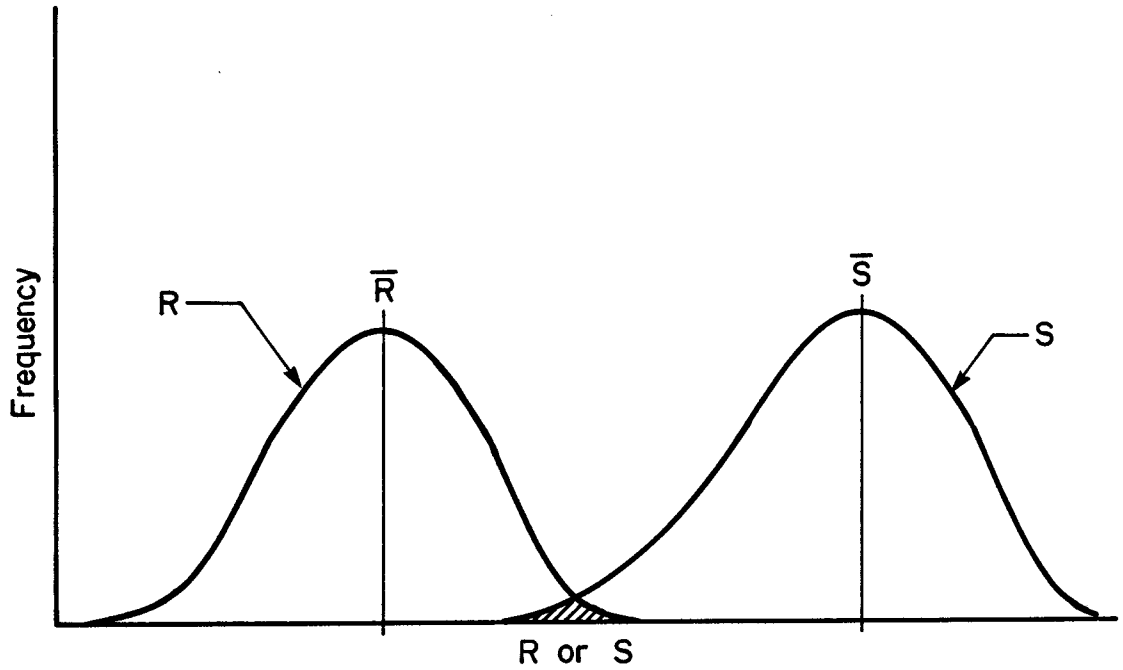

Figure 3.1 Distribution of Loading Effects and Resistances

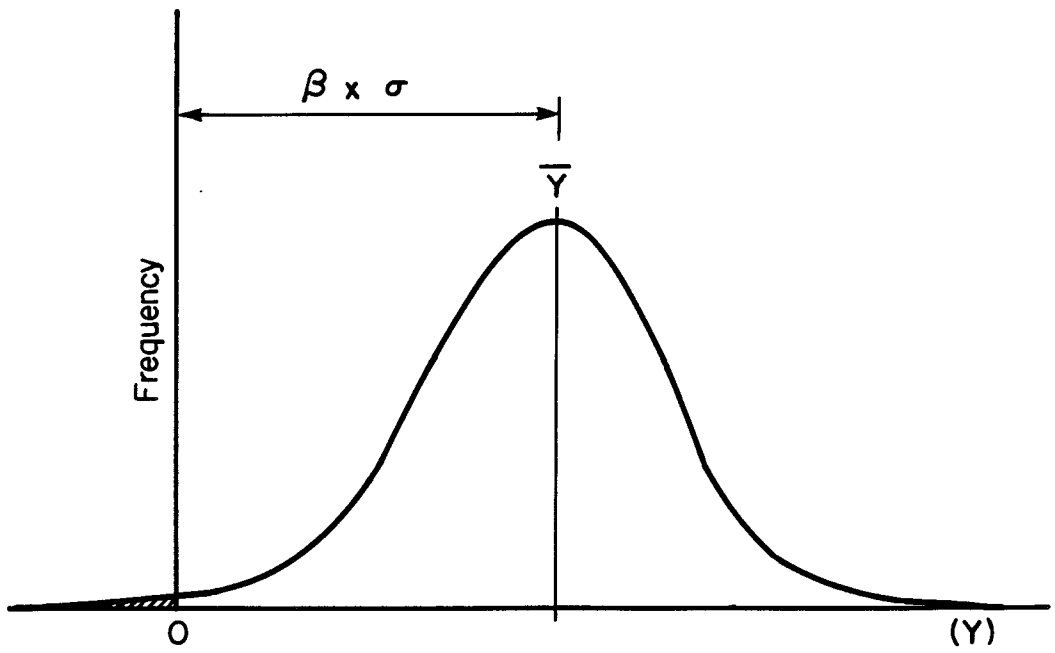

Figure 3.2 Distribution of Y

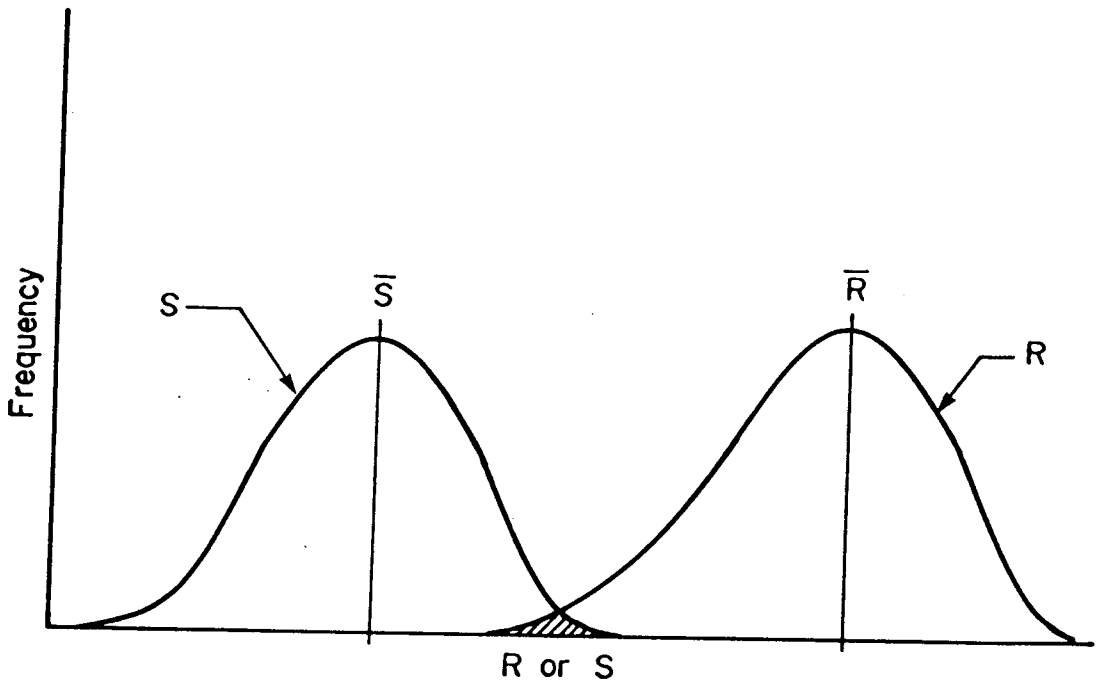

Figure 3.1 Distribution of Loading Effects and Resistances (revised)

$$\text{Prob} = P\{\ln(R/S) < 0\} \qquad [3.2]$$

If a new variable, Y, is introduced and set equal to R - S then the probability of the load effects exceeding the strength of the system is the same as the probability that Y has a value less than zero. This is shown graphically in Figure 3.2, where the area under the curve to the left of zero represents the probability of Y being less than zero. If the mean value of Y ($\bar{Y}$) is a large number β of standard deviations (σ) from zero, then the probability of this event occurring is small.

The probability that Y is less than zero is not the same as the probability of collapse. Even if the distribution of Y is known exactly, the theory does not include failures due to human error, nor does it account for simplifications in the structural analysis which become more pronounced as the indeterminancy of the structural system increases[22]. However, this parameter β does give a good relative measure of safety for evaluating design procedures.

For reinforced concrete members, it has been established that β values of approximately 3.5 give adequate safety for most ductile ultimate limit states[21,22]. However, this value was derived for building systems where the consequences of failure can be catastrophic. The consequence of masonry veneer wall system failure is generally less severe. Appropriate β values for each failure mode of the wall system will be discussed in the following sections. With these target values of β, a load factor (λ) and a

performance factor (ϕ) can be derived. These factors are applied separately to the load effects (S) and resistance of the structural system (R) as shown in Equation 3.3[21,22].

$$\lambda S \leq \phi R \qquad [3.3]$$

λ has a value greater than unity and accounts for the variability of the loading and for approximations made when calculating loading effects. The performance factor (ϕ) has a value less than unity and accounts for the variability in the resistance and for approximations made when calculating the resistance. Values of λ and ϕ range from 1.25 to 1.7 and from 0.4 to 0.9, respectively.

In recent years, Canadian Structural Standards have been moving towards a unified limit states design philosophy for all materials[22]. The various limit state codes have been modified so that all use the same load factors, load combination factors and importance factors. The common load factor used for wind loadings is 1.5. As masonry veneer wall systems are usually subjected only to wind loads, a load factor of 1.5 was chosen for the development of the limit state design procedures for this wall system.

For a given load factor, the performance factor can be calculated by Equation 3.4, based on a log normal distribution of Y[23].

$$\phi = \lambda \frac{\bar{R}\, S}{\bar{S}\, R} e^{-\beta(V_r^2 + V_s^2)^{0.5}} \qquad [3.4]$$

In addition to the variability of R and S, this equation accounts for the difference between the nominal values of R

and S and their average values $\bar{R}$ and $\bar{S}$.

If the National Building Code of Canada (NBC)[24] 1/30 year nominal wind pressures are used for design, then $S/\bar{S}$ and V_s have values of approximately 1.25 (1.0/0.8) and 0.25, respectively[22]. However, the NBC recommends the use of the 1/10 year wind pressures for design of cladding systems. For this investigation, it was assumed that the localized cladding wind loads with a 1/10 chance of exceedence per year have the same values of V_s and $S/\bar{S}$ as the overall building wind loads with a 1/30 chance of exceedence per year.

Using the values defined above, Equation 3.4 can be used to calculate ϕ factors for each limit state of the masonry veneer wall system.

3.3 Limit States Design of Masonry Veneer Systems

Applying the first step of the limit states approach to the masonry veneer wall systems results in the indentification of five limit states for out-of-plane loading:

1. Formation of a crack in one or more of the veneer mortar joints by veneer flexure.
2. Failure of the tie systems connecting the backing wall to the veneer.
3. Flexural failure of the backing wall.
4. Local failure of the backing wall, at or near the supports, under the concentrated reaction load.

5. Excessive deflection of the wall system.

Having identified the major limit states of masonry veneer wall systems, each limit state must be defined as either an ultimate limit state or a serviceability limit state. Relationships must then be developed between these limit states, the material properties and the wall system loading.

3.3.1 Ultimate Limit States

Ultimate limit states are usually defined as those limit states which result in collapse of a structural member or system. The failure of the tie systems and the failure of the backing wall, both flexurally and at the supports, fall within this definition and are classified as ultimate limit states. The classification of veneer cracking is not as straightforward as the two limit states above and is the subject of much controversy.

Veneer cracking does not cause immediate collapse of the wall system. In addition, masonry wall systems that are backed by metal stud walls exhibit significant post-cracking strength if tie systems of sufficient strength are used. Therefore, it has been suggested that veneer cracking might be considered a serviceability limit state[3]. However, it has also been suggested[10] that moisture movements through cracked veneer walls are substantially larger than moisture movements through uncracked veneers. With increased moisture movements, the possibility of corrosion of the tie systems

is increased. If corrosion sensitive tie systems and connections are used, the long term performance of the masonry veneer wall system can be seriously affected. Furthermore, little is known about deterioration of cracked masonry veneer. Repeated loading of cracked veneer will likely cause mechanical break-down of the cracked mortar joint. If ties are embedded in this mortar joint, it is likely that the strength of the tie/veneer connection will be reduced. The amount of this strength reduction is not known and must be investigated.

Until more is known about the effects of veneer cracking on the behaviour of masonry veneer wall systems, the classification of this limit state will remain difficult. However, it is proposed that veneer cracking be likened to the "Damage Limit State" designation suggested by MacGregor for reinforced concrete structures[25]. This limit state is considered to be critical in the performance of the system but, because of less severe consequences of failure, a higher probability of occurrence is acceptable.

Each of these critical limit states will be discussed separately in the following sections.

3.3.1.1 Veneer Cracking

The masonry veneer cracks when the tension stress in a mortar joint exceeds the strength of the tensile bond between the brick and mortar. These tensile stresses are primarily caused by the bending of the veneer. Thus, to preclude veneer cracking, the applied

veneer moment must be less than the veneer moment resistance. If the masonry veneer is assumed to behave elastically and the self-weight of the veneer is neglected, then Equation 3.3 can be modified to give the basic design equation for veneer flexural cracking:

$$\lambda M \leq \phi_m \frac{\sigma_r I}{y} \qquad [3.5]$$

λ and ϕ_m are, respectively, the load factor and the performance factor associated with the wind loading and veneer cracking. I is the moment of inertia of the net section of the veneer, σ_r is the nominal modulus of rupture of the veneer and y is the distance from the neutral axis to the extreme tensile fibre.

Veneer cracking usually governs the design of wall systems where the masonry veneer is backed by metal studs. Thus, this limit state should be used as a basis for design, and the resulting wall system should be checked for adequacy with respect to the remaining limit states.

The successful application of Equation 3.5 requires an accurate prediction of the applied moments and appropriate values of ϕ_m and σ_r. Modelling of the wall system to predict the load effects will be discussed in Chapter 6, as will the derivation of ϕ_m and σ_r.

The derivation of ϕ_m also requires a value of β. As mentioned previously, veneer cracking can have undesirable consequences. However, it was further argued that a higher probability of ocurrence would be

acceptable for this limit state. It is suggested that β should range between 2.3 and 3.0. These β values correspond to probabilities of occurrence for veneer cracking of approximately 1% and 0.14 %. The value of β choosen will depend on the corrosion resistance of the tie systems used, the environment to which the wall system will be subjected and the susceptibility of the tie/veneer connection to weakening by mechanical breakdown of the mortar joint.

3.3.1.2 Tie Failure

The failure of the tie system connecting the veneer to the backing wall can be very dangerous and sudden. As with connection design for steel structures, these tie "connectors" should have a higher margin of safety against failure than other more ductile modes of wall system failure. Both the CAN3-CSA-S136-M84[26] and CAN3-CSA-S16.1[27] steel design codes use β factors for connections that are greater than those for other ultimate limit states.

Failure of a single connection of a structural member may produce collapse of this member. However, the failure of a single tie system in a masonry veneer wall system does not necessarily cause failure of the the wall system. Due to the redundant nature of the wall system a significant number of the tie systems must fail before the veneer either pulls away, or collapses into the backing wall. The redundancy of the wall system

provides further safety against tie failure by re-distribution of the tie loads. As the failure load is approached, the tie systems become significantly less stiff. Therefore, a greater portion of the increasing veneer load is drawn to the surrounding ties. Thus, it is suggested that a β value of approximately 4.0 be used for tie system design. This value is greater than the β value (3.5) recommended for ductile failure modes, but is less than the β value used for structural connections (4.5).

To prevent failure of the tie system, the factored resistance must be less than or equal to the predicted factored load effects (tie loads). However, the resistance of the tie system is very difficult to analyze due to the complexities of tie system behaviour. Thus, it is proposed that the nominal resistance of the tie system be established by testing. This resistance (T_n), once factored, must be less than or equal to the predicted factored tie loads (λ T). Equation 3.6 represents this concept in equation form.

$$\lambda T \leq \phi_t T_n \qquad [3.6]$$

To establish the nominal ultimate resistance of a tie system, CAN3-A370-M84[1,2] requires that a minimum of five tests be performed on a typical veneer-tie-backup system. Because of the small sample of data, the average ultimate strength from these tests must be reduced by a factor of 1.0 - 1.5V to give the nominal resistance.

Where V is the coefficient of variation of the tie test results.

It is suggested that a minimum of five tension tests and five compression tests should be performed on a typical tie system. Each test specimen should include sections of both the veneer and the backing wall. Testing the tie system in this manner accounts for tie end effects, local stud failure, pull-out from the mortar joint, failure of the tie/backing wall connection and the failure of the tie system itself. With the wide variety of tie systems available and the complex action of some of these systems, developing equations to predict the tie resistance becomes impractical. Thus, testing of the tie configuration under consideration becomes the simpliest and most accurate alternative.

The derivation of nominal tie resistances and the value of the tie performance factor (ϕ_t) will be discussed in Chapter 6.

3.3.1.3 Flexural Failure of the Backing Wall

The flexural failure of backing walls can be categorized in two groups, flexural cracking of concrete block backing walls and flexural buckling of stud backing walls. The block backing wall usually has supports which cause it to act as a propped cantilever beam. Thus, the maximum wall moment will always be at the base of the wall and it is likely that first cracking will occur there. The block wall will have a

small reserve strength after this crack occurs because collapse of this wall will not occur until a second crack forms. However, this cracked mortar joint has a reduced shear strength. Furthermore, the behaviour of this cracked joint under repeated loadings is not known and further strength deterioration is possible. Thus, it is recommended that the ultimate flexural strength of hollow concrete backing walls should be based on the formation of a crack at its base.

If the concrete block backing wall is reinforced and sufficiently long dowels are provided between the slab and the block wall to provide full development of the bars, then the ultimate flexural capacity of the reinforced concrete block wall can be defined by the formation of a second plastic hinge. However, the lower connection must be checked to ensure that sufficient ductility is present to allow the formation of the this second hinge.

Equation 3.5 can be applied to the unreinforced (hollow) concrete block backing wall for flexural design. The factored applied moment at the base of the block wall must be less than or equal to the factored moment resistance of the connection at this location. It should be noted that the nominal modulus of rupture (σ_r) must be adjusted to account for differences in the tensile strength of the masonry veneer and the concrete block wall.

Because this ultimate limit state can result in the collapse of the wall system, a lower probability of failure is required. It is suggested that a β of 3.5 be used for the derivation of a ϕ for this limit state.

The design of steel stud backing walls for flexure should conformied in accordance to the limit states design code for cold formed steel members, CSA S136[24]. This code uses λ equal to 1.5 for wind loading and ϕ equal to 0.9 for flexure. The steel studs can be assumed to be fully braced along their length if it can be shown that the tie systems and sheathings provide adequate stiffness and strength to provide both twist and buckling bracing.

Most manufacturers of steel studs design the stud cross-sections to be fully effective. Therefore, the factored moment resistance of a fully braced steel stud (M_r) can be calculated by:

$$M_r = \phi\ S_x\ F_y \qquad [3.7]$$

where S_x is the minimum fully effective section modulus of the steel stud and F_y is the yield stress of the steel.

It should be noted that the flexural resistance of the studs is reduced by the presence of service cut-outs in the stud web. Premature stud failure will occur if the applied moment at these cut-outs exceeds this reduced stud resistance before the maximum applied moment exceeds the full flexural resistance of the stud.

The possibility of this occurrence must be checked.

If the tie systems are attached to the stud web, these studs may fail at one of the tie locations by a combined crippling of the web and flexural buckling of the flanges. This type of failure is further complicated if the tie is connected to the stud over a service cut-out. This possible stud failure mode must be investigated using the procedures outlined in CSA S136[26] for combined web crippling and bending. The minimum web area should be used in the resistance calculation.

If the ties are connected to the stud flange, the local deformation of the stud cross-section (see Chapter 6) may reduce the moment resistance of the stud to the point where the stud fails prematurely. This reduction in stud flexural resistance is increased if the tie is connected the stud at a large distance from the stud web. The deformation of the stud cross-section can be approximated from the results of the tie resistance tests and an expression relating the magnitude of the tie load to the reduction of the flexural resistance of the stud. The stud backing wall resistance must then be checked at the maximum moment region and at the tie connection locations.

However, when the veneer is uncracked the tie loads in the maximum stud moment region are usually small and it is unlikely that either of the above failure modes will significantly affect the flexural strength of the

stud in regions where the applied stud moment is sufficient to cause premature failure.

3.3.1.4 Backing Wall Failures at the Supports

The final ultimate limit state of masonry veneer wall systems is the failure of the backing wall at the supports. For steel stud backing walls, this failure is characterized by buckling of the stud web, either by crippling or shear buckling. The procedures outlined in CSA S136[26] should be used to check the adequacy of the steel studs for web crippling and shear buckling under the reaction loads. It is recommended that the performance factors specified in CSA S136 be used.

The strength of the stud track supports should also be checked. The track strength can either be determined by tests or based on the manufacturer's recommended loading.

For concrete block walls, the factored shear strength of the connection at the base of the wall must be checked to determine if it exceeds the applied shear force (F_s). The shear resistance of a plain (unreinforced) block wall can be approximated by the product of the net area of the joint (A) and the nominal shear strength of the masonry (σ_s). The design equation for shear in a concrete block backing wall therefore becomes:

$$\lambda F_s \leq \phi_{sh} A \sigma_s \qquad [3.8]$$

This equation assumes a uniform shear stress across the bedded area of the mortar joint and is only accurate if the nominal shear strength of the masonry is based on the same assumption. The performance factor for this failure mode should be based on the same β value as that used for the flexural failure of this type of backing wall.

If the backing wall is reinforced, the contributions of the reinforcement can be included in the calculation of the shear resistance.

Equation 3.8 should also be applied to the veneer in the region of maximum shear, although shear failure of the veneer was not observed in any of the 44 wall tests presented in this investigation.

There is another possible, although unlikely, failure mode of a concrete block backing wall. The top of the backing wall is usually supported by a clip angle attached to the concrete slab. This clip angle normally bears on a single block and if the clip angle has adequate strength the block may "push out" under the reaction load. It is suggested that the "push out" strength of this block be checked against the reaction load (F_R) using the following equation:

$$\lambda \, F_R \leq \phi_{sh} \, A_p \, \sigma_s \qquad [3.9]$$

where A_p is the net shear resisting area around the perimeter of the block and σ_s is the nominal shear

strength of the masonry as defined previously.

The evaluation of the adequacy of these proposed design procedures together with the wall system models developed for the prediction of the loading effects are presented in Chapter 6.

3.3.2 Serviceability Limit States

The one structural serviceability limit state of masonry veneer wall systems is excessive wall deflection under out-of-plane loading. Both the maximum deflection of the veneer and the maximum deflection of the backing wall must checked against limiting values. If the veneer is allowed to deflect excessively the caulked joints in the wall system may leak, especially around window openings. Excessive deflections of the backing wall can cause damage to windows, vapour barrier, air seal of the building closure and interior finishes.

By definition, serviceability limit states produce acceptable wall behaviour under most conditions. Maximum deflections of the wall system are computed under unfactored loading and then checked against maximum allowable limits. The maximum live load deflection allowed by CSA S-16.1[27] for plastered finishes is L/360. For the same conditions, the maximum deflection allowed by CSA A23.3[28] is L/480. Neither of these limits is likely to preclude a crack forming in a plaster wall[29]. However, the Commentary on the National Building Code of Canada[29] suggests that these limits are

applicable to most standard forms of construction. For allowable deflections in the caulking, the designer must check the manufacturer's specifications.

In most cases, a maximum live load deflection limit of L/480, should produce acceptable wall performance under service loads. It should be noted that deflections of this magnitude will almost certainly cause cracking of the veneer. Thus, deflection of the wall system rarely governs its design.

3.4 Wall Details for In-Plane Movements

The design procedures presented earlier are for masonry veneer wall systems subjected only to out-of-plane loading. However, there are large differential in-plane movements between the wall system and the building frame which, if not accommodated, will apply large in-plane loads to the wall system and possibly cause premature failure. One way to preclude significant in-plane-loading is to provide vertical and horizontal control joints in both the veneer and the backing wall[4,5,6,7].

Figure 3.3 shows typical horizontal control joints for a stud backed masonry veneer wall system. The masonry veneer is stopped below the support angle of the next floor height of veneer. The resulting gap is partially filled with a compressible material and then caulked. The size of the gap must allow for[4]:

1. thermal expansion and contraction of the veneer.

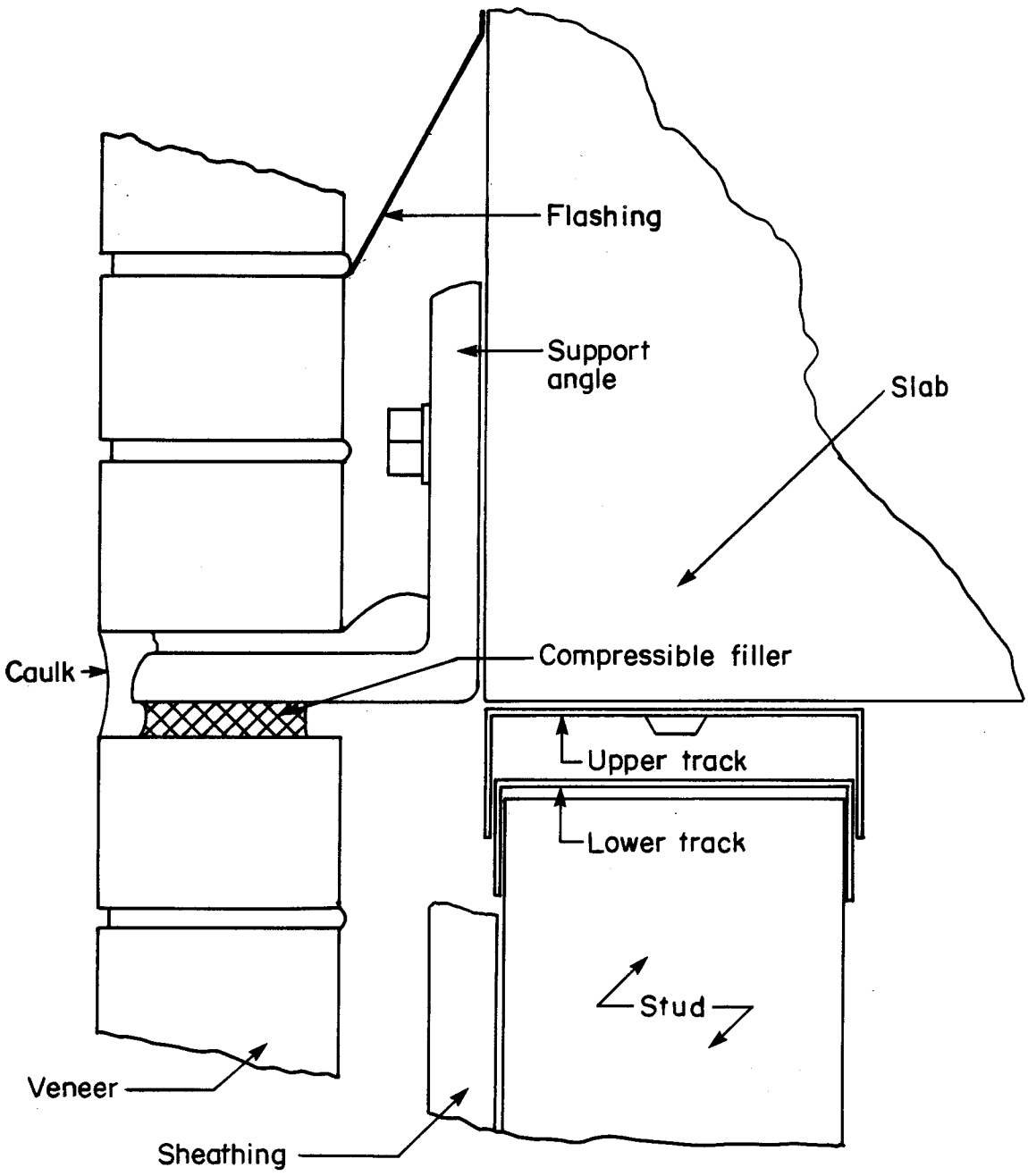

Figure 3.3 Typical Horizontal Control Joints

2. moisture expansion of the veneer.
3. shrinkage of the veneer.
4. shortening of the building frame, including shrinkage and creep effects.
5. deflection of the floor slab, including creep and shrinkage effects. (Doubly reinforced spandrel beams can be placed at the exterior edge of the floor slabs to reduce the slab deflections.)
6. maximum allowable strain in the caulking.
7. the differences in the construction tolerances allowed for the various construction materials.

There must also be caulked, compressible, vertical control joints placed in the veneer to absorb horizontal in-plane movements of the veneer due to thermal expansion, moisture expansion and shrinkage of the veneer. These joints should be located at wall offsets, at junctions, at intervals in long walls, and near corners[4].

The horizontal control joint for the stud backing wall is also shown in Figure 3.3. A double track arrangement at the top of the stud wall allows relative vertical movement between the stud and the upper slab without applying significant axial loads. The gap size for this control joint must account for shortening of the concrete frame and deflection of the floor slab, with allowance for creep, shrinkage, dimensional variation of the veneer wall and dimensional variation of the concrete slab allowed in construction.

A concrete block backing wall also requires both horizontal and vertical control joints. A caulked control joint, similiar to that used for the veneer should be placed between the top of the block wall and the bottom of the upper slab. This joint must be sized to allow for:

1. shrinkage of the block wall.
2. shortening of the building frame, including creep and shrinkage effects.
3. slab deflections, including creep and shrinkage effects.
4. maximum allowable strain in the caulking.
5. dimensional tolerances of the concrete slab and the block wall.

Vertical control joints in the concrete block wall should be designed to accommodate the horizontal shrinkage movements of the concrete block. Because of the significant axial resistance of the concrete block wall, accidental in-plane loading of these concrete block backing walls is not as critical as accidental in-plane loading of stud backing walls.

The veneer and backing wall are connected by tie systems. These tie systems must be able withstand the relative in-plane movements of the two walls without failing or applying significant axial loads to either wall. Tie systems which provide partial shear connection between the two walls also restrain shrinkage, moisture expansion and thermal movements of the veneer. The forces produced by this restraint must be considered in the wall system design.

It was mentioned earlier that construction tolerances must be taken into account when designing the expansion gaps for the in-plane movements. Variations in the slab thickness and level can significantly reduce the expected size of the control joint. If the joint is reduced by a sufficient amount, the effects of the in-plane movements are greatly increased and premature wall failure can result[30]. Contractors, architects, and site engineers must realize that control joints are not fabrication joints which make up variations in building dimensions and create an acceptable exterior finish.

4. TESTING PROGRAM

4.1 Introduction

To properly evaluate the design procedures presented in Chapter 3, a number of full-sized wall system tests were performed to confirm the theoretical model of wall system behaviour. The following chapter presents a summary of the experimental investigations of masonry veneer wall system behaviour.

There have been two extensive experimental programs conducted at the University of Alberta on the behaviour of masonry veneer and steel stud wall systems under positive pressure loading[1,17]. The results of these testing programs have already been presented in Chapter 2. These two experimental programs did not investigate certain aspects of masonry veneer wall system behaviour which are important for proper evaluation of the proposed design procedures. Thus, an additional testing program was conducted in which further aspects of wall system behaviour were investigated. These include:

1. The behaviour of stud backed masonry veneers of varying heights subjected to a positive pressure load.
2. The behaviour of stud backed masonry veneers under negative pressure loading.
3. The behaviour of block backed masonry veneers under both positive and negative pressure.
4. The behaviour of steel stud backed veneers that are

connected so that partial composite action is present between the backing wall and veneer.

This experimental program consisted of two phases. Phase one evaluated the load-deflection behaviour of the tie sytems used in the full-sized wall specimens. Phase two investigated the behaviour of full-sized wall specimens in the areas noted above. A detailed summary of the experimental program is presented in the following sections.

4.2 Tie Testing

The purpose of the tie tests was to evalute the load-deflection behaviour and modes of failure of the two tie systems used in the stud backed, full-sized wall specimens. A linear approximation of this behaviour was then used in an analysis of the load-deflection behaviour of the full-sized wall specimens.

Wall ties do not act in isolation. They interact with the masonry, the steel studs, and the exterior sheathing on stud backing walls. Previous studies have only examined the interaction of ties and masonry[3,1]. Results of these studies indicate that, below the pullout load, the masonry has little effect on the tie behaviour. For this reason, the ties used in the block backed wall specimens and the interaction of the two tie systems with the masonry veneer were not investigated. By reason of their open cross-section, the steel studs have a significant effect on the behaviour of the ties[1]. The exterior sheathing can

restrain the stud flange so that it, too, affects the performance of the ties. Because of the complex interaction of the stud, tie and sheathing, the two tie systems were tested against a typical section of backing wall.

For the first type of tie system, only the axial load-deflection behaviour was investigated because this system does not transfer any significant shear between the veneer and backing wall. However, the second tie system was designed to produce partial composite action between the veneer and backup. Therefore, shear load-deflection behaviour, as well as axial load-deflection behaviour, was investigated for this tie system.

4.2.1 Axial Load Tests

4.2.1.1 Specimen Description

The first of the two tie systems tested is shown in Figure 4.1. The tie system consists of an 18 gauge corrugated tie, bent to form a right angle and fastened to the flange of the steel stud using a 4.76 mm diameter, self-drilling screw. The tie is supported on the surface of the rigid insulation by a 16 gauge metal platform, developed in an earlier testing program[17]. This platform transfers the tie load directly to the stud flange and holds the insulation in place. The free end of the tie is laid in a veneer mortar joint.

The second tie system consists of a 18 gauge shear bracket and a 4.76 mm diameter rod tie attachment. The

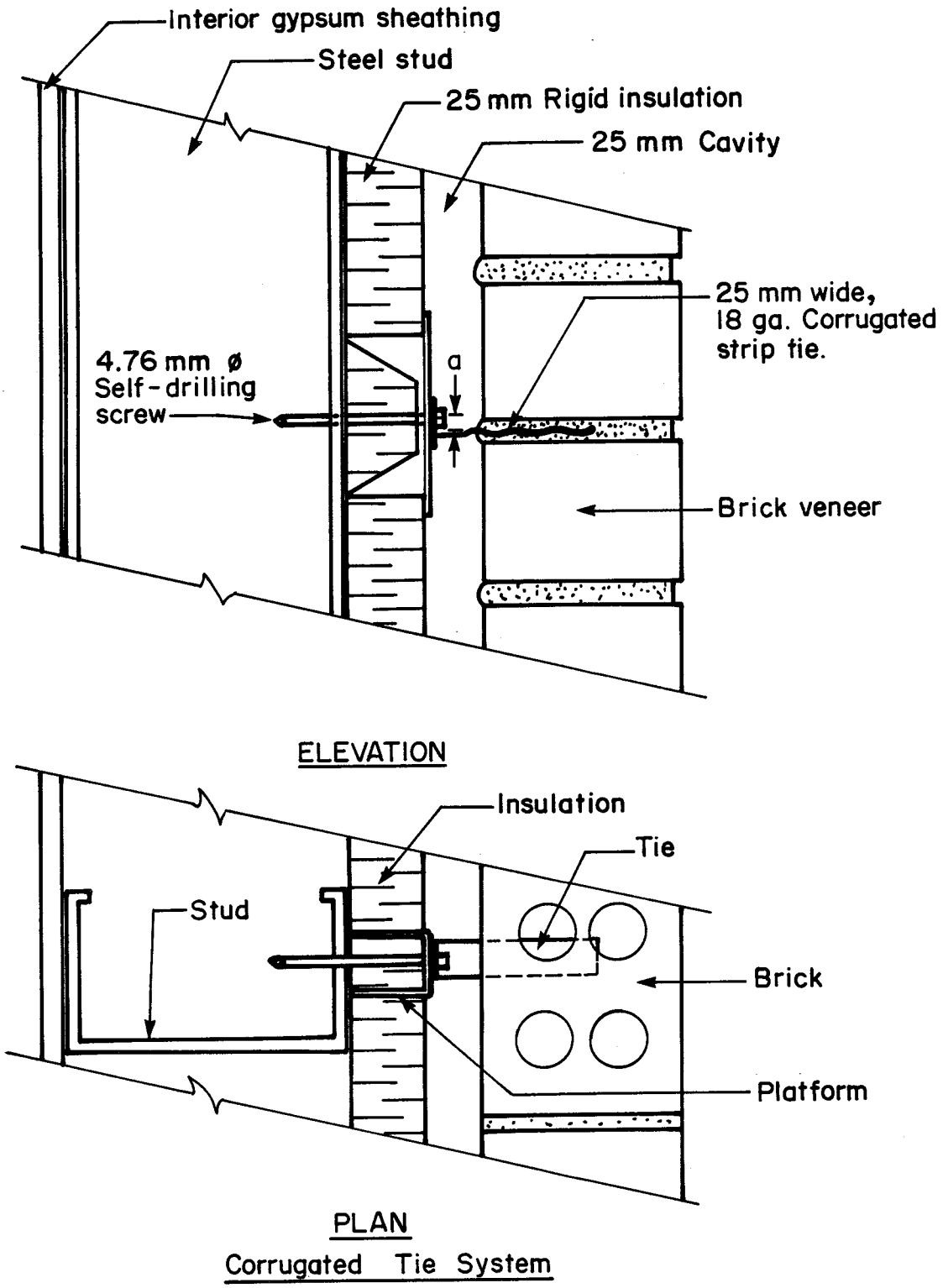

Figure 4.1 Corrugated Tie System

shear bracket is connected to the web of the steel stud by four, No. 10 self-drilling screws as shown in the Figure 4.2. Rigid insulation is attached to the exterior face of the stud wall by forcing the shear bracket through the insulation. A rod tie is then attached by insertion into one of the holes at the free end of the shear bracket. This rod attachment not only connects the veneer to the shear bracket but also acts to hold the insulation in place. Any shape of rod tie may be used providing that the rod tie produces sufficient interlock with the mortar and can be easily inserted into the holes at the end of the shear bracket. Two rod shapes were tested in this program, a "Z" shaped rod tie and a "V" shaped tie. It should be noted that this tie system is similiar to one developed to provide shear connnection between concrete block backing walls and masonry veneers in cavity wall construction[32].

The rod tie attachment is laid in a veneer mortar joint so that the rod is approximately level. A number of holes are provided on the shear bracket so that adjustment of the interior elevation of the tie is possible.

A total of nine, 18 gauge corrugated tie systems and eleven shear bracket tie systems were tested against a 1210 mm long by 1210 mm wide section of a typical stud backing wall. The pertinent information for the tie specimens is listed in Table 4.1.

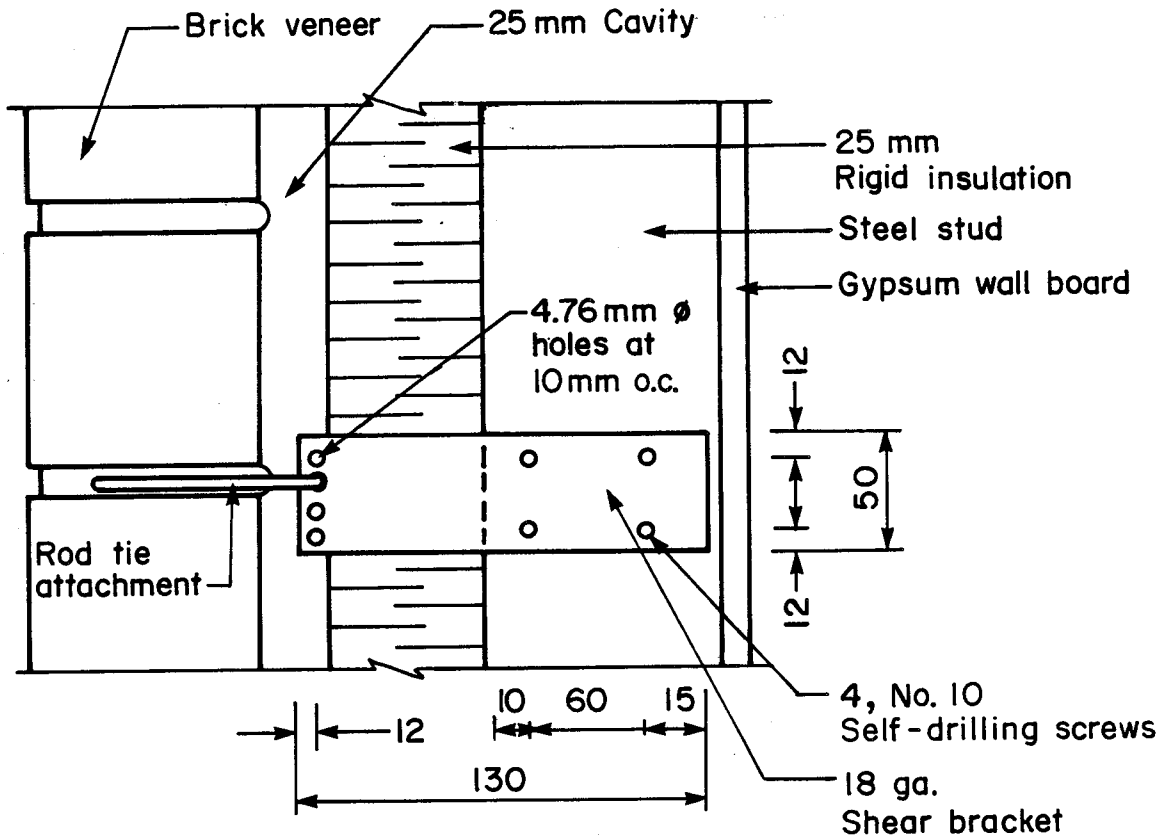

ROD TIE ATTACHMENTS

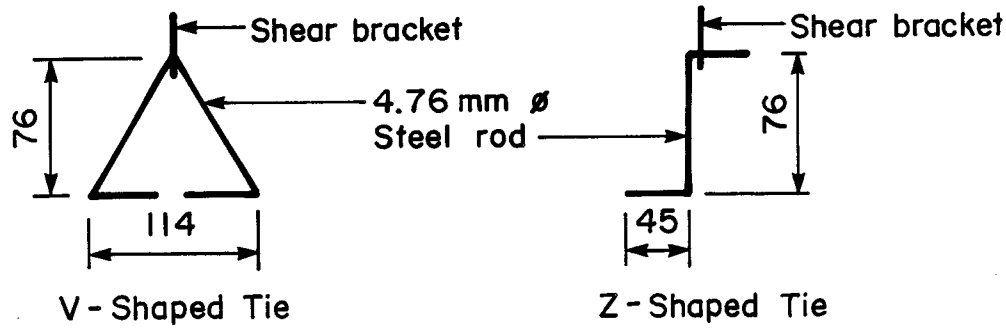

Figure 4.2 Shear Bracket Tie System

Table 4.1 A Summary of Axial Load Tie Specimens

Specimen	Tie System	a* (mm)	L& (mm)
C1	18 Corr.¢	13.0	--
C2	18 Corr.	15.0	--
C3	18 Corr.	10.0	--
C4	18 Corr.	11.0	--
C5	18 Corr.	15.0	--
C6	18 Corr.	14.0	--
C7	18 Corr.	11.0	--
C8	18 Corr.	15.0	--
C9	18 Corr.	11.0	--
SB1	SB/V#	20.0	29.0
SB2	SB/V	20.0	37.0
SB3	SB/V	20.0	33.0
SB4	SB/V	10.0	33.0
SB5	SB/V	20.0	33.0
SB6	SB/V	10.0	31.0
SB7	SB/Z#	20.0	28.0
SB8	SB/Z	20.0	34.0
SB9	SB/Z	20.0	35.0
SB10	SB/Z	20.0	38.0
SB11	SB/Z	20.0	33.0

Note: *- a - distance from centre of screw hole to bottom of tie bend, for the corrugated tie systems, and denotes the distance from the top of the shear bracket to the centre of rod attachment hole, for each of the shear bracket specimens

&- L - distance from the centre of the rod attachment hole to the stud flange

¢- 18 Corr. - 18 gauge corrugated strip tie with a 16 gauge metal backing platform

#- SB/V and SB/Z - shear bracket with "V" rod tie attachment and "Z" rod tie attachment, respectively

- all ties tested against 1220 x 1220 mm typical backing wall with 90 mm, 18 gauge steel studs at 400 mm O. C., complete with sheathing

4.2.1.2 Testing Procedures

The apparatus used to test the tie systems is shown in Figure 4.3. This testing frame consisted of a double-acting jack, tie clamp, adjustable clamp guide, jack and guide support frame, steel reaction beam, load cell, two linear variable differential transducers (LVDTs), and a backing wall consisting of three 18 gauge, 90 mm deep steel studs. This backing wall was sheathed on the tie side with 25 mm thick rigid insulation and on the opposite side with 12 mm thick gypsum wallboard. One transducer, positioned at the back side of the backing wall at the same height as the tie, provided a measurement of the beam deflection of the stud. A second transducer measured the deflection of the clamped end of the tie. The difference between these two deflections gave an accurate reading of the overall deflection behaviour of the tie system.

After the backing wall was fabricated in the testing frame, three corrugated tie specimens were fastened to the centre of each of the three stud flanges, with an even spacing over the height of the studs. Each corrugated tie specimen was then tested using the following procedure:

1. The free end of the corrugated tie was fixed in the tie clamp so that the clear distance between the tie platform and the edge of the tie clamp was 25 mm.
2. The distance (a) from the bottom of the tie bend to

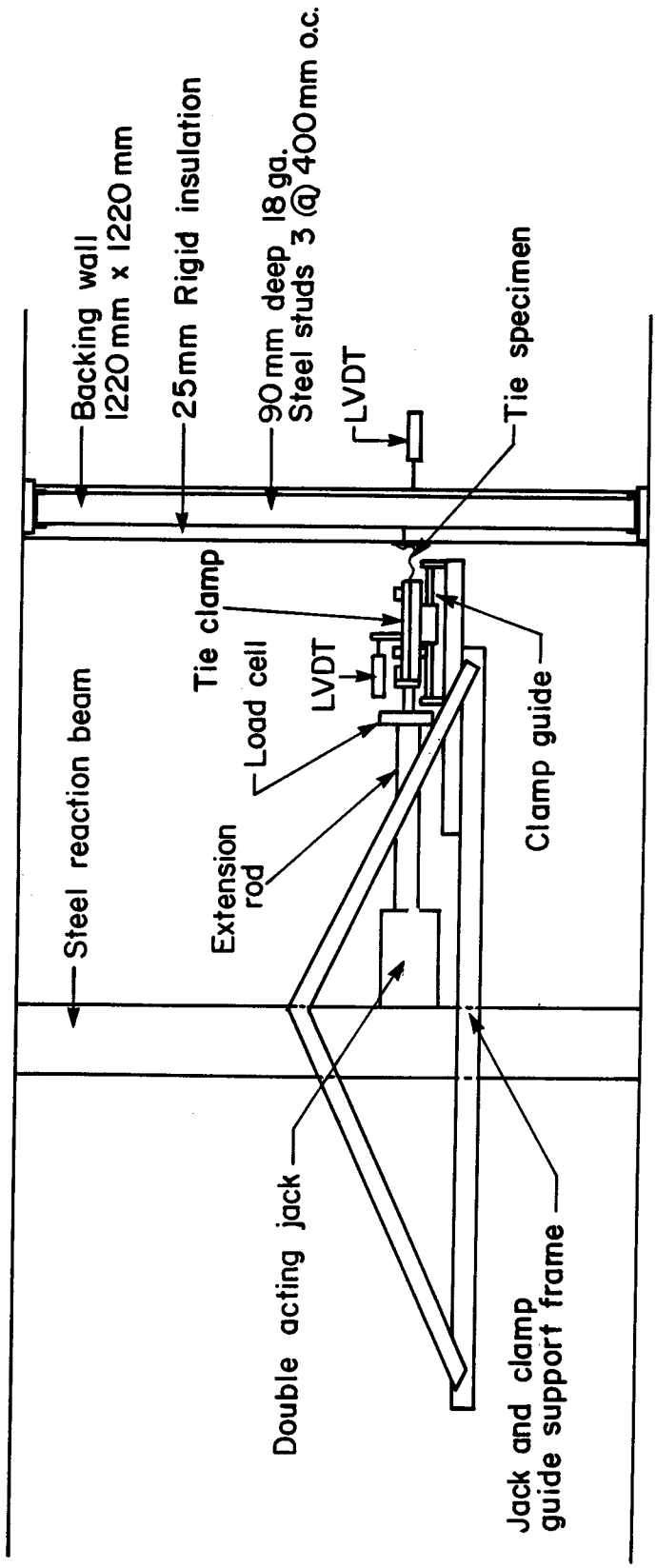

Figure 4.3 Tie and Wall Section Testing Apparatus

the centre of the fastening screw was measured.

3. An axial load was applied to the tie using a hand pump to actuate the jack.
4. The axial load was cycled four times from 0.80 kN in compression to 1.0 kN in tension. Each specimen was then loaded to failure, either in compression or tension. Measurements of deflections and load were taken at intervals during each test.

When the corrugated tie system tests were completed, a new backing wall was fabricated. Four shear bracket tie systems were fastened to the web of two of the studs and three were fastened to the third stud. These brackets were spaced evenly over the height of the studs. Each shear bracket tie specimen was tested in the following manner:

1. The rod attachment was fixed firmly in the tie clamp so that the distance from the flange of the steel stud to the edge of the tie clamp was 50 mm.
2. The distance from the stud flange to the centre of the rod attachment hole and the distance from the centre of the attachment hole to the top of the shear bracket were recorded. This information is summarized in Table 4.1.
3. An axial load was applied and cycled once to $\pm$ 1.5 kN for specimens using "V" rod tie attachments, and once to $\pm$ 1.0kN for specimens using "Z" rod tie attachments.

4. The specimen was then loaded to failure in either tension or compression. Deflections and load were recorded at intervals throughout each test.

4.2.2 Shear Load Tests

4.2.2.1 Specimen Description

A total of nine shear load-deflection tests were performed during this part of the testing program. Three tests were performed on each configuration of stud backing and shear bracket combination present in the full-sized wall specimens. Table 4.2 lists the stud configuration of each specimen tested.

4.2.2.2 Testing Procedures

Figure 4.4 shows a typical shear test specimen and the shear load-deflection testing apparatus. A threaded rod was attached to the free end of the shear bracket by means of a bolt and two plates. A shear load was then applied by slowly advancing a nut on the rod. A load cell was used to monitor the load in the rod. Deflections and load were recorded at intervals to a maximum shear load of 3.0 kN.

Two LVDTs monitored vertical deflections on the three specimens attached to a single stud. One LVDT was placed at the point of load application and one was placed at the interior side of the shear bracket. By monitoring both movements, the rotation of the shear

Table 4.2 Shear Loaded Tie Specimens

Specimen	Stud	d1* (mm)	d2& (mm)
1	18 - 90¢	35.0	80.0
2	18 - 90	39.0	76.0
3	18 - 90	36.0	81.0
4	20 - 90B#	33.0	--
5	20 - 90B	34.0	--
6	20 - 90B	35.0	--
7	20 - 150B	34.0	--
8	20 - 150B	32.0	--
9	14 - 150B**	27.0	--

Note: *- d1 - distance from stud flange to load LVDT (see Figure 4.4)
&- d2 - distance from stud flange to rear LVDT (see Figure 4.4)
¢- 18 - 90 denotes a 18 gauge , 90 mm stud
#- 20 - 90B denotes two 20 gauge, 90 mm studs back to back
**- 14 - 150B denotes two 14 gauge, 150 mm studs back to back

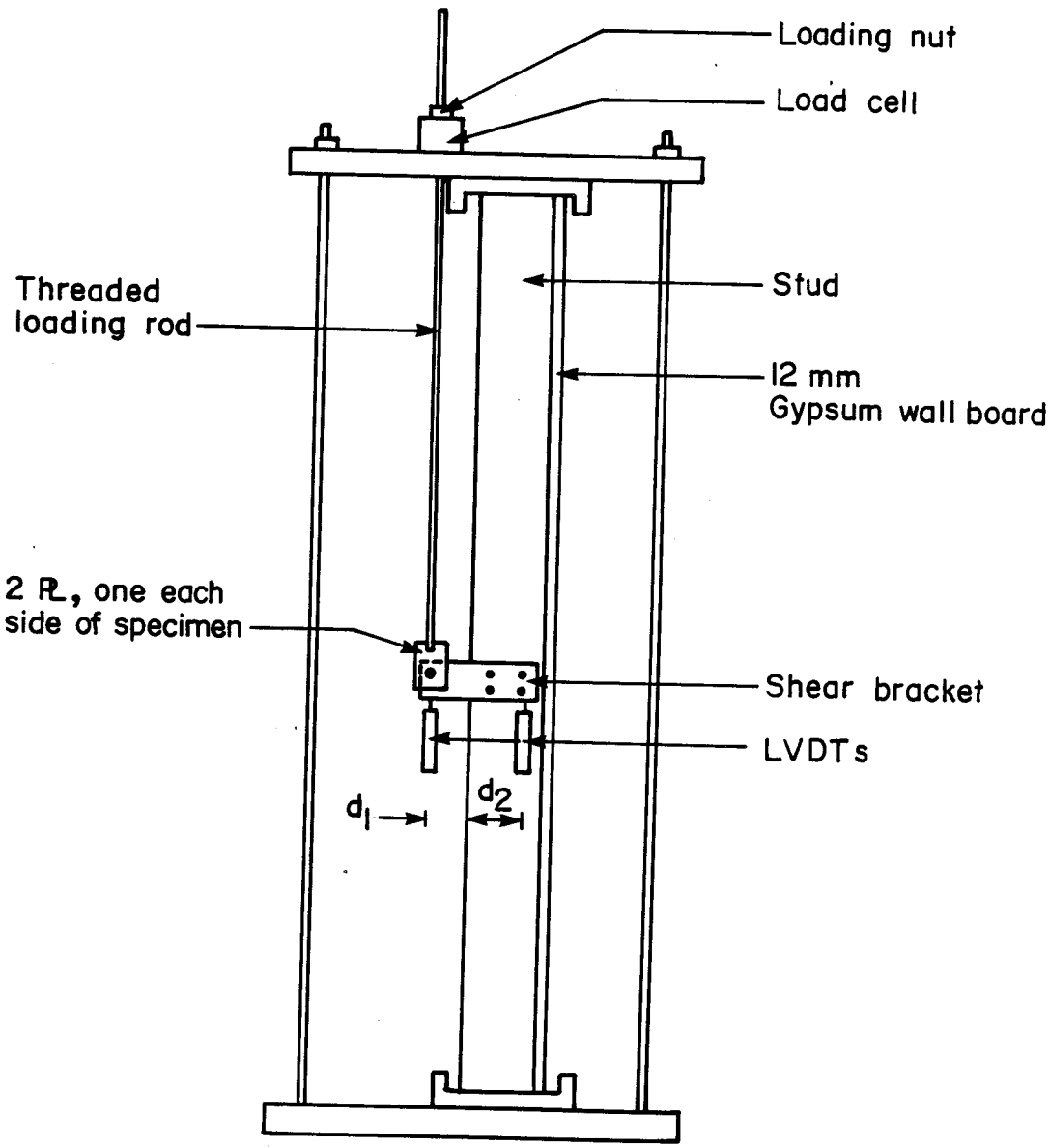

Figure 4.4 Shear Test Specimen and Testing Apparatus

bracket/stud connection can be determined. The exterior sheathing of rigid insulation was not present during testing as it provides negligible shear restraint and made deflection measurements difficult.

Six of the shear test specimens were attached to the webs of two studs placed in a back-to-back configuration. For these specimens, deflection measurement at the interior end the shear bracket was impossible. Thus, only the deflection of the loading point was measured.

For each specimen, the distance from the stud flange to the point of application of shear load and, where applicable, the distance from the stud flange to the interior LVDT were measured. These measurements are summarized in Table 4.2.

4.3 Full-Sized Wall Tests

In the second phase of the experimental program full height, masonry veneer wall sections were subjected to a simulated wind pressure loading. The first half of this phase evaluated the behaviour of wall specimens under a positive pressure loading and the second half evaluated the behaviour of wall specimens under a negative pressure loading.

As part of the the evaulation of the behaviour of the full-sized wall system, the load-deflection behaviour of the stud and track connection was investigated. The stud/track

tests and their results are summarized in Appendix B.

4.3.1 Walls Subjected to Positive Pressure

4.3.1.1 Specimen Description

The full-sized wall specimens were constructed and tested in two series of six specimens. Seven veneer wall specimens were tested under a positive pressure loading. One specimen was backed by a 190 mm deep, hollow concrete block wall and six were backed by steel stud walls.

Figures 4.5 and 4.6 show details of a typical full-sized stud backed wall specimen. The construction of all the stud backed wall specimens followed the same sequence. The stud backing wall was constructed between the two supported slabs and was then sheathed on the interior face with 12 mm gypsum wallboard. For wall specimens employing shear bracket tie systems, the shear brackets were attached to the studs in the same manner as for the small tests. The distance from the stud flange to the centre of the rod holes was kept at a constant 45 mm. Rigid insulation, 25 mm thick, was then forced over the shear brackets after thin openings were cut in the insulation at each bracket elevation.

For the specimens employing corrugated tie systems, the ties were attached to the stud after 25 mm of rigid insulation was placed on the exterior face of the stud wall. This was done sequentially for each 600 mm by 1220

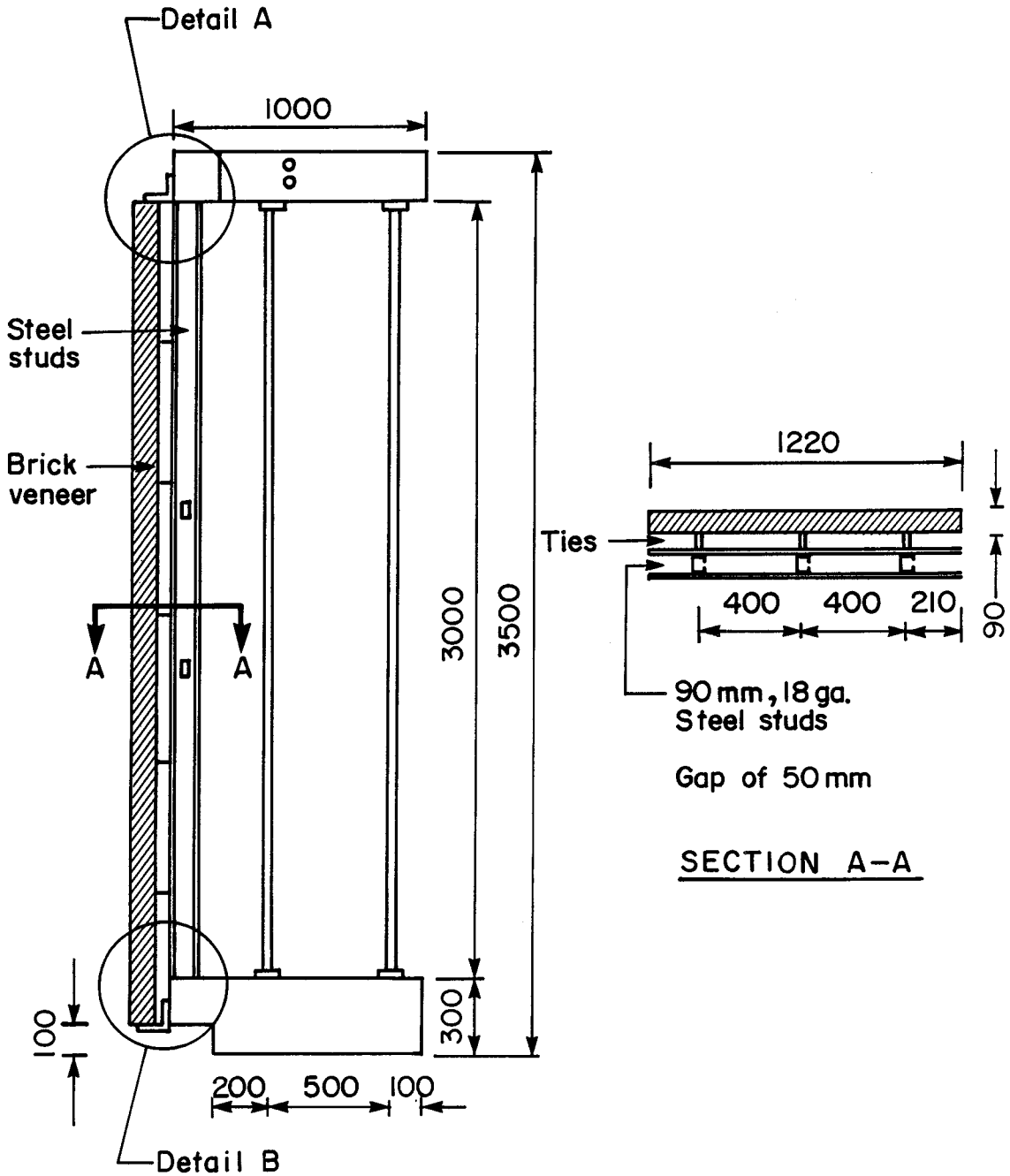

Figure 4.5 Full-Sized Wall Specimen

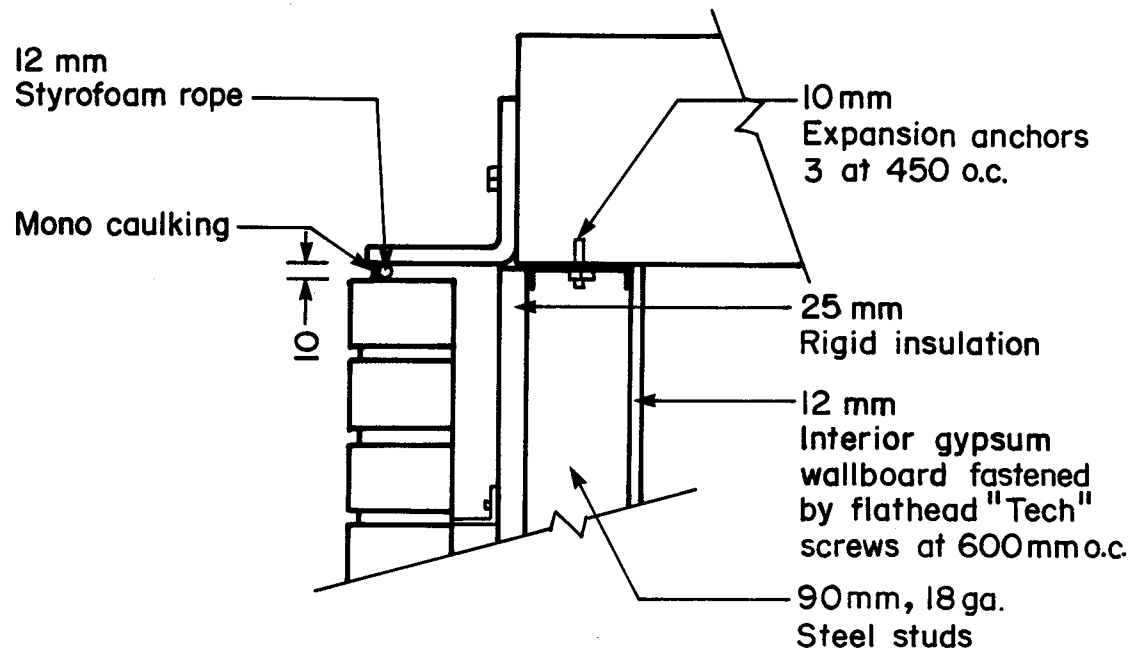

DETAIL A

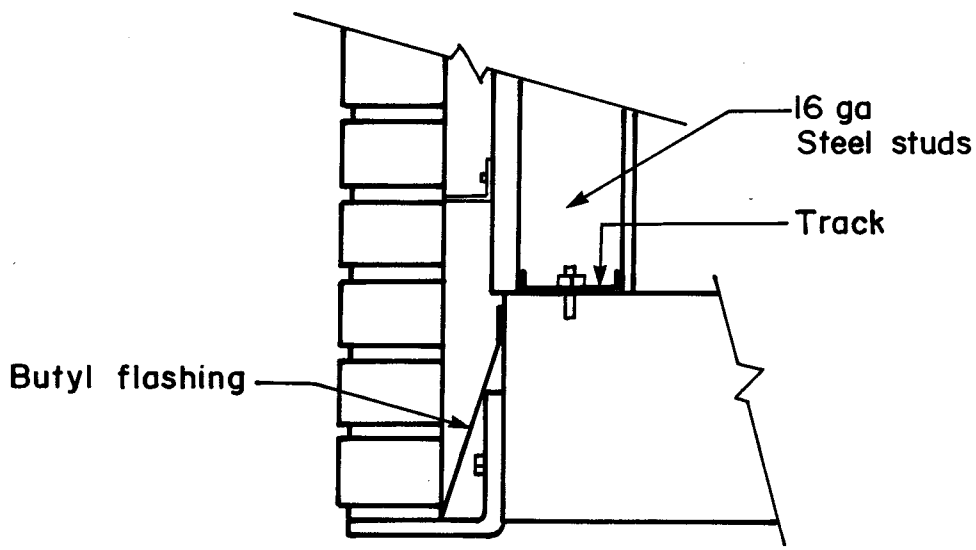

DETAIL B

Figure 4.6 Full-Sized Wall Specimen Details

mm panel of rigid insulation.

The tie pattern used for all the stud backed wall specimens is shown in Figure 4.7. The nominal tie spacing was 400 mm by 530 mm. A staggered spacing was used with an additional tie placed near the top of the middle stud line.

After the backing wall was completed, butyl flashing was applied to the support angle and backing wall. Then, the brick veneer wall was layed up. After twenty-one days of curing, the top expansion joint was filled with 12 mm Styrofoam rope and Mono brand caulking. Each wall was then cured for a minimum of 28 days.

Figure 4.8 shows the details for the block backed specimens. Specially fabricated 18 gauge flat sheet metal ties connected the two wythes of masonry and facilitated axial strain measurements on each tie. The first course of the block backing wall was mortared to the bottom slab and the top of the backing wall was supported laterally by a clip angle attached to the top slab.

Construction of the block backed veneer wall specimens followed a procedure similar to that of the steel stud backed specimens. Ties were positioned as shown in Figure 4.9. Rigid insulation, 25 mm thick, was then cut and glued to the exterior face of the block. The insulation was cut so that the panels fitted tightly

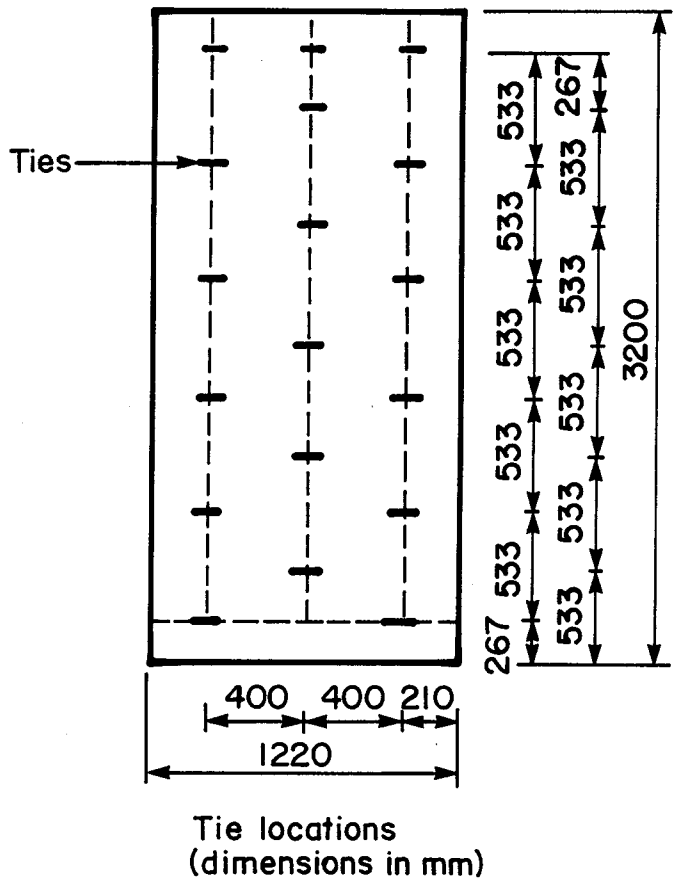

Figure 4.7 Tie Pattern of Stud Backed Specimens

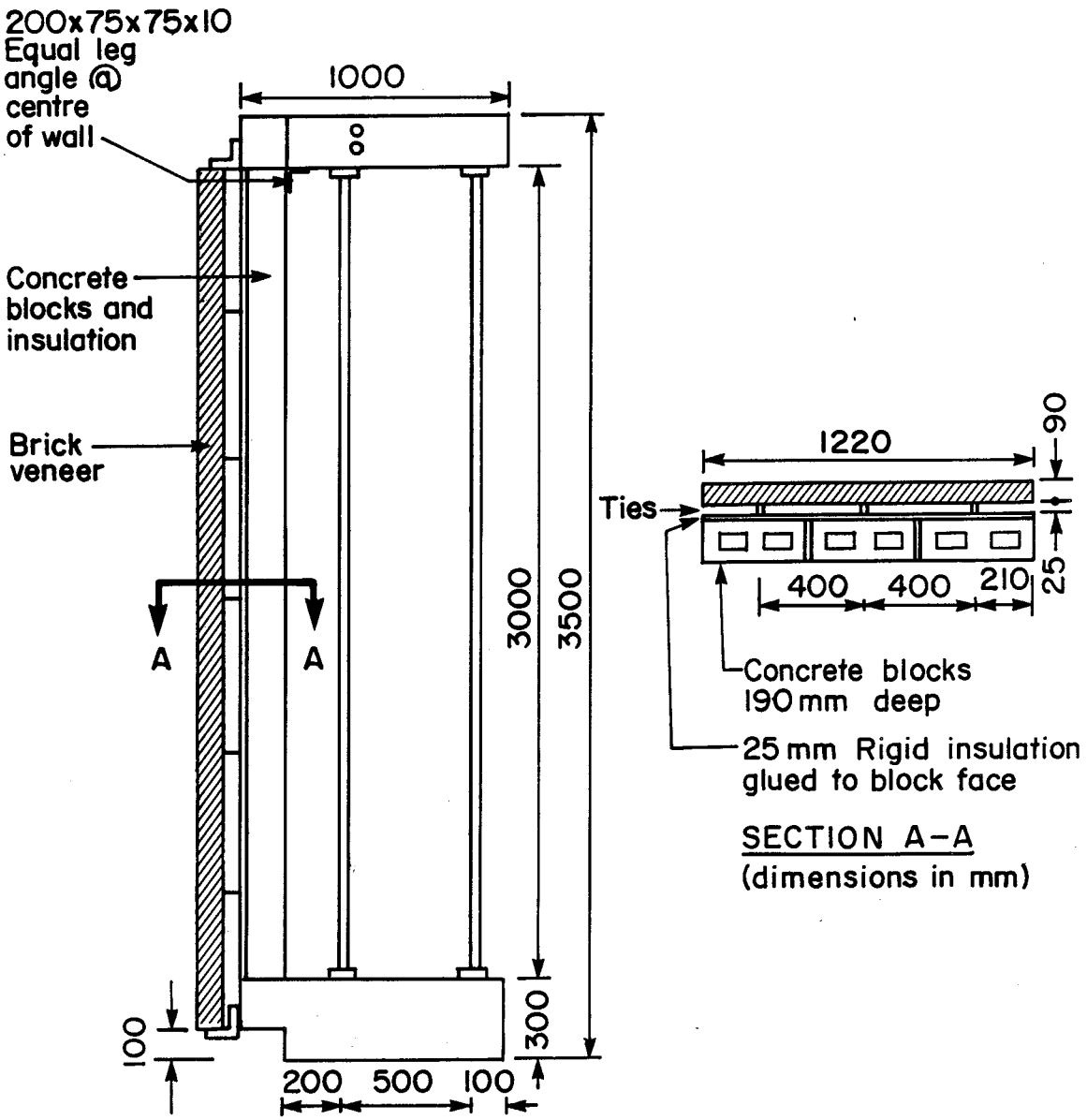

Figure 4.8 Construction Details of Block Backed Specimens

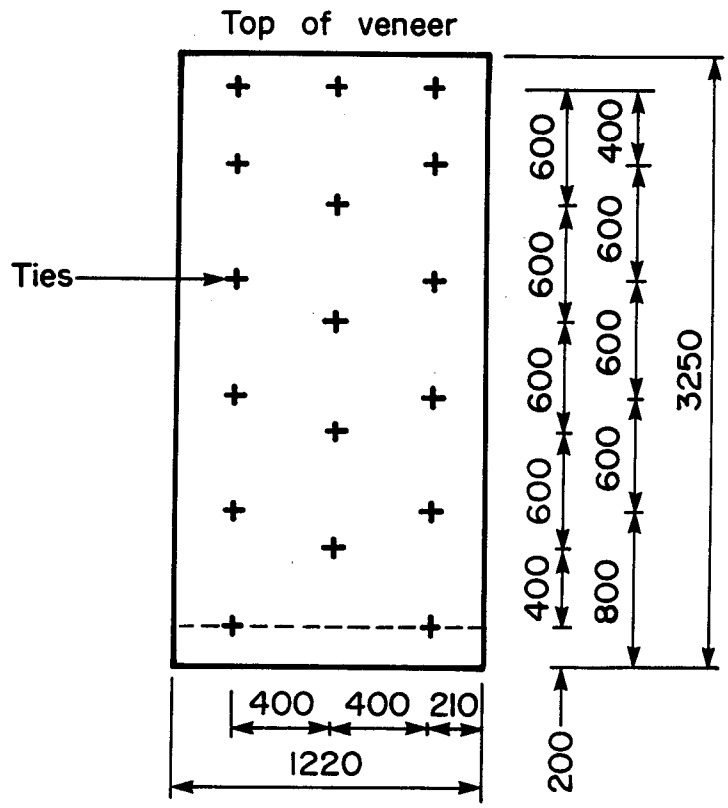

Figure 4.9 Tie Pattern of Block Backed Specimens

between the lines of ties. After the block backing was completed, the flashing was applied and the veneer was laid up.

Table 4.3 summarizes the tie system type and backing wall characteristics for all wall specimens tested under a positive pressure loading.

The masonry wall specimens were constructed by a journeyman mason. The brick mortar joints were raked 5 mm and special care was taken to ensure that the workmanship of the brickwork was comparable to a well-built wall in the field. The cavity was not cleaned.

All mortar was mixed according to CSA A-179M[33] specifications for type S mortar. Three test cubes were made from each mortar batch.

4.3.1.2 Testing Procedures

Before each wall specimen was constructed, strain gauges were attached to all the ties to measure axial strains. For the specimens that used shear bracket tie systems, the amount of composite action between the veneer and the backing wall was measured by means of four strain gauges positioned on three of the shear brackets to measure bending strains. As the maximum shear transfer is expected near the supports of the backing wall, these ties were located at the top and bottom of one of the outer stud lines and at the top of the middle stud line. Details of tie gauges and

Table 4.3 Wall Specimens Subjected to Positive Pressure

Specimen	Tie System	Ex. Sheathing	Veneer Height (mm)	Backing Wall
NS1W1	18 Corr.*	12 mm, Gyp.**	3200	S/18/90?
NS1W2	18 Corr.	12 mm, Gyp.	2600	S/18/90
NS1W3	SB/Z&	25 mm, RI&&	3200	S/20/90B##
NS1W4	SB/V¢	25 mm, RI	3200	S/18/90
NS1W5	SB/Z	25 mm, RI	3200	S/18/90
NS1W6	18 Flat.#	25 mm, RI	3200	B/190***
NS2W4	SB/V	25 mm, RI	3200	S/14/150&&&

Note: *- 18 Corr. - 18 gauge corrugated strip ties and 16 gauge platforms
&- SB/Z - shear bracket with "Z" rod tie
¢- SB/V - shear bracket with "V" rod tie
#- 18 Flat - 18 gauge flat strip tie
**- 12 mm Gyp - 12 mm gypsum wall board
&&- 25 mm RI - 25 mm of rigid insulation
¢¢- S/18/90 - 18 gauge, 90 mm steel studs
##- S/20/90 - 20 gauge, 90 mm steel studs (two back to back)
***- B/190 - 190 mm deep hollow concrete block
&&&- S/14/150 -14 gauge, 150 mm steel studs (two back to back)
- All 90 mm deep studs used 16 gauge track

calibration are given in Appendix B.

After curing for at least 28 days, specimens were moved into the testing frame shown in Plate 4.1. A set of LVDTs was attached to the both the backing wall and brick veneer as shown in Figures 4.10, 4.11 and 4.12. The specimen was then loaded by means of the air bag and bag pressure, deflections, and strains were recorded at intervals through a computerized data acquisition system. The pressure was cycled from zero to 0.90 KPa, returned to zero, then increased until the specimen failed. For Specimen No.1, the pressure was cycled to 0.90 KPa three times before the specimen was loaded to failure.

After testing each specimen, a section of the veneer was cut from the wall and used to determine the material properties of the veneer. These tests and their results are summarized in Appendix A.

4.3.2 Walls Subjected to Simulated Negative Pressure

4.3.2.1 Specimen Description

In this half of the testing program five wall specimens were subjected to a simulated negative pressure loading. Four specimens had stud backing walls and one had a hollow concrete block backing.

The wall specimens were constructed in the same manner as those subjected to a positive pressure. In addition, ten 5 mm diameter bolts were laid in veneer

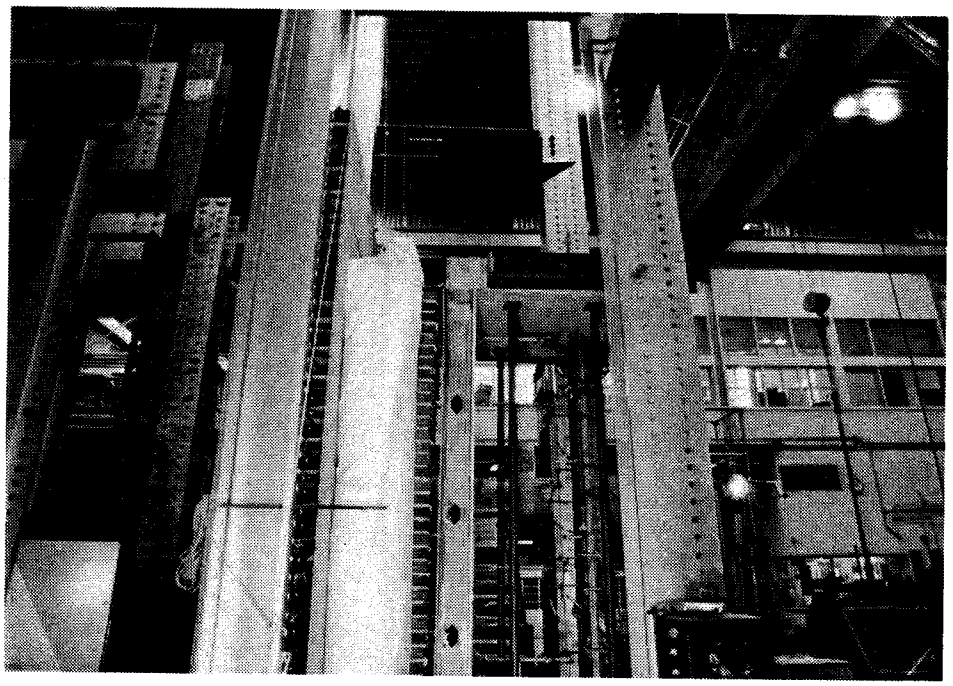

Plate 4.1 Positive Pressure Loading Apparatus

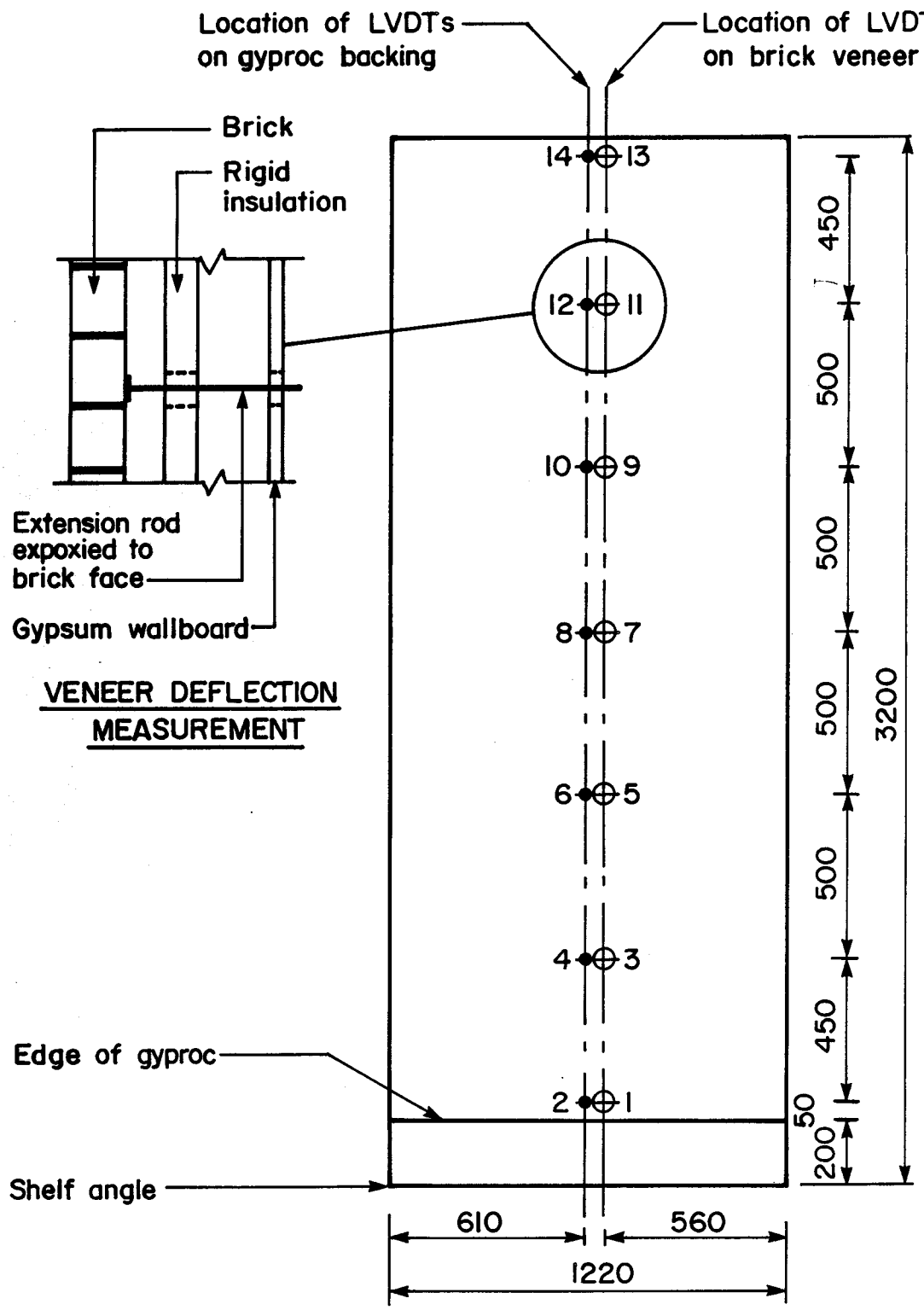

Figure 4.10 LVDT Configurations for Stud Specimens

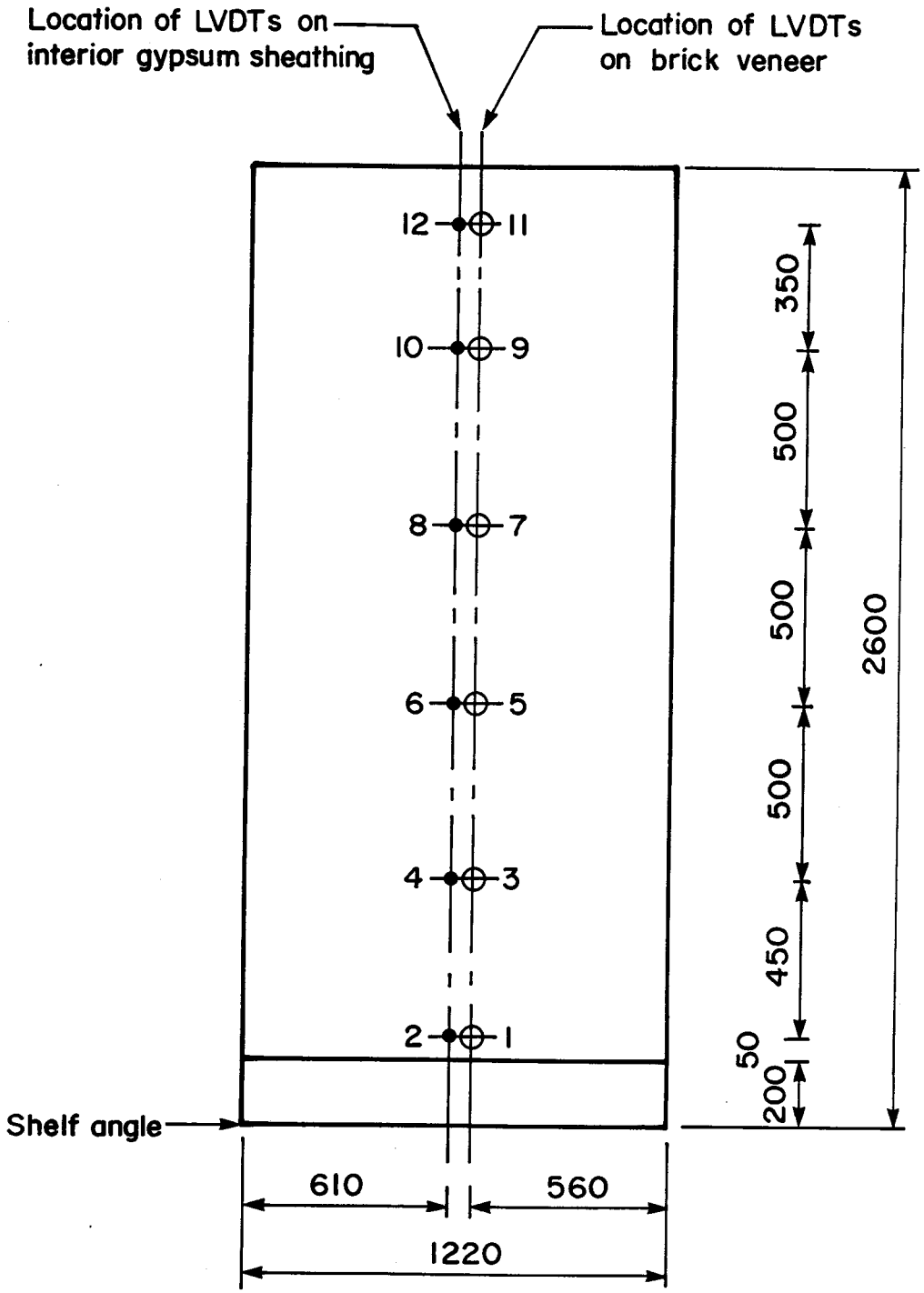

Figure 4.11 LVDT Configurations for Short Specimens (S1W2, S2W2)

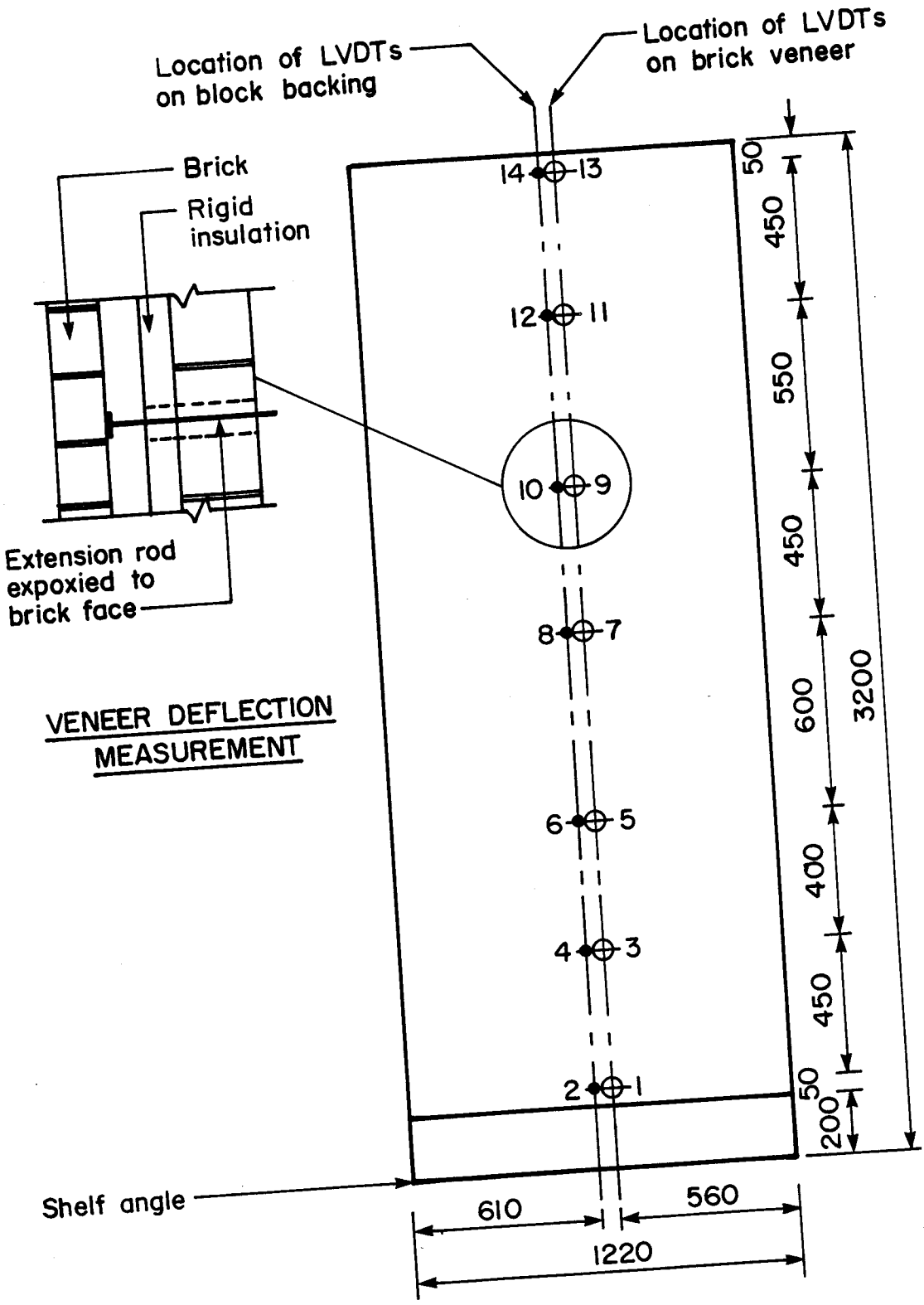

Figure 4.12 LVDT Configurations for Block Specimens

mortar joints in two lines of five each. These bolts served as anchors for the pulley mechanisms used to apply a negative load to the wall system. Each line of bolts was located midway between the outer and middle stud lines. Care was taken to ensure that the bolts were placed in veneer mortar joints in which there were no ties. Details of the anchor bolts and their locations are described in Appendix B.

The clip angle at the top of the block backed wall specimen was oriented to resist the negative lateral load. This was achieved by placing the vertical leg of the angle against the exterior face of the block wall.

The characteristics of the five full-sized wall specimens subjected to negative pressure load are summarized in Table 4.4.

4.3.2.2 Testing Procedures

Strain gauges were applied to the ties in the five wall specimens subjected to a simulated negative pressure in the same manner as those subjected to a positive pressure. After each specimen had been cured for at least 28 days, the specimen was moved into the testing frame shown in Plate 4.2 and the LVDTs were attached in the same configuration used in the positive pressure tests.

The simulated negative pressure was applied to the veneer by a continous pulley system as shown schematically in Figure 4.13. By pulling on a continuous

Table 4.4 Wall Specimens Subjected to a Simulated Negative Pressure

Specimen	Tie System	Ex. Sheathing	Veneer Height (mm)	Backing Wall
NS2W1	18 Corr.*	12 mm, Gyp.**	3200	S/18/90¢¢
NS2W2	18 Corr.	12 mm, Gyp.	2600	S/18/90
NS2W3	SB/Z&	25 mm, RI&&	3200	S/20/90B##
NS2W5	SB/V¢	25 mm, RI	3200	S/18/90
NS2W6	18 Flat.#	25 mm, RI	3250	B/190***

Note: *- 18 Corr. - 18 gauge corrugated strip ties and 16 gauge platforms
&- SB/Z - shear bracket with "Z" rod tie
¢- SB/V - shear bracket with "V" rod tie
#- 18 Flat - 18 gauge flat strip tie
**- 12 mm Gyp - 12 mm gypsum wall board
&&- 25 mm RI - 25 mm of rigid insulation
¢¢- S/18/90 - 18 gauge, 90 mm steel studs
##- S/20/90 - 20 gauge, 90 mm steel studs (two back to back)
***- B/190 - 190 mm deep hollow concrete block
- All 90 mm studs used 16 gauge track

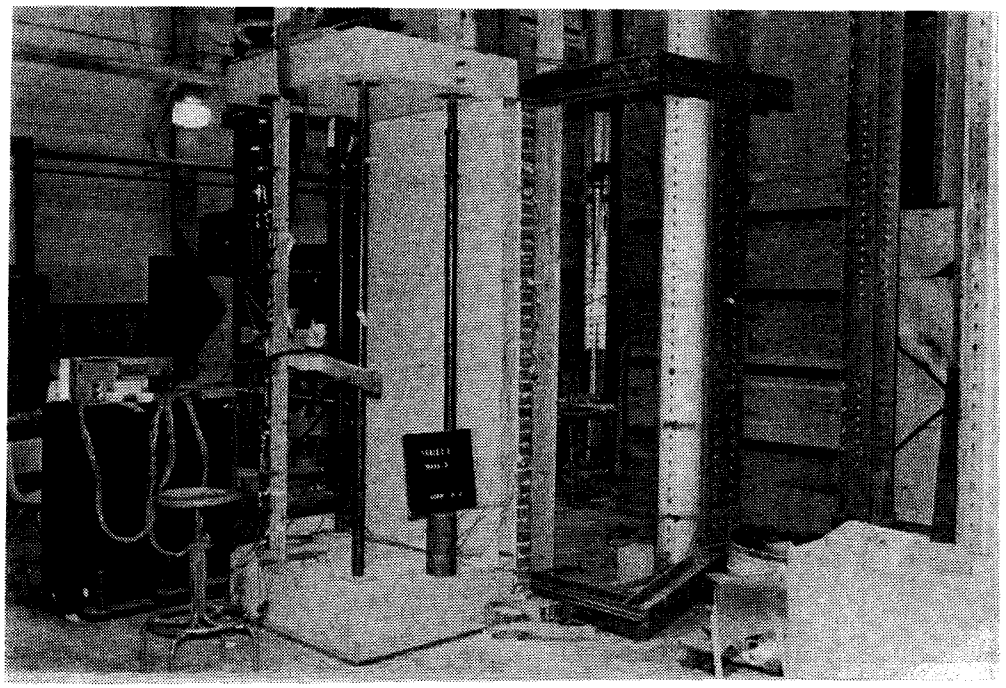

Plate 4.2 Specimen and Simulated Negative Pressure Testing Apparatus

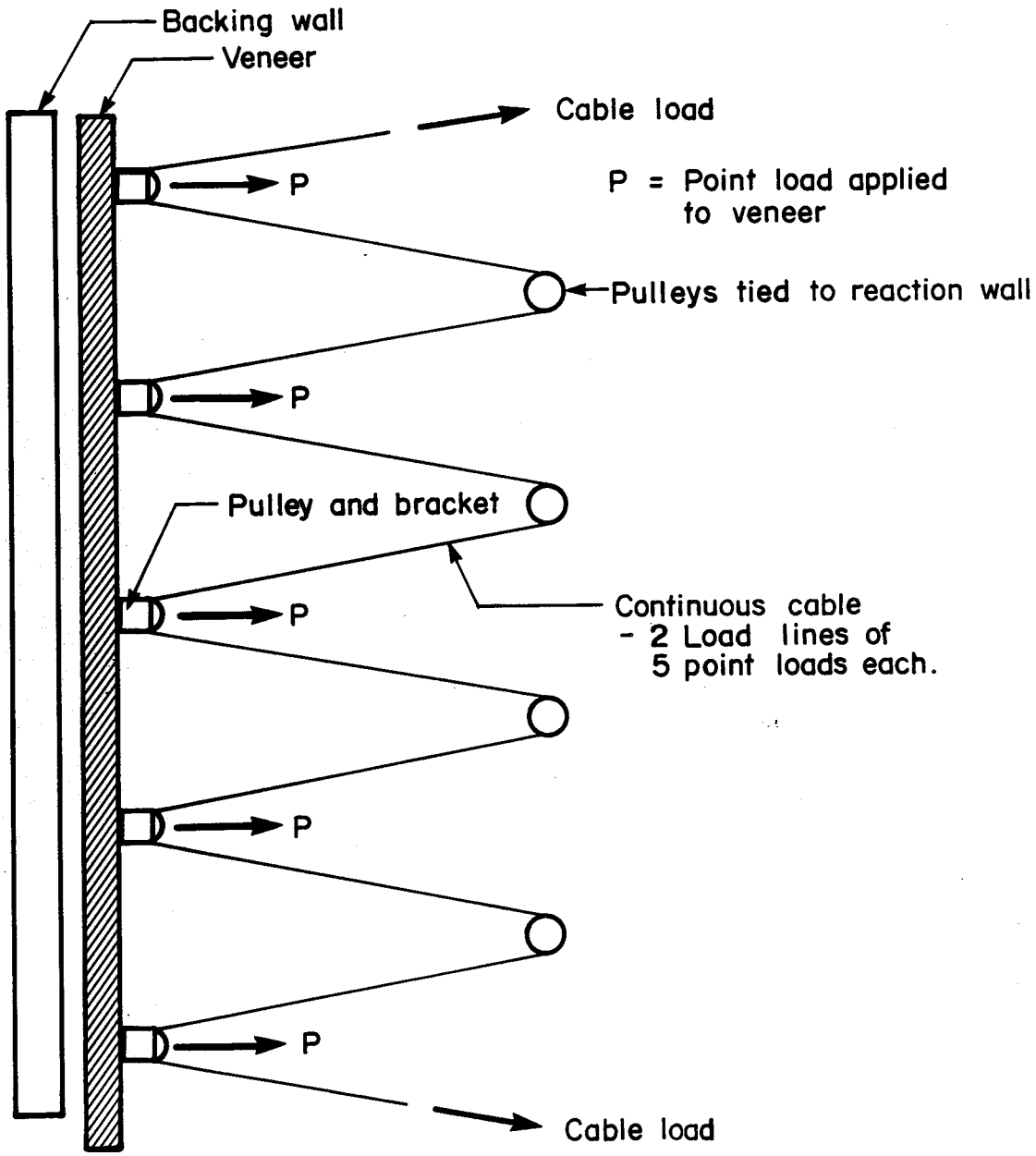

Figure 4.13 Schematic Diagram of the Simulated Negative Pressure Loading

cable on each load line, point loads were applied to the veneer through the pulley brackets and anchor bolts. These point loads are equal and horizontal if the pulleys are completely frictionless. The pulley system used to test Specimen No. 1 was found to have excessive friction and the system was modified for the remaining four tests. Details of the negative testing apparatus and the tests conducted to determine pulley friction are given in Appendix B.

Each specimen was subjected to a cycled load. The wire load was taken to approximately 80 N, dropped back to zero and then taken to the ultimate value.

After the specimens were tested, veneer prisms were cut out and tested for their material properties. The results of these tests are presented in Appendix A.

5. TEST RESULTS

5.1 Introduction

The results of the current experimental program are presented in this chapter. The first section reports the findings of the tie system tests and the subsequent section presents the results from the tests conducted on the full-sized wall specimens.

5.2 Tie Test Results

5.2.1 Axial Load-Deflection Behaviour

5.2.1.1 18 Gauge Corrugated Tie System

The load-deflection responses of two corrugated tie specimens are shown in Figure 5.1. Specimen C3 was tested to failure in tension and Specimen C6 was tested to failure in compression. The load-deflection curves of these specimens are very similar. At lower load levels, the deflection of the tie system varied linearly with the load. For higher loads, the relationship between load and deflection was nonlinear. The area within the hysteresis loop of the cyclic loading is small and little degradation of the tie system stiffness was observed. However, the failure mode of the two specimens differed significantly. Specimen C3 failed abruptly by a sudden pullout of the fastening screw threads, resulting in a large drop in the load. Specimen C6 failed by a

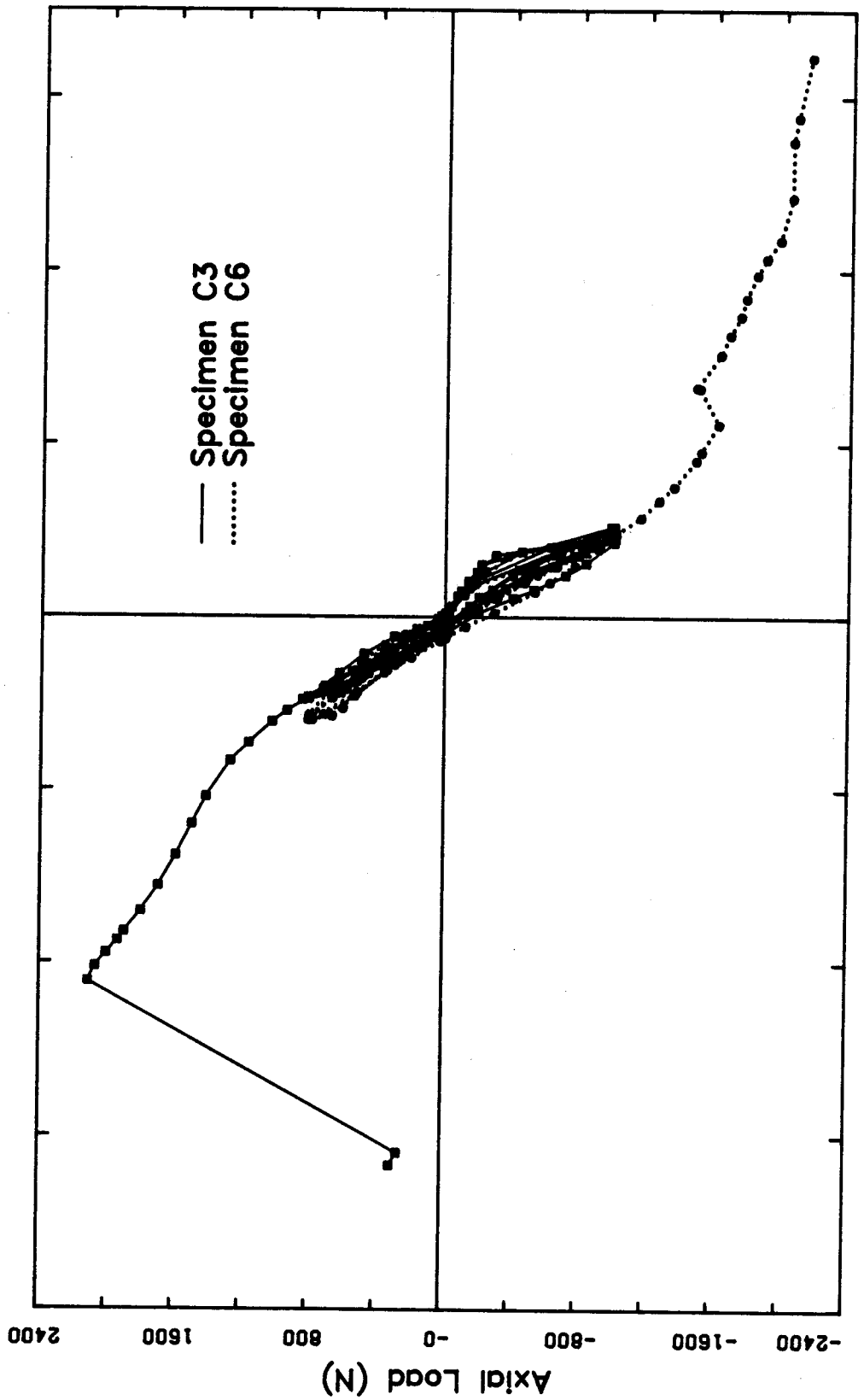

Figure 5.1 Axial Load-Deflection Behaviour of the Corrugated Tie Systems

progressive permanent bending of the tie, the tie platform and the stud flange. This bending eventually resulted in the buckling of the corrugated tie. The behaviour of these two specimens is typical of all the corrugated tie specimens.

For each of the tie tests, a straight line was fitted to the initial linear portion of the load-deflection curve using a linear regression analysis. It was observed that the slope of the load-deflection curve in the tension load region differed from the slope of the load-deflection curve in the compression load region. Therefore, independent analyses were performed for each of these load regions. The two slopes from each of the test curves are recorded in Table 5.1. Also presented in Table 5.1 are the standard deviations for each slope, the maximum linear load and the ultimate load for each tie specimen.

5.2.1.2 Shear Bracket Tie System

Figure 5.2 shows the typical load-deflection response of the shear bracket tie systems. Specimen SB3 was tested to failure in compression and Specimen SB5 was tested to failure in tension. As with the corrugated tie system response, the deflection of the shear bracket specimens varied linearly with load at lower load levels. For each shear bracket specimen, however, the slopes of the load-deflection curve in the tension load region and the compression load region were

Table 5.1 Axial Load Corrugated Tie Test Results

Specimen	Compression		Tension		Max. Linear Load		Ult. Load (N)
	Slope (N/mm)	Sdev. (N/mm)	Slope (N/mm)	Sdev. (N/mm)	Comp. (N)	Tens. (N)	
C1	--	--	330.	75.	--	+792	+2003
C2	344.	13.	180.	7.	-1031	+808	+1953
C3	460.	16.	392.	6.	-1010	+1307	+2153
C4	392.	13.	389.	8.	-1035	+1019	+1567
C5	313.	7.	519.	20.	-1024	+997	+2051
C6	503.	18.	327.	8.	-1357	+809	-2195
C7	568.	20.	576.	19.	-1503	+837	-2680
C8	494.	19.	289.	11.	-1237	+817	-2380
C9	373.	24.	338.	29.	-1298	+827	-2163

Note: - Compression is negative (-) and tension positive (+)
- Average slope in compression is 456 N/mm (Sdev=82.0 N/mm)
- Average slope in tension is 347 N/mm (Sdev=103.5 N/mm)

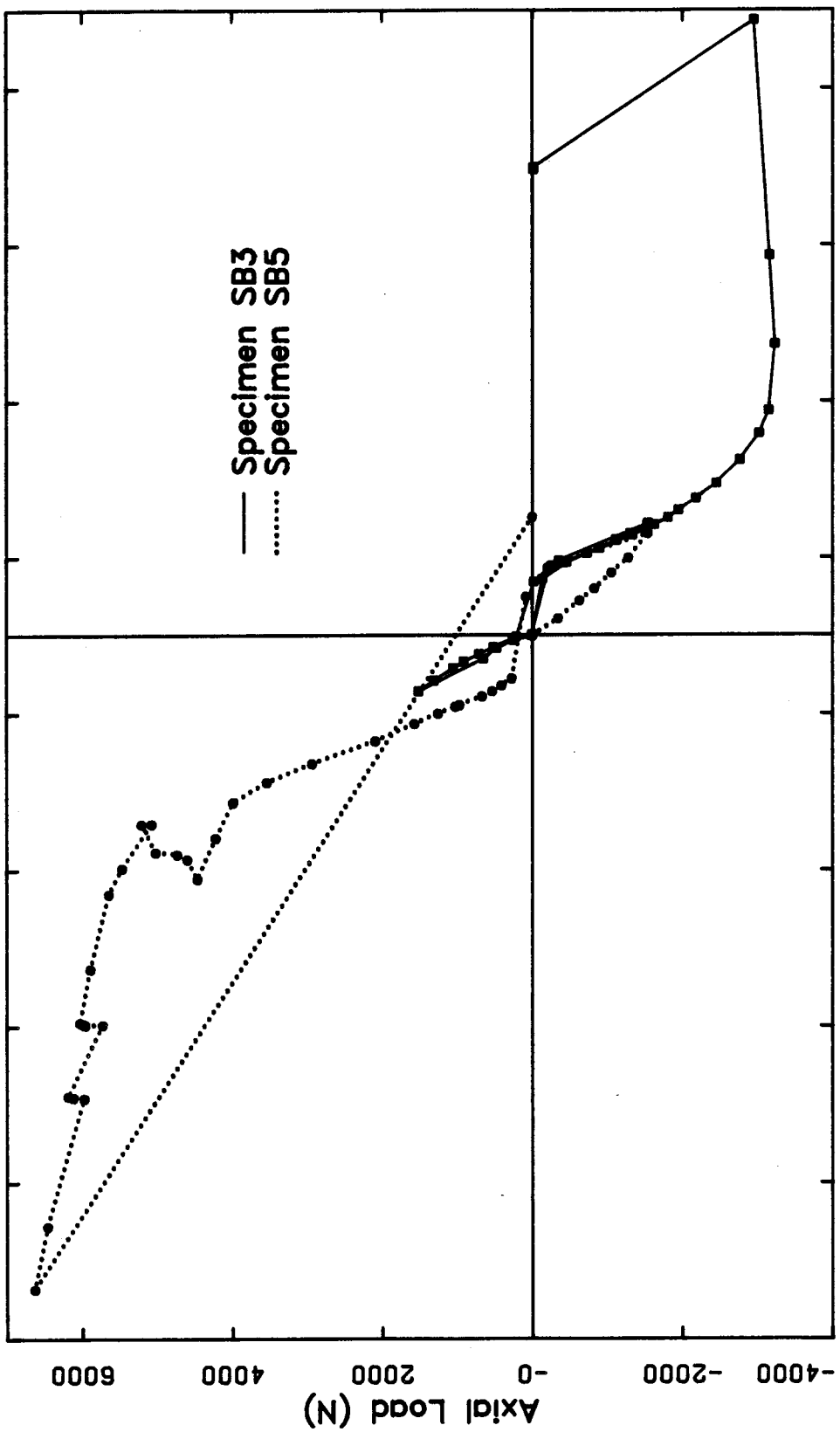

Figure 5.2 Axial Load-Deflection Behaviour of the Shear Bracket Tie Systems

approximately the same. In addition, the play in the rod tie attachment hole allowed a certain amount of free movement of the tie system, resulting in the observed shift in the load-deflection curve near the zero load level.

A linear regression analysis was again used to determine the slope of the initial linear portion of the load-deflection curves for each of the shear bracket specimens. A separate regression was performed on the tension load region and on the compression load region of load-deflection curves, with allowance for an intercept. Table 5.2 summarizes the slopes, intercepts, standard deviation of the slopes and intercepts, maximum linear load and ultimate load for each of the shear bracket tie specimens. Also listed in this table is the value of the slope and standard deviation obtained from a regression analysis performed on all the data from the eleven shear bracket tests. This analysis assumed that the slopes of the load-deflection curves were equal, in both the tension zone and compression zone, and the slope intercept was zero.

Four modes of ultimate failure were observed in the shear bracket tests. The mode of failure varied with type of rod tie attachment and type of loading. Compression failure of shear bracket specimens with "V" rod tie attachments started with significant permanent bending of the rod tie over the thickness of the shear

Table 5.2 Axial Load Test Results on Shear Bracket Ties

Specimen	Load Deflection Approximation				Max. Linear Load		Ult. Load (N)
	Intrc.(N/mm)	Sdev. (N/mm)	Slope (N/mm)	Sdev. (N/mm)	Comp. (N)	Tens. (N)	
SB1	1126.	73.	493.	52.	-1065	+1176	-2500
SB2	1126.	130.	698.	145.	-1276	+1124	-2910
SB3	2627.	110.	434.	60.	-2180	+1519	-3160
SB4	1843.	74.	25.	45.	-1489	+2419	+6200
SB5	2250.	195.	29.	81.	-1539	+2091	+6205
SB6	1416.	60.	70.	36.	-2134	+1568	-2190
SB7	943.	137.	585.	122.	-1430	+1485	-1550
SB8	718	141.	104.	108.	-1108	+1100	-1500
SB9	667.	142.	293.	74.	-1106	+1105	-1300
SB10	1149.	115.	----	----	-1143	+1365	+1660
SB11	1796.	541.	----	----	-1126	+1000	+1661

Note: - For SB10 and SB11, only the initial compression curve was used because of a LVDT malfunction.
- Compression is negative (-) and tension positive (+).
- Slopes for a linear regression fit of all the data below the linear loads are 938 N/mm (sdev=58 N/mm) for V rod tie attachments and 523 N/mm (Sdev=72N/mm) for Z rod tie attachments. This regression was forced to have a zero intercept.

bracket and a partial bearing failure of the rod attachment hole. This was followed by buckling of the shear bracket as shown in Plate 5.1. The shear bracket sway-buckled as the veneer end of the bracket slid along the cross-piece of the rod tie. The mode of tension failure for this tie system was similar to its mode of compression failure. Tension failure was initiated by permanent bending of the rod tie and a bearing failure at the attachment hole. However, the final mechanism of the tension failure was plastic hinge formation at the centre of the "V" rod tie cross piece as shown in Plate 5.2.

Shear bracket tie specimens with "Z" rod tie attachments failed in compression by significant permanent bending of the rod tie cross-piece, followed by lateral bending of the shear bracket as the deformation of the rod cross piece produced lateral thrust. The tension failure of this tie system was similiar to its compression failure except the lateral bending of the shear bracket was not as severe and the "Z" tie eventually pulled out of the attachment hole.

5.2.2 Shear Load-Deflection Behaviour

Figure 5.3 shows the shear load-deflection response of three shear bracket specimens up to a shear load of approximately 3.0 kN. A single 90 mm, 18 gauge steel stud backed Specimen 2, while two 90 mm, 20 gauge studs and two

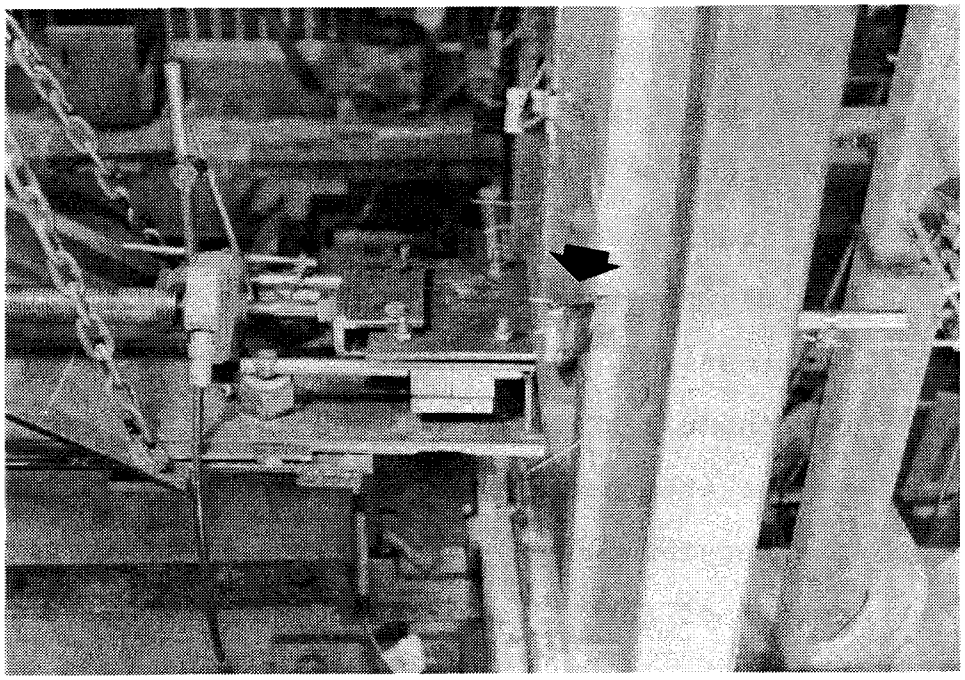

Plate 5.1 Compression Failure of the Shear Bracket and V Rod Tie

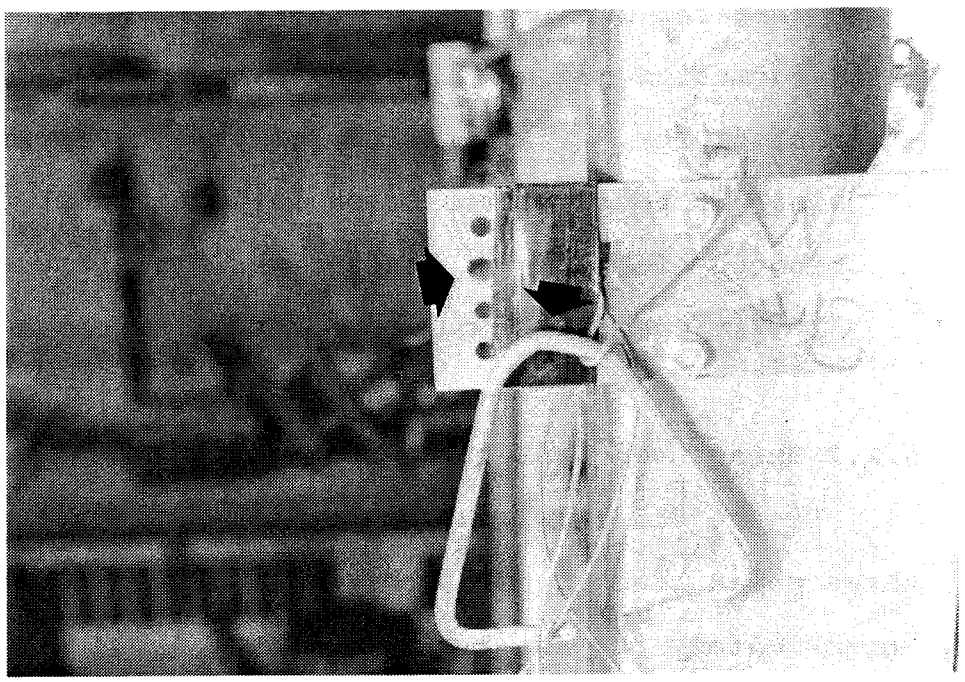

Plate 5.2 Tension Failure of the Shear Bracket and Z Rod Tie

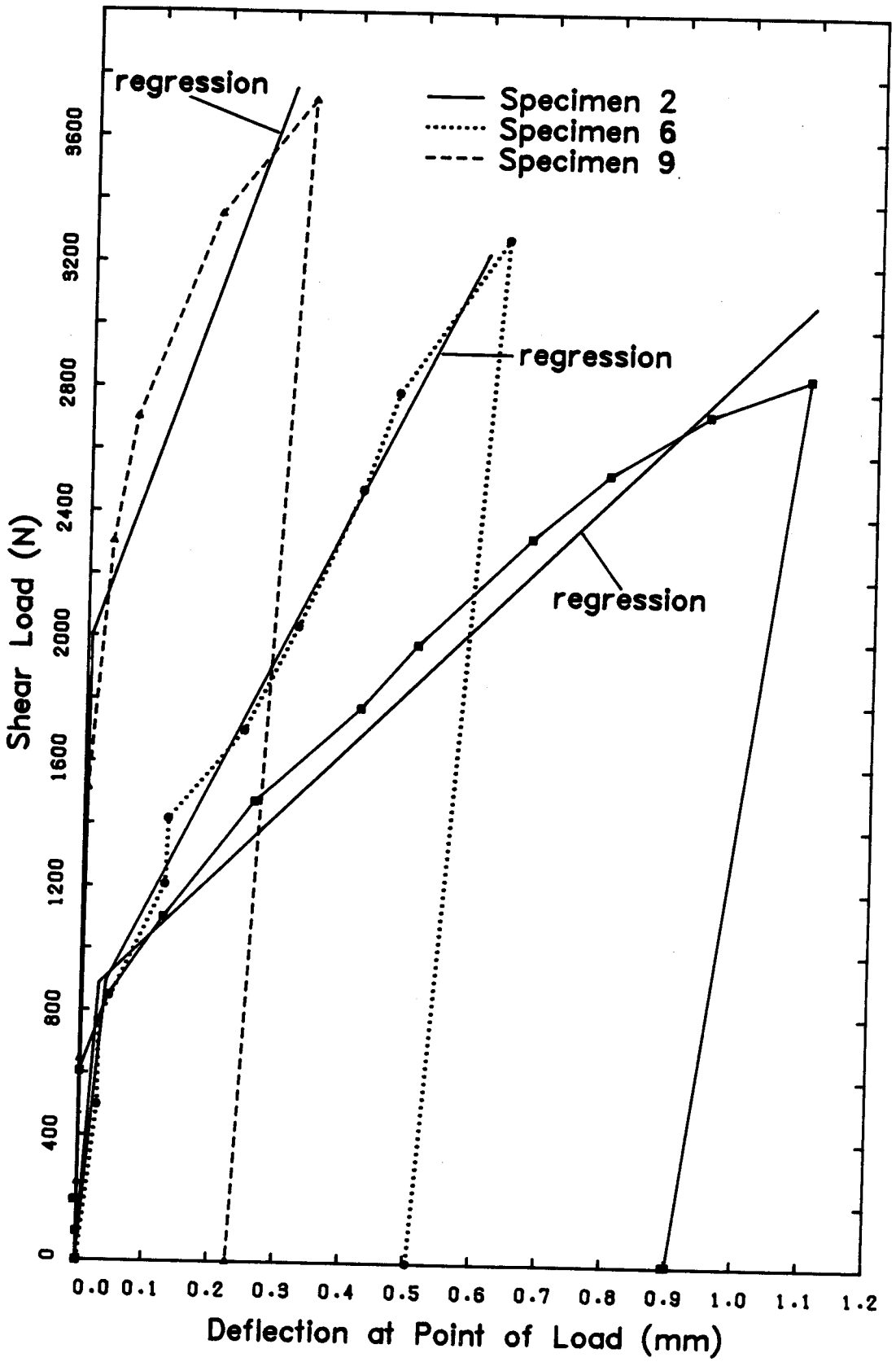

Figure 5.3 Shear Load-Deflection Behaviour of Shear Brackets

150 mm, 14 gauge studs backed Specimens 6 and 9, respectively. Each specimen type behaved similarly, with very little deflection at lower load levels; this was followed by much larger deflections once slip in the connection occurred.

The shear load-deflection behaviour of the shear bracket specimens can be approximated by a bilinear relationship. Using a linear regression analysis, a bilinear approximation was obtained for each shear load-deflection curve. While not perfect, this bilinear approximation has the advantage of being simple and reasonably accurate. Figure 5.3 shows graphically the accuracy of the approximations for Specimens 2, 6 and 9. The resulting two equations for bilinear approximation of each shear-load deflection curve are summarized in Table 5.3. Also presented in Table 5.3 are the load and deflection at the intersection of the two equations.

5.3 Results of the Full Sized Wall Tests

Presented in the following section are the test results for the twelve full-sized wall specimens. A brief description of the observed behaviour and a load-deflection plot of the veneer is presented for each specimen. Deflected shape plots for both the veneer and backing wall of each specimen are shown in Appendix C.

Measured tie loads and transfer shear are discussed in Chapter 6.

Table 5.3 Shear Load-Deflection Approximations

Specimen	Equation 1	Equation 2	Int. Dfl. (mm)	Int. Load (N)
1	S=11675(d)	S=1018+1949(d)	.105	1222
2	S=31452(d)	S=831+2042(d)	.0285	889
3	S=10296(d)	S=1166+2018(d)	.141	1450
4	S=58448(d)	S=913+3514(d)	.034	1986
5	S=343015(d)	S=1860+3720(d)	.005	1880
6	S=22875(d)	S=736+4160(d)	.039	896
7	S=84752(d)	S=1207+2985(d)	.015	1251
8	S=154051(d)	S=2647+4152(d)	.018	2720
9	S=339291(d)	S=1965+5970(d)	.006	2000

Note: - Equation 1 governs from zero load to intercept
- Equation 2 governs from intercept to approximately 3000 N
- these equations are only linear APPROXIMATIONS
- Int. Dfl. - intercept deflection
- Int. Load - intercept load

5.3.1 Wall Specimens Subjected to Positive Pressure

5.3.1.1 Specimen S1W1

Figure 5.4 shows a plot of wall pressure versus veneer deflection at an elevation of 1700 mm, for Specimen S1W1. A bilinear representation of the load-deflection curves providesa good representation of the test results, for at least two thirds of the pressure range. At a pressure 0.61 kPa, the veneer cracked in the mortar joint located at an elevation of 2015 mm. The slope of the load-deflection curve was significantly reduced after cracking, indicating that there was a significant loss in wall system stiffness when the veneer cracked. Cracking occurred during the load cycling portion of the test and the post-cracking load-deflection curve exhibits the same reduction in slope over the entire pressure cycling range. No further significant reduction in curve slope was observed when a second veneer crack occurred at a pressure of 2.24 kPa. This crack was located in the mortar joint at an elevation of 995 mm.

On both the outer studs, the tie and stud flange showed signs of permanent deformation at an elevation of 1870 mm as the wall pressure neared maximum. When the pressure reached its maximum value of 3.84 kPa, the outer studs buckled flexurally. The flexural buckling of all the steel studs consisted of a local buckling of a portion of the stud web and compression flange as shown

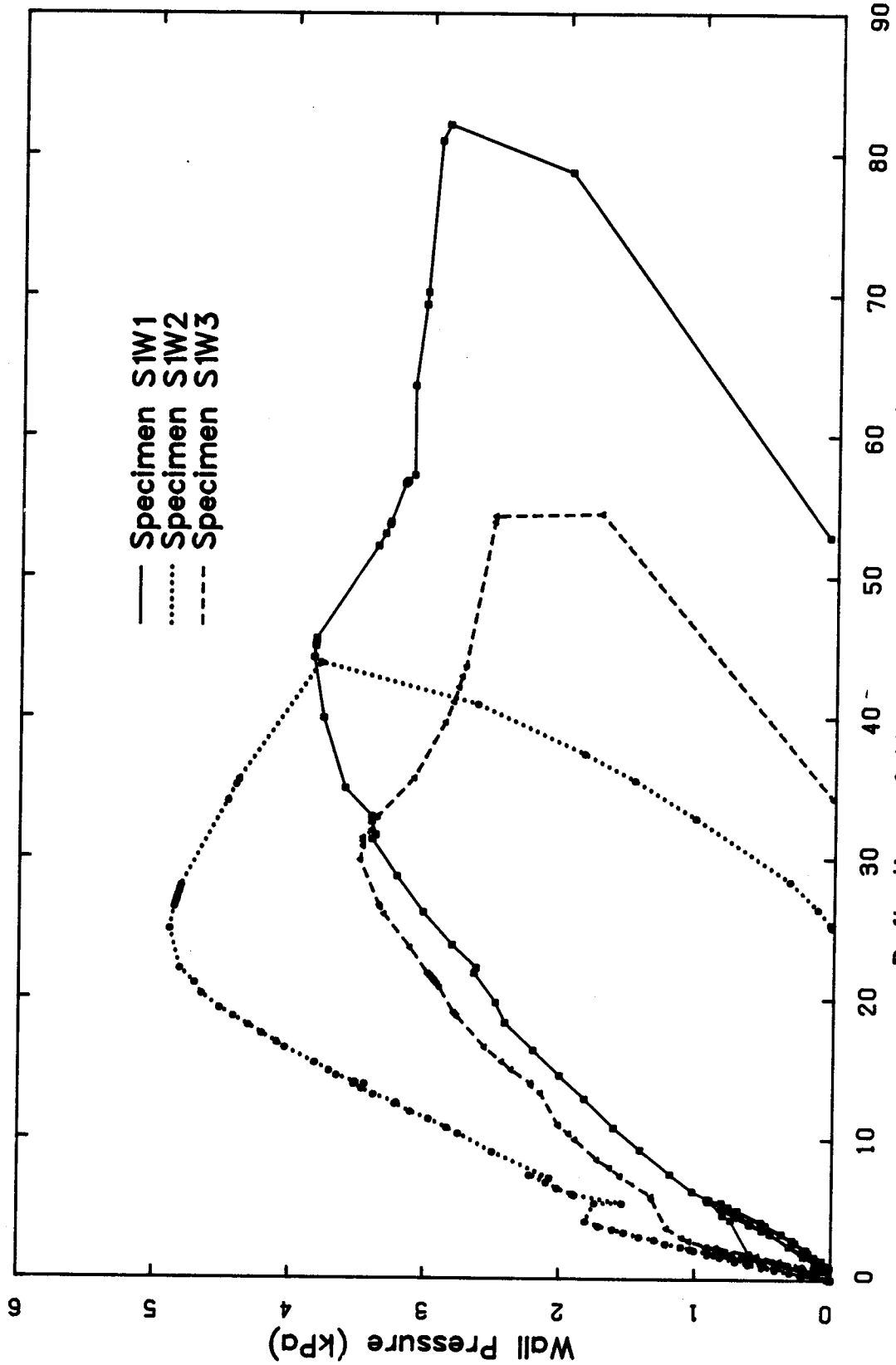

Figure 5.4 Positive Pressure Load-Deflection Curves for Specimens S1W1, S1W2 and S1W3

in Plate 5.3. After the test was completed, examination of the inner stud showed that this stud had buckled flexurally very near a tie connection at an elevation of 2070 mm.

Figures C-1 and C-2 show the deflected shape of both the veneer and stud backing wall for specimen S1W1. These plots show the significant deformation of the top of the veneer and the top and bottom of the steel stud backing wall.

5.3.1.2 Specimen S1W2

The veneer load-deflection plot for Specimen S1W2 is also shown in Figure 5.4. The load-deflection behaviour for this specimen was similar to that of Specimen S1W1, although Specimen S1W2 was stiffer than Specimen S1W1 and the veneer of Specimen S1W2 cracked only once, at a pressure 1.81 kPa. This crack occurred in the mortar joint at an elevation of 1285 mm. At an elevation of 1325 mm the two outer studs buckled flexurally very near tie connections at a wall pressure of 4.89 kPa. Post test examination showed that the centre stud buckled near a tie connection at an elevation of 1595 mm.

Figures C-3 and C-4 show the deflected shapes of the veneer and backing wall for Specimen S1W2. These plots indicate the stud supports and top of the veneer deformed significantly over the entire range of wall pressure.

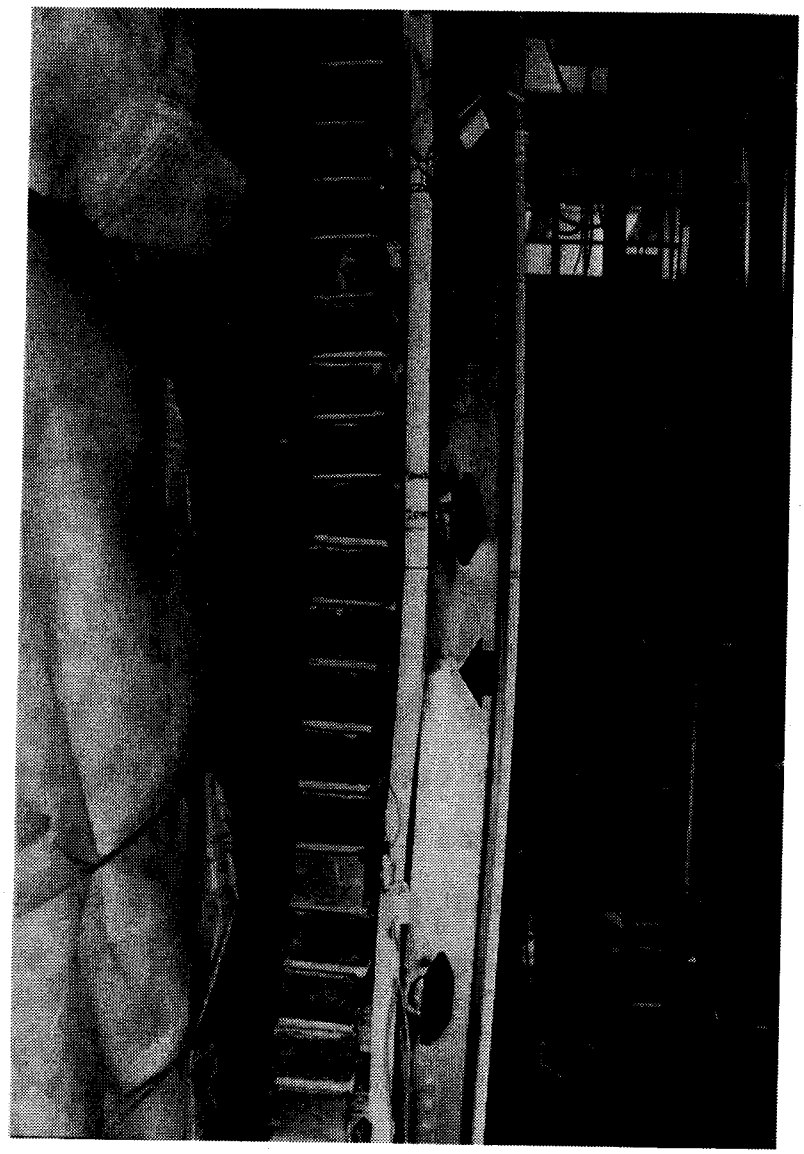

Plate 5.3 Buckling of Stud at Tie Locations (S1W1)

5.3.1.3 Specimen S1W3

Figure 5.4 shows the veneer load-deflection behaviour of Specimen S1W3. This load-deflection curve was approximately bilinear for most of the wall loading, with a significant reduction in curve slope after veneer cracking. Cracking occurred at a pressure of 1.21 kPa in the mortar joint located at an elevation of 1710 mm. The plot also shows that the two slopes of the load-deflection curve for S1W3 are greater than those for specimen S1W1 and less than those for S1W2. This indicates that Specimen S1W3 was stiffer than Specimen S1W1 and not as stiff as Specimen S1W2.

When the maximum pressure of 3.49 kPa was reached, the studs buckled flexurally. The east outer studs buckled at an elevation of 1970 mm, the west outer studs buckled at an elevation 1935 mm and the centre studs buckled at an elevation of 2100 mm. As shown in Plate 5.4, the compression flange and web of the studs buckled near, but not at, a tie connection. It appears that the compression flange of the stud has rotated away from the centre line of the stud, indicating a lateral torsional buckling of at least the sections of the stud cross-section subjected to compression.

When the wall specimen was dismantled, it was observed that the "Z" tie attachments at the upper and lower tie locations had undergone severe shear deformation, as shown in Plate 5.5. It was also observed

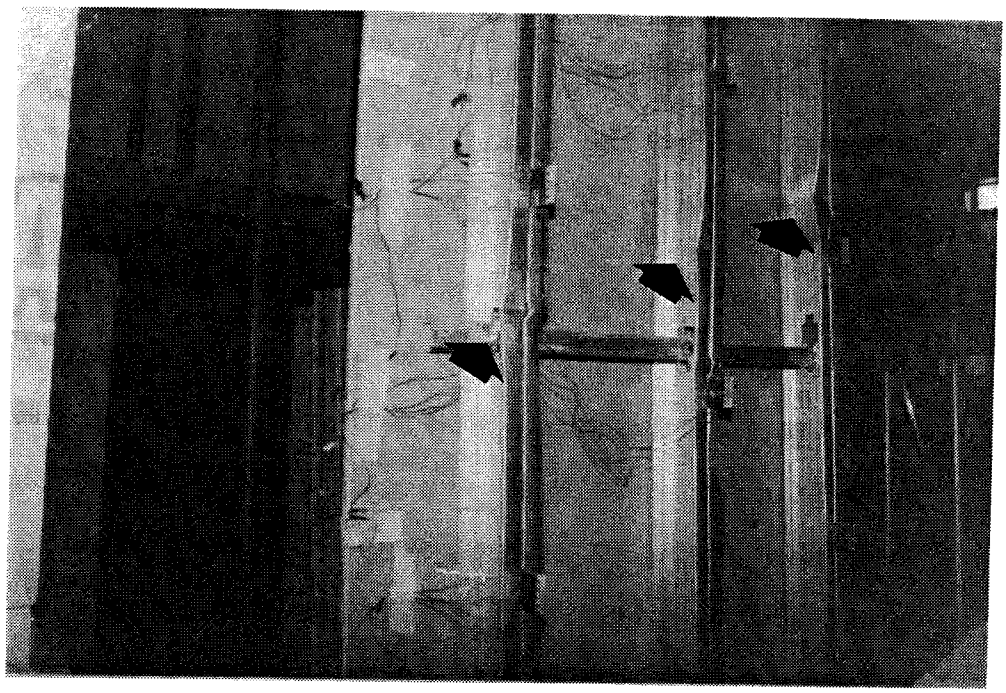

Plate 5.4 Flexural Buckling of Studs (S1W3)

Plate 5.5 Shear Deformation of Rod Tie Attachment (S1W3)

during this examination that the top of the veneer had shifted significantly to the east.

During loading, Specimen S1W3 exhibited significant deformation of the stud supports and the top edge of the veneer as shown in Figures C-5 and C-6.

5.3.1.4 Specimen S1W4

Figure 5.5 shows the veneer load-deflection behaviour of Specimen S1W4. The load-deflection behaviour of this specimen closely resembled that of Specimen S1W3. At pressures below 2/3 of the maximum specimen capacity, the veneer deflection varied bilinearly with pressure, with a change in curve slope after first cracking. Specimen S1W4 had approximately the same apparent stiffness as Specimen S1W3, both before and after cracking. The veneer of Specimen S1W4 cracked at pressures of 1.01 kPa and 2.58 kPa in mortar joints at elevations of 1330 mm and 860 mm, respectively. Specimen S1W4 withstood a higher pressure than did S1W3 before the backing studs buckled flexurally at a pressure of 4.64 kPa. All studs buckled at approximately the same elevation of 1330 mm. As with Specimen S1W3, the observed lateral movement and twisting of the compression flange of the stud suggests that the stud failure was due to lateral torsional buckling.

Plate 5.6 shows that the "V" rod tie attachments of Specimen S1W4 experienced severe shear deformation at

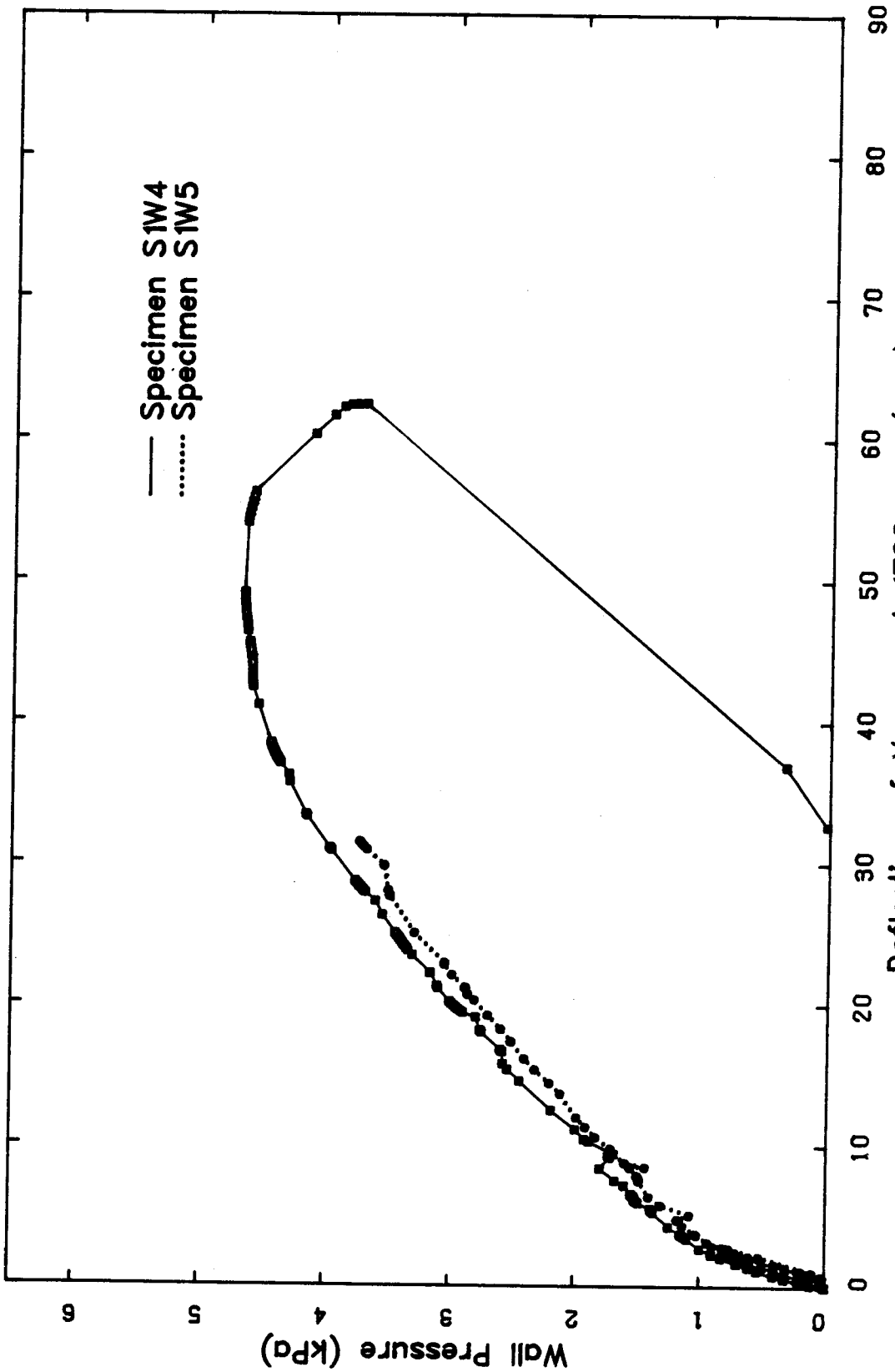

Figure 5.5 Positive Pressure Load-Deflection Curves for Specimens S1W4 and S1W5

the upper and lower tie elevations. In addition, some of the shear brackets near the crack elevation and at the top and bottom of the veneer showed signs of buckling.

The stud backing wall supports and the top of the veneer exhibited significant deformation as shown in Figures C-7 and C-8.

5.3.1.5 Specimen S1W5

Also shown in Figure 5.5 is the veneer load-deflection behaviour of Specimen S1W5. This load-deflection behaviour follows closely that of the Specimen S1W4. The first veneer crack occurred at a pressure of 1.18 kPa and the second occurred at a pressure of 1.57 kPa. These cracks were located in the mortar joints at elevations of 1475 mm and 1940 mm, respectively. Significant reduction in the slope of the load-deflection curve was only observed after the first veneer crack.

At a load of 3.74 kPa the loading air bag burst. After the air bag was repaired, this specimen was loaded to its ultimate pressure of 6.48 kPa, at which point the backing studs buckled flexurally. This buckling occurred at an elevation of approximately 1500 mm for all three studs. The shape of these buckling patterns suggests that the studs failed by a lateral torsional buckling. Only the initial loading curve of Specimen S1W5 is shown in Figure 5.5.

Plate 5.6 Shear Deformation of V Tie Attachment (S1W4)

During dismantling of the specimen, it was observed that the rod tie attachments of this specimen had undergone shear deformations similar to those of Specimen S1W3.

As with all the previous specimens, the veneer top and the top and bottom of the stud backing wall deflected significantly during the loading of Specimen S1W5 (see Figures C-9 and C-10).

5.3.1.6 Specimen S1W6

Specimen S1W6 was backed by a hollow concrete block wall and as a result exhibited significantly different load-deflection behaviour than that previously described for the stud backed specimens. Figure 5.6 shows the veneer load-deflection behaviour of this wall specimen. The veneer deflection varied linearly with pressure up to 2.50 kPa. After this pressure was exceeded, there was an approximately simultaneous cracking of the veneer and block wall, causing the wall system to "snap through" with a large increase in deflections and a large drop in load. The veneer cracked in the mortar joint located at an elevation of 2180 mm and the block backing wall cracked in mortar joints at its base and at an elevation of 2240 mm.

Because of the small shear connection provided by the flexible ties in this wall specimen, the pressure did not drop to zero but was able to maintain a value of approximately 0.7 kPa over a large deformation. The test

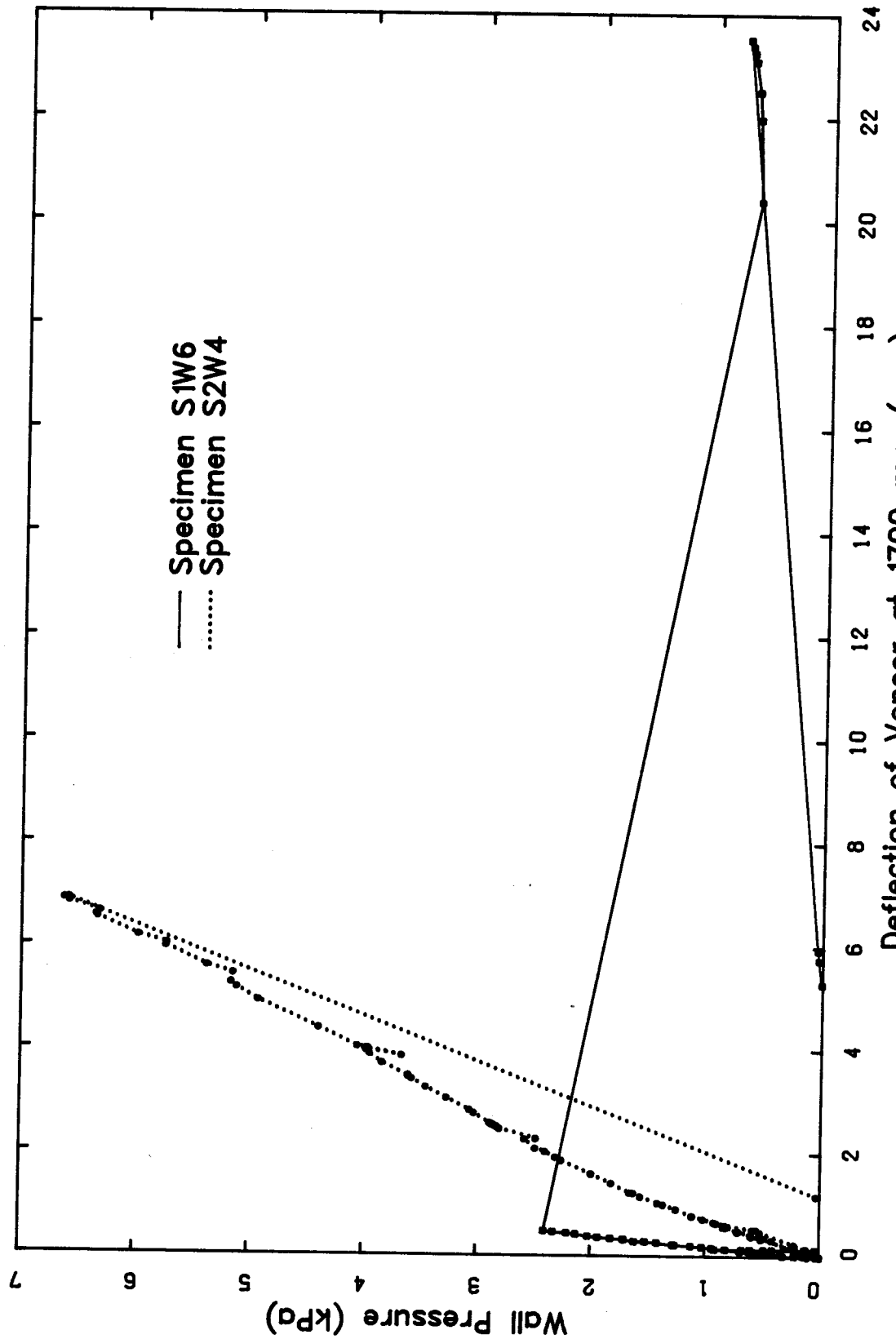

Figure 5.6 Positive Pressure Load-Deflection Curves for Specimens S1W6 and S2W4

was halted when the top of the block backing wall had rotated so that its corner began to bear against the top slab.

This block backed specimen was much stiffer than any of the stud backed specimens, but it sustained a much lower ultimate pressure. It also failed in a brittle manner, while the ultimate failure of the studs was ductile.

As shown in Figures C-11 and C-12, Specimen S1W6 deformed very little under load.

5.3.1.7 Specimen S2W4

Specimen S2W4 was designed to determine if the stiffness of a steel stud backing wall specimen could approach the stiffness the block backed wall specimen. This specimen was not tested to failure because of limited capacity of the testing apparatus.

Figure 5.6 shows the veneer load-deflection behaviour of Specimen S2W4. The load-deflection curve remained approximately bilinear over the entire pressure range. At a pressure of 1.66 kPa, the veneer cracked in the mortar joint at an elevation of 1600 mm. After veneer cracking, there was a small reduction in the slope of the load-deflection curve. An additional veneer crack occurred at 5.16 kPa in the mortar joint located at an elevation of 750 mm. No significant change in the slope of the load-deflection curve was observed after the second veneer crack. The test was stopped

arbitrarily at 6.5 kPa.

While the stiffness of this wall specimen was less than that of the block backed specimen S1W6, it was much greater than any of the other stud backed specimens. However, it is unlikely that two 150 mm, 14 gauge steel studs in a back-to-back configuration would be used because of economic considerations, and therefore the practicality of this wall system configuration is questionable.

Figures C-13 and C-14 show the deflected shapes of the veneer and the backing wall for this specimen. These plots show small deformations of the stud supports and the top of the veneer during the loading of this specimen.

5.3.2 Wall Specimens Subjected to Simulated Negative Pressure

Due to the fact that these wall specimens were subjected to point loads in a simulation of a negative pressure loading, direct comparison to identical specimens subjected to positive pressure is not possible. However, the observed load-deflection behaviour and modes of failure of each specimen gives important information on the performance of this type of wall system.

5.3.2.1 Specimen S2W1

Specimen S2W1 was identical to Specimen S1W1 but subjected to a simulated negative pressure loading. In

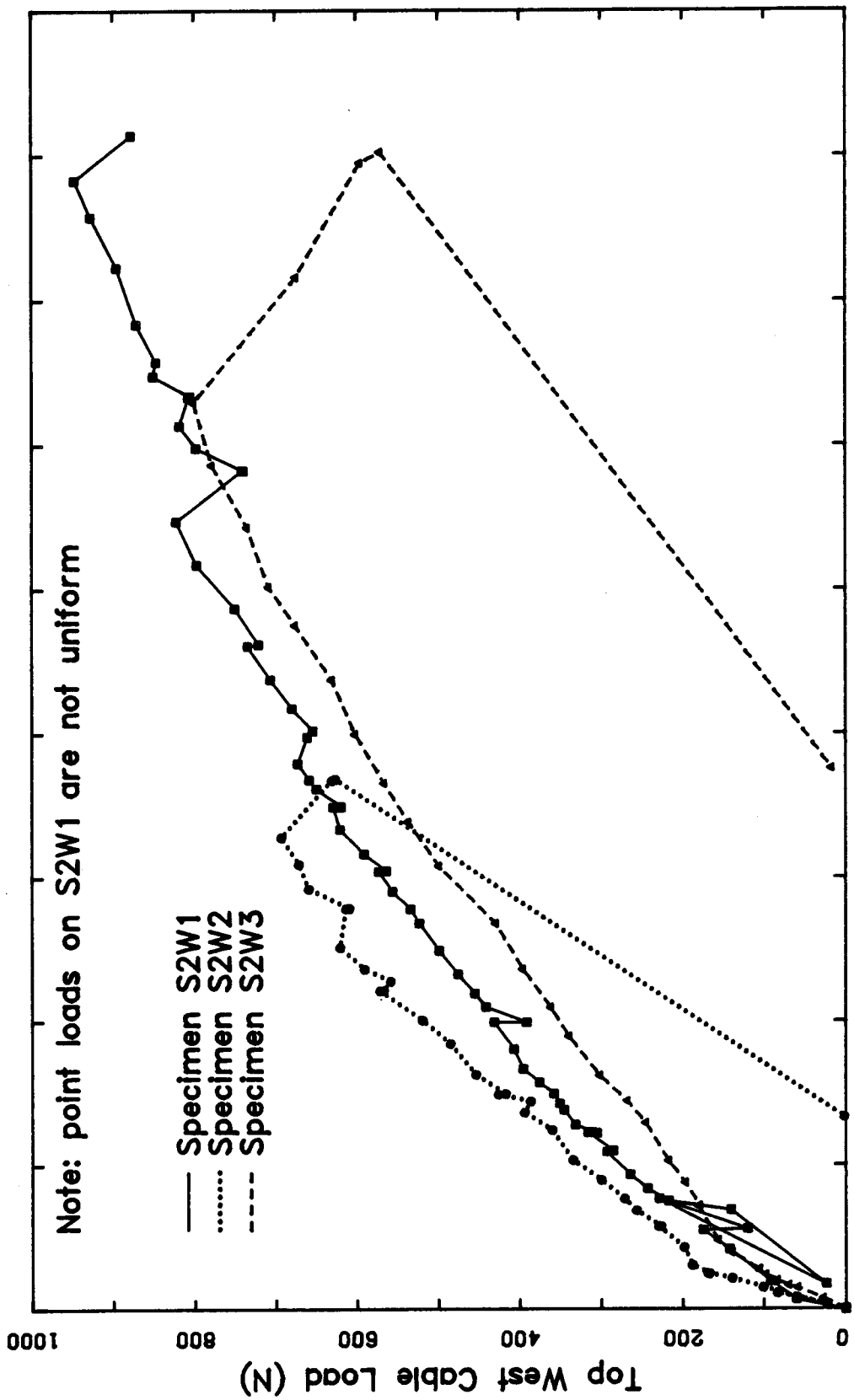

Figure 5.7 Negative "Pressure" Load-Deflection Curves for Specimens S2W1,S2W2 and S2W3

Figure 5.7, the observed veneer deflection at an elevation of 1700 mm is shown for an increasing cable load. Because of excessive pulley friction, this specimen was subjected to point loads which decreased by approximately half their value from the top to the bottom of the specimen (see Appendix B). However, even with varying point loads, the load-deflection behaviour is very similar for positive and negative loadings. The load-deflection curve was bilinear for most of the load range, with a curve slope change occurring after the first veneer crack. Cracking occurred at a cable load of 316 N, in the mortar joint located at an elevation of 1800 mm. The curve showed abrupt shifts when the screws fastening the ties to the outer studs started to pull-out. This screw pullout first occurred at a cable load of 603 N, and it took place on those ties located at an elevation 1870 mm. As shown in Plate 5.7, subsequent increases in loading caused the continued pull-out of the remaining threads of these fastening screws. The fastening screws of the ties, both immediately above and below, also showed signs of pull-out.

Final wall failure is shown in Plate 5.8. At a cable load of 941 N, the panel of veneer below the crack abruptly pulled away from the steel studs.

The plots of the deflected shapes for the veneer and backing wall for Specimen S2W1 are shown in Figures

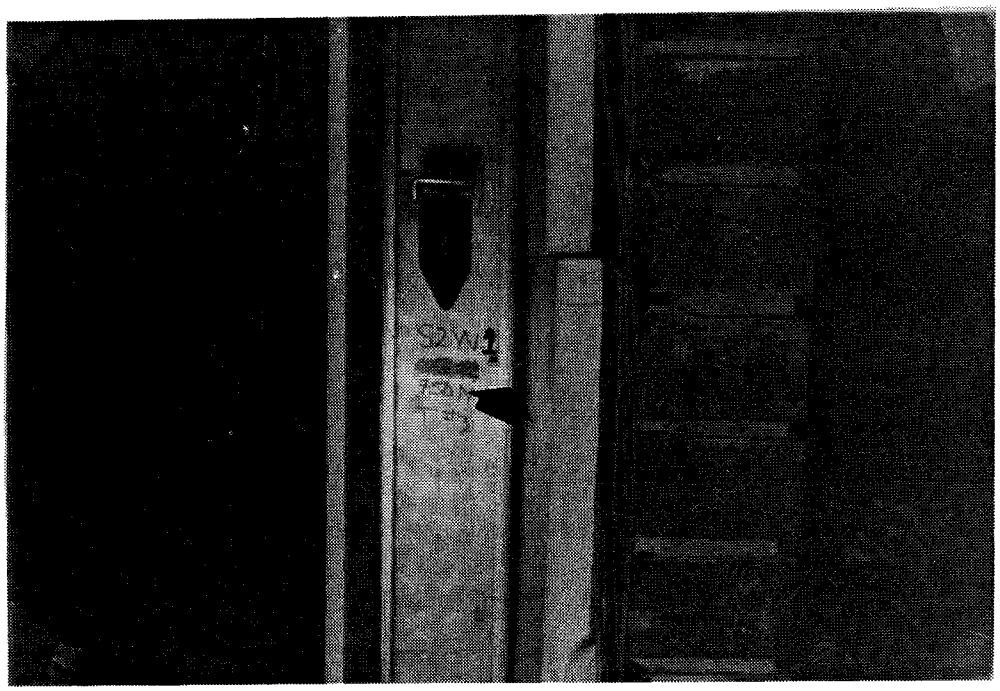

Plate 5.7 Pullout of Tie Attachment Screw Threads (S2W1)

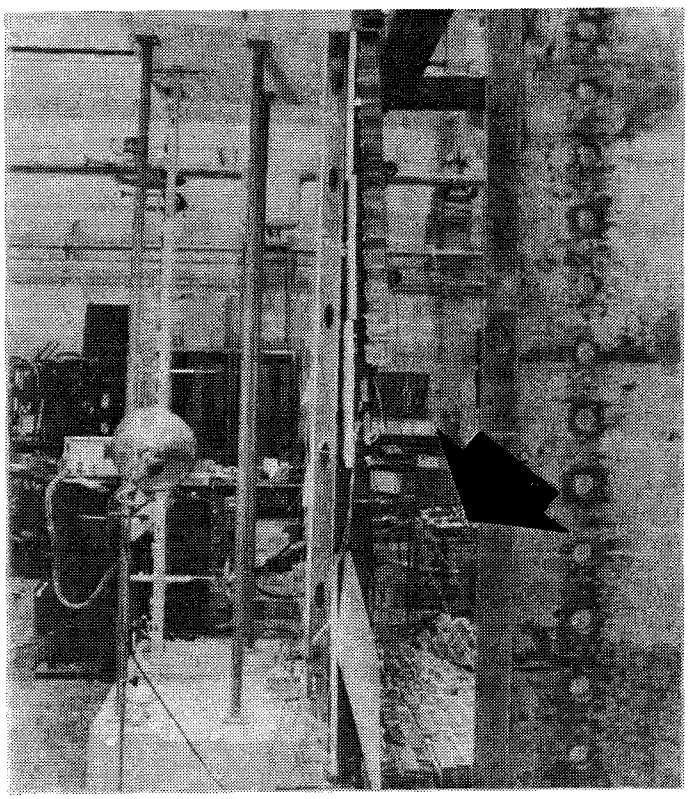

Plate 5.8 Veneer Panel Pulloff (S2W1)

C-15 and C-16. These curves show that the top of the veneer and the top and bottom of the stud backing wall deflected significantly during loading.

5.3.2.2 Specimen S2W2

Figure 5.7 also shows the veneer load-deflection behaviour of Specimen S2W2. The load-deflection behaviour of this specimen is similar to that of Specimen S2W1, even though the point loads were considerably more uniform than those applied to Specimen S2W1 because of a loading apparatus modification (see Appendix B). The load-deflection curve for this specimen was approximately bilinear for most of the loading range, with a curve slope change occurring when the veneer cracked. Cracking occurred at a cable load of 189 N in the mortar joint at an elevation of 1330 mm. The cracked mortar joint contained two anchor bolts for the pulley brackets. On both of the outer studs pull-out of the tie fastening screws started at a cable load of 426 N at an elevation of 1270 mm. Shifts in the load-deflection curve show the subsequent screw pull-out as the load was increased. The maximum cable load was 750 N and the test was stopped when the load started to decline. It was obvious that further loading would have pulled off a portion of the veneer panel.

Specimen S2W2 was stiffer but had a lower maximum load than Specimen S2W1. However, the apparent higher ultimate resistance of Specimen S2W1 may have been due,

in part, to the reduction of the point loads over the height of this specimen.

There was a substantial movement of the top of the veneer and top and bottom of the steel stud backing wall during the loading of Specimen S2W2, as shown in Figures C-17 and C-18.

5.3.2.3 Specimen S2W3

The veneer load-deflection curve of Specimen S2W3 is shown in Figure 5.7. Again, the typical pattern of stud backed veneer load-deflection behaviour is repeated. The load-deflection curve is approximately bilinear, with the change in slope occurring at veneer cracking. The veneer cracked at a cable load of 156 N in a mortar joint containing pulley anchor bolts. This mortar joint was located at an elevation of 1130 mm. At the maximum cable load of 830 N, the backing studs buckled flexurally at elevations of 1860 mm for the east studs, 1700 mm for the west studs and 1790 mm for the middle studs. The local buckling of the compression flange and web of the steel studs occurred near, but not at, tie connections. Significant lateral movement and twist of the compression flanges suggests that the studs failed by a lateral torsional buckling.

Specimen S2W3 was significantly less stiff but withstood a higher cable load than Specimen S2W2. Like Specimen S2W2, however, the top of both the veneer and backing wall and the bottom of the backing wall deformed

significantly under load (see Figures C-19 and C-20).

5.3.2.4 Specimen S2W5

Figure 5.8 shows the veneer load-deflection behaviour of Specimen S2W5. The load-deflection curve for this specimen is approximately bilinear and is very similar to that of Specimen S2W3. The first veneer crack occurred at a cable load of 199 N in the mortar joint at an elevation of 2205 mm. This mortar joint contained two pulley bracket anchor bolts. After the slope change at first veneer cracking, the load was increased to 555 N. When this load was exceeded, the veneer cracked again in the mortar joint located at an elevation of 1600 mm. No significant change in the slope of the curve was observed after this second veneer crack. All three of the backing studs buckled flexurally at the maximum cable load of 953 N at at an elevation of 1950 mm.

Figures C-21 and C-22 indicate that the supports of the stud backing wall and the top of the veneer deformed significantly during the test.

5.3.2.5 Specimen S2W6

The veneer load-deflection curve for Specimen S2W6 is also shown in Figure 5.8. Similar to positive pressure load-deflection behaviour, the "negative" load-deflection behaviour of this block backed specimen was different from that of the stud backed specimens. The veneer load-deflection curve for Specimen S2W6 was

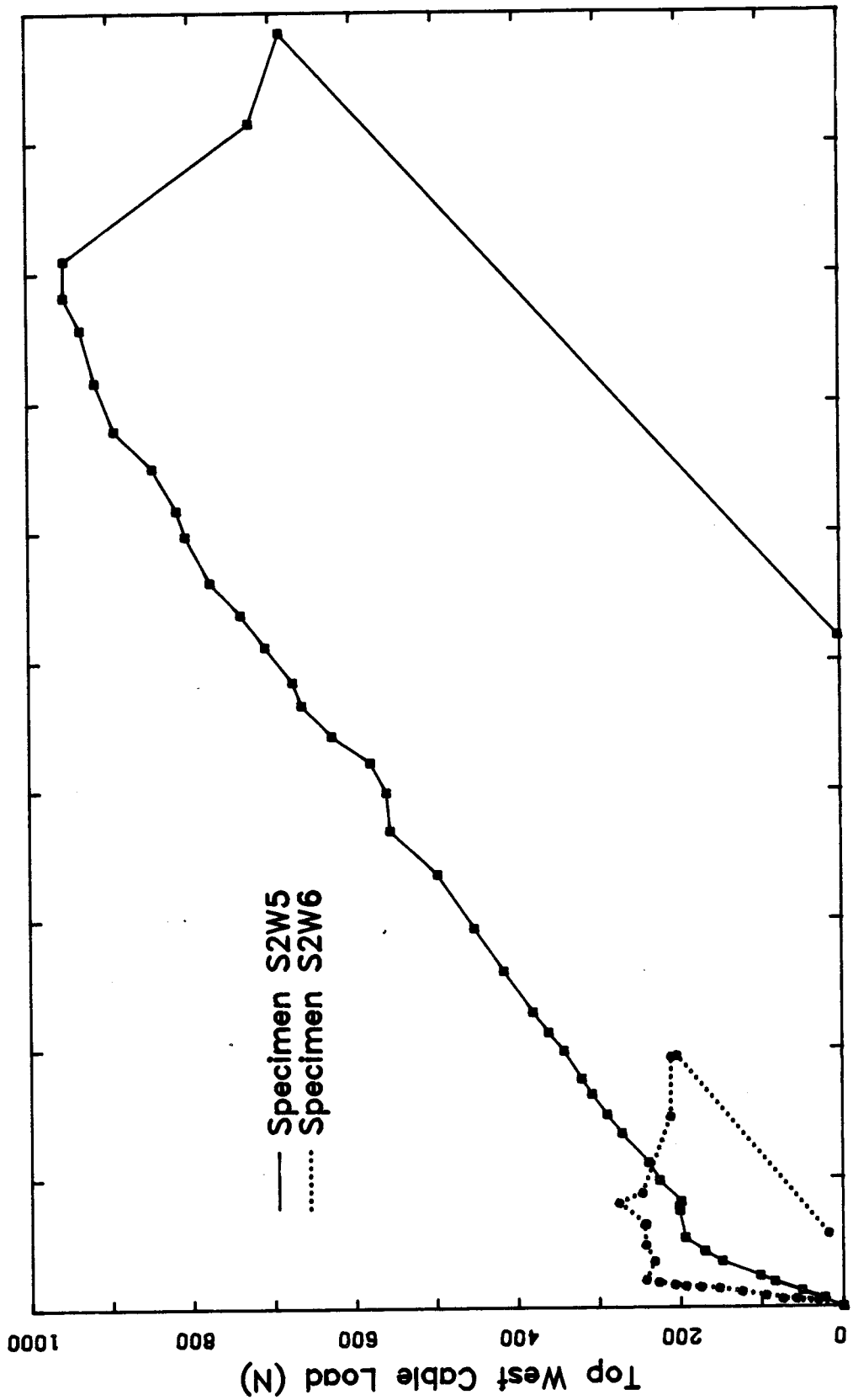

Figure 5.8 Negative "Pressure" Load-Deflection Curves for Specimens S2W5 and S2W6

linear up to a cable load of 243 N. When this load was exceeded, the block wall cracked in the mortar joint at an elevation of 1000 mm. After a large jump in the deflections, the load rose to a maximum value of 276 N before dropping off. After completion of the test, it was observed that mortar joints at an elevation of 1730 mm on the veneer and at the base of the the block wall had cracked. The small amount of shear connection provided by the flexible ties in this specimen, along with the stroke control loading of the pulley system, kept the load from dropping off abruptly, and a long portion of the unloading curve of this specimen was obtained.

Specimen S2W6 deformed very little under load, as shown in Figures C-23 and C-24. However, the top of the block wall deflected significantly under the load. By comparison, Specimen S2W6 was much stiffer but withstood a lower ultimate "negative" load than any of the stud backed specimens.

6. ANALYSIS AND DISCUSSION

6.1 Introduction

A discussion of masonry veneer wall system behaviour and an evaluation of the proposed limit states design procedures for out-of-plane loading are presented in this chapter. The first section includes analytical models developed for prediction of wind load effects. Subsequent sections evaluate the adequacy of the proposed design procedures, derive performance factors and review the relative safety margins for each primary ultimate limit state. A design example showing the application of these design procedures is presented in Appendix D.

Because the possibility exists that veneer cracking may be found to be a serviceability limit, approximate methods for the calculation of tie loads, backing wall moments and backing wall shears are developed and evaluated.

The final section of this chapter presents a discussion of the effects of partial shear connection between stud backing walls and masonry veneer.

6.2 Analytical Models

To better understand the analytical models, the out-of-plane load carrying mechanism of a masonry veneer wall system must first be evaluated. As shown in Figure 6.1, the system must support the applied wind loads over each floor height and transfer these loads to the building frame.

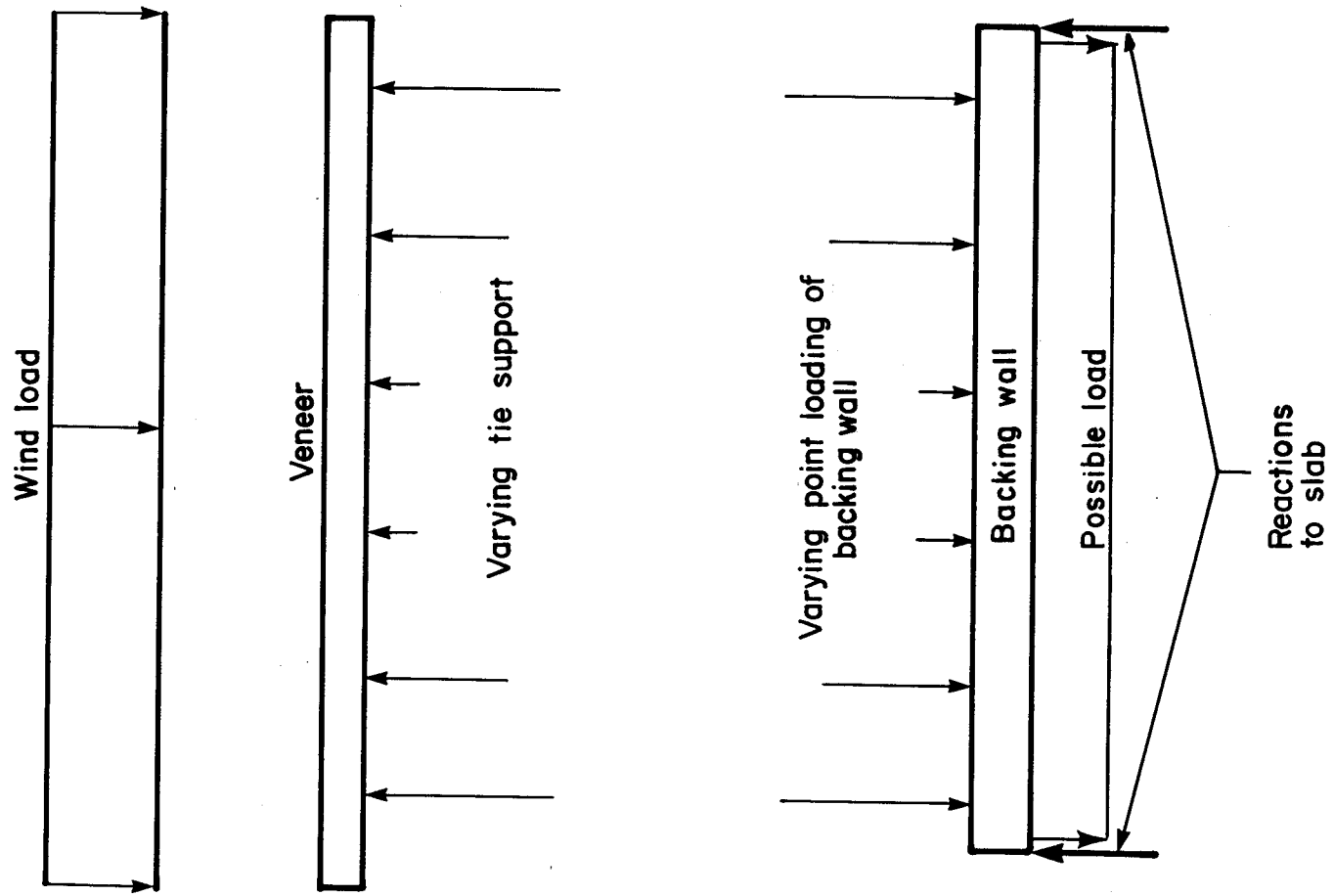

Figure 6.1 Load Carrying Mechanism of Masonry Veneer Wall Systems

Wind loads are applied to both the veneer and the backing wall. However, in most cases the majority of the load is applied to the exterior face of the veneer. The masonry veneer must therefore be able resist the applied load with support from the ties. This tie support varies according to relative deflection of the backing wall and veneer, and with the relative stiffness of the ties. The ties transfer the load to the backing wall as point loads of unequal magnitude. Finally, the backing wall spans the story height and transfers the entire wind load to the supporting slabs. Near openings and wall junctions, a portion of the wall load is transfered across the width of the wall system so that the wall system is subjected to two way bending action.

Two analytical models were used to predict deflections, moments and tie loads of uncracked masonry curtain wall systems under out-of-plane loading - a three dimensional space-frame model and a two dimensional plane-frame model. The following sections discuss and evaluate each of these models separately.

6.2.1 Three Dimensional Space-Frame Model

The three dimensional wall system model is shown in Figure 6.2. Each 400 mm width of veneer (based on a full stud spacing, centred on a stud) is assumed to act independently forming continuous vertical beam members. Horizontal veneer members span continuously between the vertical veneer members at the outer tie elevations. These

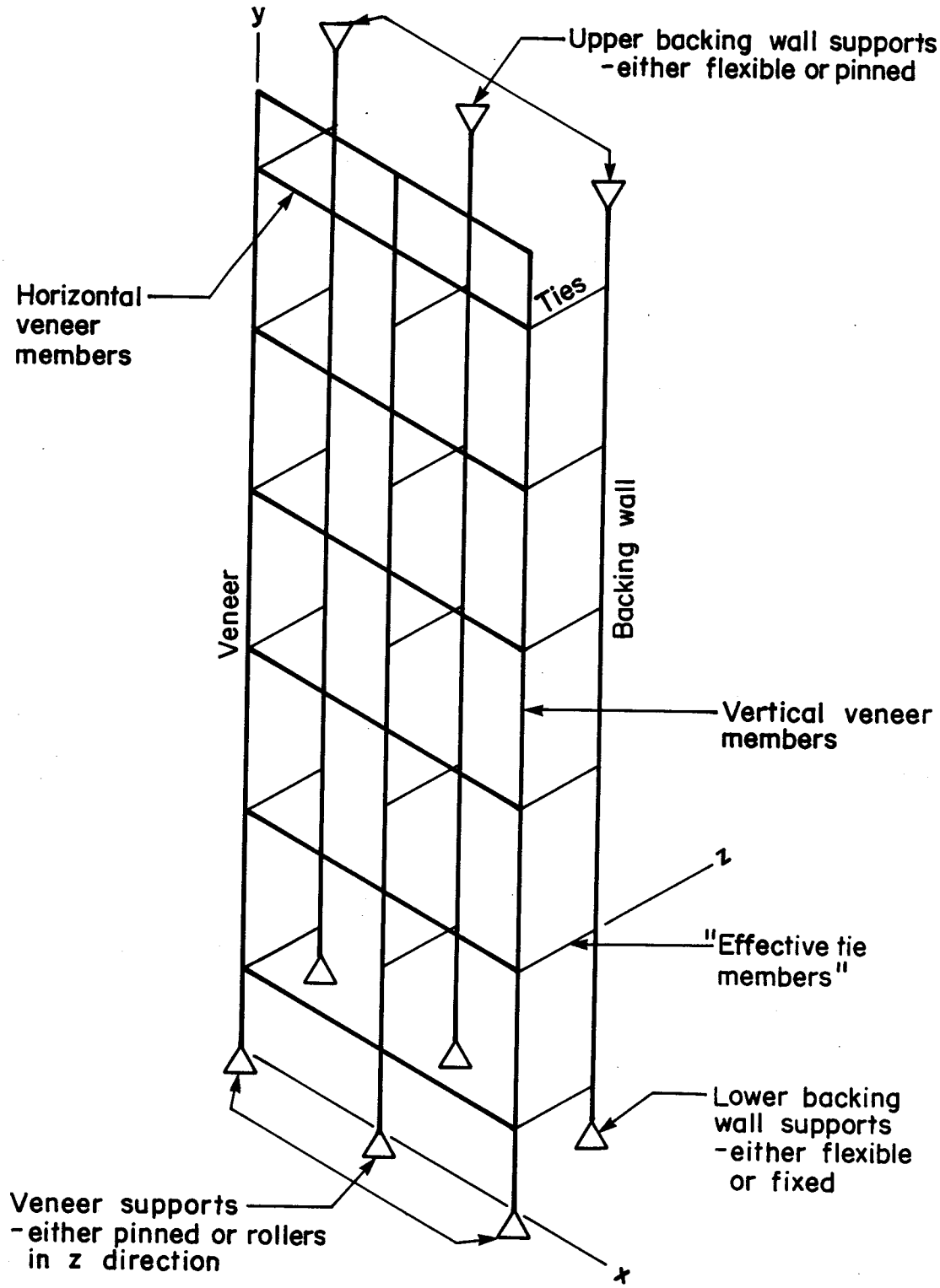

Figure 6.2 3-D Wall System Model

horizontal members have the same material properties as the vertical members and an effective width of 100 mm. For stud backing walls, the studs are modelled as continuous beam members and it was assumed that the backing wall sheathing and the ties provide sufficient twist bracing so that the studs are only subjected to bending about their strong axis. Other than for its bracing action, the backing wall sheathings are neglected. Masonry backing walls are modelled in the same manner as the veneer, with both vertical and horizontal members.

Mortar droppings in the cavity and friction between the veneer and support angle prevent out-of-plane movement of the base of the veneer under positive pressure loading. Therefore, the veneer is assumed to be pinned at its base. Under negative pressure, only the friction between the veneer and support angle restrains out-of-plane movement at the base of the veneer. Thus, at the ultimate load, the veneer base is likely to slip and this support is conservatively modelled as a roller for negative loads. For both types of loading, the top of the veneer is assumed to be free to move out-of-plane.

Masonry backing walls are modelled as fixed at the base and pinned at the top. Stud backing wall supports are flexible, however, and their load-deflection behaviour is modelled with effective track members.

Effective members are also used to model the complicated load-deflection behaviour of the various tie

systems.

6.2.1.1 Effective Members

The tie systems and the track supports of stud backing walls are modelled with effective members which are developed to approximate the load-deflection behaviour of these systems for an elastic analysis. The properties of these members are determined from testing and classical elastic beam-column theory.

Figure 6.3 shows the action of a typical flange connected tie system without sheathing and platforms. The tie system and the flange of the stud deflect as a unit. The open cross-section of the stud can be assumed to act as a cantilevered frame which deflects significantly upon loading. Factors affecting the deflection of this frame include restraint of the exterior sheathing, lateral flexibility of the ties, thickness of the stud metal, dimensions of the stud, flexiblity of the stud tie connection and distance from the tie connection to the stud web[1]. The three most important factors are the distance from the stud web, the gauge of the stud and restraint of the exterior sheathing. It is obvious that the farther the tie is connected from the web, or the thinner the stud metal, the greater the deflection of the tie system. In addition, a stiff exterior sheathing reduces the deflection of the tie system.

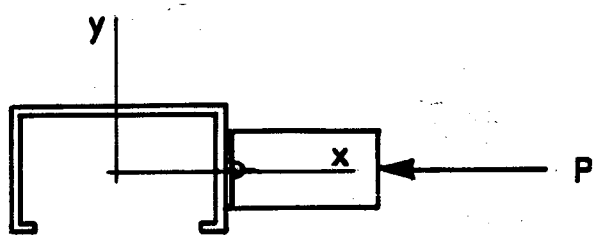

TYPICAL TIE AND STUD SYSTEM

SYSTEM MODEL

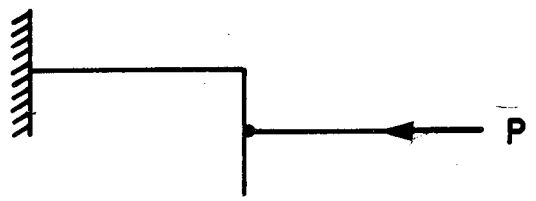

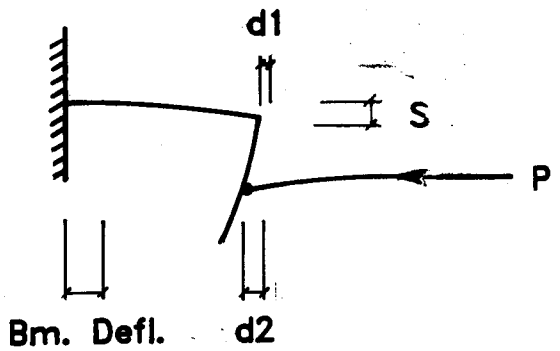

ACTION OF SYSTEM UNDER LOAD

Figure 6.3 Action of Flange Connected Ties Under Load

In the model, the tie and stud system is replaced with an effective tie member whose cross-sectional area is such that its deflection under axial load is equal to the total deflection of the tie and stud system under the same load. This "effective" area can be calculated using Equation 6.1, which is simply a rearrangement of the classic elastic formula for the deformation of a concentrically loaded axial member.

$$A_e = \frac{P\ L}{\Delta\ E} \qquad [6.1]$$

A_e is the effective area of the member, E is the modulus of elasticity, L is the assumed length of the member, and P/Δ is the average slope from the linear portion of the axial load-deflection test curve for each stud and tie system.

Because test results are used to derive the effective areas of the flange mounted tie systems, tie systems which include deformable backing platforms can be modelled with equal ease and accuracy as those which do not include backing platforms. Determining the effective area of the tie system in this manner also accounts for the effects of the different types of tie/stud connections.

Equation 6.1 approximates the load-deflection behaviour of tie systems fairly well upto the linear load limit. Beyond this limit, the approximation becomes increasingly inaccurate. However, for most of the critical wall loads, the tie loads are near the maximum

linear load of the tie, so the inaccuracy in the approximation of the tie system behaviour is small and within the variation of the slope data.

Slope variations are produced by variations in tie location, sheathing restraint, tie flexibility, and tie/stud connection flexibility. The tests on the 18 gauge corrugated tie systems were conducted on tie systems placed as close to the centre of the stud line as possible. Thus, the variation in the slope data produced by this distance variation was reduced. Average effective areas and corresponding standard deviations were calculated for this tie system, and are listed in Table 6.1.

It should be noted that in the full-sized wall specimens the placement of the tie systems followed typical field procedures and it is therefore expected that the stiffness of these ties will vary more than the component test results. Furthermore, for the tie systems subjected to tension loading the distance from the horizontal leg of the corrugated tie to the screw fastener also affects its load-deflection behaviour. As this distance becomes smaller, the stiffness of the tie system increases. However, the effective tie stiffness for the 18 ties in a full-sized wall specimen is assumed to be constant for analysis of the overall system behaviour.

Table 6.1 Material Properties of Effective Members

Member	Effect. Area (mm^2)	Effect. Stiffness (mm^2)
18C-18-90(+)	0.174 (.032)*	-----
18C-18-90(-)	0.132 (.039)*	-----
SBV(+-)	0.36 (.022)*	1500 - 4000&
SBZ(+-)	0.20 (.028)*	1500 - 4000&
Trac-16ga(+-)	0.30 (.008)*	-----
Trac-14ga(+-)	0.80&	-----
Bric-Bloc(+-)	33.1	-----

Note: 18C-18-90 - 18 gauge corrugated tie systems,
with backing platform, on 18 ga. 90 mm steel studs
SBV - shear bracket tie systems with V rod ties
SBZ - shear bracket tie systems with Z rod ties
Trac-16ga - 16 gauge 90 mm track supports
Trac-14ga - 14 gauge 150 mm tracke supports
Bric-Bloc - Brick to block ties (E=201,000 MPa)
(-) - compression loading
(+) - tension loading
* - standard deviations
& - estimated values

The effective track members are modelled in the same manner as the effective tie members. Effective area values based on an average test slope for the 16 gauge track tests are listed in Table 6.1. These effective areas vary due to variations in the distance from the stud end to the track web. Furthermore, the flexibility of the stud/track connection decreases if any axial load is applied to the stud. Friction between the stud and track web restrains the out-of-plane movement of the stud. Due to the manner in which Specimens S2W1 and S2W2 were attached to the loading frame, an axial load was applied to the stud backing walls of these specimens. Therefore, the effective area of the track members was increased to a value of 1.0 mm^2.

Because the track members are fastened at discrete points, the deformation of the tracks include the bending deflections of the track between these supports. However, these deflections are insignificant compared to the deflection of the track flanges and are ignored in the analysis.

Effective tie members are also used to model the behaviour of the shear bracket tie systems. Figure 6.4 shows the action of these tie systems under both shear loading and axial loading. The axial load-deflection behaviour of this tie system is modelled in the same manner as the flanged connected tie systems. This approximation must account for the bending deformations

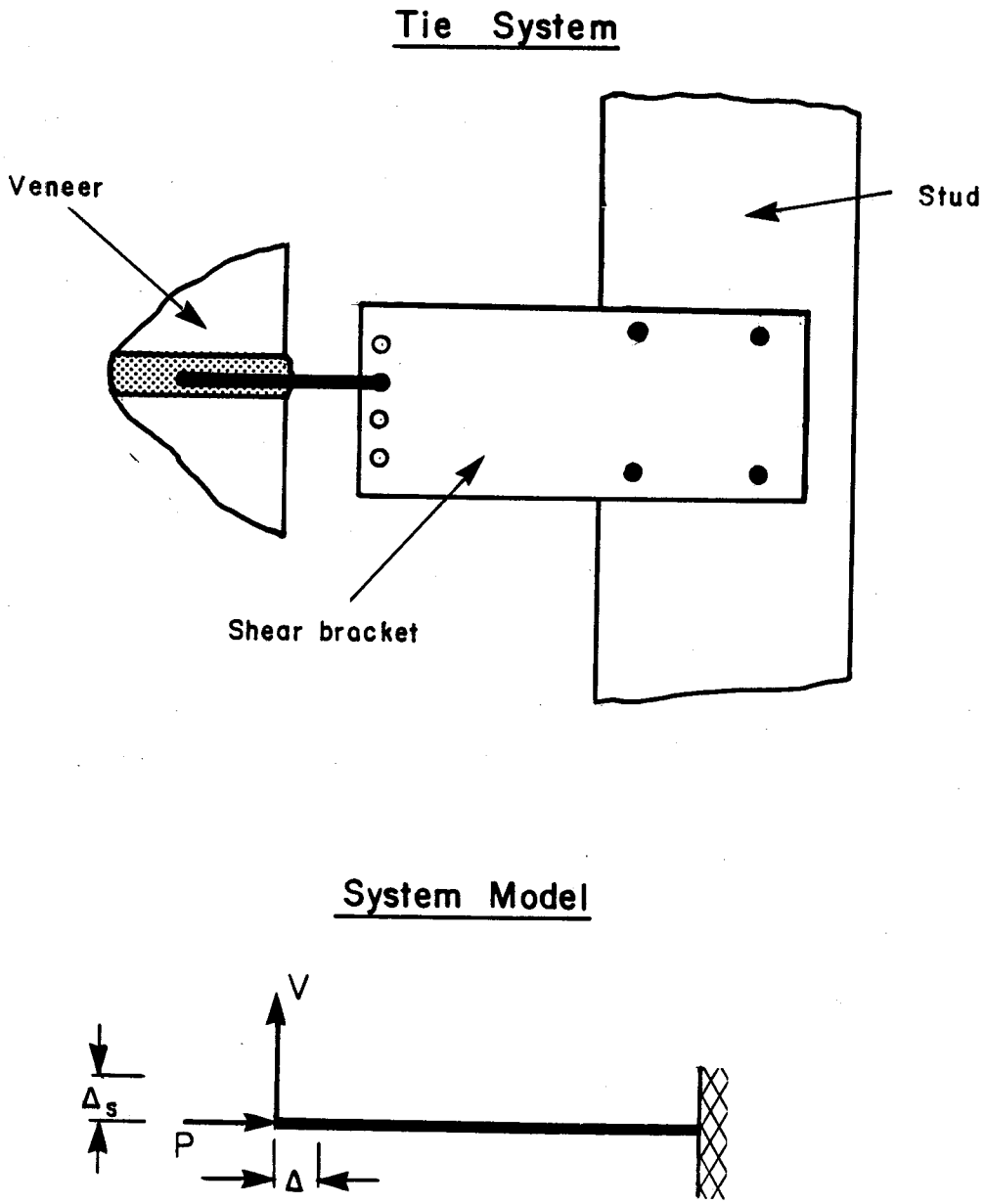

Figure 6.4 Deformations of the Shear Bracket Tie System

of the rod attachments, in addtion to the axial deformations of both the shear bracket and the rod attachments. However, as shown in Figure 5.2, there is significant play in the rod tie attachment hole. This unrestrained movement must also be accounted for in the model of the shear bracket load-deflection behaviour. The simplest way to accomplish this is to force the equation of linear approximation through zero. As outlined in Chapter 5, a linear regression analysis was used to fit a straight line through the initial linear portion of all the load-deflection curves of the shear bracket specimens. This line was forced to have a zero intercept. The resulting slopes of the axial load approximation were 938 N/mm, for the shear bracket specimens employing V tie attachments and 523 N/mm, for the shear bracket specimens employing Z tie attachments. The standard deviations of these slopes were 58 N/mm and 72 N/mm, respectively. Effective areas corresponding to these slopes are listed in Table 6.1.

The deformation of the shear bracket tie system, under the loads induced by the partial shear connection, must also be approximated. If the vertical movement of the interior face of the veneer is used as a reference deflection, the deformation of the shear bracket tie system is comprised of bending deformation of the rod tie, bending of the shear bracket, slip at the bracket/stud connection and play in the rod tie

attachment hole. "Shear" load-deflection tests, performed only on the shear brackets, show that slip of the bracket/stud connection occurs only after significant shear load is applied to the bracket. Until this load threshold is exceeded, the data shows that the bracket acts as if fully fixed to the stud. The results of these tests also show that the effective location of the fixed support of the shear brackets moves from 30 mm off the stud centre to the exterior face of the stud flange.

If the tie system is considered a cantilevered beam loaded by a point load at its end, then classic elastic beam theory gives the deflection at the end of the tie system as:

$$\Delta_s = \frac{V L^3}{3 E I} \qquad [6.2]$$

where V is the point load, L is the length of the tie system, I is the moment of inertia of the tie system and E is its modulus of elasticity.

Using Equation 6.2, a moment of inertia of the effective shear bracket tie member is calculated in the following manner:

1. Both the rod tie and the bracket are assumed to act as cantilevered beams, joined by a hinge.
2. The dimensions of the rod tie and bracket, shown in Figure 4.2, are used to calculate moments of inertia for each of these members. The modulus of elasticity (E) of both members is assumed to be 210,000 MPa.

3. The veneer end of the rod tie is given a unit deflection in the vertical direction (δ_s) and the vertical reaction load at this location is calculated.
4. This vertical load is then applied to the end of a 80 mm long cantilevered beam and the moment of inertia required to produce a unit deflection at the end of the beam is determined, assuming E is 210,000 MPa. This moment of inertia is taken as the moment of inertia of the effective shear bracket tie member.

The length of the rod tie and the bracket have a significant effect on the value of the moment of inertia of the effective tie member. Varying the lengths of these components from the values shown in Figure 4.2, produces "effective" moments of inertia that range from 0.500×10^3 mm^4 to 200×10^3 mm^4. It should be noted that these values can be significantly reduced by the play in the rod attachment hole.

Within the wall specimens, the variation in the lengths of the tie system and play in the rod tie attachment hole result in a variable effective stiffness of the shear bracket tie systems. Furthermore, the axial load is applied eccentrically to the axis of the shear bracket, producing an additional moment at the bracket/stud connection. This moment can either reduce or increase the shear load at which this connection will

slip. If moment produced by the shear force and moment produced by the eccentricity of the axial load are in the same direction, the slip load decreases. Thus, the stiffness of any one connection in the wall system is impossible to predict with any accuracy. However, for the 18 ties in each wall specimen, it is assumed that the effective shear connection can be approximated by a constant value. It was assumed that the value of this constant moment of inertia was within the range of 1.5 x 10^3 mm^4 to 4.0 x 10^3 mm^4.

The connections of the effective members to the backing wall and veneer depend on the nature of the actual connections used. All the effective corrugated tie members are assumed be fixed to the veneer and pinned to the stud backing. The effective members of the shear bracket tie systems are assumed to be pinned at the veneer and fixed at the stud backing.

The tie systems used in the masonry backed wall specimens are assumed to have a fully effective cross-sectional area. The supports of these members are assumed to be fixed at both the veneer and the backing wall.

6.2.2 Evaluation of 3-D Model

A three dimensional direct stiffness frame analysis program is used to analyze each of the twelve full-sized wall specimens tested in this investigation. This analysis

method was chosen over the more "elegant" Finite Element Method because there is essentially no difference between a direct stiffness analysis and a linear-elastic Finite Element analysis using beam elements. Furthermore, most consulting engineers are more familiar with the direct stiffness method and are more likely to possess a direct stiffness frame analysis program.

To accurately predict the behaviour of the masonry veneer wall systems, appropriate values of the material properties and dimensions of each wall system component must be chosen. The measured dimensions of both the veneer and the backing wall are used for the analysis. For each specimen, the elastic modulus of the veneer is obtained from prism tests (see Appendix A) and it is assumed that the elastic modulus of all the steel components is 210,000 MPa.

For the analysis of the overall behaviour of the wall system, it is assumed that the stiffnesses of the effective members can be approximated by constant values. The area of the effective members is assumed to be near the average effective areas calculated from the component load-deflection tests. However, the magnitude of the effective area does not appear have a signficant effect on the accuracy of the predicted system behaviour when the effective area is chosen within 50 % of the average component test value'. The values for the effective moments of the shear bracket tie systems are assumed to fall within the range of values defined previously. It should be noted

that the stiffness of the shear bracket tie systems can significantly affect the behaviour of the wall system. However, reasonable estimates of the wall system behaviour are obtained using values in the specified range. Listed in Table 6.2 are the material properties used for the analysis of each wall specimen.

The positive pressure loading is applied as a uniformly distributed load over the entire length of the vertical veneer members. This uniform load was calculated based on a uniformly distributed pressure and a tributary width of 400 mm. In the tests, the simulated negative pressure loading was applied as point loads, located halfway between each stud line on the stud backed specimens, and at this same spacing for the testing of the block backed specimen (see Appendix B). For the analysis of these specimens the negative loads are applied as point loads. The elevations of the horizontal veneer members are adjusted so that they were at the same elevation as the point loads, and these loads are assumed to act at the midpoint of each of the horizontal members. The magnitudes of the point loads varied due to friction in the pulley systems. Based on the friction tests performed on the pulley systems, normalized point loads for the three different pulley arrangements are calculated. Figures 6.5, 6.6 and 6.7 show the average normalized loads of each loading configuration for a given cable load.

Table 6.2 Measured and Estimated Material Properties

Specimen	Is (mm^4)	As (mm^2)	Em (MPa)	Ate (mm^2)	Atr (mm^2)	Ibr (mm^4)
S1W1	301,000	241.5	9947	0.17	0.30	----
S1W2	301,000	241.5	10076	0.20	0.30	----
S1W3	404,000	311.0	10471	0.20	0.30	4000
S1W4	301,000	241.5	8853	0.36	0.40	2500
S1W5	301,000	241.5	7583	0.36	0.40	1500
S1W6	155,000,000	24000.	11364	30.0	----	----
S2W1	301,000	241.5	7016	0.20	1.00	----
S2W2	301,000	241.5	8861	0.13	1.00	----
S2W3	404,000	311.0	8435	0.20	0.30	2500
S2W4	3,220,000	1023.	6323	0.50	0.80	3000
S2W5	301,000	241.5	9947	0.40	0.30	4000
S2W6	155,000,000	24000.	10471	30.0	----	----

Note:
1. The elastic modulus of the steel studs was taken as 210,000 MPa.
2. The elastic modulus of the concrete block taken as 10,000 MPa (750 f'm).
3. The net area of the veneer is 8200 mm^2 and has a I of 1.56×10^7 mm^4.
4. (Is) is the measured moment of inertia of the backing wall and (As) is its measured area.
5. (Ate) is the estimated effective area of tie systems.
6. (Atr) is the estimated effective area of the track supports.
7. (Ibr) is the estimated effective stiffness of the shear bracket tie systems.

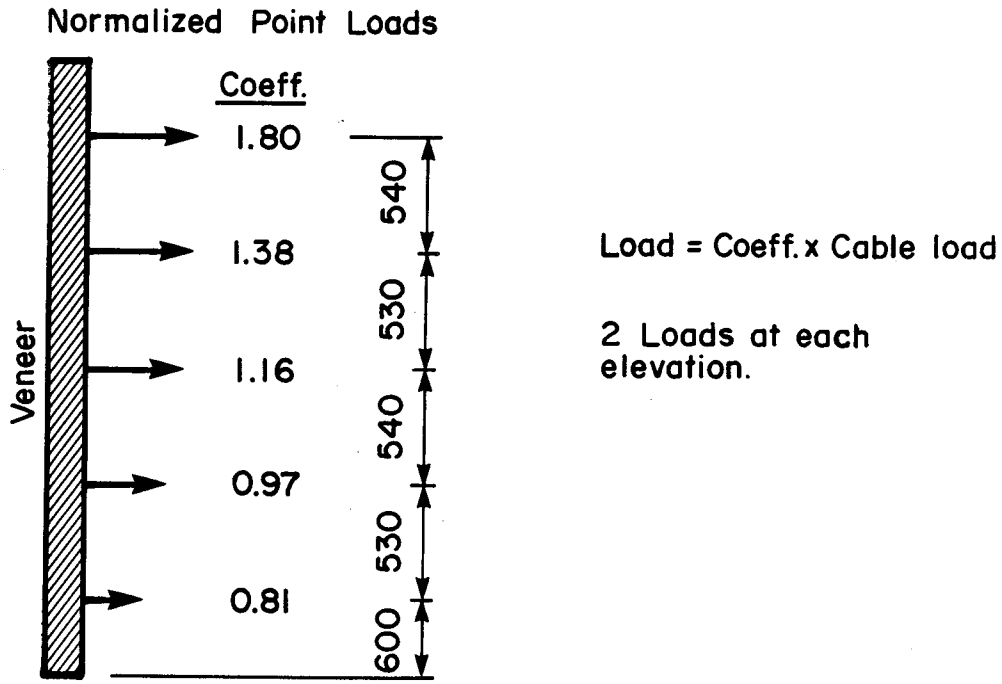

Figure 6.5 Normalized Average Point Loads on Specimen S2W1

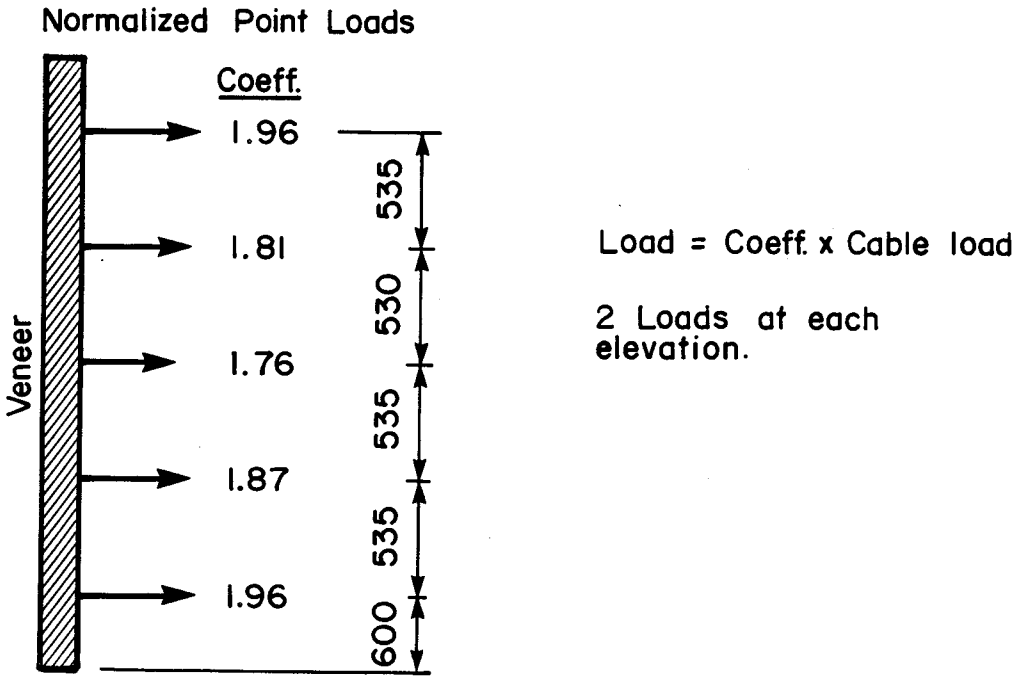

Figure 6.6 Normalized Average Point Loads on Specimen S2W2

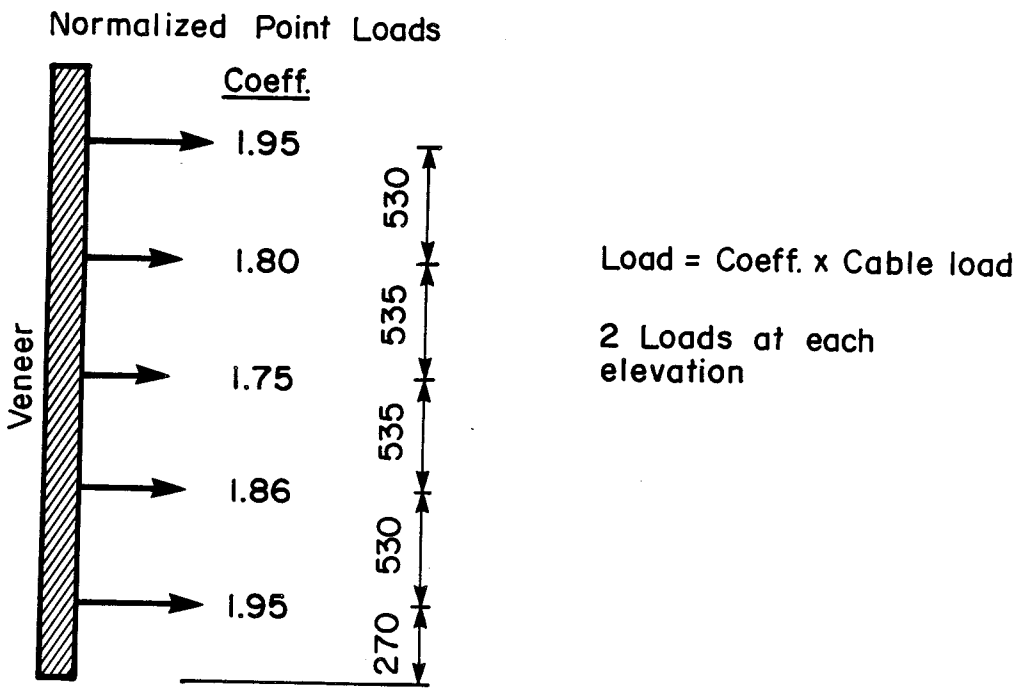

Figure 6.7 Normalized Average Point Loads on Specimens S2W3, S2W5 and S2W6

6.2.2.1 A Comparison of Deflected Shapes - Measured to Predicted

Figures 6.8 and 6.9 show the veneer and backing wall deflected shapes for Specimen S1W1 under a positive pressure load of 0.50 kPa. These figures show good agreement between the predicted and measured deflected shapes. Figures 6.10 and 6.11 show similar agreement between the predicted and measured deflections of the veneer and stud backing wall of Specimen S1W4 under a positive 1.00 kPa load.

Predicted and measured veneer deflected shapes are shown in Appendix C for the remaining ten wall specimens (Figures C-25 to C-35). In all cases the agreement is good, with the exception of the block backed specimen under negative load. During this test the support of the block wall settled significantly, causing the block wall to crack prematurely at its base. There were also indications that the deflection measuring devices shifted during loading as positive deflections were measured whereas none were possible.

6.2.2.2 A Comparison of Tie Loads - Measured to Predicted

Figures 6.12, 6.13, 6.14 and 6.15 show a comparison of predicted and measured tie loads for Specimens S1W1 and S1W4. Although the general shape of the tie load patterns agree, the measured magnitudes vary and are, on the whole, larger than expected. Similiar agreement was

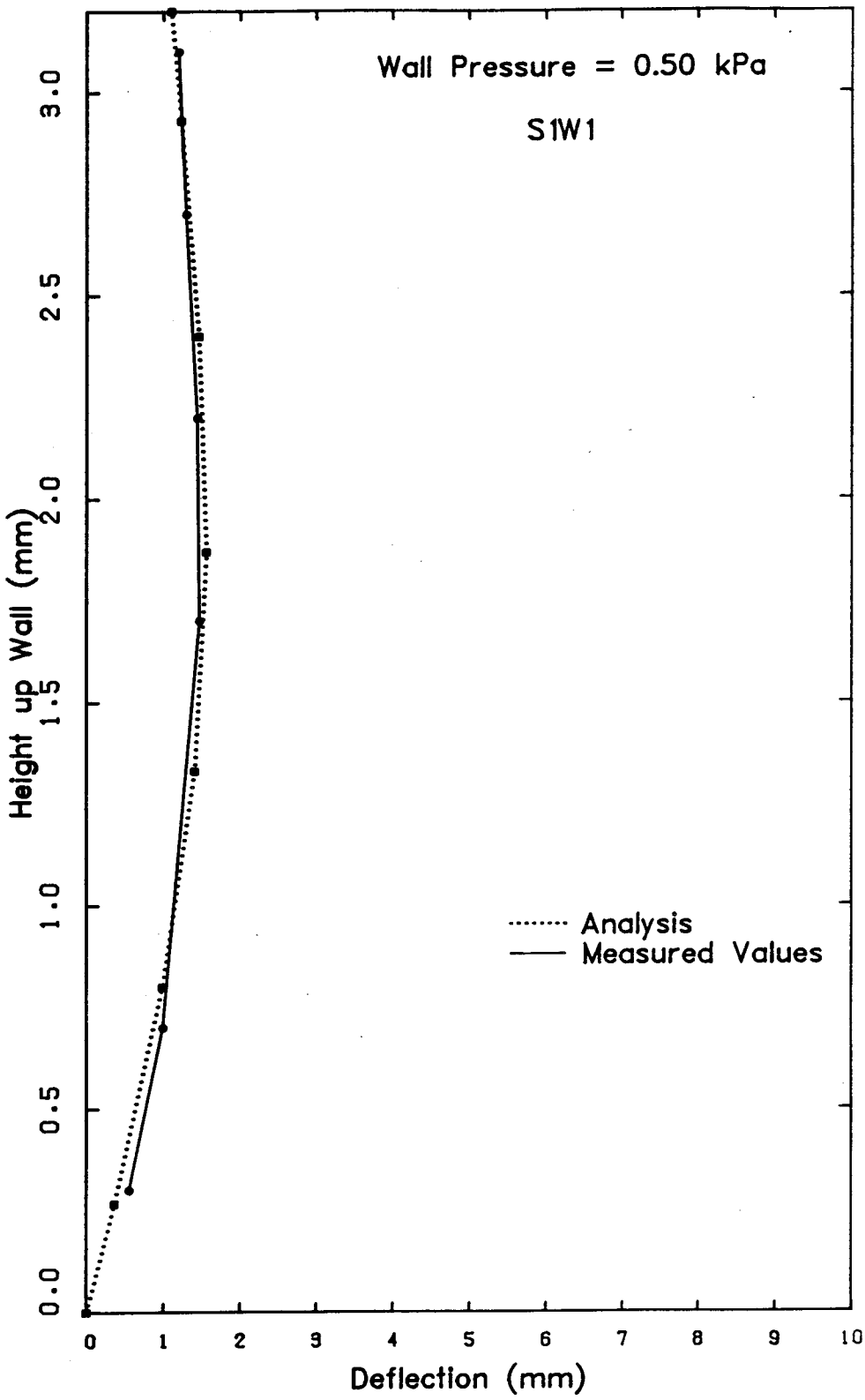

Figure 6.8 Veneer Deflection for Specimen S1W1 - Measured and Predicted

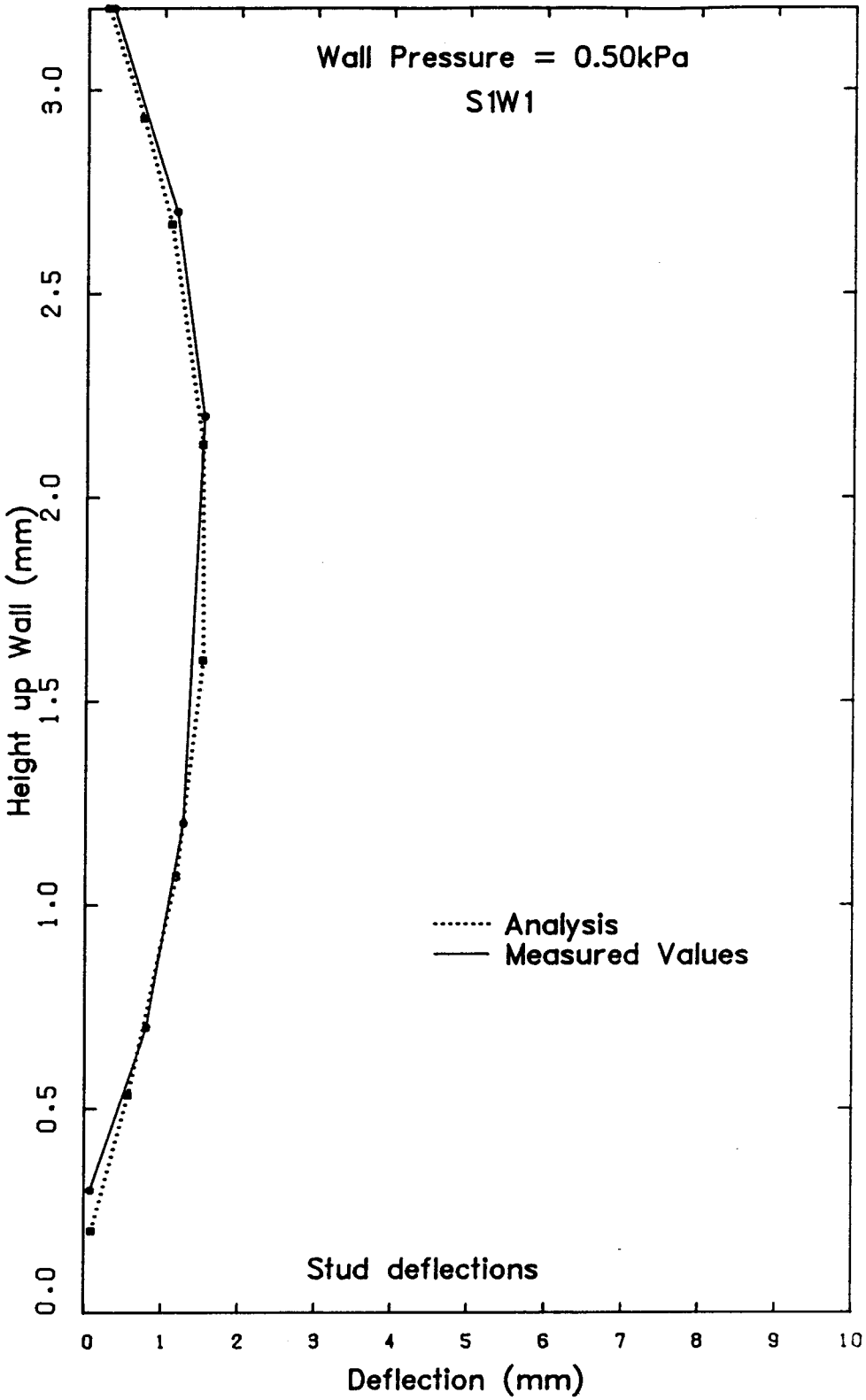

Figure 6.9 Stud Backing Wall Deflection for Specimen S1W1 - Measured and Predicted

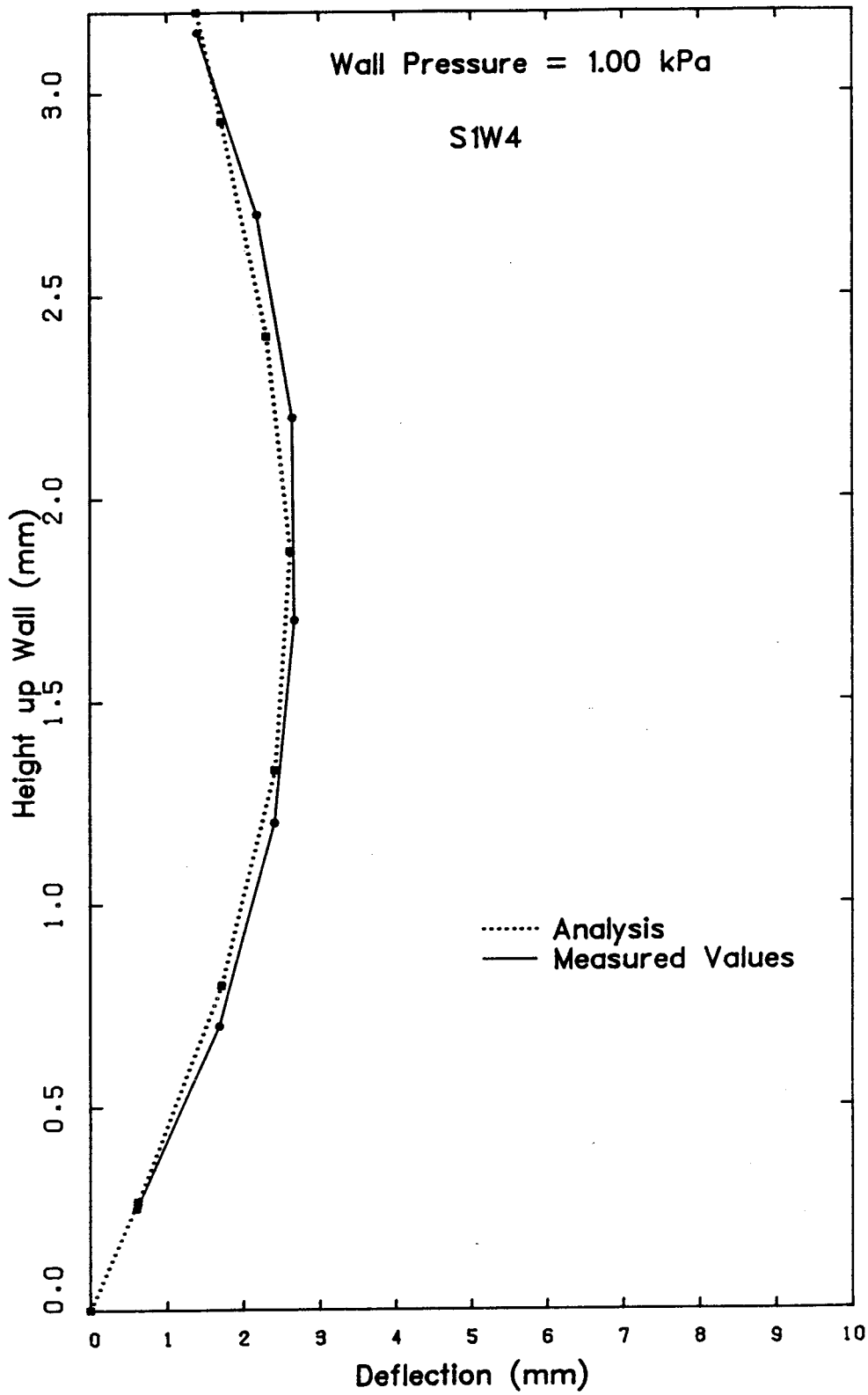

Figure 6.10 Veneer Deflection for Specimen S1W4 - Measured and Predicted

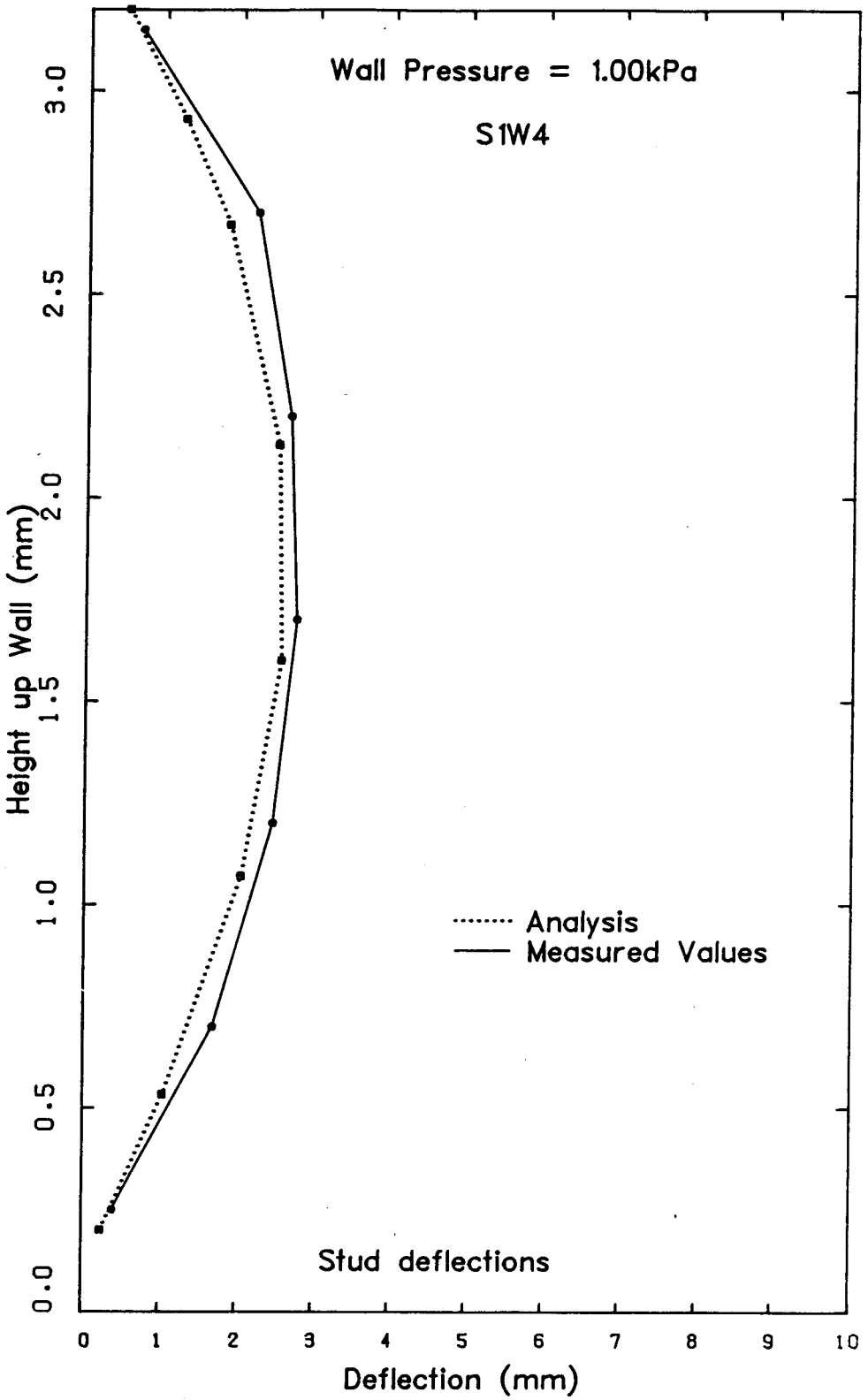

Figure 6.11 Stud Backing Wall Deflection for Specimen S1W4 - Measured and Predicted

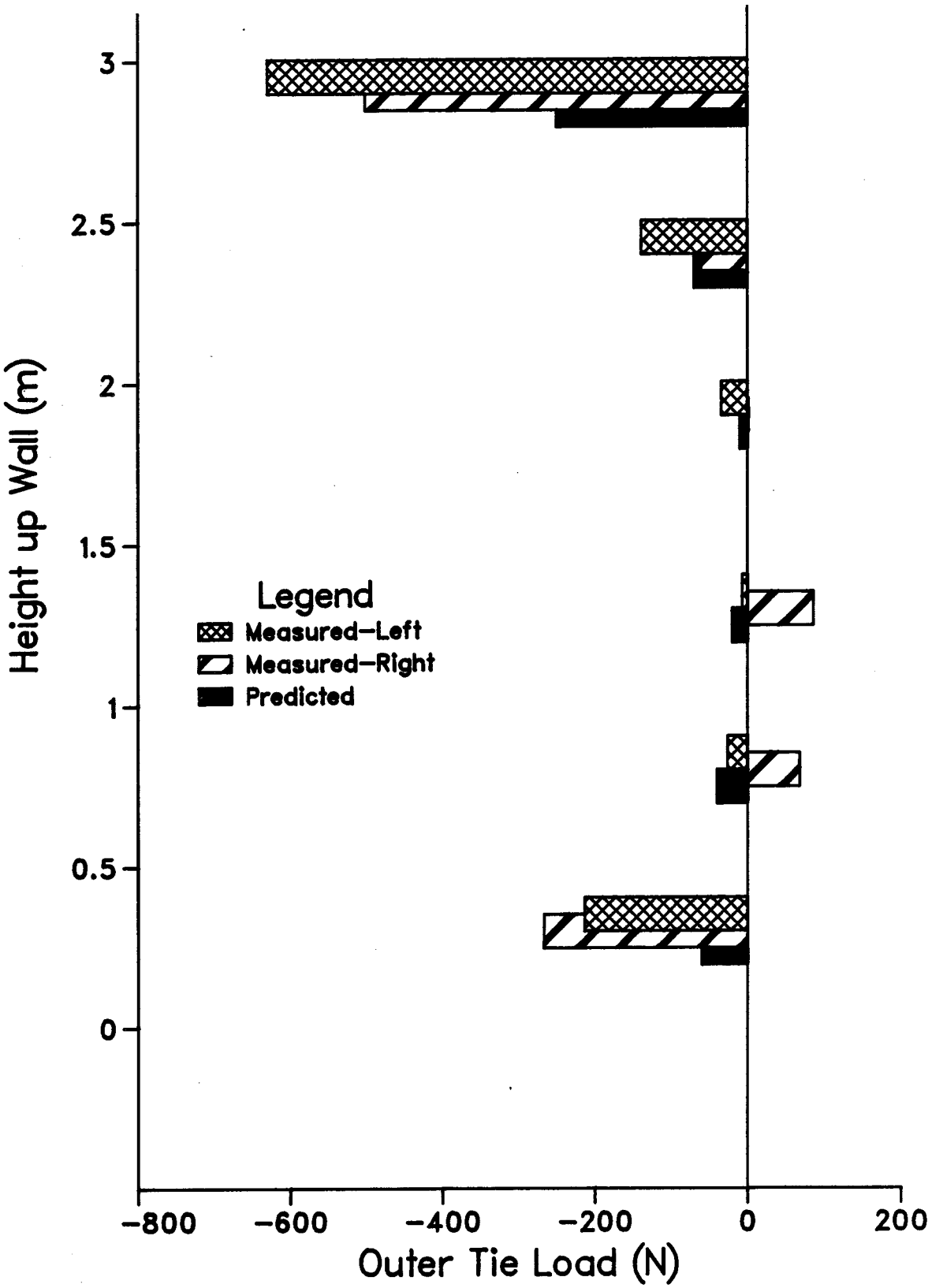

Figure 6.12 Outer Tie loads for Specimen S1W1 - Measured and Predicted

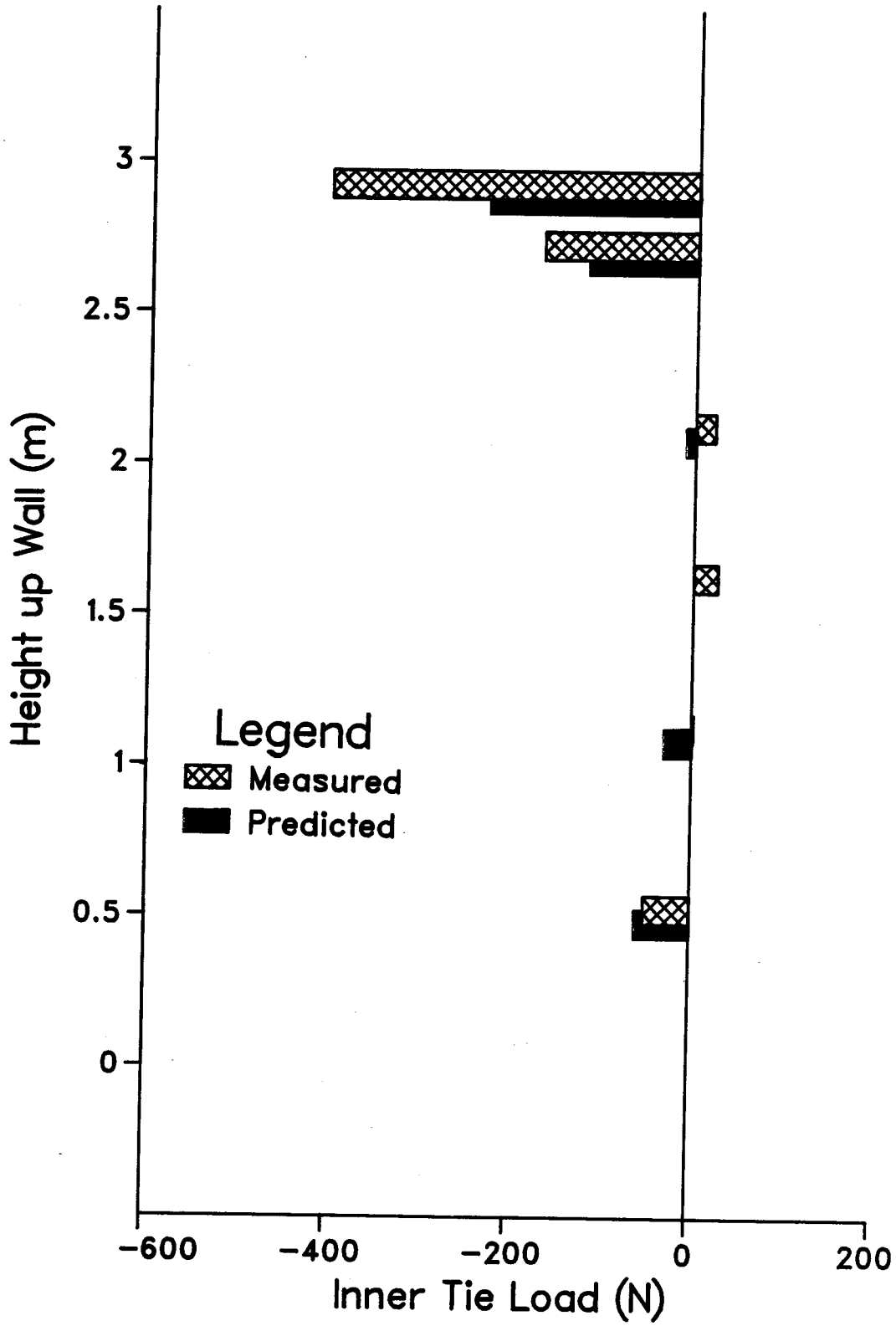

Figure 6.13 Inner Tie loads for Specimen S1W1 - Measured and Predicted

observed for the other ten wall specimens, for both positive pressure and "negative pressure" loading.

Some of the differences between the measured and the predicted tie loads are due to the variation in the relative tie system stiffnesses over the height and width of the wall specimen. In this highly redundant wall system a tie which is stiffer than those adjacent will attract a greater amount of the veneer load.

However, this variation in tie stiffness does not account for all the discrepancies between the predicted and measured tie loads. The moment produced by the measured tie loads about the base of the veneer was calculated and compared to the moment produced by the applied uniform load about the same point. The applied load produced moments that were up to 57 % (S1W1) smaller than moments produced by the measured tie loads. The measured tie loads do not statisfy statics. In general, the method of measuring these tie loads overestimates the actual tie loading.

Load calibration of the tie systems was performed and the results are shown in Appendix B. The linear load-strain calibration of the 18 corrugated tie systems showed a standard deviation of 33 % for loads below 1.0 kN. A linear load-strain calibration performed on the shear bracket tie systems showed a standard deviation of 15 % for loads below 1.2 kN. These relatively large standard deviations account for part of the large

differences between the predicted and measured tie loads. Tie load measurement inaccuracies could be caused by the following reasons:

1. In the thin tie metal, any small differences in placement of the strain gauges can result in an incorrect measurement of the axial strains. This is particularly significant in the presence of a large moment gradient.
2. The ties are subjected to substantial flexural stresses which can force the measured strains beyond the proportional limit of the tie metal even at low axial loads.
3. Because of space limitations, the strain gauges were placed near enough to the rod tie attachment holes and the tie corrugations to be subjected to stress concentration effects.

Although there is not close agreement between the measured and predicted tie loads, a large portion of this difference can be explained by inaccuracies in measurement. Furthermore, it is suggested that the inaccuracies in tie load prediction caused by variations in the relative stiffnesses of the tie systems may not be critical in the design of the wall system. Because the load-deflection behaviour becomes nonlinear at higher load levels, heavily loaded ties will become significantly less stiff. Thus, as the wall systems approach their failure load it is likely that the

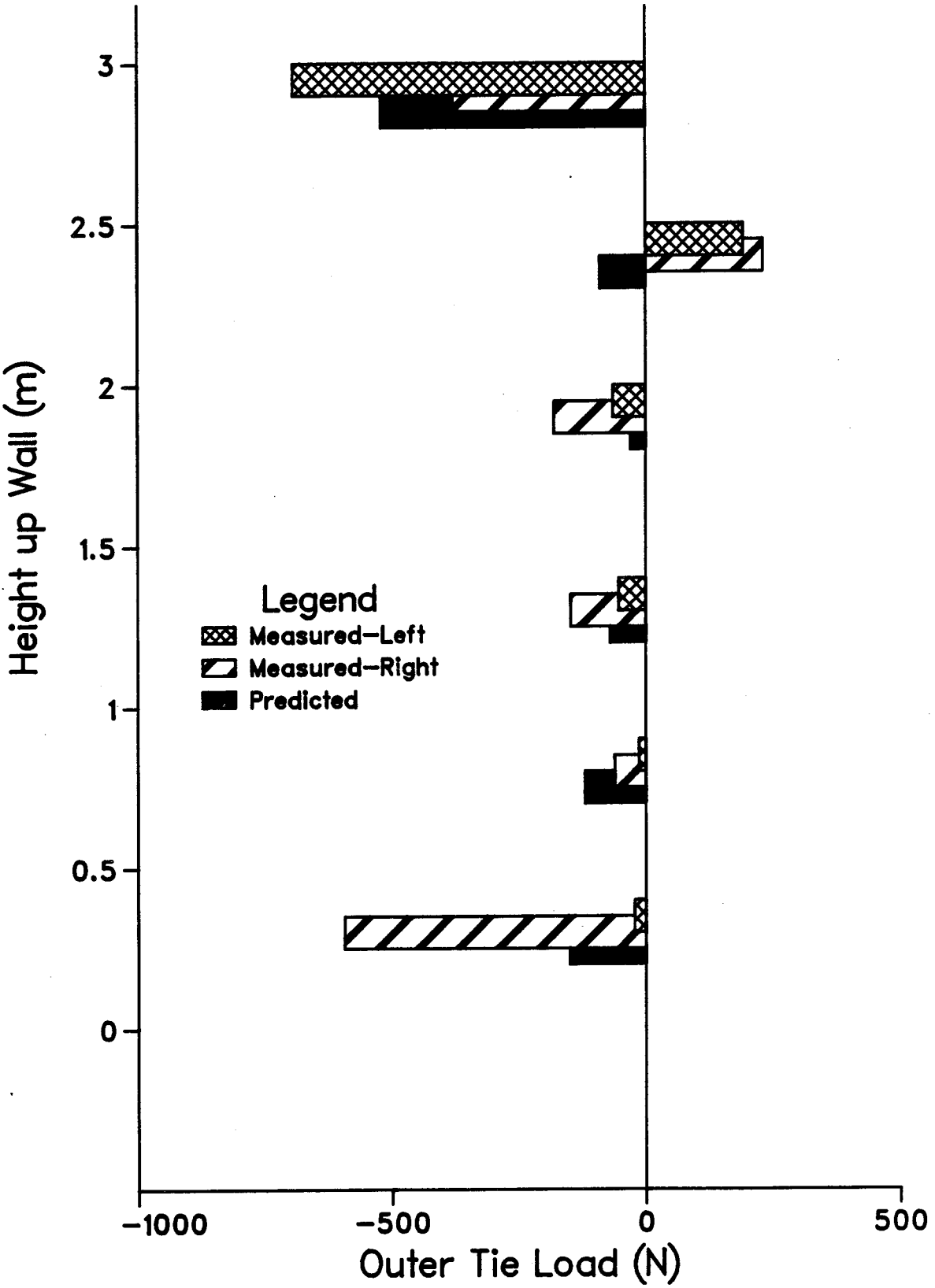

Figure 6.14 Outer Tie loads for Specimen S1W4 - Measured and Predicted

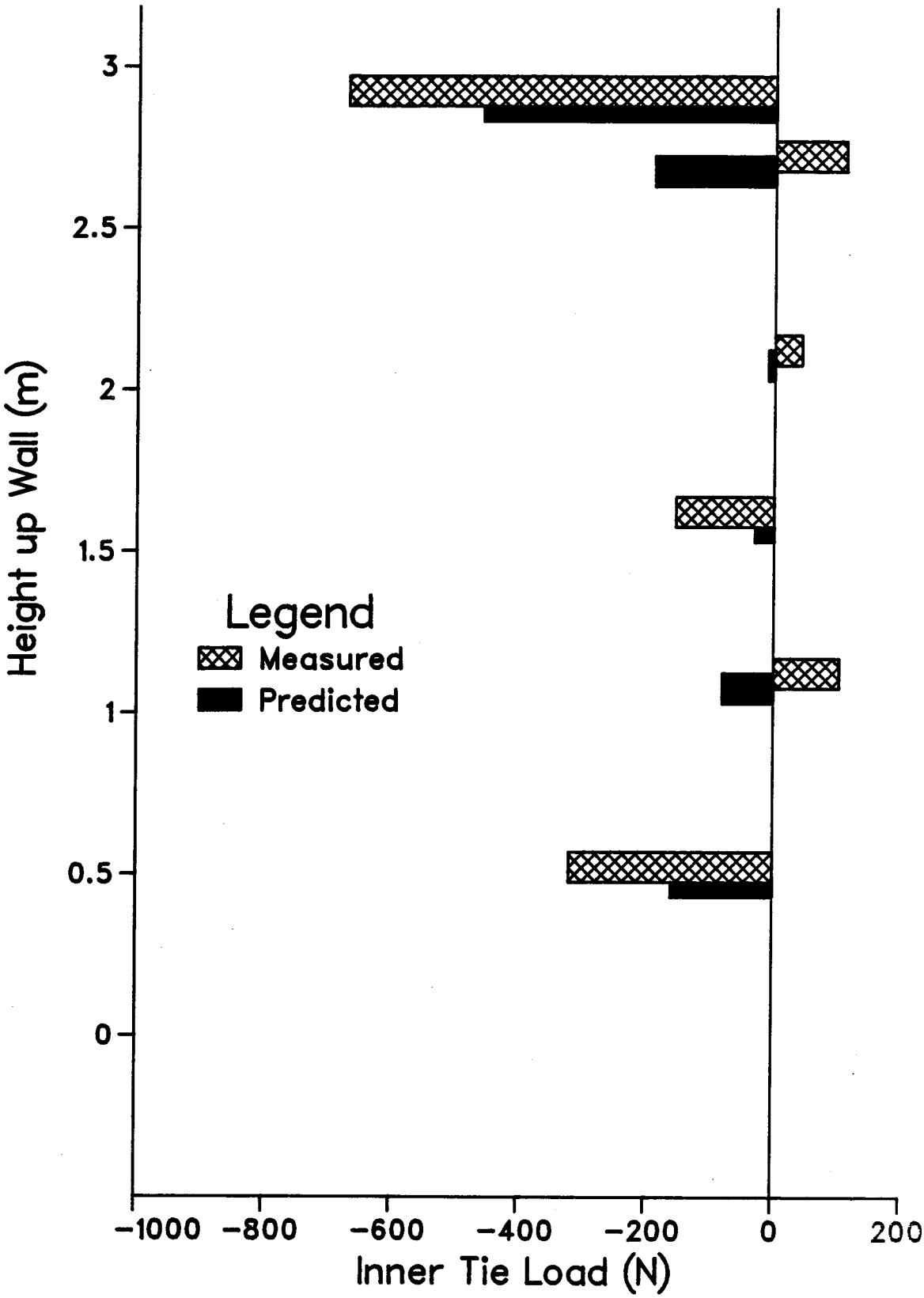

Figure 6.15 Inner Tie loads for Specimen S1W4 - Measured and Predicted

effective stiffness of the tie systems will be approach a uniform value. Therefore, it is proposed that the wall model and analysis can be used to provide sufficiently accurate prediction of tie loading for design purposes.

Examination of the shear transfer data confirms that the degree of shear connection provided by the shear brackets is highly variable. The results vary widely for the three shear brackets instrumented. Since only three tie systems out of 18 were instrumented, this large random variation supports the use of approximate uniform values of shear connection because more accuracy is not possible and of questionable validity.

The test data suggests that the three dimensional frame model predicts the behaviour of a masonry wall system adequately for design purposes. This three dimensional model can also be used to predict masonry veneer wall system behaviour near openings, corners and wall junctions. However, further testing is required to confirm the accuracy of this model for these conditions.

6.2.3 Two Dimensional Plane-Frame Model

Away from openings, corners and wall junctions, the masonry wall system is bent primarily in single curvature and therefore supports the wind load through one-way bending between floor slabs. Thus, the three dimensional wall system model can be reduced to a two dimensional plane-frame model with little loss in accurracy.

Figure 6.16 shows the two dimensional plane-frame model. Each 400 mm width of veneer and backing wall is assumed to act independently and form a plane-frame. Both the veneer and stud are assumed to span continuously over their entire length. The effective tie and track members are the same as those described previously, as are the wall support conditions. The wind load is applied to the vertical veneer members and it is assumed to be uniformly distributed. This load is calculated based on a tributary width equal to a full stud spacing of 400 mm. The plane-frame model is analyzed using a direct stiffness, frame analysis computer program. Although any elastic frame analysis technique can be used, this method is the most convenient. The same material properties used for the three dimensional analysis are used for the two dimensional analysis.

Figure 6.17 shows a comparison of measured veneer deflections with veneer deflections predicted by the two dimensional plane-frame model and veneer deflections predicted by the three dimensional space-frame model for Specimen S1W1. Figure 6.18 shows the predicted and measured stud deflections of Specimen S1W1, again using both models. The predicted shapes from both models show almost identical agreement between the measured and predicted shapes. Similiar agreement was obtained for each the 12 wall specimens.

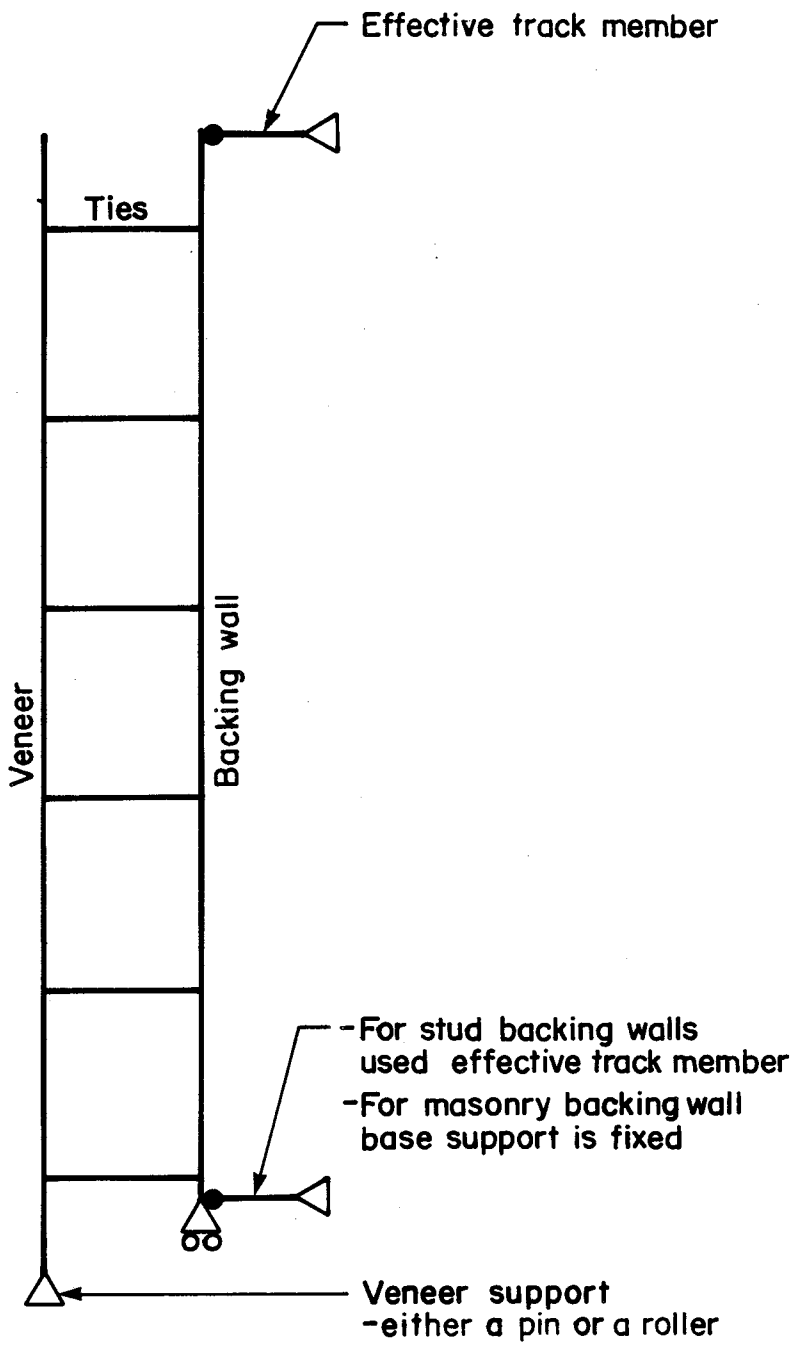

Figure 6.16 2 Dimensional Wall System Model

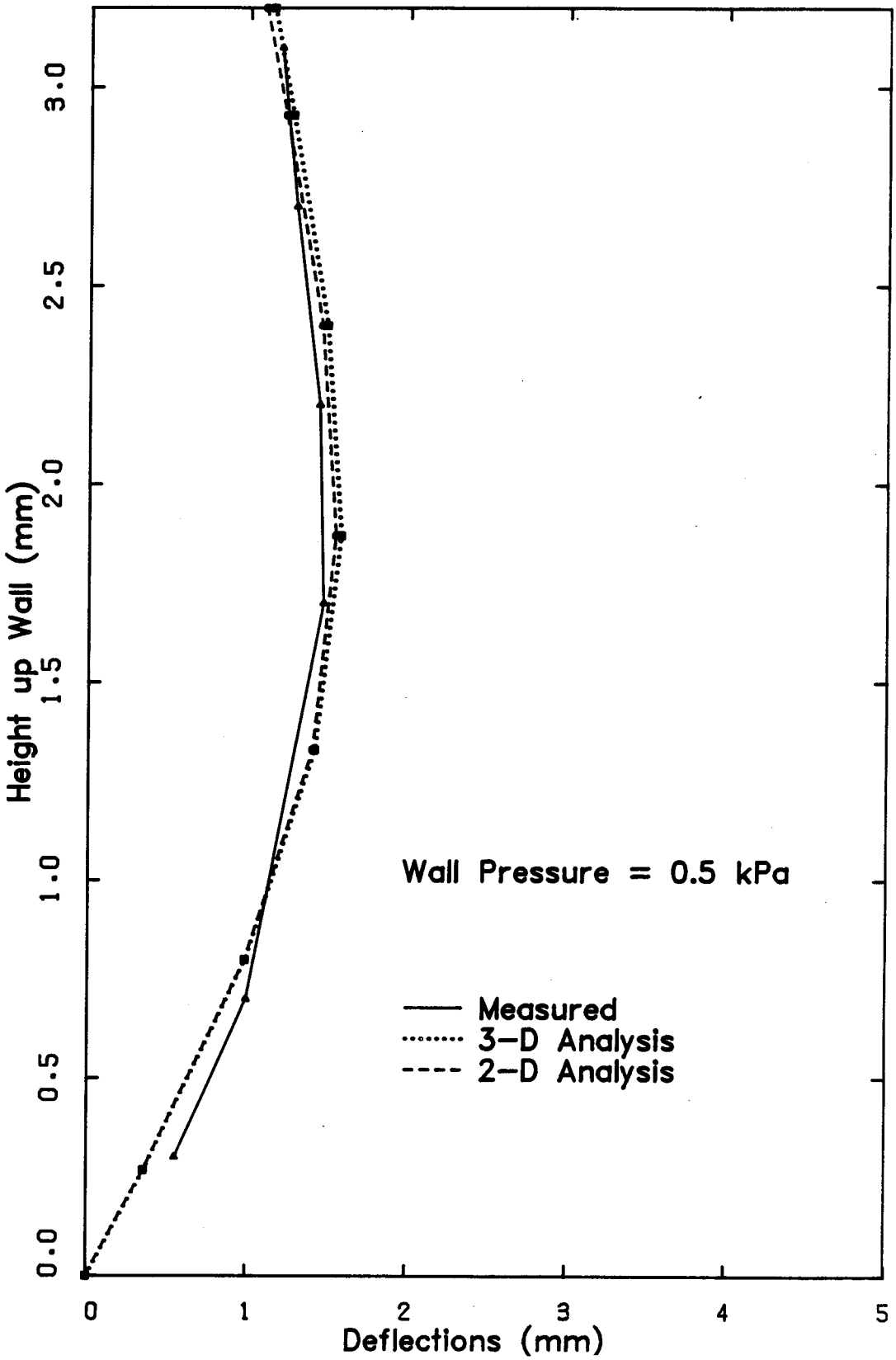

Figure 6.17 Comparison of Predicted Veneer Deflections - 2D and 3D (S1W1)

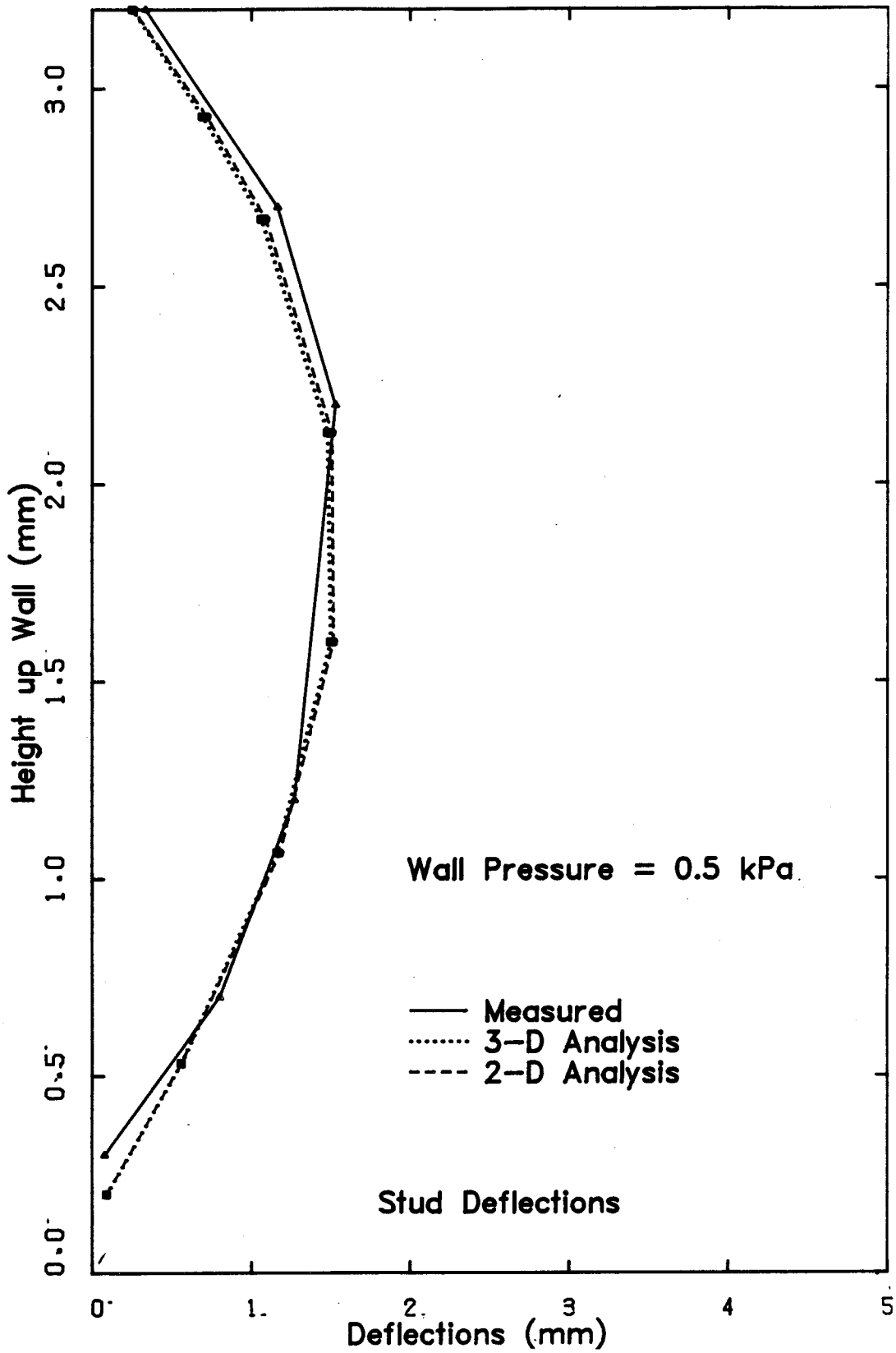

Figure 6.18 Comparison of Predicted Stud Deflections - 2D and 3D (S1W1)

Thus, a two dimensional wall model can be used to predict the load-deflection behaviour of a masonry veneer wall system with reasonable accuracy. However, care must be exercised when calculating the loads applied to the two dimensional wall model. These loads should account for tie pattern at the top of the walls'. If the tie pattern is staggered, the stud lines with ties closest to the top of the veneer will be more heavily loaded. It is recommended that ties be placed at one-half a tie spacing for the top of the veneer on each stud line. This procedure not only simplifies the modeling but it also evens out the loading of the upper ties.

The two dimensional model can also be used to predict the behaviour of masonry wall systems around openings. A narrow width of veneer and backing wall on each side of the opening can be assumed to act as a plane frame. The wind load on a section of wall defined by the opening is transferred to the stiffer wall sections on either side. Therefore, the loading of these frames includes loads from the section with the opening as well as any wind loads applied directly to the design section. Depending on the connection details, the wind load from the section with the opening is applied to the veneer or to the backing wall. It should be noted that all these assumptions are based on the results of analyses preformed using the three dimensional model and must be confirmed by tests.

6.3 Evaluation of Design Procedures

In order to evaluate the design procedures a comparison between the measured load effects and average member resistances must be made. This comparison must also be made when resistance factors are to be derived. However, direct measurement of most of the applied load effects was impractical, and in the case of the tie loads, subject to high variation. Furthermore, the masonry veneer wall system is a highly redundant structural system. Variations in the stiffness of individual members of the system can change the distribution of the wall loads. However, this investigation is concerned with the accuracy of the predicted failure load. Therefore, the wall model and analysis procedures were used to generate veneer loads based on the capacity of each wall system component. By comparing these predicted wall loads to the measured wall loads an evaluation of the design procedures can be performed.

The accuracy of the predicted veneer loads will include the accuracy and variation of:

1. the wall system models and the component capacity equations;
2. the material properties (modulus of elasticity);
3. the geometric properties of each member (including effective area and stiffness).

Using the approach described above the results of the twelve wall specimens tested in this investigation were evaluated.

6.3.1 Veneer Cracking

Ten of the twelve wall specimens exhibited veneer cracking as their primary ultimate limit state. The results of these ten tests were used to evaluate the design procedures for veneer cracking resistance.

In order to predict the veneer load that will cause cracking of the veneer a value for the veneer flexural resistance must be determined. If this resistance is calculated by Equation 3.5, then a value for the modulus of rupture of the veneer must be chosen. In general the modulus of rupture of masonry depends on a number of factors, including:

1. workmanship;
2. absorption of the masonry units;
3. water content of the mortar;
4. curing environment;
5. mortar mix portions and ingredients.

Each factor affects the bond between the masonry unit and the mortar, producing large variations in the modulus of rupture.

In each test series the veneer was constructed and cured under approximately the same conditions. Thus, for each series the average modulus of rupture was assumed to be indicative of the modulus of rupture of the veneer of each wall specimen in the series. The results of the prism tests give an average modulus of rupture, σ_r, of 0.511 MPa for Series 1 veneer and 0.685 MPa for Series 2 veneer (see

Appendix A).

Using these σ_r values and a veneer width of 400 mm, Equation 3.5 was used to calculate the average moment resistance of the veneer for each test series. The moment of inertia of the net bedded area of the veneer and a y of 42 mm were used for this calculation. The average moment resistance was 0.189 kNm for Series 1 veneer and 0.255 kNm for Series 2 veneer.

Using the three dimensional wall model and the measured and approximated member properties listed in Table 6.2, veneer loads were calculated for each specimen so that the veneer moment at the crack location equalled the corresponding average moment resistance of the veneer. These loads are the predicted failure loads for the specimen and their values are listed in Table 6.3. The ratios of measured veneer load to predicted veneer load were calculated for each specimen, and are listed in Table 6.3. The average value of this ratio is 1.103 with a coefficient of variation of 0.325. Although the average value of the test to predicted ratio is close to unity, the coefficient of variation is large. The variation in the test to predicted ratio includes the variations and accuracy of:

1. the prediction of the wall model and resistance equation;
2. the properties of the wall system members;
3. the experimental procedures;
4. the modulus of rupture of the veneer.

Table 6.3 Test to Predicted Ratios Based on Veneer Cracking Resistance

Specimen	*Pred. Load	&T/P Ratios
S1W1	0.642 kPa	0.95
S1W2	0.950 kPa	1.90
S1W3	0.953 kPa	1.27
S1W4	0.844 kPa	1.20
S1W5	0.840 kPa	1.41
S2W1	255 N	1.24
S2W2	250 N	0.74
S2W3	175 N	0.89
S2W4	2.54 kPa	0.47
S2W5	170 N	1.17

* Predicted veneer load for cracking of the veneer - pressure (kPa) or cable load (N)
& Test to predicted load ratios

If the variations of all except the modulus of rupture of the veneer are assumed to be insignificant, variation of the ratio of estimated applied moment and average moment resistance should be the same as the variation of the modulus of rupture. An average modulus of rupture of 0.607 MPa and a coefficient of variation of 0.47 were calculated using the results of the twelve prism tests. For a similar sample size, the coefficient of variation of the modulus of rupture is greater than the coefficient of variation of the test to predicted ratio. It can therefore be concluded that the design procedures are reasonably accurate.

One reason that the coefficient of variation of the test to predicted ratio is less than coefficient of variation of the modulus of rupture of the veneer is due to the fact that a weak veneer mortar joint is likely to be less stiff than a strong mortar joint. As a result, the redundant structural behaviour of the wall system will cause redistribution of the veneer moment, reducing the moment at the weak joint. This action will tend to reduce the effect of the variability of the modulus of rupture of the veneer on the variability of the veneer cracking load.

6.3.2 Backing Wall and Tie System Failure

None of the 12 wall specimens tested exhibited tie failure as a primary ultimate limit state. However, both specimens backed by hollow concrete block walls failed by the formation of a crack at the base of the backing wall

followed by further crack formation in the veneer and backing wall near mid-height. The top support of the backing wall for Specimen S2W6 settled significantly. Therefore, the mortar joint at the base of the wall was likely to have cracked at a low load even though the crack was not observed until after the test was completed.

The values for the member properties listed in Table 6.2 and the three dimensional wall model were used to predict the backing wall moment at the crack location under the measured cracking load. Specimen S1W6 was assumed to have a fully fixed support at the base of the block wall and the maximum moment was calculated at this location. For Specimen S2W6, the backing wall was assumed to be pinned at both the top and bottom, and the maximum moment was calculated at the crack location near mid-height of the backing wall. The measured cracking load was assumed to be the maximum wall load for specimen S1W6 and the first maximum wall load was used as the cracking load for Specimen S2W6.

In order to calculate the moment resistance of the block backing wall an average value for the modulus of rupture of the block is required. However, there was no test data with which to determine this value because of the difficulties experienced in attempting to cut block prisms from the backing walls. Therefore, it was assumed that the modulus of rupture of the concrete block and the modulus of rupture of the veneer have the same ratio as their allowable

stresses as specified in CSA S304[11] (0.16/0.25). Based on the average moduli of the veneer, this assumption results in moduli of rupture of the concrete block of 0.33 MPa and 0.44 MPa, for Specimens S1W6 and S2W6, respectively. For these σ_r values, I equal to 1.55 x 10^8 mm^4 and y equal to 95 mm, Equation 3.5 gives a moment resistance for the concrete block wall of 0.534 kNm for Specimen S1W6 and 0.438 kNm for Specimen S2W6.

Comparing the estimated applied moment to the moment resistance of the backing walls results in tested to predicted ratios of 1.03 (S1W6) and 0.74 (S2W6). These values indicate that the design and modeling procedures can be applied to concrete block wall backed masonry systems with a reasonable degree of accuracy.

6.4 Performance Factors

Performance factors must be derived for each of the ultimate limit states. In the derivation of these performance factors a comparison of measured load effects and predicted member resistance is required. It is again assumed that the three dimensional wall model can be used to predict the veneer load that will produce failure of the components of the wall systems. Thus, the ratio of test to predicted veneer load can be used for the performance factor (ϕ) calculations. As mentioned previously, this ratio will include allowances for inaccuracies of the wall model, design equations, member properties, testing accuracy and

member resistance.

Deriving ϕ values based on this ratio is not strictly correct as some allowance has already been made for the accuracy of prediction of loading effects in the determination of the load factor (λ). However, in keeping with a uniform load factor philosophy, λ must be 1.5. Therefore, any additional uncertainty in load effect prediction associated with this wall system must be included in the value of ϕ. Calculating performance factors in this manner will produce conservative values of ϕ. However, for the relatively small amount of data available to this investigation, this is considered acceptable.

A more accurate determination of ϕ can be made if variations in the material properties can be determined and their effects on the resistance and performance of the wall system evaluated. It is suggested that, at some later date, a Monte Carlo simulation be performed on this wall system to evaluate these effects.

If Equation 3.4 is applied to the results of the ten full-sized tests, a performance factor for the moment resistance of the veneer (ϕ_m) can be derived. The ratio of $\bar{R}/R$ ratio was taken as 1.103, with a coefficient of variation of 0.325. If the value of λ is 1.5, $S/\bar{S}$ is 1.25, V_s is 0.25, and β is 2.3, ϕ_m has a value of 0.81. However, because this value of ϕ_m is based on a sample of only ten tests, its statistical significance is questionable.

In design the average material properties are not usually known. Therefore, nominal material properties and geometry values are used for the calculation of member resistances and prediction of load effects. The following sections show the derivation of performance factors for ultimate limit states of the masonry veneer wall systems based on these nominal values. Included in these derivations are the results of the twelve full-sized wall tests, together with the 36 full-sized wall test results from the previous two investigations[1,17].

6.4.1 Veneer Moment Resistance Performance Factor

The three dimensional wall system model was used to predict the veneer load that would cause cracking of the veneer for all steel stud backed specimens which exhibited veneer cracking as their primary limit state. Nominal values for the material properties of the veneer and studs, together with average material properties determined for the effective members, were used for the analysis. Table 6.4 lists these material properties for each wall specimen.

The nominal material properties and dimensions of the studs were obtained from the manufacturer's handbooks and the dimensions of the veneer were obtained from the brick manufacturer's manual. Calculation of the area and moment of inertia of the veneer was based on the net bedded area and a 4 mm raking.

Table 6.4 Veneer Moment - Nominal Material Properties and Measured to Predicted Load Ratios

Specimen	Stud I ($\times 10^5$ mm^4)	Stud A (mm^2)	Ae Tie (mm^2)	Ae Track (mm^2)	Ratios
NS1W1	3.0	183.	0.176	0.30	0.54
NS1W2	3.0	183.	0.176	0.30	1.21
NS1W3	4.0	254.	0.20	0.30	0.84
NS1W4	3.0	183.	0.36	0.30	0.68
NS1W5	3.0	183.	0.20	0.30	0.84
NS2W1	3.0	183.	0.132	0.30	1.31
NS2W2	3.0	183.	0.132	0.30	0.68
NS2W3	4.0	254.	0.20	0.30	0.84
NS2W4	32.0	1100.	0.36	0.50	1.05
NS2W5	3.0	183.	0.36	0.30	1.16
MS1W3	3.0	183.	0.14	0.30	0.96
MS1W4	3.0	183.	0.14	0.30	1.43
MS2W1	3.0	183.	0.14	0.30	1.54
MS2W2	3.0	183.	0.14	0.30	0.66
MS2W3	3.0	183.	0.14	0.30	1.94
MS2W4	3.0	183.	0.14	0.30	1.45
MS3W3	7.2	159.	0.10	0.20	1.10
MS3W4	7.2	159.	0.10	0.20	1.51
MS4W2	7.2	159.	0.10	0.20	1.35
MS4W3	7.2	159.	0.10	0.20	1.31
MS4W4	7.2	159.	0.10	0.20	1.12
DS1W1	3.0	183.	0.14	0.30	1.50
DS1W2	3.0	183.	0.14	0.30	1.66
DS1W3	3.0	183.	0.14	0.30	1.20
DS1W4	3.0	183.	0.14	0.30	1.40
DS2W1	2.05	127.	0.10	0.20	2.83
DS2W2	7.2	157.	0.10	0.20	1.68
DS2W3	9.76	224.	0.14	0.30	1.29
DS2W4	3.7	226.	0.20	0.40	2.37
DS2W6	4.52	297.	0.30	0.50	1.58
DS3W1	2.05	127.	0.10	0.20	2.54
DS3W2	7.2	157.	0.10	0.20	1.18
DS3W3	7.2	157.	0.10	0.20	1.93
DS3W4	9.76	224.	0.14	0.30	1.24
DS3W5	12.6	226.	0.20	0.40	1.82
DS3W6	4.52	297.	0.30	0.50	2.42

Note: 1. The masonry E is calculated as 750f'm
-Block=10000 MPa, Brick=10500 MPa
2. All other values are as defined in Table 6.1.
3. The I of the veneer is taken as 1.56×10^7 mm^4
4. The effective areas for the ties and and track used with the 14 and 16 gauged studs were estimated based on the data of the other studs.
5. NS1W1 indicates the first wall of the first series of this present investigation.

CSA CAN3-S304-M78[11] specifies procedures for estimating the elastic modulus of masonry. It has been found that these procedures may be unconservative[34]. Therefore, the nominal elastic modulus was assumed to have a value of 750 x (f'm), as suggested by Hatzinikolas, et al[34].

It is expected that tie manufacturers and steel stud manufacturers will provide member load-deflection data in their design aids. For this reason, values for the effective area of the ties and track were used in the analysis. Some of these values were obtained from tests conducted in previous investigations[1,17]. It was assumed that the effective moment of inertia of the shear bracket tie systems was 2500 mm^4.

To calculate the nominal moment resistance of the masonry veneer, a value for the modulus of rupture must be chosen. For the veneer prisms tested during all three investigations, the average of the measured moduli of rupture was 0.695 MPa. Based on this average, the "nominal" modulus of rupture for this type of brick and mortar was conservatively estimated as 0.600 MPa. For this σ_r, a moment of inertia of 15.6 x 10^6 mm^4 and a y of 42 mm, the nominal veneer moment resistance was 0.223 kNm. Veneer cracking loads were then calculated using the analysis described above. The veneer cracking load was defined as the veneer load which produced a maximum veneer moment equal to the "nominal" moment resistance. Using the measured loads at cracking, test to predicted ratios were calculated for each

wall specimen and these values are listed in Table 6.4. The average of test to predicted ratio is 1.39, with a coefficient of variation of 0.39.

The coefficient of variation of these ratios is large. However, as discussed previously, this value includes the variation of a number of factors. If the variations of all but the modulus of rupture of the veneer are again assumed to be insignificant, comparison of the coefficient of variation of the modulus of rupture to the coefficient of variation of the test to predicted ratio indicates the value of this latter coefficient is reasonable.

The test to predicted ratio has a value greater than one and therefore leads to the conclusion that the design equation and analysis methods are conservative. A portion of this conservatism results from the use of a nominal modulus of rupture which is lower than the average value. In addition, the nominal modulus of elasticity of the veneer is larger than the measured values, causing the analysis to predict larger veneer moments than would likely be experienced by the veneer.

Based on the average ratio and its coefficient of variation, Equation 3.4 was used to calculate a performance factor for veneer moment resistance, ϕ_m. The ratio of $\bar{R}/R$ was taken as the 1.39 and V_r was taken as 0.390. The remaining variables in the equation had the same values as presented previously. These calculations resulted in values of ϕ_m of 0.85 for a β of 2.3, and a ϕ_m of 0.65 for a β of

3.0. Since these ϕ_m values are based on the results of 36 wall tests, there is a greater confidence in their statistical validity than in the value of ϕ_m calculated previously.

The Uniform Building Code[35] suggests ϕ values of 0.6 and 0.4 for "specially inspected" and "inspected" reinforced masonry, respectively. However, these values are based on a live load factor of 1.7 , a dead load factor of 1.4, and a β of approximately 3.5. For veneer cracking, ϕ_m has a value of 0.58 for a β of 3.5 and a λ of 1.7. Thus, the calculated ϕ_m value of 0.85 (for a λ of 1.5 and β of 2.3) compares reasonably with the UBC values. This value is slightly lower than expected for the "specially inspected" conditions in the lab. However, these wall systems are highly redundant and susceptible to variations in the material properties. Thus, the lower ϕ_m value seems reasonable for this type of wall system where ϕ_m accounts for the variability in the prediction of the loading effects as well as variability in resistance.

For the partially shear-connected specimens, the veneer moment resistance calculation ignored the axial loads in the veneer produced by the partial shear connection and the self-weight of the veneer. For the amount of shear connection provided by the shear bracket tie systems, the axial loads are small and highly variable. The axial stresses are usually less than 20 % of the modulus of rupture and were neglected.

In order to derive the performance factors above, it was necessary to estimate a nominal value of the modulus rupture of the veneer. The performance factor is therefore dependent upon the value chosen. There are are no guidelines for estimating this value in any of the North American codes; only allowable tensile stresses are given. The British Standard BS 5628 Part1 1985[36] provides values of the "characteristic tensile strength" of unreinforced masonry. For the type of mortar and brick used, this code recommends a value of 0.500 MPa. If this value is taken as the nominal modulus of rupture of the veneer, different values of the performance factor result. These values of ϕ_m are 1.08 and 0.78 for values of β of 2.3 and 3.0, respectively.

The derivation of the performance factor, ϕ_m, account for the accuracy of the load effect prediction as part of the derivation. Therefore, the design load effects must be predicted by an equally accurate method for these values of ϕ_m. It is recommended that frame models (either two dimensional or three dimensional) be used for the prediction of veneer moments produced by the applied factored load. These analyses must include the effective members or serious inaccuracies in prediction will result[37].

6.4.2 Tie Resistance Performance Factor

In six wall specimens tie failure was the primary ultimate limit state. The ties in these specimens failed before either the veneer cracked or the backing wall failed.

Using the same analysis as previously described for the prediction of the estimated veneer moment, the maximum tie load was calculated for each of these specimens. These loads were then compared to the nominal values of the tie resistances given by Equation 3.6.

To use Equation 3.6, a nominal tie load must be chosen. Using the procedures outlined in Chapter 3 and the average tie strengths from tests[1], nominal compressive strengths were calculated for 22 and 24 gauge corrugated tie systems. The nominal ultimate compressive strength for 22 gauge corrugated ties was 550 N for a cavity of 50 mm and 790 N for a cavity of 25 mm. It should be noted that this latter value is slightly less than the working load compressive strength value (800 N) recommended by CAN3-A370[1,2] for this tie type and cavity width. In a cavity width of 50 mm, 24 gauge corrugated ties are calculated to have a nominal ultimate compressive strength of 390 N.

There is a further consideration in the selection of the nominal ultimate strength of the tie system. This ultimate strength should be reasonably close to the proportional limit of the tie system so that the inaccuracies in the elastic analysis are small. For these tie types, the buckling load is close to the proportional limit so this criteria is satisfied[1].

Table 6.5 lists the tie type, cavity width, and ratios of estimated tie failure load to predicted nominal resistance for each wall specimen. The average ratio of

Table 6.5 Tie Failure - Measured To Predicted to Predicted Ratios

Specimen	Tie Type	Gap (mm)	Ratios
MS1W1	22 Corr.	50.	2.18
MS1W2	22 Corr.	50.	2.22
MS3W1	22 Corr.	50.	2.22
MS3W2	22 Corr.	50.	1.65
MS4W1	24 Corr.	50.	1.03
DS2W5	16 Corr.*	25.	2.99

Note: 1. 22 Corr. - 22 gauge corrugated ties without backing platform
2. 24 Corr. - 24 gauge corrugated ties without backing platform
3. 16 Corr.* - 16 gauge corrugated ties with backing platform (Pt=1200N)

measured to predicted load is 2.05, with a coefficient of variation of 0.32. This results in a ϕ_t of 0.76 for a β of 4.0. This safety index is higher than that for veneer cracking so that it is more likely that veneer cracking will be the governing limit state. However, this performance factor was calculated based on the results of only 5 tests and is of questionable validity. Further testing is required to derive a more statistically significant performance factor for tie resistance.

The average value of the ratio of "measured" tie load and predicted tie resistance is large; this results in a large ϕ factor. However, this value depends on the nominal value of the tie resistance chosen. Each of the nominal tie resistance values is less than the average test value. Thus, the average of $\bar{R}/R$ is expected to be greater than one.

The average value of tie load ratio is also increased by the highly redundant nature of the wall system. The tie systems become less stiff as they approach their failure load. Therefore, more of the veneer load is transfered to surrounding ties, thus reducing the amount of wall load which is applied to the heavily loaded tie. As a result of this load sharing between ties, the wall specimens were able to withstand significantly greater loads than predicted. In addition, the failure of one tie did not significantly alter the performance of the wall specimen. Collapse or "pull off" of the veneer occurred only after a number of tie systems had failed. Thus, the wall load for first tie failure was

likely overestimated.

It should be noted that for each of the five wall specimens that exhibited tie failure as the primary limit state, the analysis predicted that the veneer would crack before the ties fail. The design and analysis predicted that the tie failure load was a maximum of 30% larger than the veneer cracking load. For tie failure to precede veneer cracking in this specimen, the moment in the veneer at tie failure would require the veneer to have a modulus of rupture of 0.780 MPa. This value is well within the observed variability of the modulus of rupture of the veneer. Thus, the design procedures, while not predicting the actual failure mode, can be used to provide adequate levels of safety for both limit states.

6.4.3 Backing Failure and Serviceability Limit States

Only the two hollow block backed specimens exhibited backing wall failure as their primary limit state. The adequacy of the design procedures for this limit state has already been discussed. However, there is insufficient data to derive performance factors for the failure of concrete block backed masonry veneer wall systems and it is recommended that further testing be performed.

The stud backed wall specimens exhibited significant reserve strength after veneer cracking. If veneer cracking is not overly detrimental to the performance of stud backed masonry veneer wall systems, this additional wall strength

can utilized. The following section discusses the performance of stud backed wall specimens after cracking.

The final limit state of the masonry veneer wall system is excessive deflection. For all the wall specimens, the maximum deflections of the veneer and backing wall were within 10 % of the L/480 deflection limit at the veneer cracking load. Therefore, if the wall system is designed to preclude veneer cracking under the factored wind load, deflection of the wall system under service loads is rarely a problem.

6.5 Post-Cracking Behaviour

There remains the possibility that, after further investigation, there may be some conditions where the cracking of the veneer may be considered a serviceability limit. This section presents procedures for the design of masonry curtain wall systems with cracked veneers.

The three dimensional wall model or the two dimensional wall model could be used to predict the loading effects. However, the accuracy of these models becomes questionable because of:

1. the increased effect of tie stiffness variability caused by the reduction in the effective aspect ratio of the veneer;
2. uncertainty of the actual location of the veneer crack;
3. possible slip between the two surfaces of the veneer at the crack interface.

Therefore, for the cracked wall system, an approximate analysis procedure will likley be as accurate as the frame models.

Examination of the measured tie loading patterns show that the post-cracking tie loading pattern is highly variable. If the veneer cracks near the top or bottom of the wall and there is no slip at the crack, then the top and bottom ties are heavily loaded. If the veneer cracks near mid-height and there is slip at the interface, the tie load is distributed between the top ties, bottom ties and the ties near mid-height of the wall system.

Figure 6.19 shows the tie load pattern for Specimen S1W3 after veneer cracking. This specimen cracked at an elevation of 1710 mm, very near mid-height of the backing wall. This plot confirms that the tie loading is far from uniform. The top and bottom ties are heavily loaded, as are the ties near the centre of the wall.

The highest possible loading of the top and bottom ties can be approximated conservatively using the uncracked veneer reactions. The veneer can be assumed to span between floor slabs with no support from the interior ties. Therefore, the top and bottom ties must resist the entire veneer reaction at these locations.

The tie spacing should be chosen to be within the limits specified by the applicable codes. Tie capacity should then be checked by apportioning the reaction load to these ties in relation to the distance of each tie from the

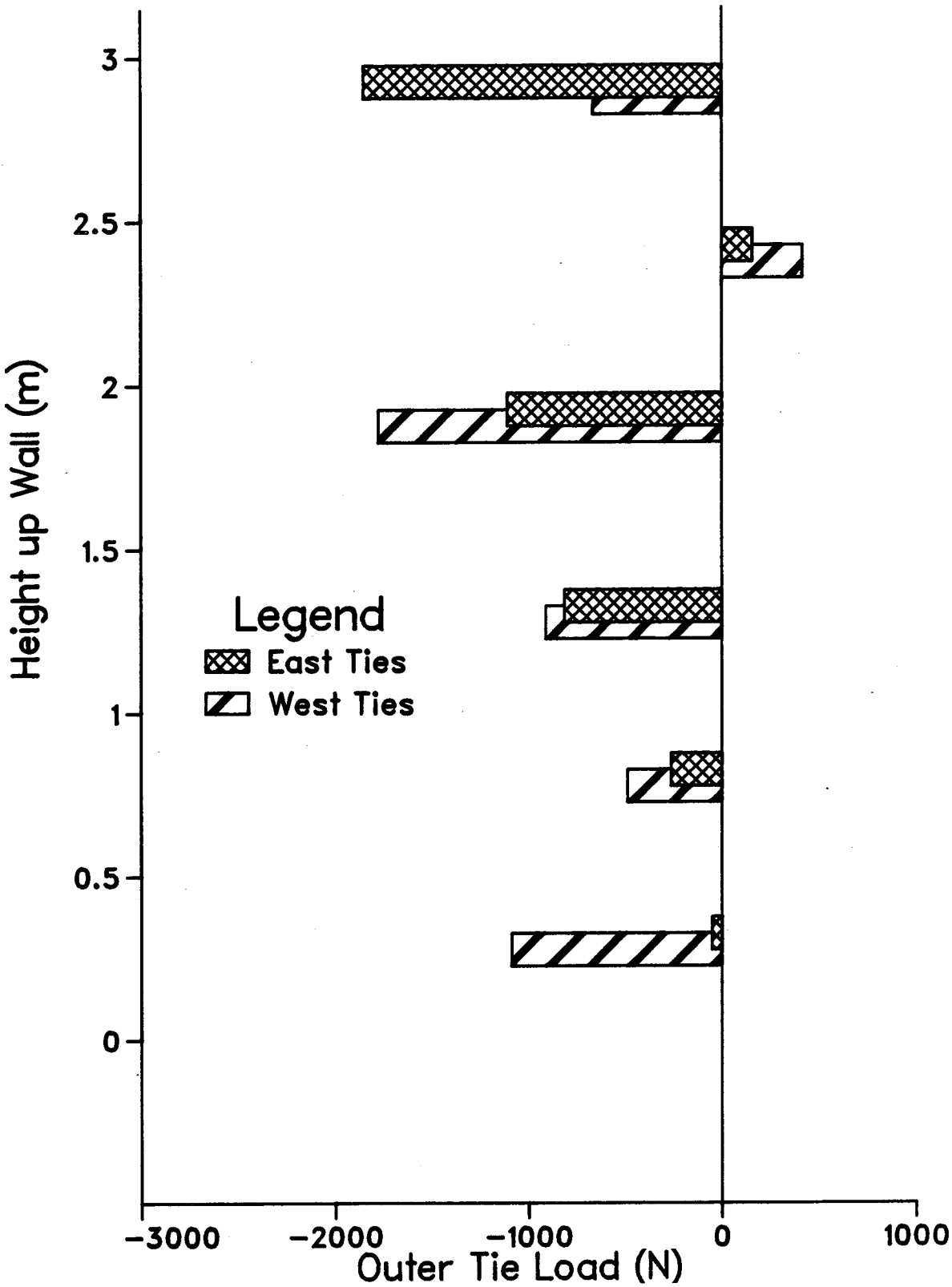

Figure 6.19 Outer Tie Loads of Specimen S1W3 After Veneer Cracking

top or bottom tie row. Ties on the top and bottom rows should be designed for a full share of the reaction loads and ties at a 1/2 tie spacing away should be designed for a half share of the reaction load. Any tie beyond a 1/2 tie spacing from the top and bottom tie rows should be neglected.

The magnitudes of the tie loads near mid-height vary widely and depend on the location of the veneer crack, the relative effective stiffness of the interior ties and the stiffness of the backing wall. The worst possible loading case would occur if the veneer is cracked near mid-height and there is slip at the crack interface. This loading can be approximated conservatively by the model shown in Figure 6.20. It was assumed that the veneer acts as two independent, simply supported beams spanning between the wall ends and mid-height. The support of the ties near the centre of these members was ignored. Therefore the ties near the crack must be able to resist the two reactions, 2 x Rv (or, one-half the total veneer load). The assumption that the interior ties provide neglible support simplifies the analysis and should provide safe, although conservative, results.

It is recommended that the ties within a full tie spacing from the mid-height of the wall system be designed to resist 1/2 the total veneer load. This load can be distributed to the ties in a uniform manner.

POST CRACKING MODEL

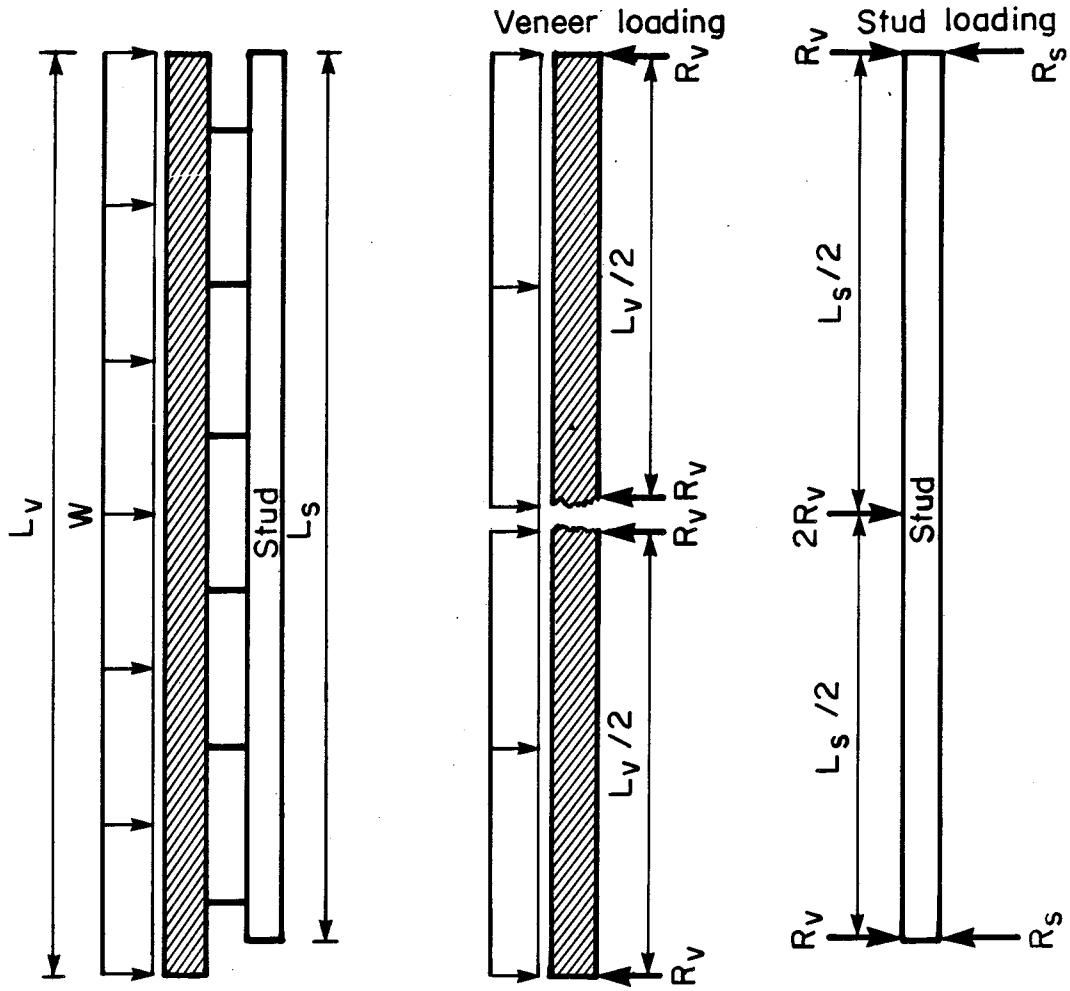

NOTE : Ignore support of interior ties

Figure 6.20 Post Cracking Wall Model

A similar approximation can be applied to the stud loading. The worst possible loading case consists of 1/2 the veneer load applied as a point load at the centre span of the backing wall and 1/4 of the veneer load applied near each of the stud supports (see Figure 6.20). Although, it is very unlikely that this type of loading will occur, large centralized tie loads are possible and can be approximated conservatively by this type of loading.

The uncracked portions of the veneer must be designed for these conditions or further cracking will result. The veneer of each side of the crack can be assumed to span simply supported between the crack and the ends of the wall system. Based on this assumption, the maximum applied factored moment can be calculated and must be less than, or equal to, the veneer moment resistance given by Equation 3.5.

The above procedures were used to predict the measured loading effects (tie loads and backing wall moments) for those wall specimens which exhibited either tie failure or backing wall failure as a primary failure mode after veneer cracking.

6.5.1 Tie System Failure

Twelve walls exhibited tie failure as their primary failure mode in the post-cracking state. The nominal resistance of each tie system type was determined based on the average results of the component tie tests. These

resistances are listed in Table 6.6. Using the procedures outlined previously, maximum tie loads were calculated for the measured wall failure load. Ratios of maximum tie load to tie system resistance were calculated for each wall specimen and these values are shown in Table 6.6.

Some tie systems exhibited two load limits. The average first load limit for these tie systems was taken as the nominal ultimate strength because of the permanent and detrimental deformations that occurred after this load was exceeded'. These average values were rounded off but were not reduced as outlined in CSA A370 because of the significant reserve strength of these tie systems. The wall specimen tie failure load was therefore defined as the load at which tie distress was first observed. Most of the wall specimens exhibited significant reserve strength after this load limit.

The average tie load ratio was 3.01, with a coefficient of variation of 0.36. If this ratio can be taken as the ratio of measured load effect to nominal resistance, then Equation 3.4 can be used to calculate a performance factor for tie resistance. These values result in a ϕ_t of 0.98 for a β of 4.0.

As expected, the conservative approximation of the tie loading results in high values of the tie load ratios and therefore a high value for ϕ_t. Load sharing between the ties and difficulties associated with determining the wall load at which tie failure occurred also increased these values.

Table 6.6 Post-Cracking Failure - Measured to Predicted Ratios

Specimen	Nominal Resistance	Ratios
	Stud-Flexural* (kNm)	
NS1W3	0.714	2.35
NS1W4	0.642	3.52
NS1W5	0.642	4.91
NS2W3	0.714	2.71
NS2W5	1.480	1.50
	Stud-Flex-Crp (in terms of load&)	
NS1W1	2.84 kPa	1.35
NS1W2	3.33 kPa	1.47
DS1W3	2.84 kPa	2.18
DS3W1	2.17 kPa	2.48
DS3W2	3.60 kPa	2.60
DS3W3	3.40 kPa	3.36
DS3W4	4.48 kPa	3.00
DS3W5	4.46 kPa	3.11
	Tie Resistance (N)	
NS2W1	1550	1.56
NS2W1	1550	1.94
MS1W3	-790	5.06
MS1W4	-790	3.26
MS2W1	-550	2.47
MS2W2	-550	4.19
MS4W2	-390	1.93
DS1W1	-790	2.93
DS1W2	-790¢	2.28
DS2W1	-790	3.61
DS2W2	-790	4.31
DS2W4	-2000#	2.60
	Stud-Crippling (kN)	
DS2W4	1.40	1.61
DS2W6	1.40	1.61
DS3W1	1.40	1.44
DS3W2	1.40	1.21

Note: 1. Fy was taken as 320 MPa for the 20 ga. steel and 230 MPa for the rest.
* - flexural resistance based on a laterally unsupported length of 3.0 m.
& - this load was calculated based on a combined flexural and crippling failure of the stud
¢ - The tie is applied directy to rigid insulation and the nominal load is likely to be lower.
- Estimated nominal load.

It is usually preferable to have resistance factors that are independent of the procedures used for the prediction of the load effects. Examination of the two values of ϕ_t suggests that the performance factor for tie resistance should be approximately 0.7. This value will result in conservative designs if the post-cracking model is used. However, these performance factors were based on the results of only 17 tests and further testing is required. For the small sampling of data evaluated, further refinement was not attempted.

6.5.2 Flexural Failure of the Studs

Thirteen wall specimens were loaded so as to cause flexural failure of the stud backing wall. Two types of flexural failure were observed. The specimens employing shear bracket ties failed by buckling of the compression flange and the compression zone of the stud web. These failures occurred near the maximum stud moment regions and all but one (NS2W5) of these failures appeared to be due to lateral-torsional buckling. The specimens employing flange connected ties exhibited combined flexural buckling and web crippling at tie locations near the centre of the stud span.

Lateral-torsional buckling of these studs indicates that the combination of shear bracket ties and an exterior sheathing of rigid insulation did not adequately brace the compression flange of the stud. The amount of bracing provided by these components is unknown. However, if the

studs are assumed to be laterally unsupported over their entire length, a conservative value for the stud resistance can be calculated using the procedures outlined in CSA S136 for laterally unsupported beams[26].

From the failure mode of the studs it was obvious that the shear brackets and rigid insulation did not provide sufficient bracing to prevent lateral-torsional buckling of the stud. However, these wall components have sufficient strength to provide some bracing action. Since it was assumed that the stud was unbraced with respect to bending, it was further assumed that the shear brackets and rigid insulation provided sufficient bracing to allow the small torsional loading of the studs to be ignored.

In the wall specimens that were loaded by a simulated negative pressure (NS2W3 and NS2W5), the stud compression flanges were braced by gypsum sheathing. However, for the specimen that used two back-to-back 90 mm 20 gauge steel studs (NS2W3) the gypsum sheathing was fastened to only one of the flanges. Therefore, the resistance of this stud assembly was limited by the strength of the laterally unsupported stud. For Specimen NS2W5, the studs were assumed to be fully braced.

For the two wall Specimens, NS2W3 and NS2W5, the action of the shear bracket tie systems produces compressive axial loads on the studs which can reduce their effective moment resistance. However, the uncertainty of the loading and bracing of the stud make it difficult to accurately

determine the magnitude of this effect. It was assumed that this refinement of the stud resistance calculation was not warranted for the relatively small axial loads and the conservatism of the post-cracking model.

Using the nominal stud dimensions, nominal material properties and the assumptions discussed above, a stud moment resistance was calculated for each of the wall specimens employing shear bracket tie systems. These nominal moment resistances and the ratio of estimated applied moment to nominal moment resistance are listed in Table 6.6.

For each of the eight wall specimens employing flange connected tie systems, the nominal stud resistance was calculated using procedures outlined in CSA S136[26] which recommends that the crippling resistance of cold formed steel members be calculated using Equation 6.3.

$$P_r = \phi_s \, 16 \, t^2 \, Fy \, A \, B \, C \, D \qquad [6.3]$$

where

$A = (1.22 - 0.22k)$

$B = (1.06 - 0.06R_c)$

$C = (1.00 + 0.007N)$

$D = (1.0 - 0.0014H)$

R_c, N, and H are the ratios of the cross-section bend radius (r), bearing length (n) and web dimension (h), to the material thickness (t) respectively. The value of k is taken as the ratio of the nominal member yield stress, Fy, to the reference yield stress of 230 MPa. It should be noted that this equation is limited to values of $R \leq 4$, $60 < N \leq 200$,

and $n/h \leq 1$.

Using the nominal dimensions of the studs, crippling resistances for each stud and tie configuration were calculated. The bearing length for tie systems employing platforms was assumed to be 30 mm. For the remaining tie systems the bearing length was assumed to be 15 mm.

Nominal stud cross-sectional dimensions and material properties were also used to calculate the nominal moment resistance for each stud. It was assumed that the ties provided adequate lateral and torsional bracing where no exterior sheathing was present or when rigid insulation was used as the exterior sheathing. Thus, the studs were assumed to behave as if fully braced.

The local deformations in the stud cross-section associated with the flange connected ties were ignored. This effect was small compared to the moments produced by the point loads.

The interaction equation for combined flexural failure and web crippling is[26]:

$$\frac{M_f}{M_r} + \frac{P_f}{P_r} \leq 1.3 \qquad [6.4]$$

M_f and P_f are the moment and concentrated load produced by the factored loads, respectively. M_r and P_r are the factored moment resistance of the stud and web crippling resistance, respectively. Using the nominal stud resistances, this equation was used to calculate the maximum central point load that each stud could support. A maximum veneer load was then calculated based on the approximate procedures outlined

previously and this maximum point load. These veneer wall loads and the ratios of measured wall failure load to this approximate resistance load are shown in Table 6.6

Examination of the ratios of measured and predicted stud flexural resistance show that the approximate procedures for stud design are, on the whole, quite conservative. The large values of these ratios reflect the conservative approximations made in both the loading and resistance calculations. To simplify the design procedures it is suggested that the code[26] performance factors of 0.9 (flexure) and 0.8 (web crippling) be used when calculating the stud resistance.

A number of the wall specimens have resistance ratios that are lower than expected for the conservatism of the design approximations. It is suggested that further testing and analysis is required to evaluate the resistances of the metal studs under tie loading. In particular the effect of localized bending of the stud flange and web, at the location of a flange mounted tie, should be investigated. It is expected that this bending reduces both the flexural and crippling capacity of the stud. In addition, the effective bracing action of different types of wall sheathings and tie system combinations should also be evaluated.

If the flexural resistance of the studs can more accurately determined, further refinement of the cracked wall model might be possible. However, although the proposed wall model produces conservative wall designs, it has the

advantage of being simple to use.

6.5.3 Stud Web Crippling at the Supports

There was one further type of stud backing wall failure observed, namely the failure of the stud web at the top support of the backing wall. This failure was typically a web crippling failure and occurred in four of the wall specimens. The stud crippling resistance at the supports was calculated using the procedures outlined in CSA S136[24]. Equation 6.5 is the recommended equation for the support crippling resistance of a single web member with stiffened flanges.

$$P_r = \phi_s \, 10 \, t^2 \, Fy \, A \, B \, C \, D \qquad [6.5]$$

$$A = (1.33 - 0.33k)$$

$$B = (1.15 - 0.15R_c)$$

$$C = (1.00 - 0.01N)$$

$$D = (1.00 - 0.0018H)$$

The limits of this equation are the same as for Equation 6.3, with the exception that the lower limit on N no longer applies.

The bearing length of the stud reaction load was assumed to be 75 % of the depth of the track (30 mm). The nominal crippling resistance of the stud was calculated using Equation 6.5 and the nominal values of the stud properties.

For each of the five wall specimens, the nominal stud resistance and the ratio of estimated reaction load to

nominal resistance are listed in Table 6.6. The measured stud reaction was estimated as 1/2 the total veneer load. The mean ratio was 1.46, with a coefficient of variation of 0.13. For the five wall specimens which exhibited this failure mode, the code design procedures appear to be adequate. It is recommended that the specified performance factor of 0.8 be used for the calculation of the stud crippling resistance.

It should be noted that some of the wall specimens were not loaded to failure. Thus, the calculated post-cracking ϕ values will tend to be conservative. However, for the small sampling of data evaluated, further refinement was not attemped.

6.6 Effects of Partial Shear Connection

Six of the wall specimens were constructed so that partial shear connection was produced between the veneer and stud backing walls. This was done to evaluate the possibility of improving the performance of stud backed masonry wall systems under lateral loading.

Figure 6.21 shows a comparison of the veneer deflection at an elevation of 1700 mm for three of the positively loaded wall specimens. These specimens were all backed by 18 gauge, 90 mm deep steel studs. Two specimens had partial shear connection between the veneer and stud backing wall (S1W4 & S1W5) and one did not (S1W1). The load-deflection plots show that there is a decrease in the deflection of the

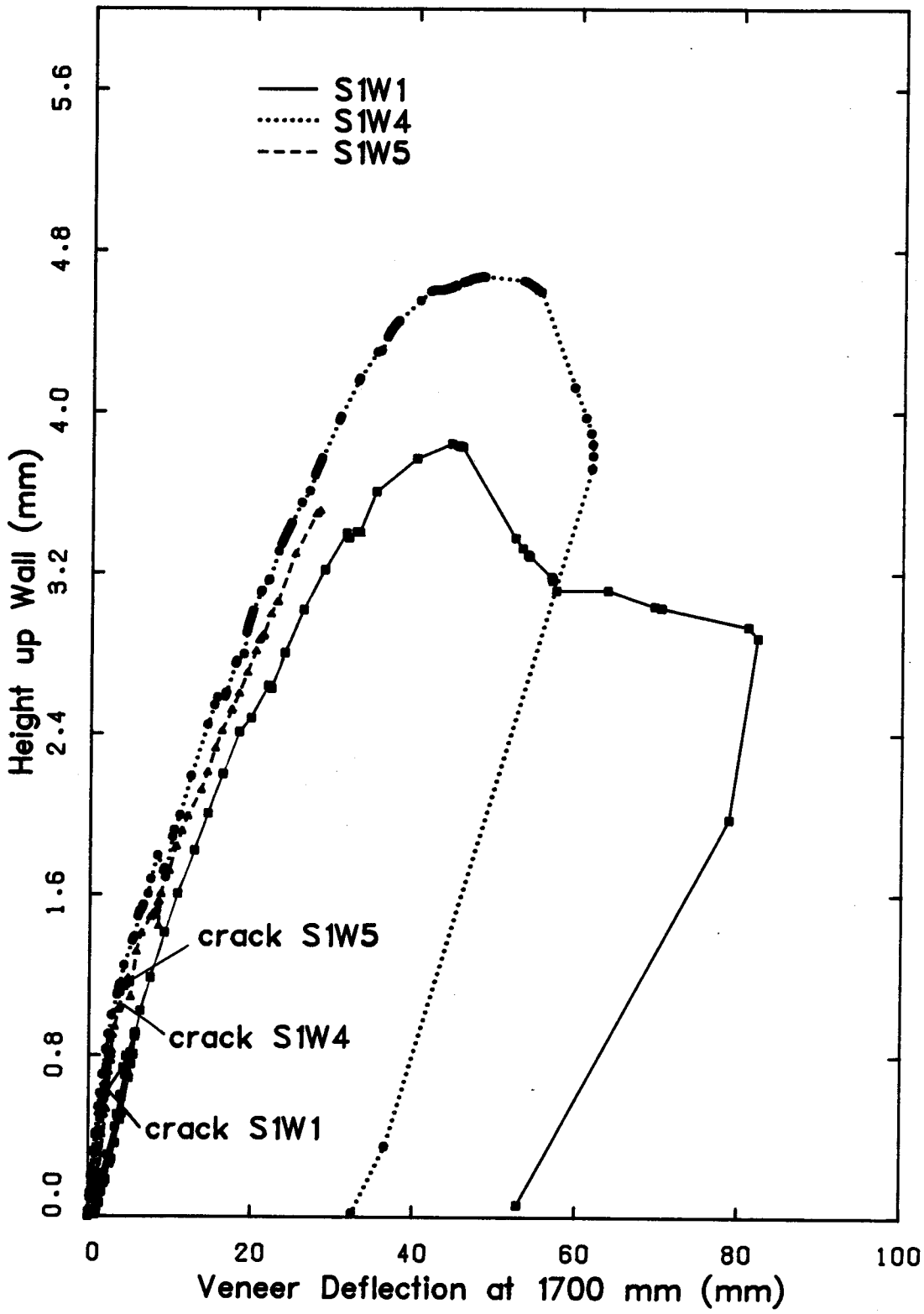

Figure 6.21 Effect of Shear Connection on Veneer Deflections

veneer when partial shear connection was present, most noticeably after veneer cracking. As mentioned previously, the amount of shear connection varied widely because of play in the rod tie attachment holes. Thus, there is only a small difference between the curve for Specimen S1W4 which used the stiffer "V" rod tie attachment and Specimen S1W5 which used the less stiff "Z" rod tie attachment.

Analysis shows that the veneer moments are reduced by approximately 15 % with the relatively small shear connection provided by the shear bracket tie systems. For positive pressure loading, this shear connection also increases the axial load on the veneer which tends to lessen the tension strain in the veneer and increase the cracking load. However, this effect is usually small.

Care should be exercised in assuming that shear connection will solve the problem of low veneer cracking loads. In-plane movements of the veneer will likely become critical as the amount of shear connection increases. Contraction of the veneer due to thermal effects will increase the veneer moments and also apply a tensile force to the veneer. Expansion of the veneer due to thermal and moisture effects will increase the compressive axial load on the veneer, but will also increase the veneer moments. If partial shear connection is to be used, the effects of the in-plane veneer movements must be accounted for.

The first critical loading case is a positive wind pressure combined with the lowest relative veneer

temperature (highest thermal contraction) and the lowest possible moisture expansion. The second critical loading case is a negative wind pressure combined with the highest possible relative veneer temperature (highest thermal expansion) and the highest possible moisture expansion. Either the two dimensional or three dimensional wall model should be used to determine the effect of these loading conditions on the masonry veneer wall system if partial shear connection is contemplated for the design.

The National Building Code of Canada[24] specifies that, for the load combination of temperature effects and wind loads a load combination factor of 0.7 be used. This code also specifies a temperature load factor, λ_t, of 1.25. Thus, the wind load effects must be increased by a factor of 1.5 and it is suggested that all in-plane movement effects be increased by a factor of 1.25.

Whether partial shear connection between the veneer and stud backing wall can improve the performance of a particular masonry veneer wall system depends on the environment in which the wall system will be used. It is likley that partial shear connection will not be advantageous in many applications.

However, even if partial shear connection does not prove to be desirable, the configuration of the shear bracket tie systems provide another performance benefit. The susceptibility to corrosion weakening is reduced because of the reserve capacity of this connection and the redundancy

of the connectors. It is recommended that, where possible, this type of tie/stud connection be used.

7. SUMMARY, CONCLUSIONS AND RECOMMENDATIONS

7.1 Summary

This investigation developed analysis and design procedures for masonry veneer wall systems. A three dimensional space-frame wall system model and a two dimensional plane-frame wall system model were developed to predict the uncracked wall system behaviour under out-of-plane loading. Because the possibility exists that veneer cracking might be considered a serviceability limit state, approximate methods for determining the backing wall and tie design loads were also developed. Based on a total of 44 full-sized wall tests, a limit states design procedure was formulated and evaluated. Finally, the effects of partial shear connection between the veneer and steel stud backing walls were discussed.

7.2 Conclusions

The results of this investigation lead to the following conclusions:

1. If the tie systems and deformable supports are modelled with effective members, the three dimensional wall model predicts the behaviour of the masonry veneer wall systems adequately for design purposes.
2. The two dimensional wall model predicts the wall system behaviour reasonably well if the tie pattern at the top of the veneer is accounted for in the loading of the

plane-frame. As with the three dimensional model, effective tie and support members must be included in the analysis or serious inaccuracies can result.

3. The limit states design procedures will provide adequate levels of safety against failure of the wall system if the applied factored load effects are less than, or equal to, the corresponding factored system resistances (limit states).
4. Masonry veneer wall systems have four ultimate limit states, flexural veneer cracking, tie failure, backing wall flexural failure and backing wall failure at its supports.
5. For veneer cracking, the moment resistance of the veneer can be calculated using the proposed moment resistance equation, a veneer nominal modulus of rupture and a performance factor. The values of this performance factor varied depending on the the level of safety required and the value of the modulus of rupture chosen. Based on thirty-six wall tests the performance factor ranged from 0.65 to 1.08.
6. For tie failure, the resistance of the tie systems should be obtained from tests and then modified by a performance factor. There was insufficient data to derive a statistically significant performance factor for tie resistance, athougth the test results suggest a value near 0.7.
7. Although only two wall specimens were backed by hollow

concrete block walls and these two results are inadequate to derive statistically significant preformance factors, the proposed design methods seem to produce acceptable results for this type of masonry veneer wall system.

8. If the veneer is allowed to crack, the tie systems and backing wall of stud backed masonry wall systems can be conservatively designed for the load effects given by the proposed approximate methods. However, some studs failed earlier than expected due to localized bending of the stud flange and web.
9. Allowance must be made in the construction of masonry veneer wall systems for the relative in-plane movements of the wall system and the supporting frame. Compressible expansion joints must be placed in the veneer and backing wall to accommodate these movements.
10. The differences in the construction tolerances between masonry and the supporting frame materials must be accounted for in the design of the expansion joints.
11. Partial shear connection between the veneer and steel stud wall improves the performance of this type of masonry veneer wall system under out-of-plane loading. However, if significant shear connection is present, the veneer, ties and backing wall must be designed for both the loads produced by the in-plane movements of the veneer and the out-of-plane loading effects.

7.3 Recommendations

The results of the investigation lead to the following recommendations:

1. Further testing and analysis is required to evaluate the performance of steel studs under tie loading.
2. Further testing is also needed to evaluate the influence of openings on the out-of plane load-deflection behaviour of the wall system.
3. Additional testing is required to evaluate the performance of hollow concrete block backed masonry veneer wall systems and to derive statistically significant performance factors for this type of wall system.
4. The performance of masonry veneer wall systems which use various types of mortar and brick should be experimentally evaluated in order to confirm the analysis and design procedures over a larger variety of wall systems and to determine appropriate moduli of rupture for each masonry and mortar type combination. These tests will also serve the create a larger body of data upon which to derive statistically meaningful performance factors.
5. Statistically significant performance factors for tie resistance must be derived. This will require further experimental evaluation.
6. A Monte Carlo study should be performed to determine the effects on wall system performance and member resistance

produced by the variability in the material properties of each member of the masonry veneer wall system.

References

1. W. M. McGinley, "The Interaction of Masonry Veneer and Steel Studs in Curtain Wall Construction", M.Sc. Thesis, University of Alberta, Edmonton, Alta., April 1985.
2. J. Arumala and R. H. Brown, "Performance Evaluation of Brick Veneer and Steel Stud Backup", Department of Civil Engineering Clemson University, Clemson, South Carolina, 1982.
3. G. L. Bell and W. H. Gumpertz, "Engineering Evaluation of Brick Veneer/Steel Stud Walls. Part 2 Structural Design, Structural Behaviour, and Durability", Proceedings, Third North American Masonry Conference, Arlington, TX, June, 1985.
4. C. T. Grimm, "Design for Differential Movement in Brick Walls", Journal of the Structural Division, American Society of Civil Engineers, Vol. 101, No. ST 11, Proc. Paper No. 11739, November, 1975, pp. 2385-2403.
5. J. G. Borchelt. "Masonry Curtain Walls on Tall Buildings", Proceedings of the 5th International Brick Masonry Conference, Washington, D. C., 1979.
6. P. Ameny and E. L . Jessop, "Masonry Cladding: A Report On Causes and Effects of Failures", Procedings of the 7th International Brick Masonry Conference, Melbourne, Australia, 1985.
7. A. A. Hamid, I. J. Becica and H. G. Harris, "Performance of Brick Masonry Veneers", Proceedings of the 7th International Brick Masonry Conference, Melbourne,

Australia, 1985.

8. United States Gypsum Company, "System Folder - USG Curtain Wall Systems - SA-805", United States Gypsum Company, Chicago, IL., 1984.
9. J. A. Wintz and Allan H. Yorkdale, "Brick Veneer Panel and Curtain Wall Systems - A Designer's Guide", in The Construction Specifier, Alexandria, Vt., Dec., 1983.
10. C. T Grimm, "Brick Veneer: A second Opinion", Letter to the Editor, in The Construction Specifier, Alexandria, Vt., April, 1984.
11. CAN3-S304-M86, "Masonry Design and Construction for Buildings", Canadian Standards Association., Rexdale, Ontario, 1986.
12. CAN3-A370-M84, "Connectors for Masonry", Canadian Standards Association., Rexdale, Ontario, 1984.
13. American Concrete Institute Standard, ACI 531-79, "Building Code Requirement for Concrete Masonry Structures", Detroit, Michigan, 1979.
14. National Concrete Masonry Association, "Specifications for the Design and Construction of Load-Bearing Concrete Masonry", National Concrete Masonry Association, Herdon, NA., 1983.
15. Brick Institute of America, "Brick Veneer Panel and Curtain Walls", Brick Institute of America Technical Note 28B revised, Maclean, Virginia, 1980.
16. R. H. Brown and J. A. Murden, "Effect of Lateral Load Cycling on Composite Action Between Gypsum Sheathing and

Metal Studs", Proceedings of the 3rd Canadian Masonry Symposium, Fredericton, NB, 1985.

17. M. A. Hatzinikolas, R. Lee, J. Longworth and J. Warwaruk "The Behaviour of Styrofoam SM Insulation as Exterior Sheathing in Brick Veneer and Metal Stud Wall Systems", Report of Commissioned Tests, Department of Civil Engineering, University of Alberta, Edmonton, 1986.
18. National Concrete Masonry Association, "The Masonry Veneer/Metal Stud Exterior Wall System - How Well Does it Perform?", Informational Document by The National Concrete Masonry Association, Herdon, NA., 1983.
19. M. J. Marchello, "USG Tests Provide New Data for Determining Limiting Heights of Steel-Stud/Brick Veneer Curtain Wall Assemblies", Form and Function, United States Gypsum Company, Chicago, IL., 1981.
20. R. H. Brown and R. Elling, "Lateral Load Distribution in Cavity Walls", Proceedings of the 5th International Brick Masonry Conference, Washington, D. C., 1979.
21. J. G. MacGregor, "Safety and Limit States Design for Reinforced Concrete", Canadian Journal of Civil Engineering, Vol. 3, pg. 484-513, 1976.
22. D. E. Allen, "Limits States Design - A Probabilistic Study", Canadian Journal of Civil Engineering, Vol. 2, pg. 36-49, 1975.
23. A. S. Nowak and N. C. Lind, "Practical Bridge Code Calibration", ASCE Journal of the Structural Division, Vol. 105(ST12), pg. 2497-1509, 1979.

24. The National Building Code Committee, "The National Building Code of Canada", Ottawa, Ontario, 1985 edition.

25. Mac

26. CSA Standard CAN3-S136-M84, "Cold Formed Steel Structural Members", Canadian Standards Association, Rexdale, Ontario, 1984.

27. CSA Standard CAN3-S16.1-M84, "Steel Structures for Buildings - Limit States Design", Canadian Standards Association., Rexdale, Ontario, 1984.

28. CSA Standard,CAN3-A23.3-M84, "Design of Concrete Structures for Buildings", Canadian Standards Association., Rexdale, Ontario, 1984.

29. "Commentary on the National Building Code of Canada", Canadian Standards Association, Rexdale, Ontario, 1986.

30. J. G. Borchelt, "Brick Veneer and Structural Frames: Dimensional Tolerances, Design Errors and Construction Problems", Proceedings, Third North American Masonry Conference, Arlington, Tx., June, 1985.

31. M. Hatzinikolas, J. Longworth, J. Warwaruk, "Strength and Behaviour of Metal Ties in 2-Wythe Masonry Walls", Alberta Masonry Institute, Edmonton , Alberta, 1981.

32. K. W. Pocholok, M.Hatzinikolas, J. Warwaruk, "Shear Connectors for Masonry Cavity Walls", Proceedings, 4th North American Masonry Conference, Los Angeles, 1987.

33. CSA Standard, A179 M-76, "Mortar and Grout for Unit Masonry", Canadian Standards Association., Rexdale, Ontario, 1976.

34. M.Hatzinikolas, J. Longworth, J. Warwaruk, "Concrete Masonry Walls", Structural Engineering Report No. 70, Department of Civil Engineering, University of Alberta, Edmonton, Alberta, 1978.

35. International Conference of Building Officials, "The Uniform Building Code", Section 2411, Whittier, CA., 1985 Edition.

36. British Standard, BS 5628, Part 1, "Code of Practice for Structuraluse of Masonry: Part 1 Unreinforced masonry", British Standards Institution, London, England, 1985.

37. W. M. McGinley, J. Warwaruk, J. Longworth, M. Hatzinikolas, "Analysis of Masonry Curtain Wall Systems", Proceedings, ASCE, Structures Congress 86, New Orleans, 1986.

APPENDICES

APPENDIX A - MASONRY MATERIAL TESTS

For each wall specimen, a minimum of eight mortar cubes were made and tested according to CSA Standard A-179 M-76[33]. The average cube compressive strengths and their standard deviations are listed in Table A-1.

Two brick prisms were cut from the veneer of each wall specimen. One prism was tested under third point loading to determine the modulus of rupture of the veneer and one prism was compressed under axial load to determine an the elastic modulus of the veneer. To determine the modulus of rupture, each eight brick long, one and one-half brick wide prism was tested so that three mortar joints were within the maximum moment region. These tests were performed horizontally and a total of seven mortar joints were subjected to flexure. The modulus of rupture for each prism was calculated using the maximum moment at the location of the crack. Included in this calculation was the self weight of the brick. Table A-1 lists the modulus of rupture for each prism.

For the elastic modulus tests, Demec Gauge points were affixed on each side of the prism, along its centre line. Each end of the prism was then capped with high strength plaster. A 10 inch gauge length was used and Demec Gauge readings were taken at intervals during the loading. Based on the net area of the veneer prism, average axial stresses were calculated. A linear regression was performed on the average stress-strain data points for each prism. An elastic modulus was derived based on these slopes, and these values

are listed in Table A-1.

Five brick units were tested in accordance to CSA Standard CAN3-A82.2-M78[33]. The average compressive failure stress of these brick units was 52.4 MPa, with a standard deviation of 4.6 MPa. Using the equation outlined in clause 4.3.3.3 of CSA Standard CAN3-S304-M-78, the compressive strength of the brick units is 45.6 MPa'. For this strength of brick and type S mortar, this standard also suggested that a value of 14000 Mpa be used for the nominal elastic modulus of the brick and mortar composite. However, Hatzinikolas et-al[34], conclude that this equation is inaccurate and suggest that the elastic modulus of concrete block masonry walls has a value of 750 f'm. The results of the veneer prism tests indicate that that this equation might also be unconservative for clay brick masonry. Based on E = 750 f'm, a nominal modulus of elasticity of 10,500 MPa was calculated for the clay brick veneer.

Table A-1 Summary of Masonry Veneer Tests

Specimen	Ave. Cube Strength (MPa)	Em* (MPa)	Modulus& (MPa)
NS1W1	8.69 (3.7)¢	9947 (77)	0.96
NS1W2	8.32 (2.7)	10076 (56)	0.26
NS1W3	8.01 (1.5)	10471 (98)	0.51
NS1W4	9.43 (2.0)	8853 (274)	0.43
NS1W5	15.08 (1.7)	7583 (75)	0.41
NS1W6	17.54 (4.4)	11364 (179)	0.60
NS2W1	5.66 (1.7)	7106 (71)	0.27
NS2W2	3.68 (2.2)	8861 (47)	0.86
NS2W3	7.48 (2.8)	8435 (111)	1.10
NS2W4	6.46 (1.9)	6323 (180)	0.95
NS2W5	5.35 (0.9)	6658 (148)	0.52
NS2W6	4.61 (2.1)	10071 (41)	0.41

* - Em is the elastic modulus of the veneer
& - Modulus is the modulus of rupture of the veneer
Average mudulus for Series 1 (NS1...) = 0.528 MPa (Sdev=0.24 MPa)
Average mudulus for Series 2 (NS2...) = 0.685 MPa (Sdev=0.331 MPa)
¢ - all values enclosed by brackets,(), indicate standard deviations

APPENDIX B - DETAILS OF EXPERIMENTAL PROGRAM

B-1 Track Tests

The deflection of the stud supporting track was investigated in this section of the experimental program.

Two specimens were tested, both fabricated from 16 gauge 90 mm studs and track. Each specimen consisted of a 470 mm length of stud fixed between two 300 mm sections of track. A 200 mm wood bearing stiffener was placed at midspan of each of the studs. This stiffener was used to preclude buckling of the stud at the centre point load.

Each track and stud assembly was placed between a pair of fixed channels. The track was fastened using 12 mm grade 2 capscrews spaced at 200 mm centres. Two metric dial gauges were then set at 30 mm from each end of the specimen. The loading apparatus, a single-action jack and load cell, was then located over midspan (see Figure B-1).

Using a hand hydraulic pump to actuate the jack, the specimen was loaded at its centre. Static loads and deflections were recorded up to the specimen's failure.

A linear regression analysis was used to fit a straight line through the initial linear portion of the load-deflection curve for the supports of each track specimen. Equation 6.1 was used to calculate an average effective track member area of 0.30 mm^2.

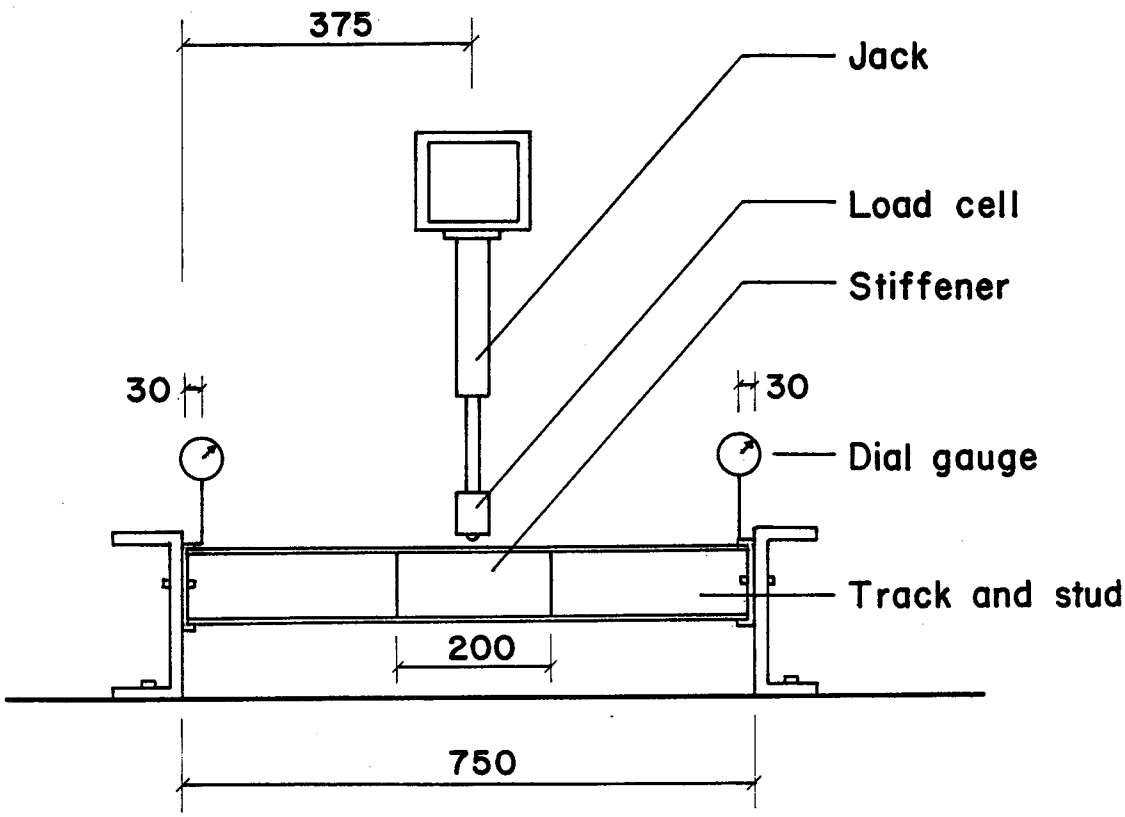

Figure B-1 Track-Stud Testing Apparatus

B-2 Tie Strain Gauges - Location and Calibration

Figures B-2, B-3 and B-4 show the placement of the strain guages used to measure axial load on each type of tie system. Figure B-5 shows the locations of strain gauges used to measure the shear bracket moment.

The 18 gauge corrugated tie systems and the shear bracket tie systems were calibrated during the axial load-deflection tie tests. Eight of the 18 gauge corrugated tie system specimens and all eleven of the shear bracket specimens were gauged for axial load measurement. During these tests, the strains from each strain gauge were recorded. One of the gauges on a 18 gauge corrugated tie specimen was damaged and the results from this specimen were discarded.

The strains from the two gauges on each specimen were averaged to produce an axial strain. For each tie type, a straight line was fitted to the data below the axial load-deflection proportional limit using a linear regression analysis. The analyses produced an axial load-strain slope of 8.4×10^6 N/mm/mm (Std. Deviation = 32.0%) for the 18 gauge corrugated tie systems, and a slope of 10.7×10^6 N/mm/mm (Std. deviation = 15.2%) for the shear bracket tie systems.

Calibration of the flat 18 gauge veneer-brick ties and the calibration of the "moment" strain gauges on the shear brackets was performed using a different procedure. Strain gauges were affixed to three specimens of the block-veneer

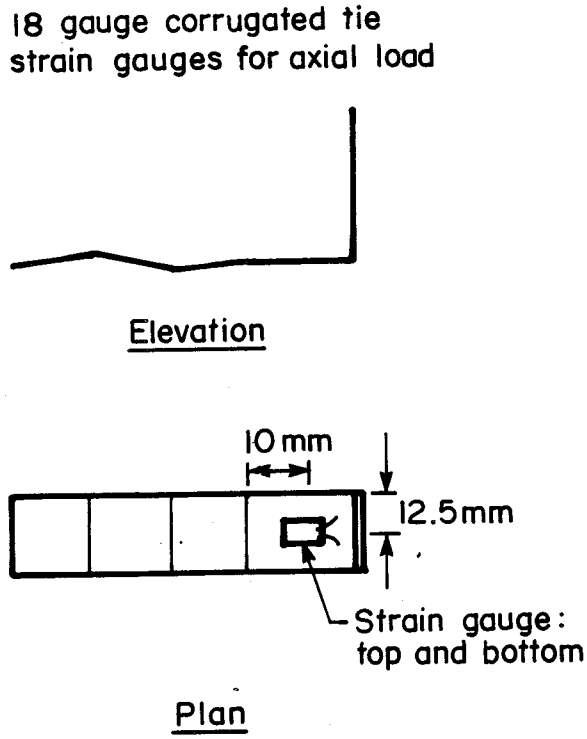

Figure B-2 Strain Gauge Details for Axial Load on 18 ga. Corrugated Ties

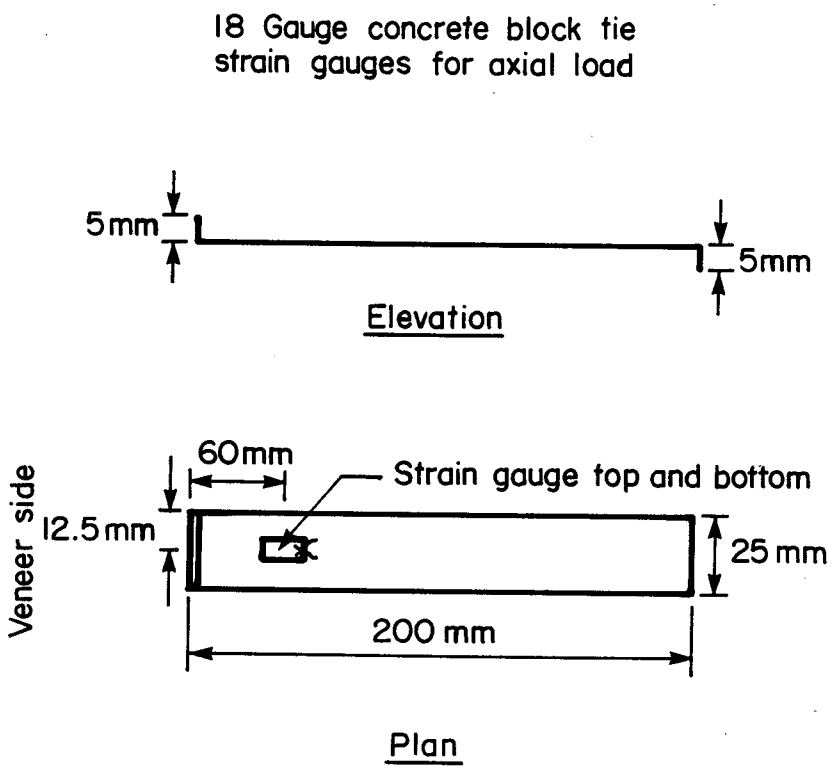

Figure B-3 Strain Gauge Details for Axial Load on Block-Veneer Ties

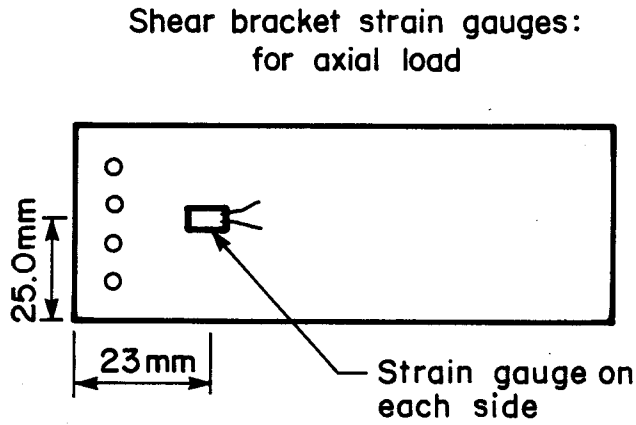

Figure B-4 Strain Gauge Details for Axial Load on Shear Bracket Ties

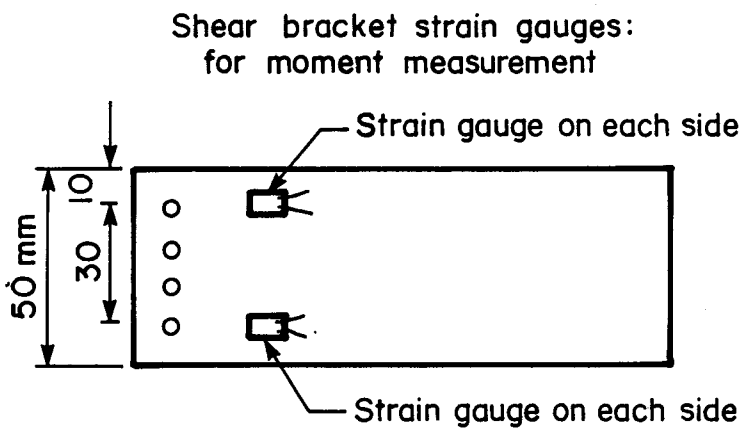

Figure B-5 Strain Gauge Details for Moment on Shear Bracket Ties

ties and to three shear brackets. These specimens were then placed in a tension coupon testing machine and loaded until the specimens yielded. Based on the measured stress-strain data, an average elastic modulus for each tie type was calculated. The block-veneer ties and the shear brackets had average moduli of elasticity of 199,980 MPa (Std. deviation = 572 MPa) and 185,110 MPa (Std. deviation = 623 MPa), respectively. For a measured strain, the elastic moduli and the average measured dimensions of each tie system were used to calculate the axial load and moment on each tie. It was assumed that these ties behaved elastically.

Simulated Negative Pressure - Testing Apparatus and Procedures

Figures B-6 and B-7 show the two pulley configurations used for the testing of the full-sized wall specimens under a simulated negative pressure. Table B-1 summarizes the dimensions shown in these figures for the four wall specimens tested and Figure B-8 shows the details of the pulleys and the pulley brackets.

During the testing of Specimen S2W1 it was observed that excessive friction was present in the pulley systems. Therefore, the brass bushings used for this first test were removed and replaced with needle bearings for the remaining wall tests. The configuration of the testing apparatus was altered so that the cable load was applied at both the top and bottom of each pulley line. Applying the cable load in

Table B-1 Dimensions of Testing Apparatus

Specimen	Dimensions (mm)											
	d1	d2	d3	d4	d5	d6	d7	d8	d9	d10	d11	d12
NS2W1	436	549	535	530	545	548	125	600	530	540	530	540
NS2W2	135	525	540	545	535	515	130	270	530	535	535	530
NS2W3	436	549	535	530	545	548	125	600	530	540	530	540
NS2W5	436	549	535	530	545	548	125	600	530	540	530	540
NS2W6	436	549	535	530	545	548	125	600	530	540	530	540

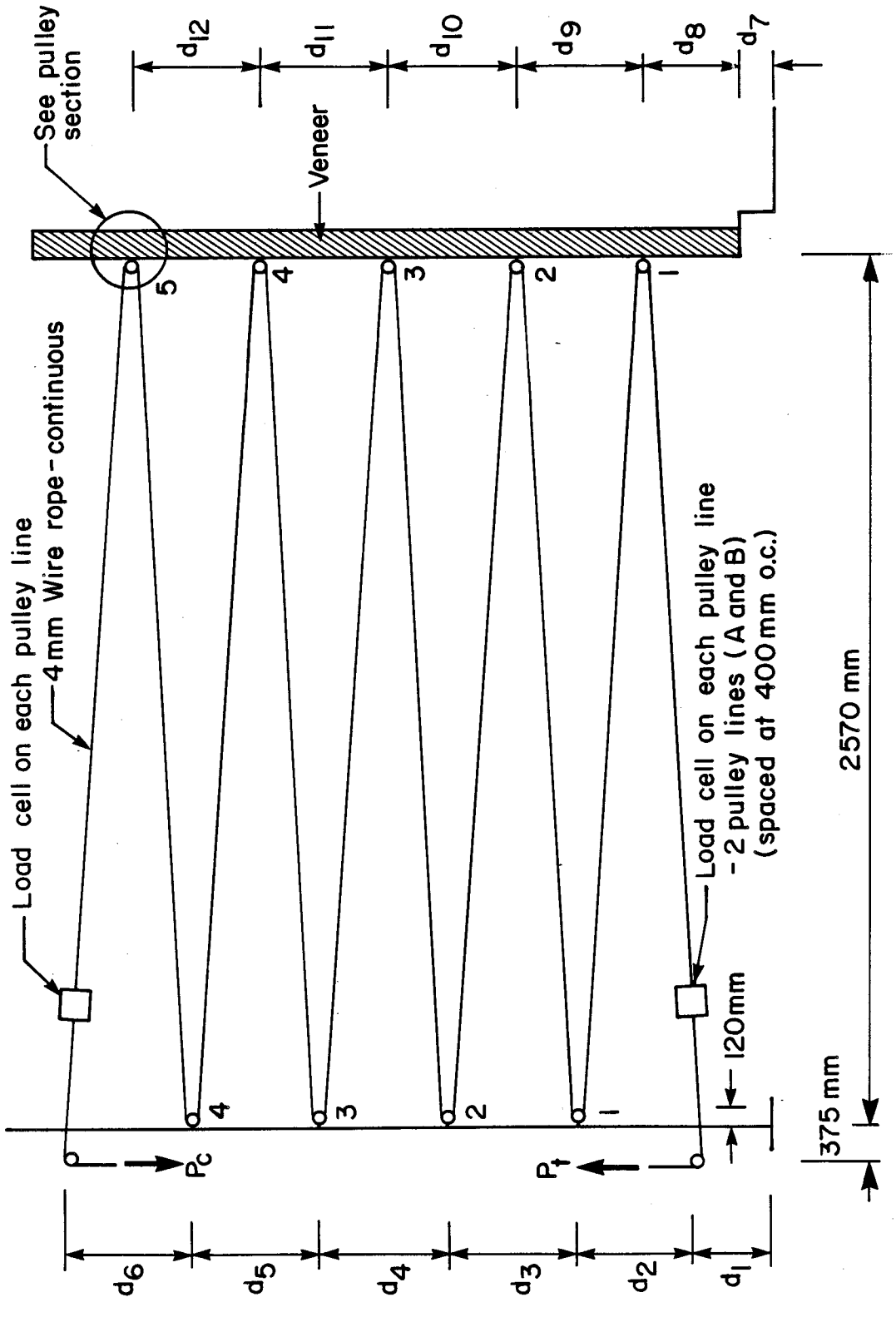

Figure B-6 Negative Testing Apparatus Configurations For All But Specimen S2W1

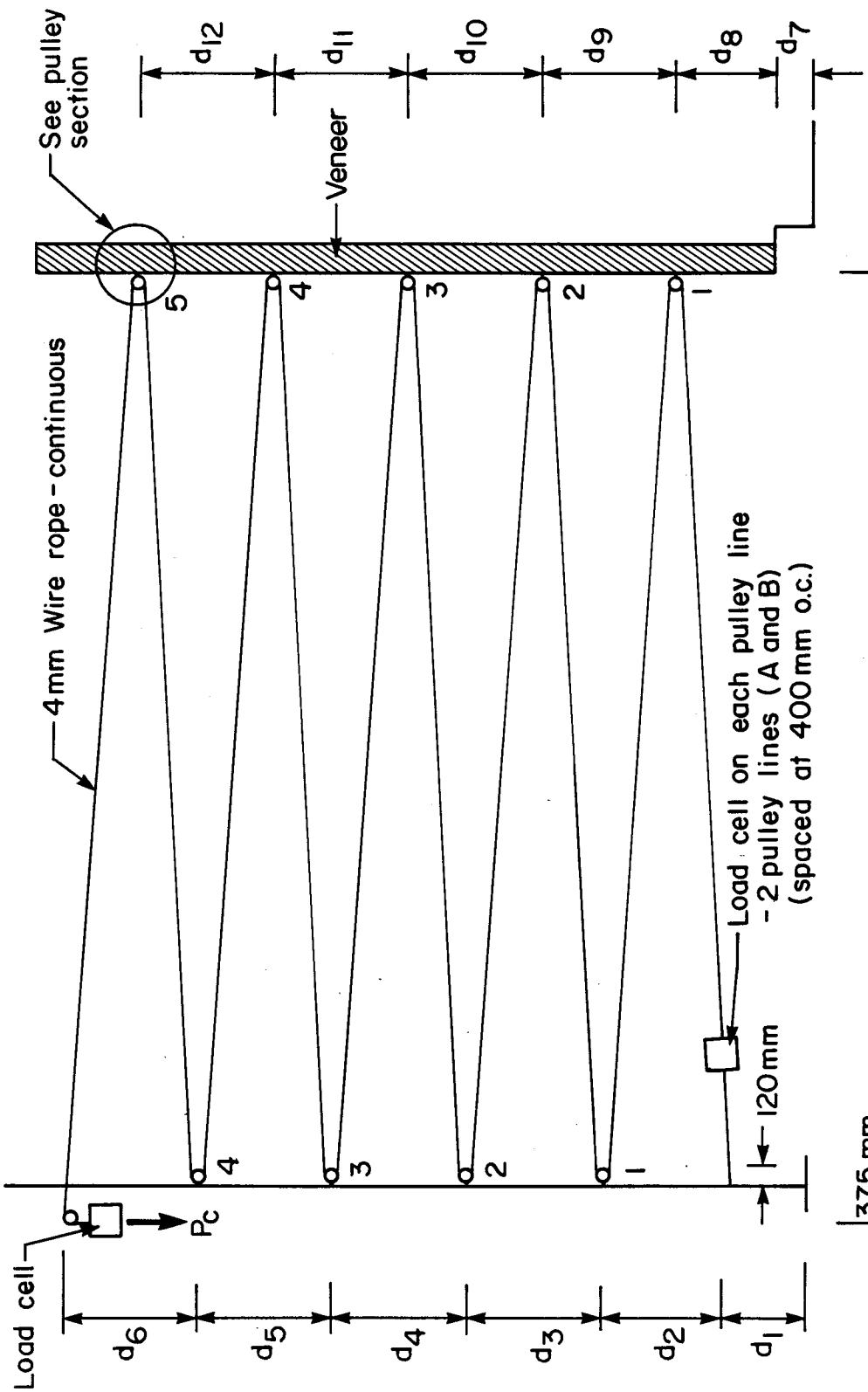

Figure B-7 Negative Testing Apparatus Configuration For Specimen S2W1

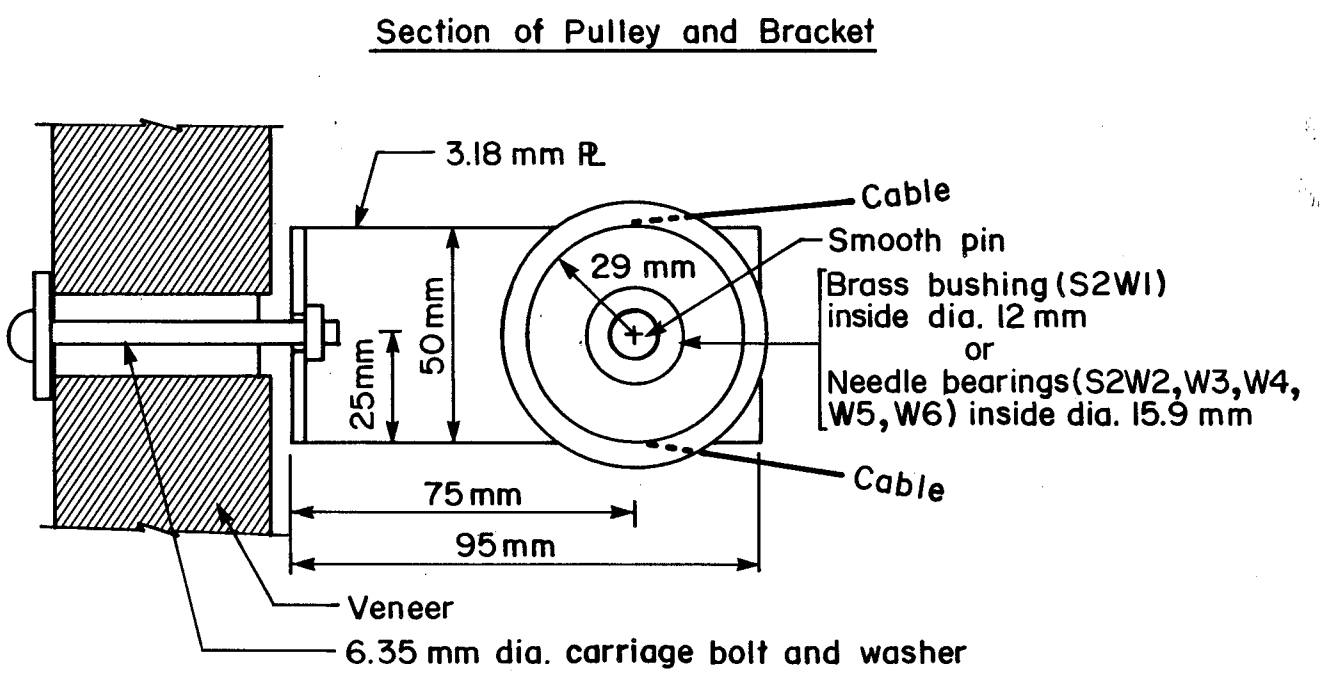

Figure B-8 Pulley and Pulley Bracket Details

this manner minimized the reduction in the applied loads caused by the pulley friction.

Cable loads were applied by advancing the nuts on the threaded bars shown in Plate B-1. In this manner the negative load was applied to the wall specimen under stroke control. The smaller threaded bars allowed the loads on each cable to be adjusted so that these loads remained approximately equal.

Five of the pulleys using brass bushings were tested to determine the amount of friction associated with the pulley configuration. These friction tests were conducted by suspending two 50 LB weights on each side of the pulley by a cable. Weight was then added to one side of the pulley until motion occurred. This procedure was performed twice for each pulley. An average coefficient of friction was then determined based on statics and the assumption that the pulley, pin and bracket were true and round. This procedure was repeated for all of the needle bearing pulleys. The pulley friction test results are summarized in Table B-2.

Table B-2 Pulley Friction Test Results

Pulley	Average Coef. of Friction
P1BL1	0.040*
P2BL1	0.051
P3BL1	0.055
P4BL1	0.038
P5BL1	0.064
P1BL2	0.072
P2BL2	0.055
P3BL2	0.041
P4BL2	0.046
P5BL2	0.046
P1RL1	0.056
P2RL1	0.071
P3RL1	0.043
P4RL1	0.103
P1RL2	0.056
P2RL2	0.059
P3RL2	0.044
P4RL2	0.045

P1BL1 - pulley 1 on brick line 1
P1RL1 - pulley 1 on reaction wall line 1
* - average of two tests

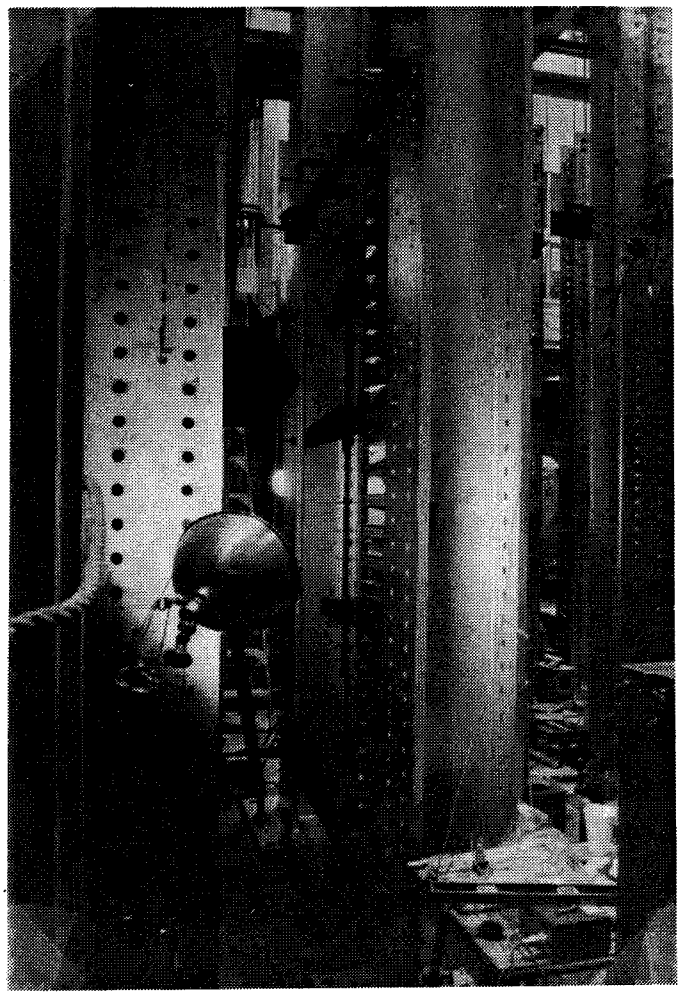

Plate B-1 Load Application Mechanism for Negative Pressure Apparatus

APPENDIX C - LOAD DEFLECTION CURVES

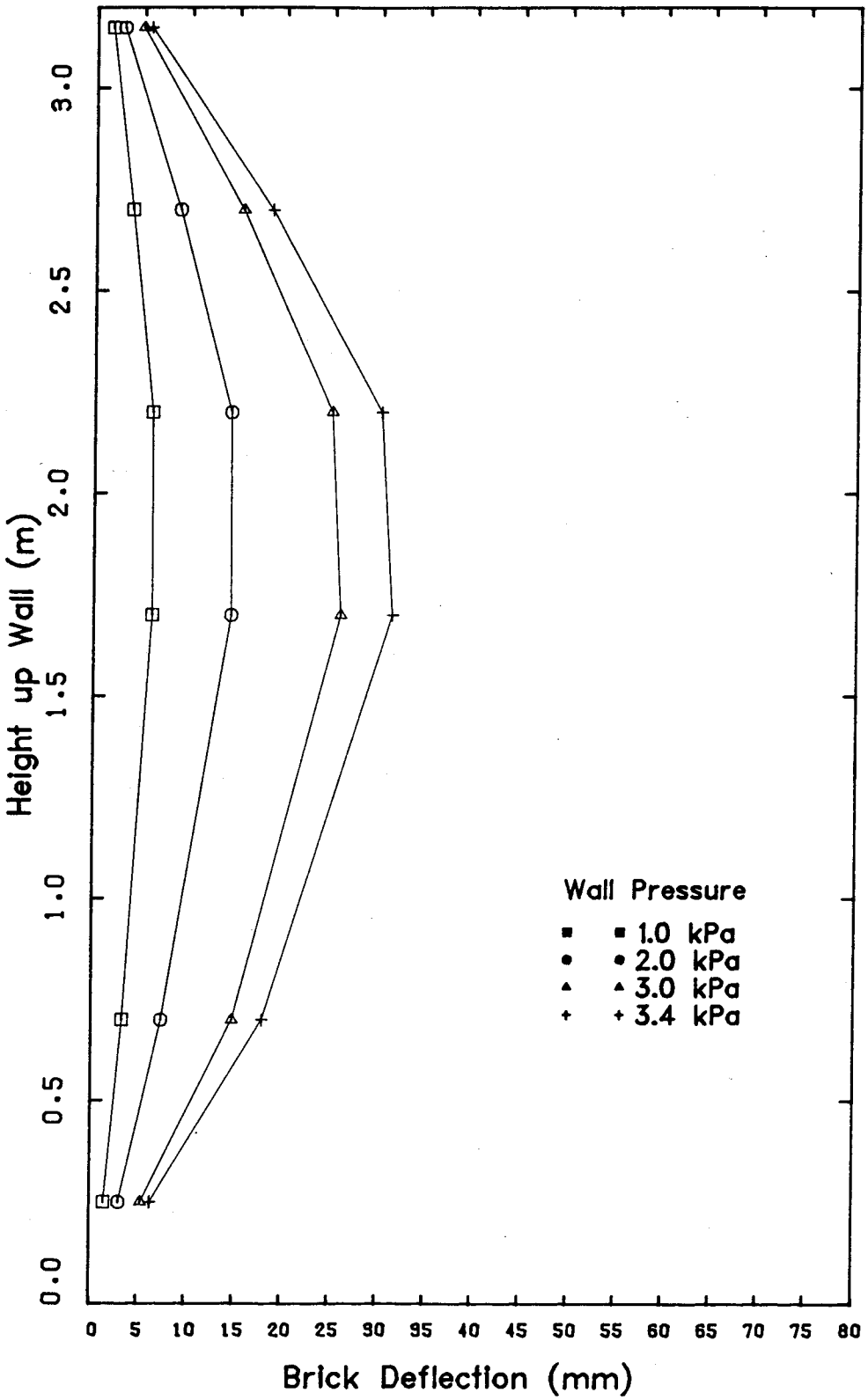

Figure C-1 Brick Veneer Deflections - Series No.1 Wall No.1

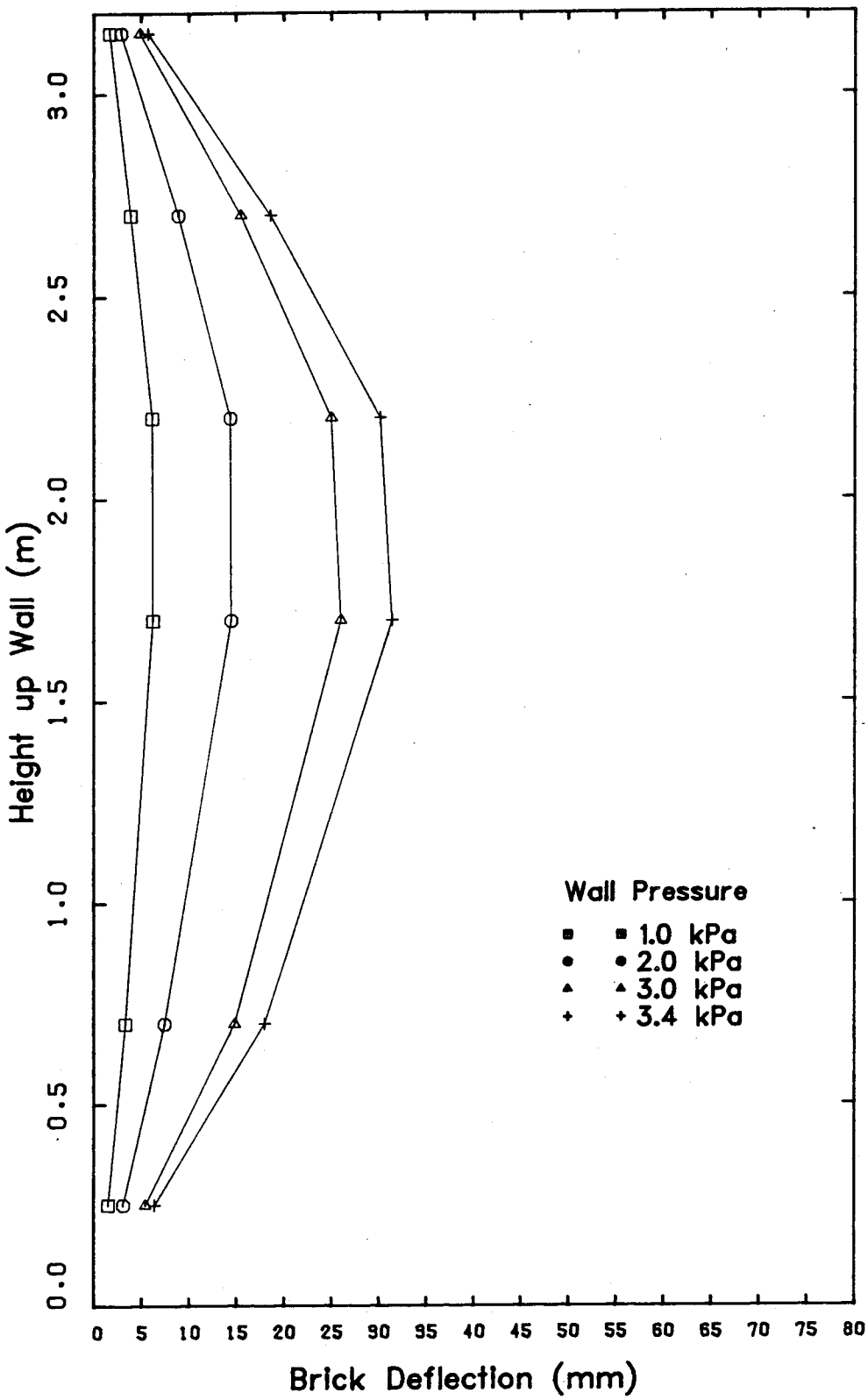

Figure C-2 Stud Wall Deflections - Series No.1 Wall No.1

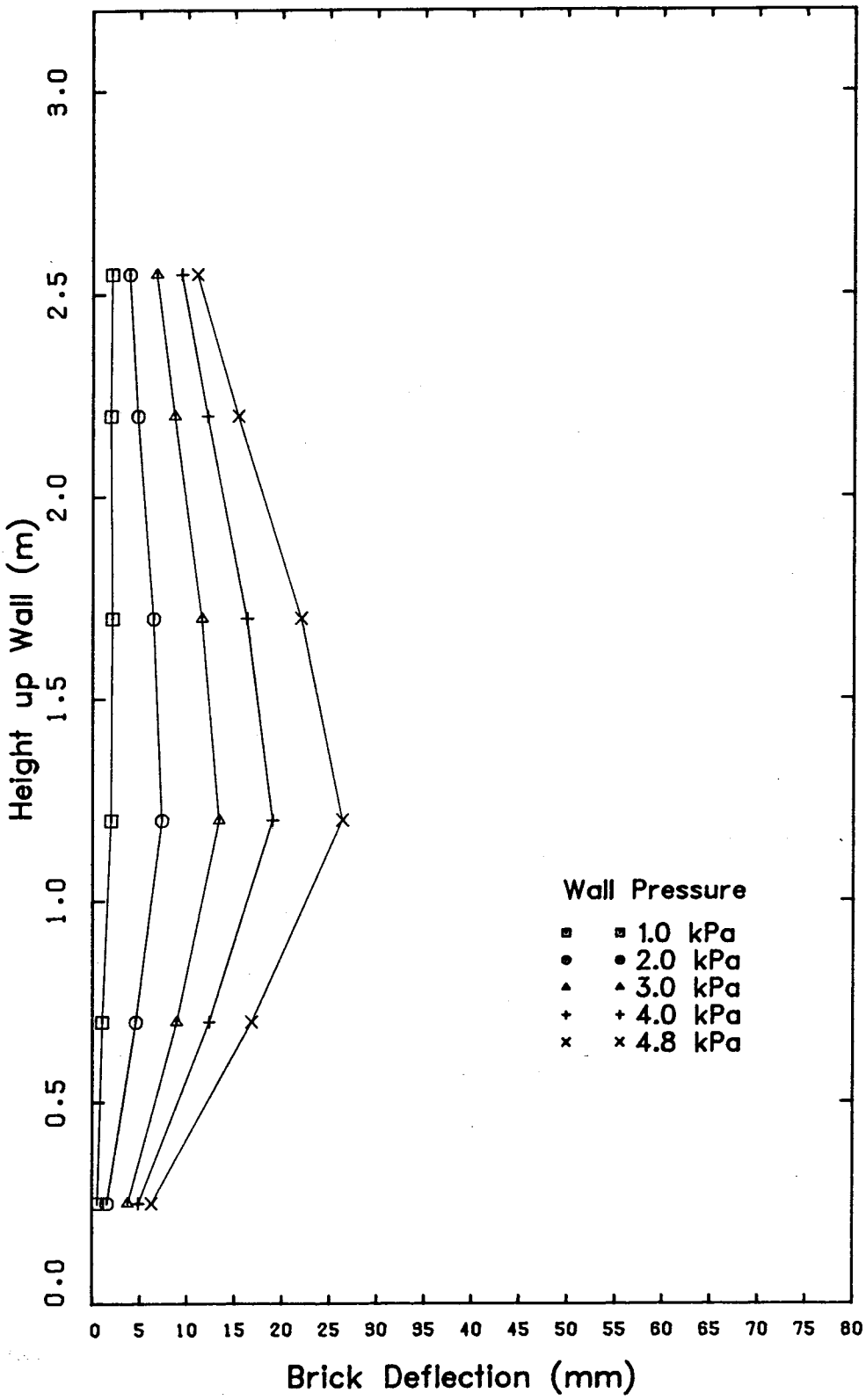

Figure C-3 Brick Veneer Deflections - Series No.1 Wall No.2

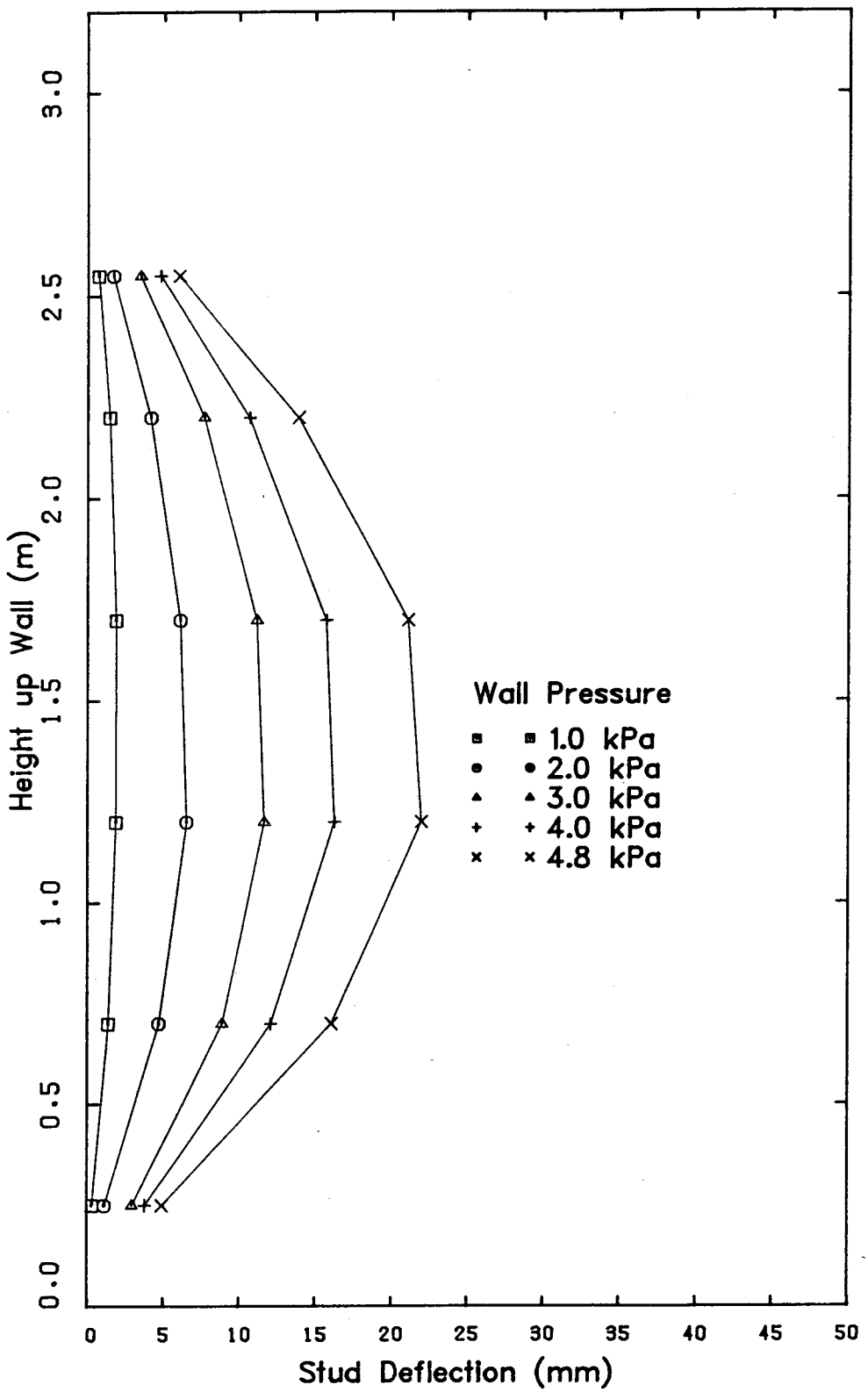

Figure C-4 Stud Wall Deflections - Series No.1 Wall No.2

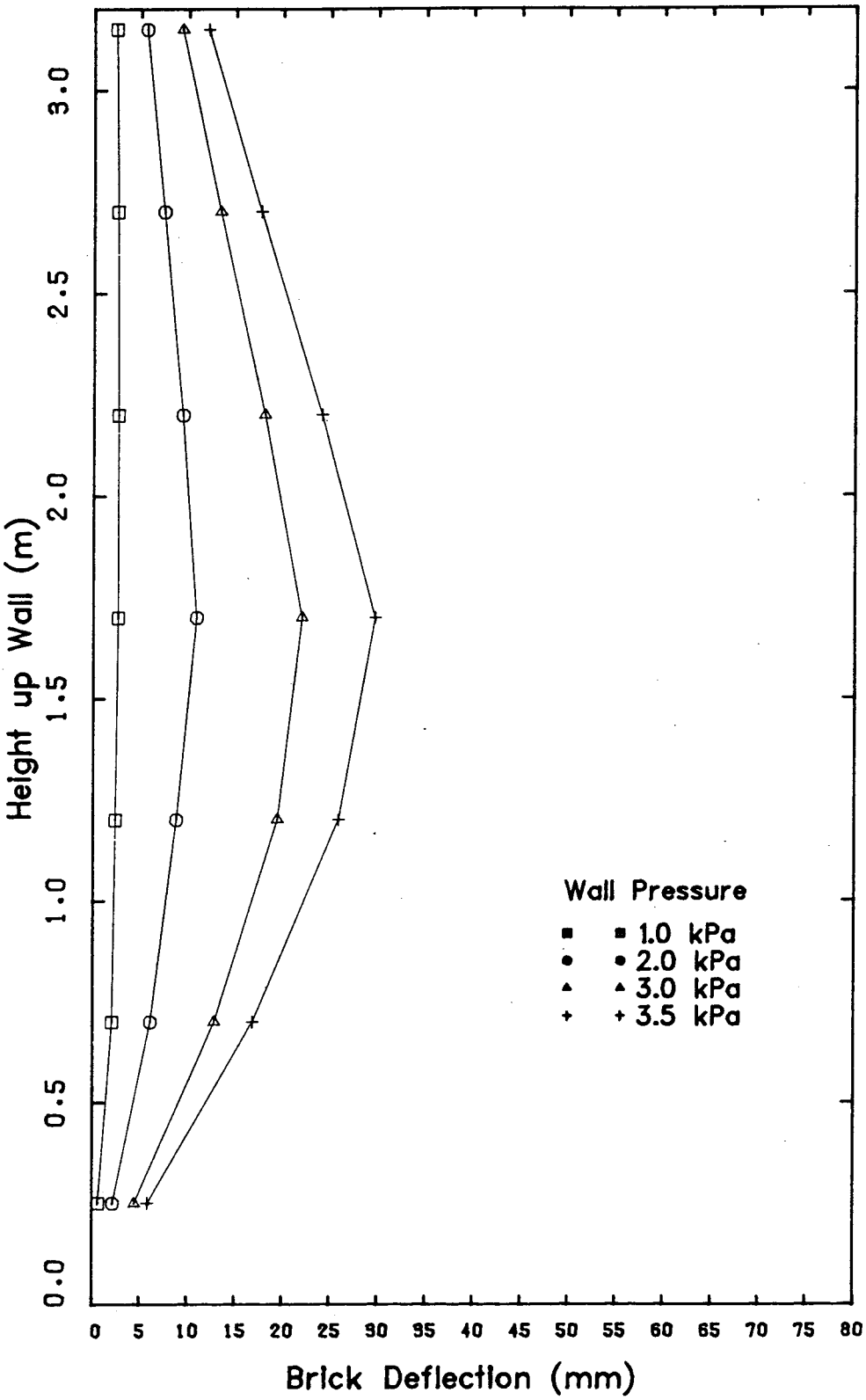

Figure C-5 Brick Veneer Deflections - Series No.1 Wall No.3

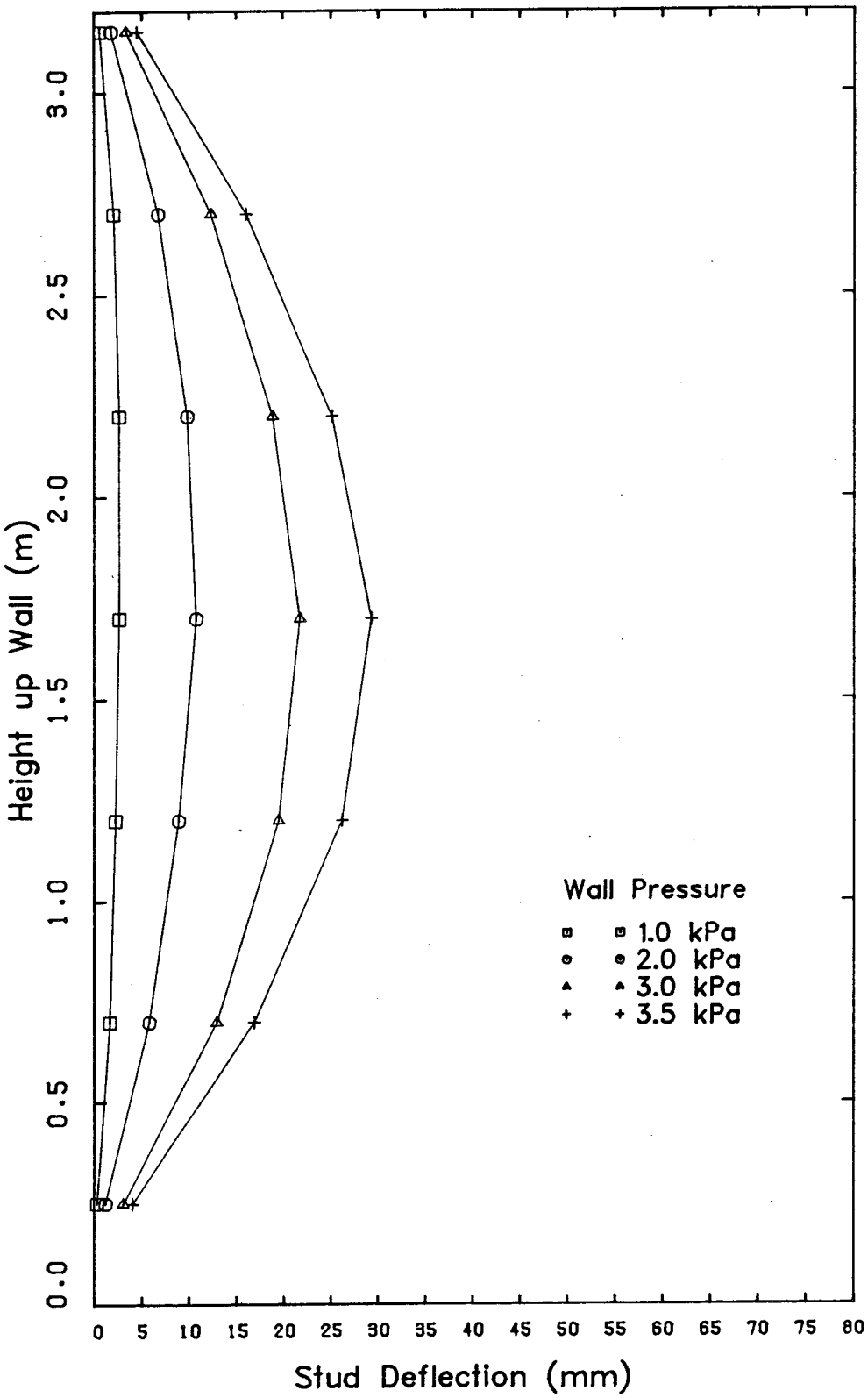

Figure C-6 Stud Wall Deflections - Series No.1 Wall No.3

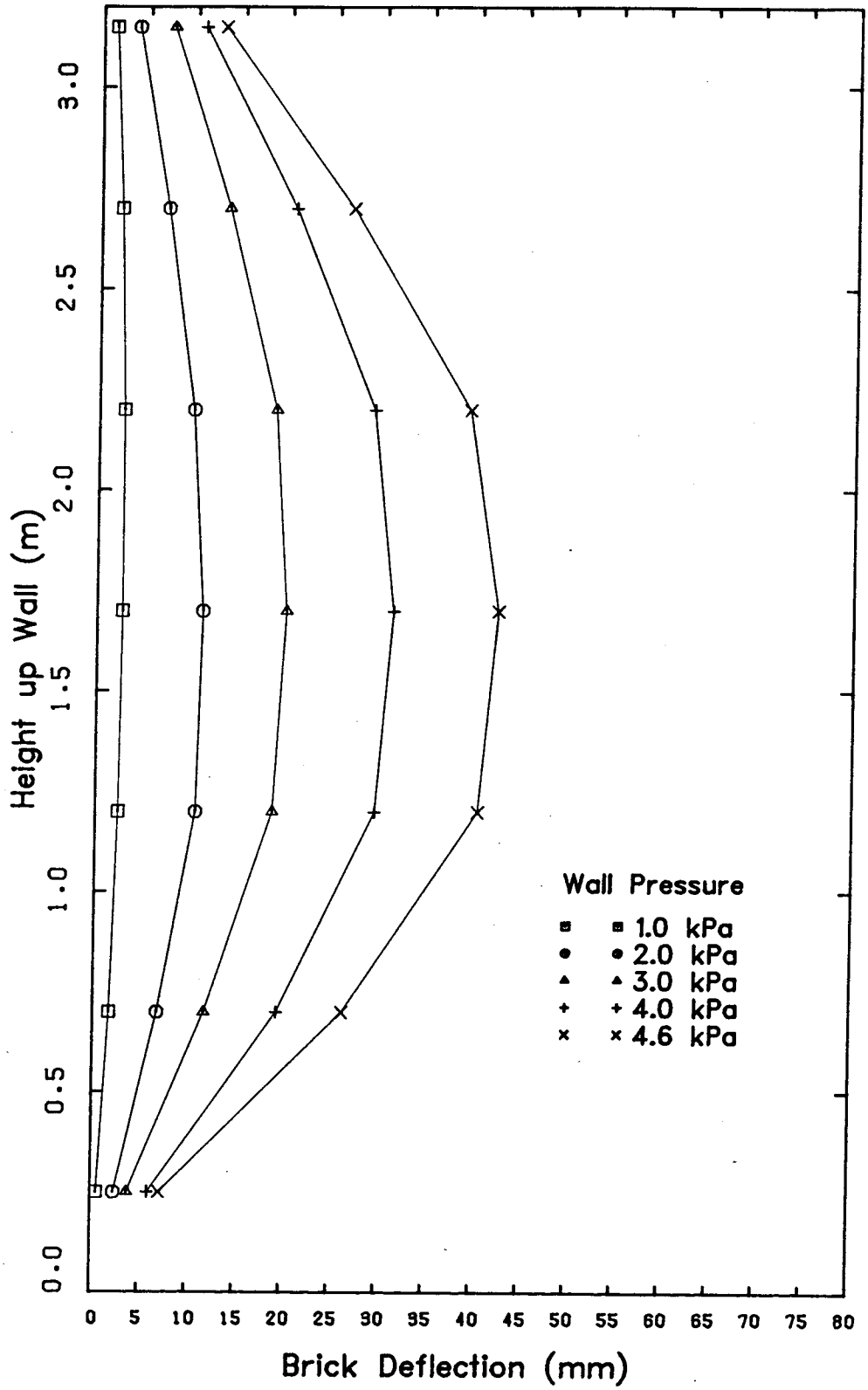

Figure C-7 Brick Veneer Deflections - Series No.1 Wall No.4

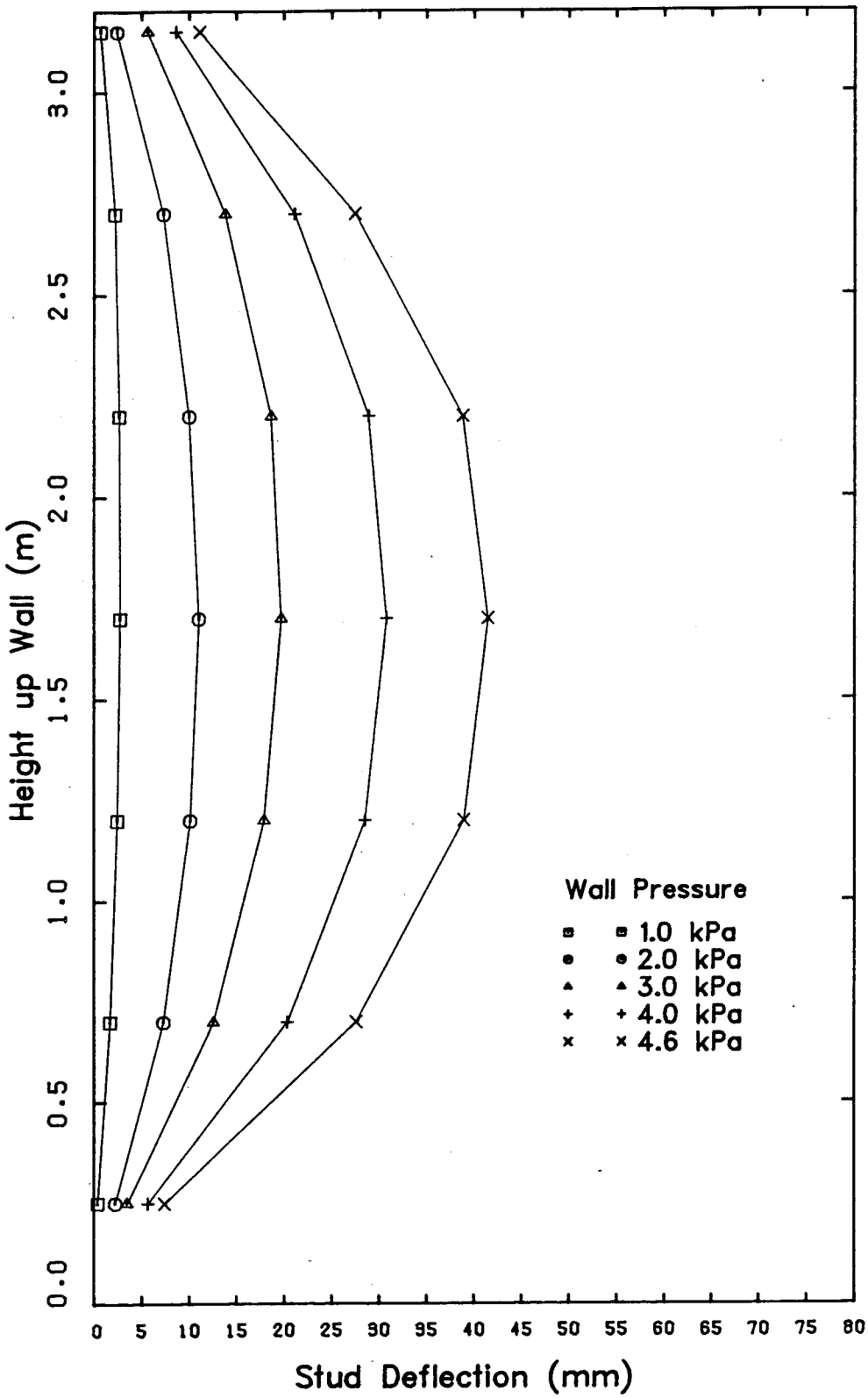

Figure C-8 Stud Wall Deflections - Series No.1 Wall No.4

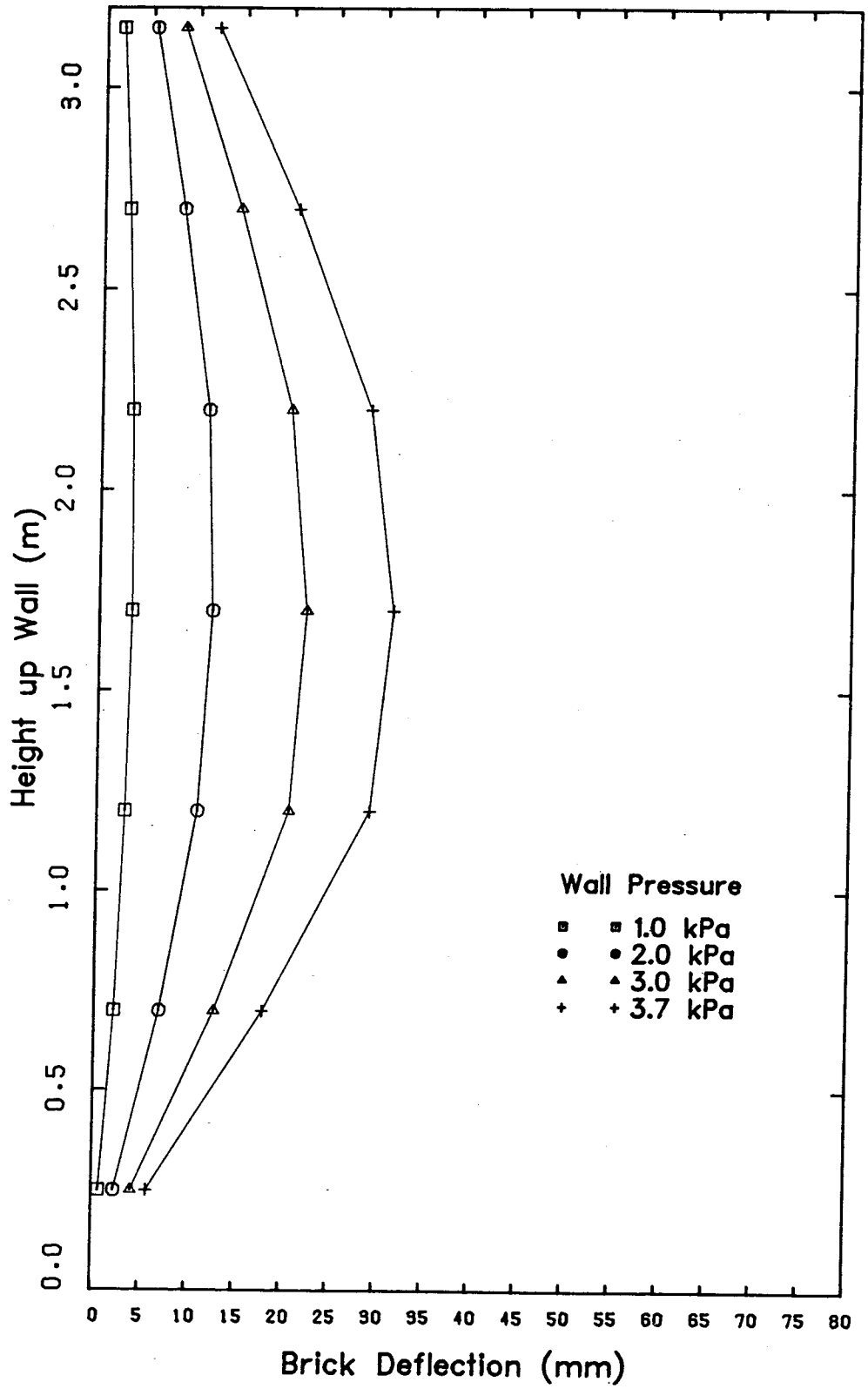

Figure C-9 Brick Veneer Deflections - Series No.1 Wall No.5

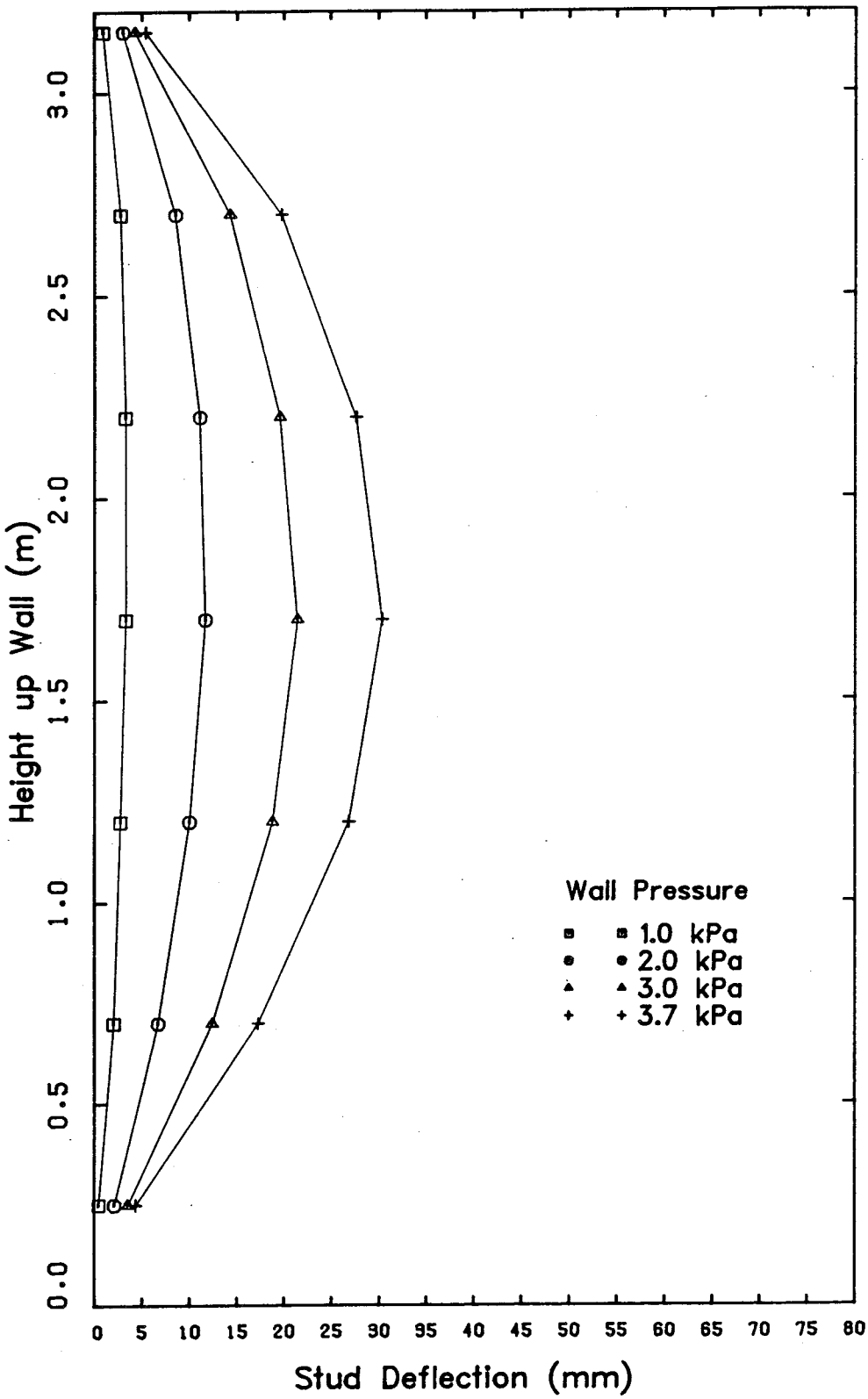

Figure C-10 Stud Wall Deflections - Series No.1 Wall No.5

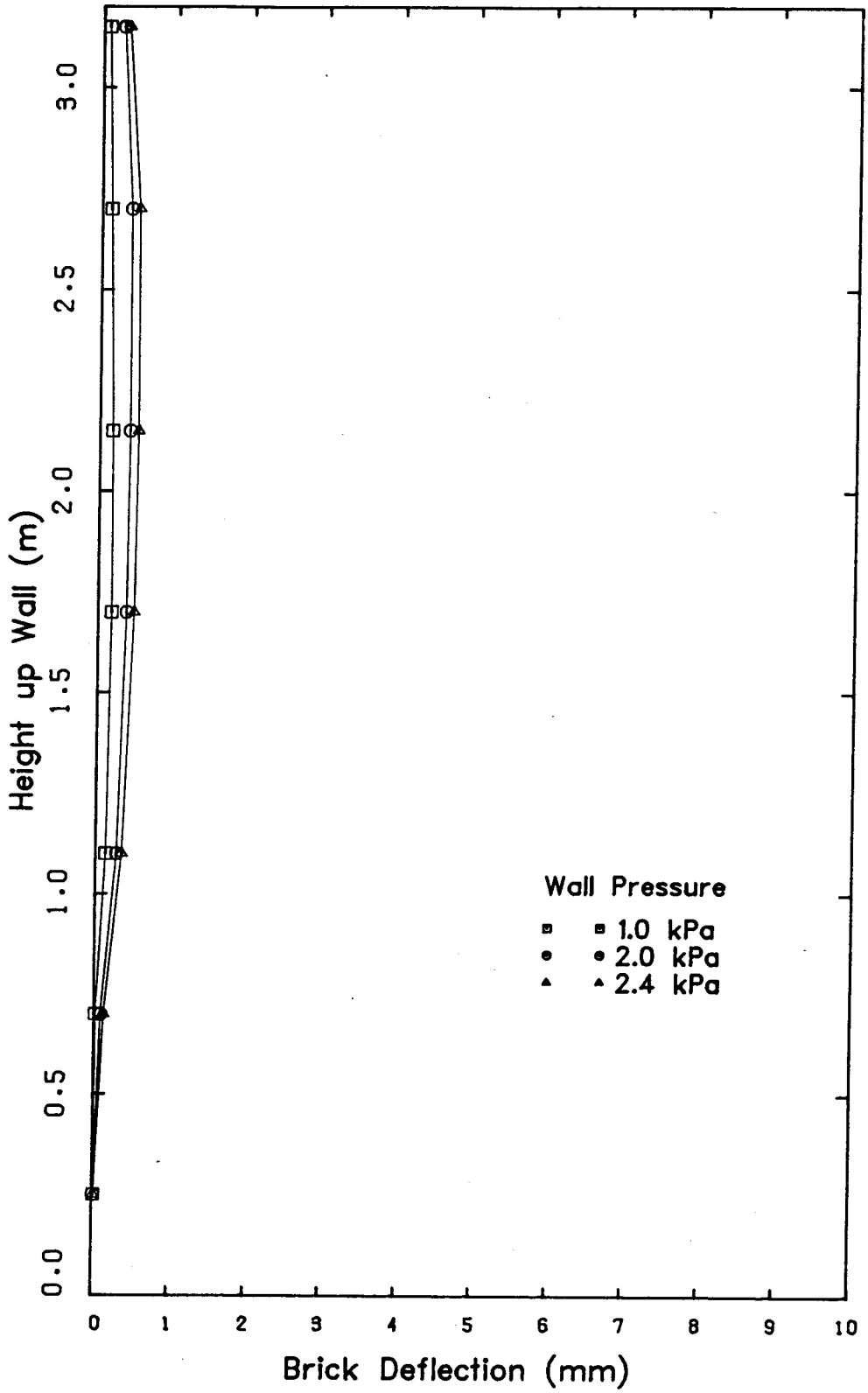

Figure C-11 Brick Veneer Deflections - Series No.1 Wall No.6

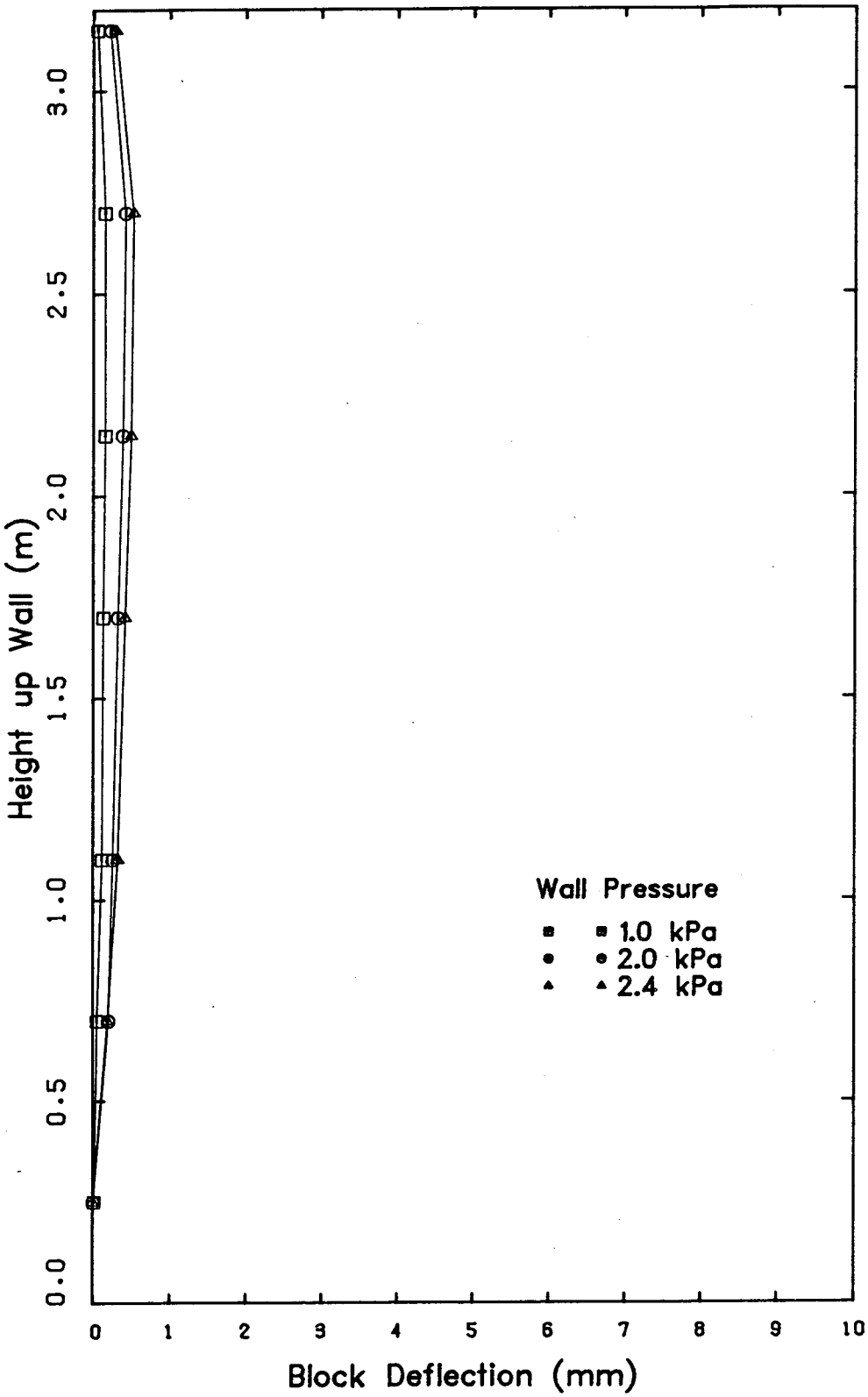

Figure C-12 Block Wall Deflections - Series No.1 Wall No.6

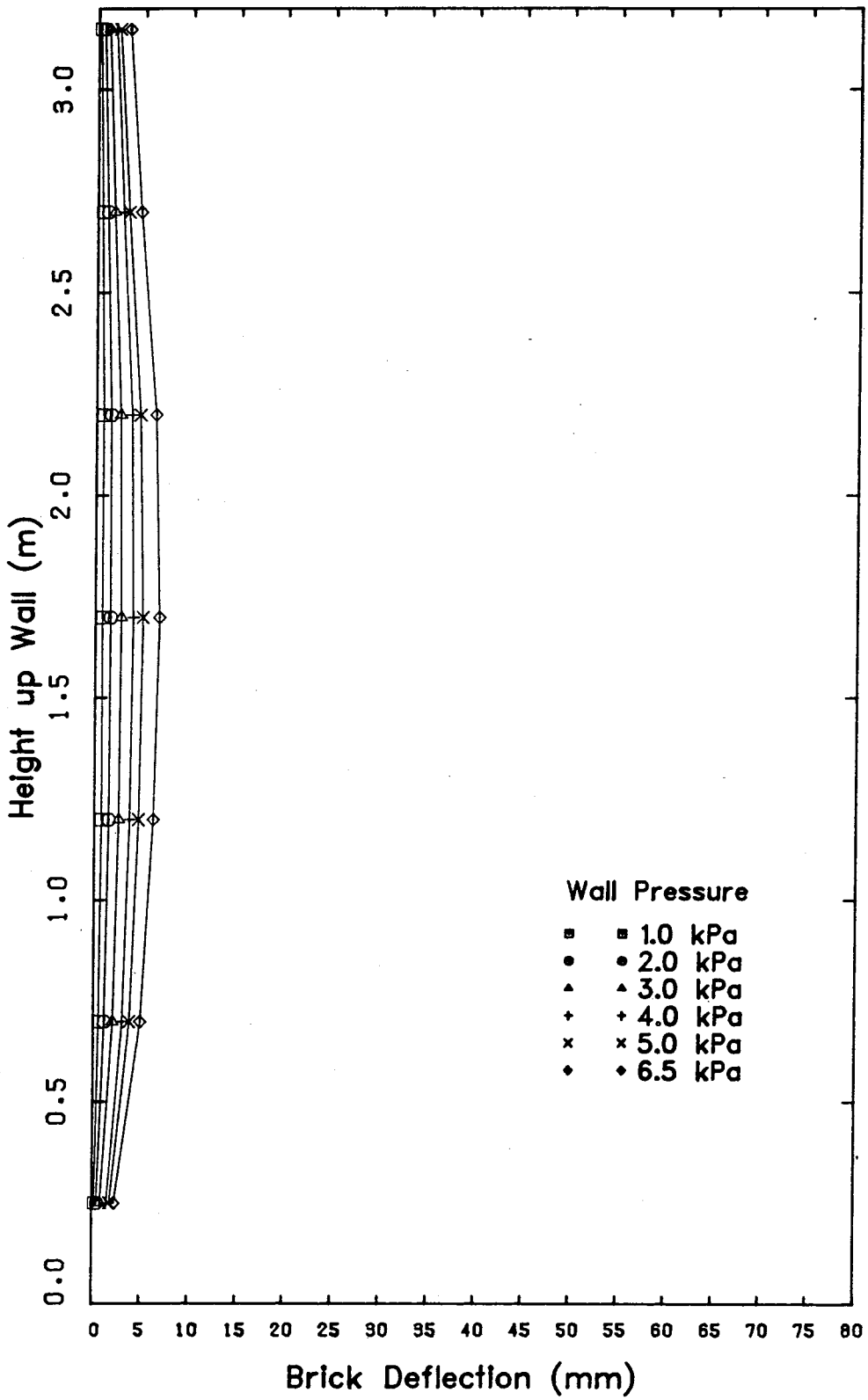

Figure C-13 Brick Veneer Deflections - Series No.2 Wall No.4

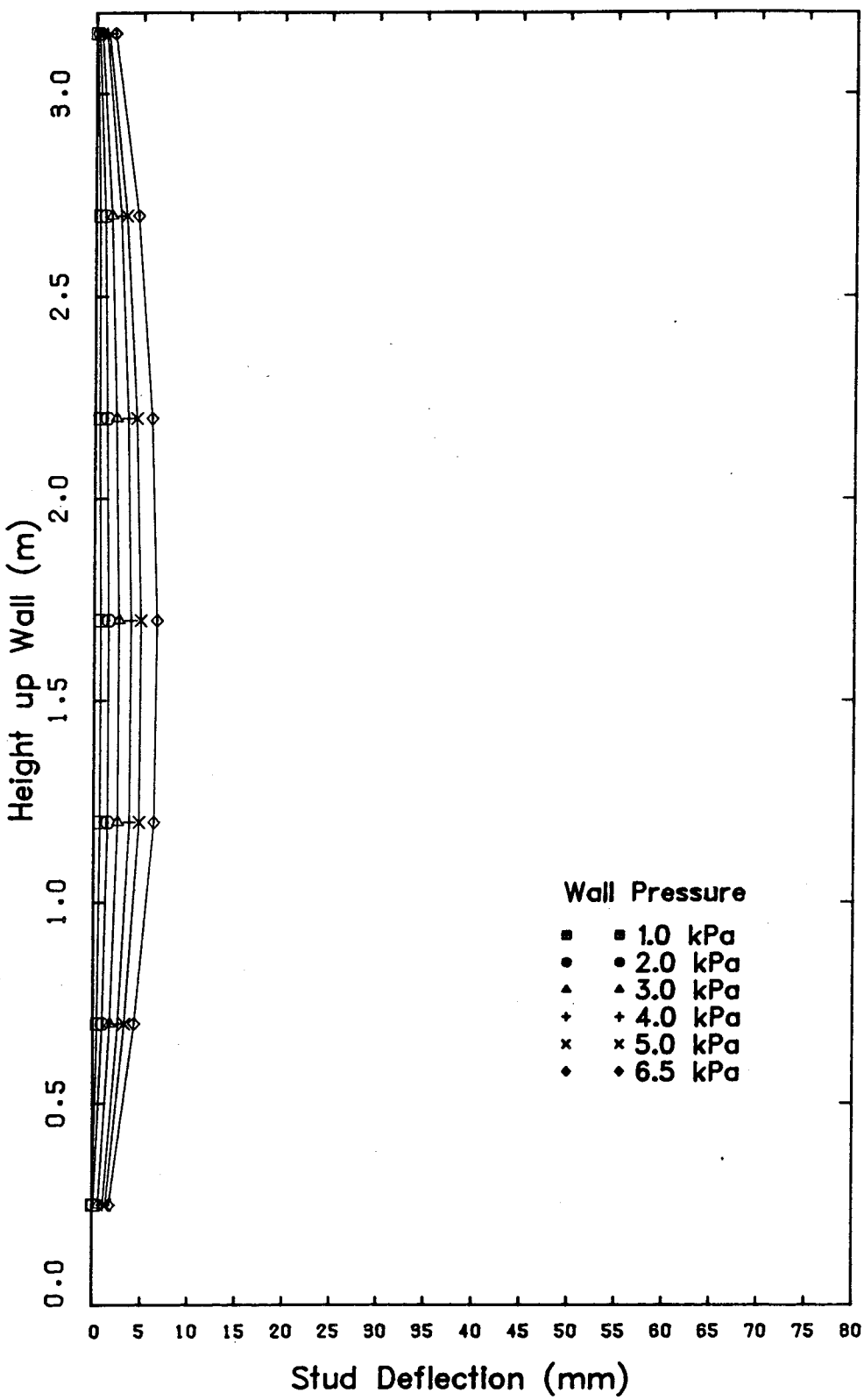

Figure C-14 Stud Wall Deflections - Series No.2 Wall No.4

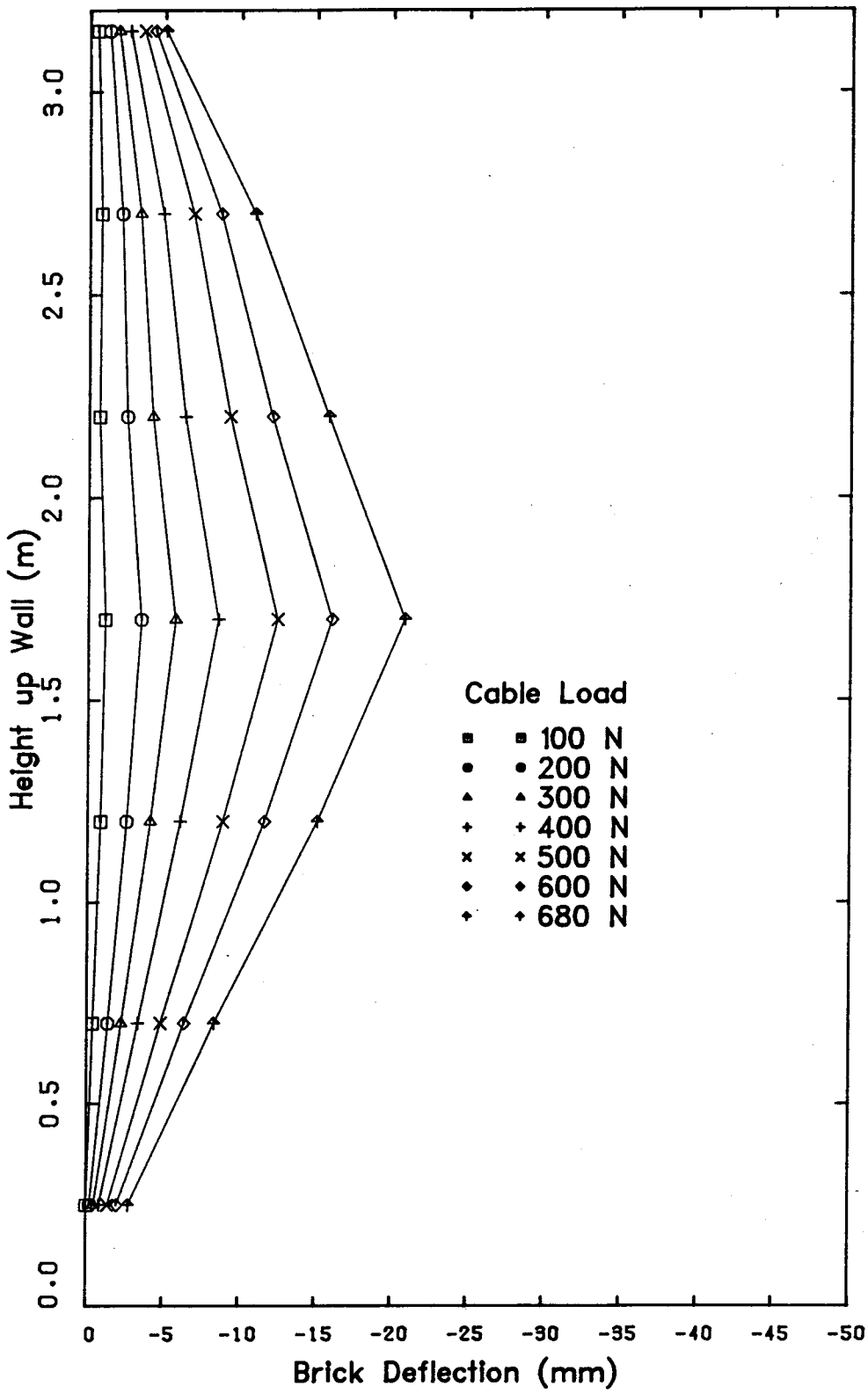

Figure C-15 Brick Veneer Deflections - Series No.2 Wall No.1

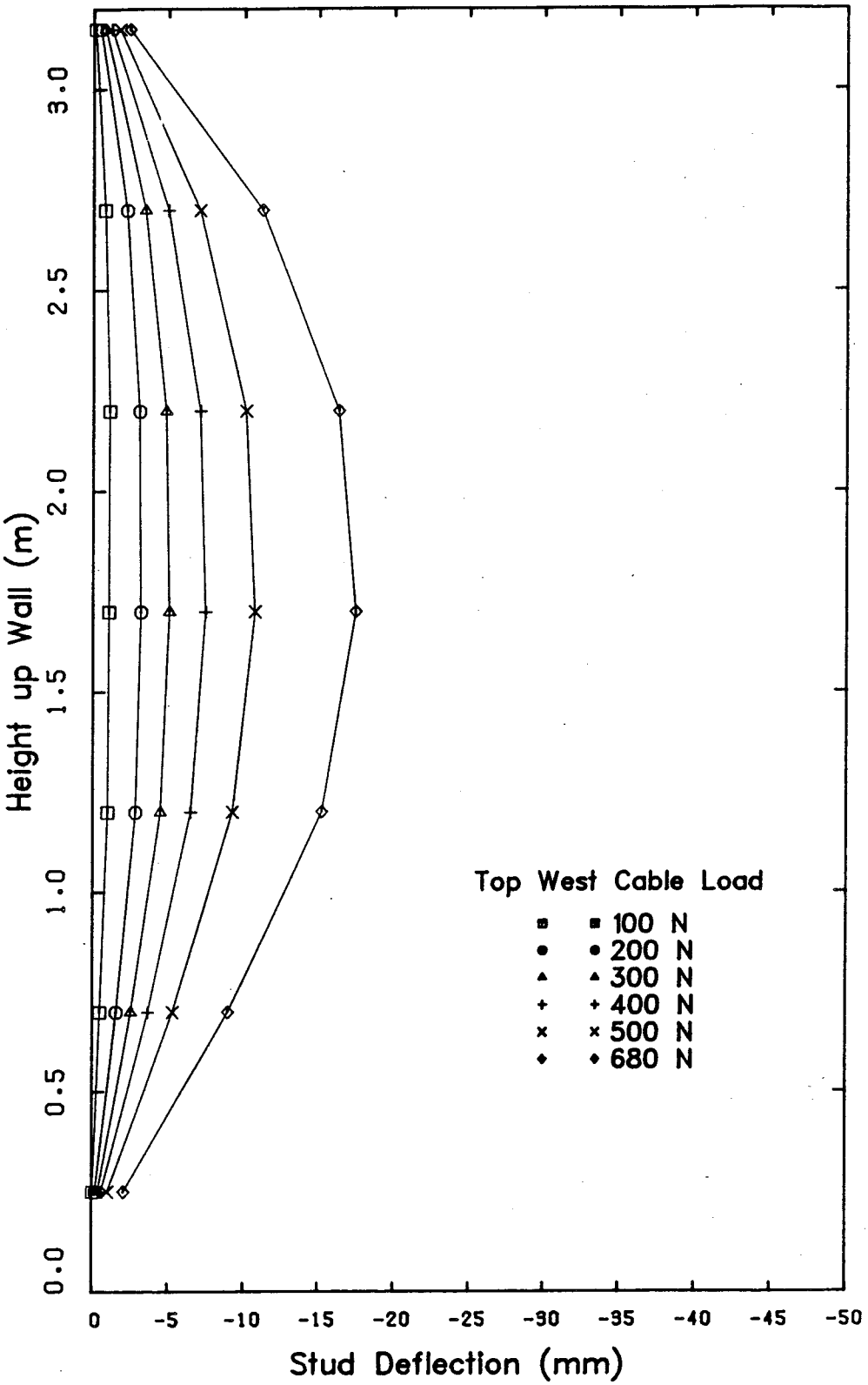

Figure C-16 Stud Wall Deflections - Series No.2 Wall No.1

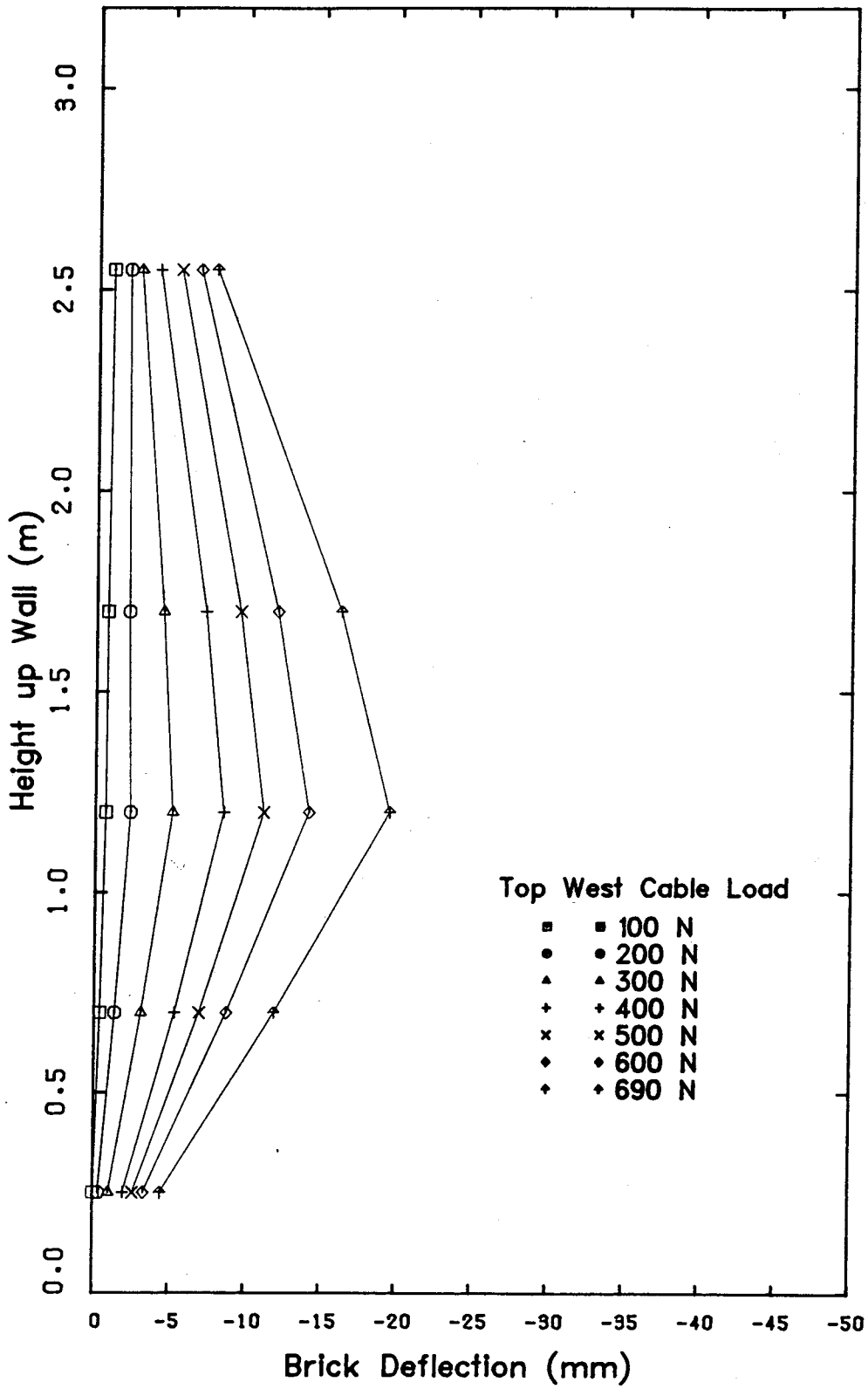

Figure C-17 Brick Veneer Deflections - Series No.2 Wall No.2

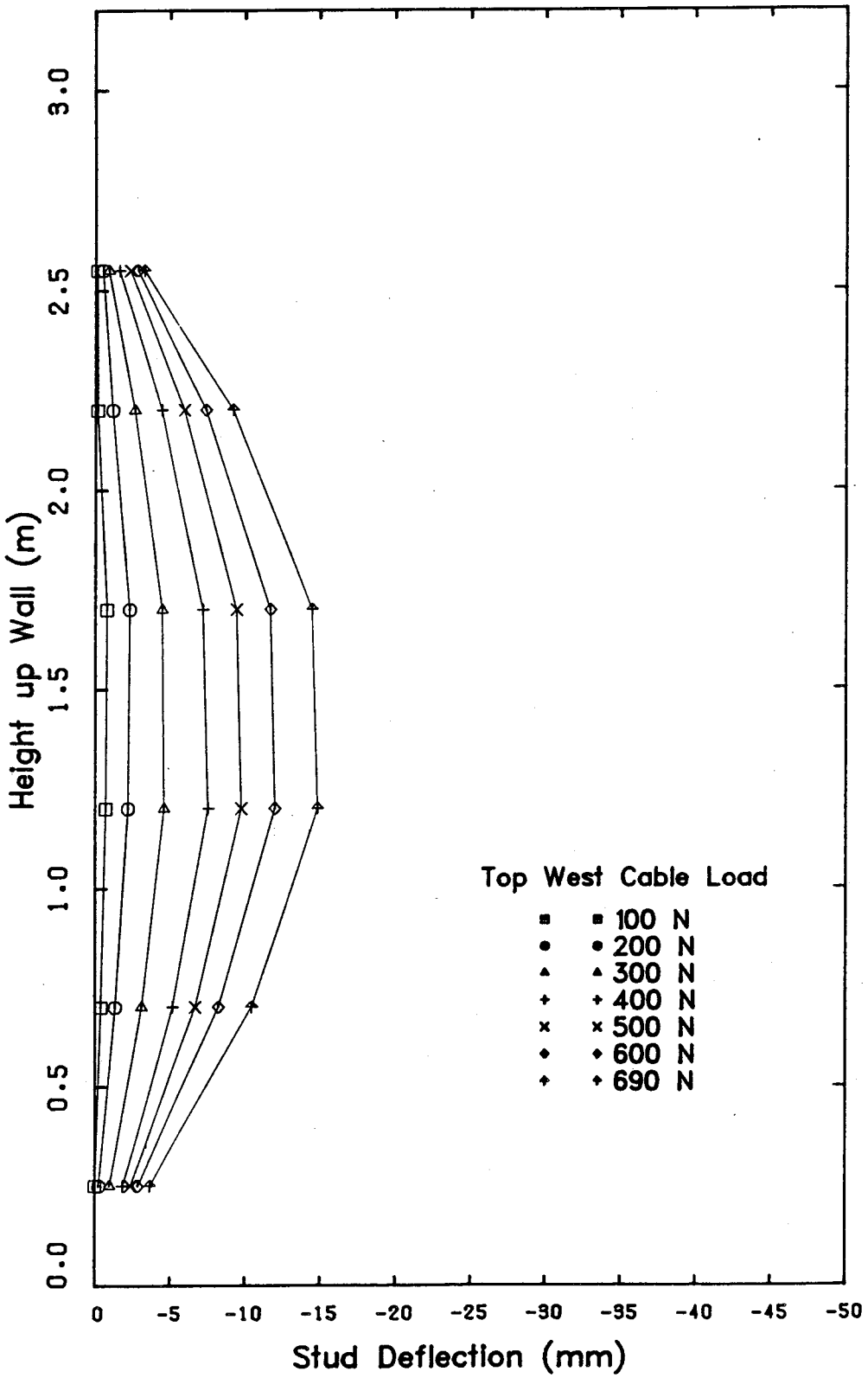

Figure C-18 Stud Wall Deflections - Series No.2 Wall No.2

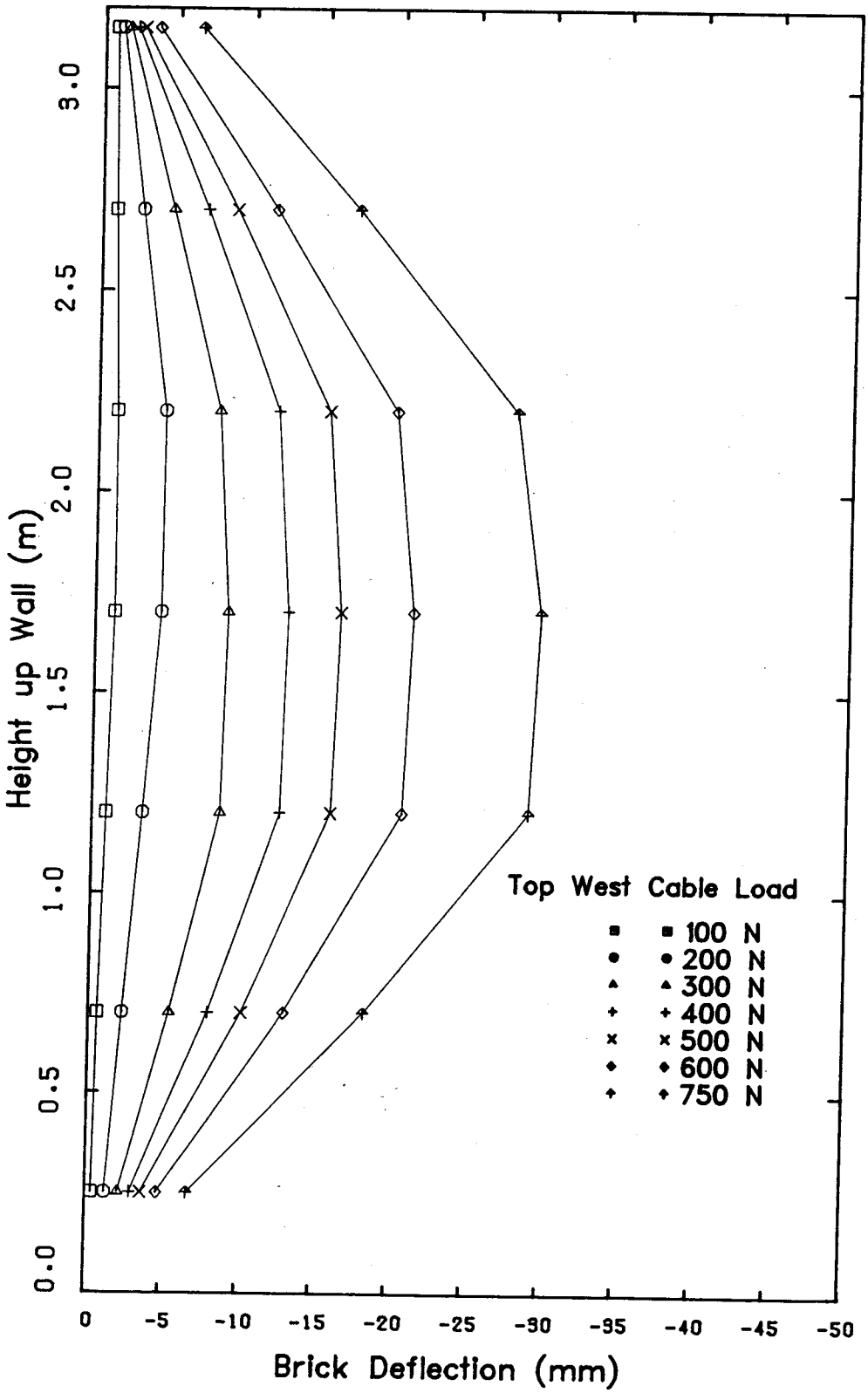

Figure C-19 Brick Veneer Deflections - Series No.2 Wall No.3

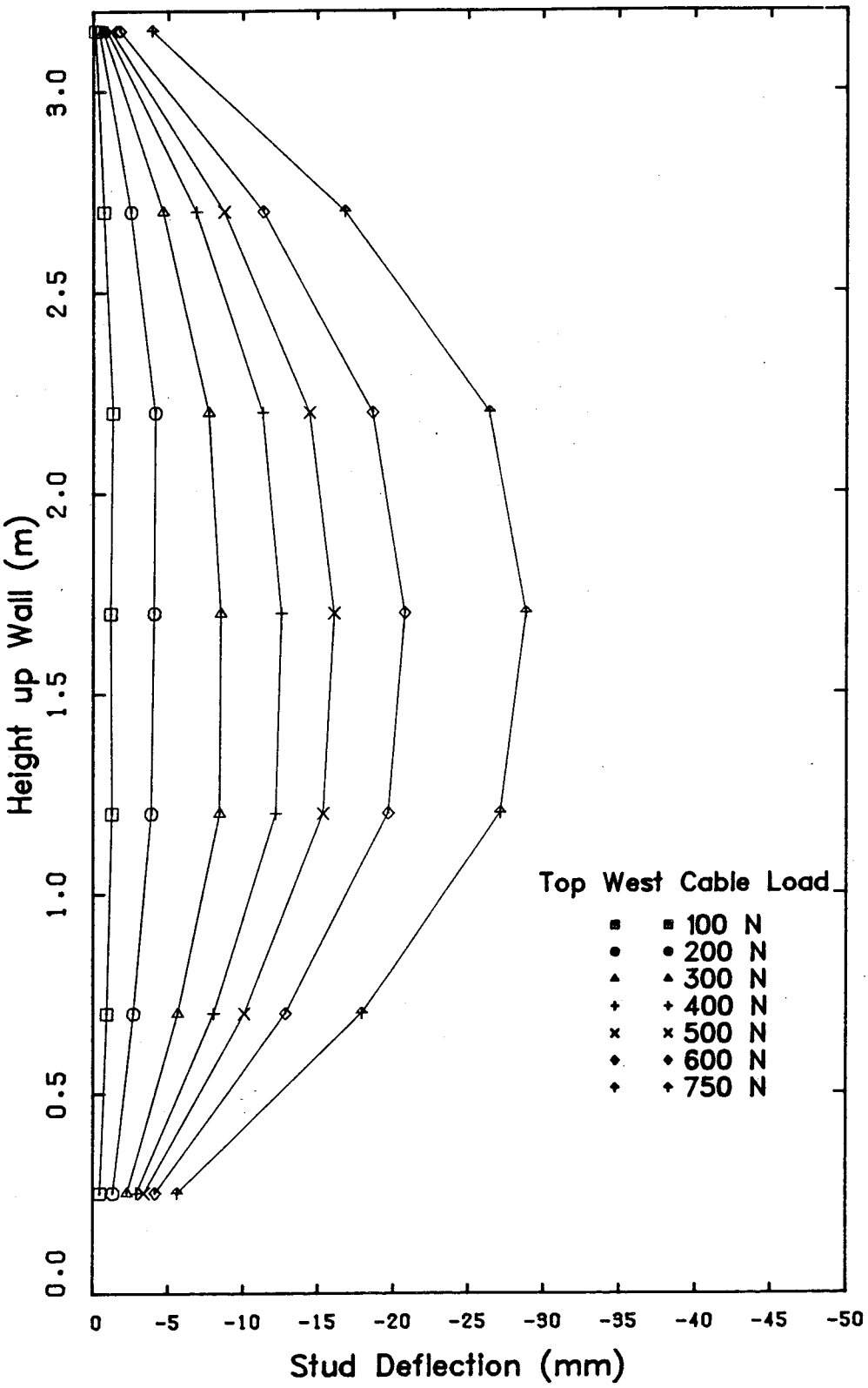

Figure C-20 Stud Wall Deflections - Series No.2 Wall No.3

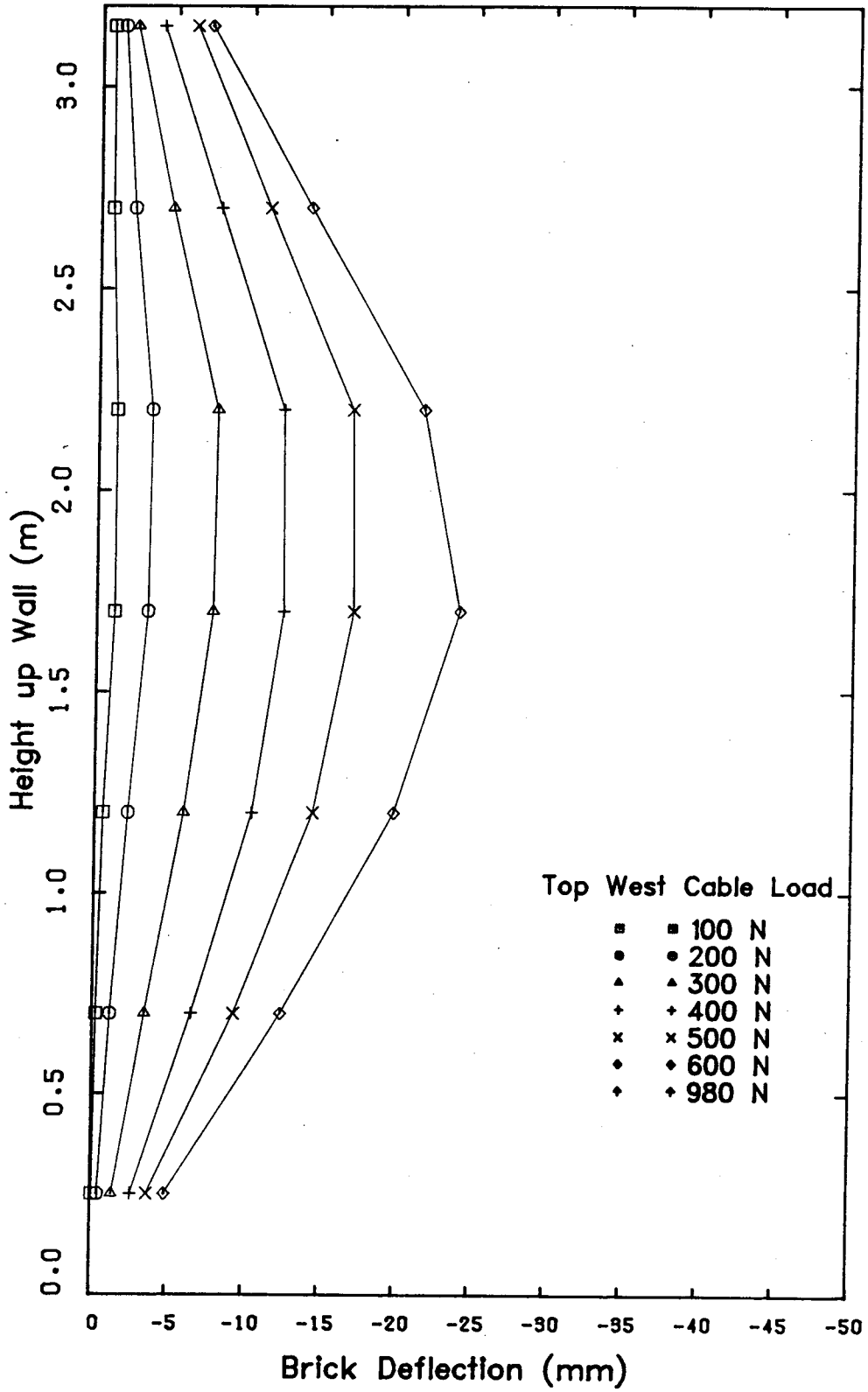

Figure C-21 Brick Veneer Deflections - Series No.2 Wall No.5

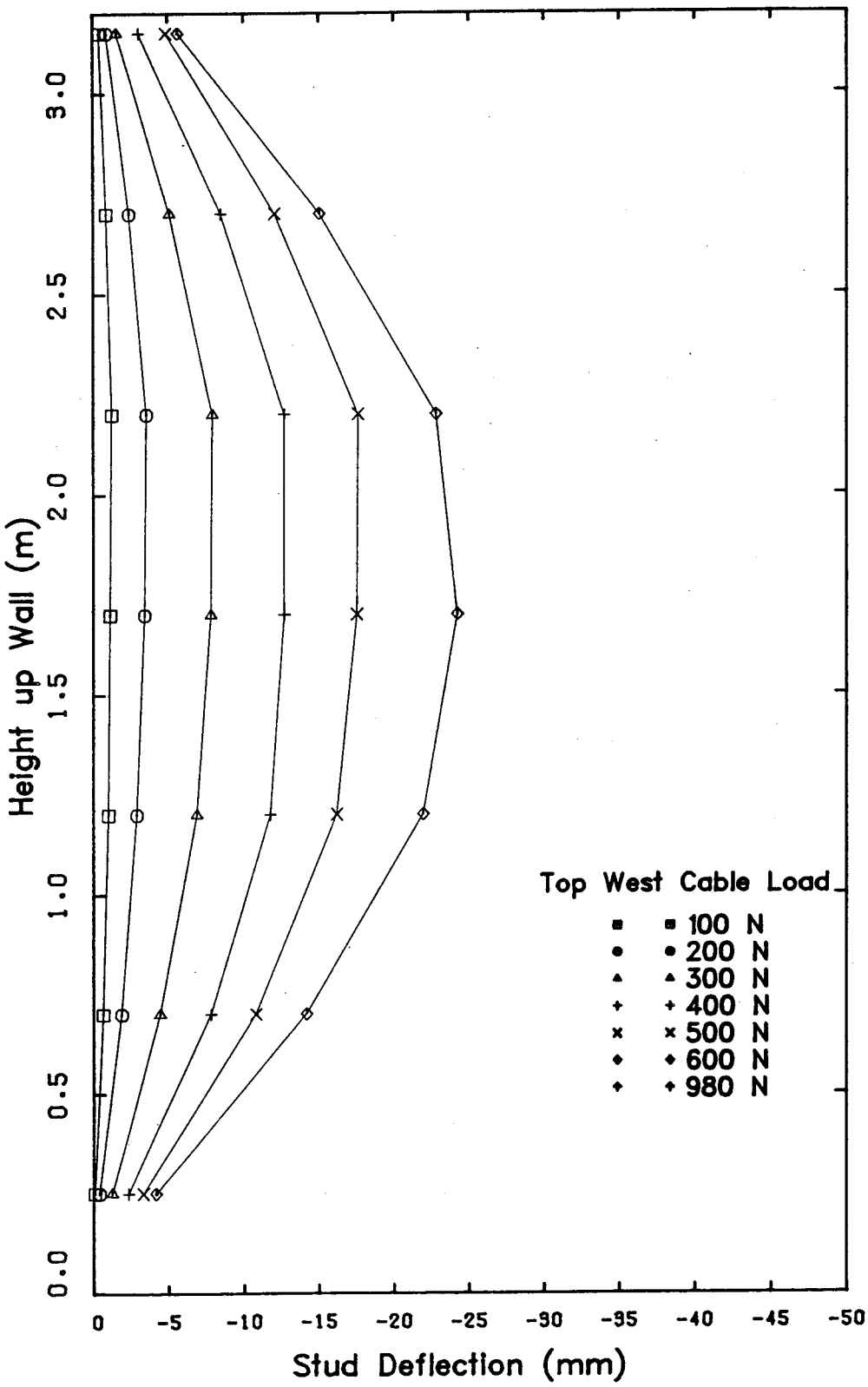

Figure C-22 Stud Wall Deflections - Series No.2 Wall No.5

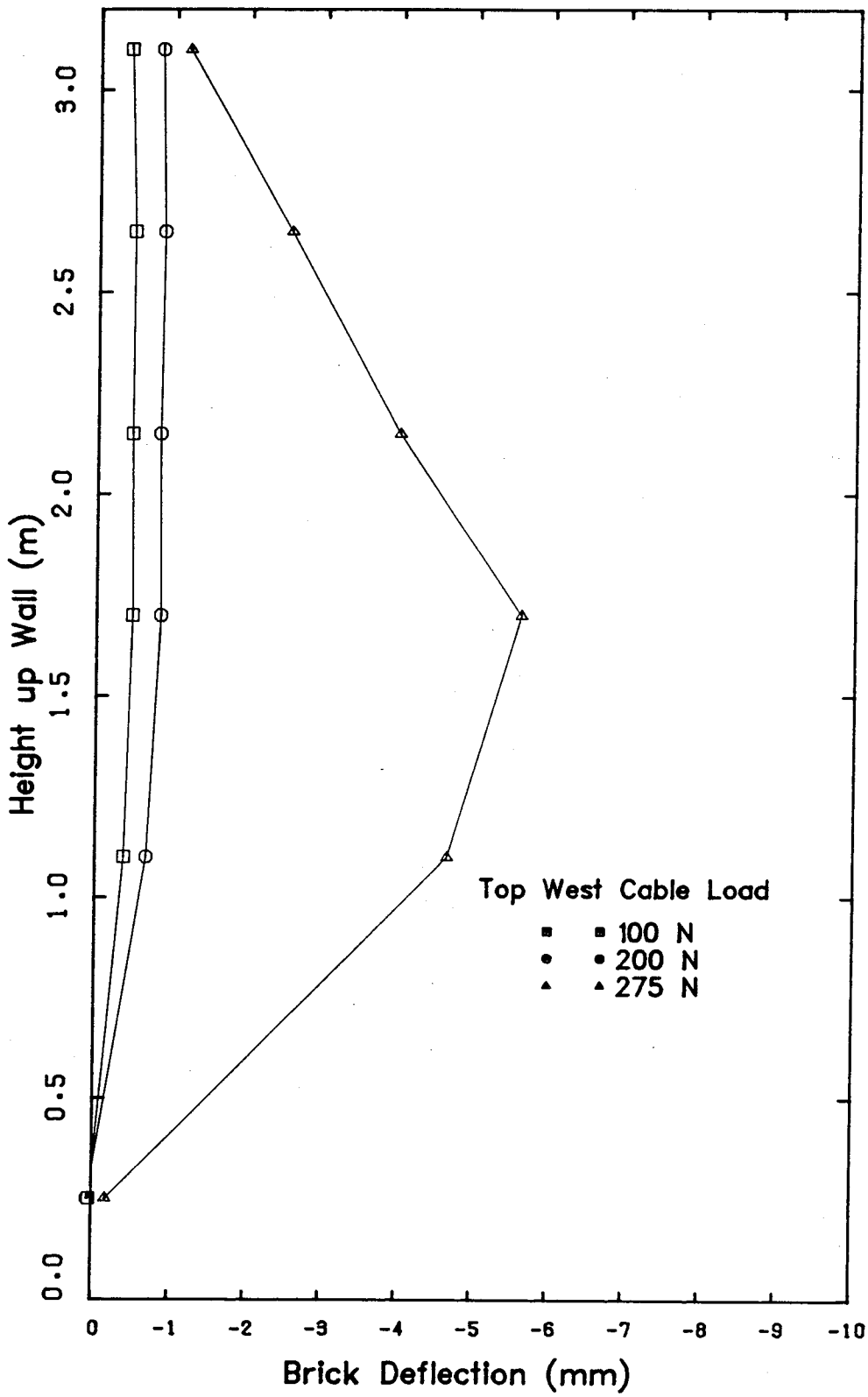

Figure C-23 Brick Veneer Deflections - Series No.2 Wall No.6

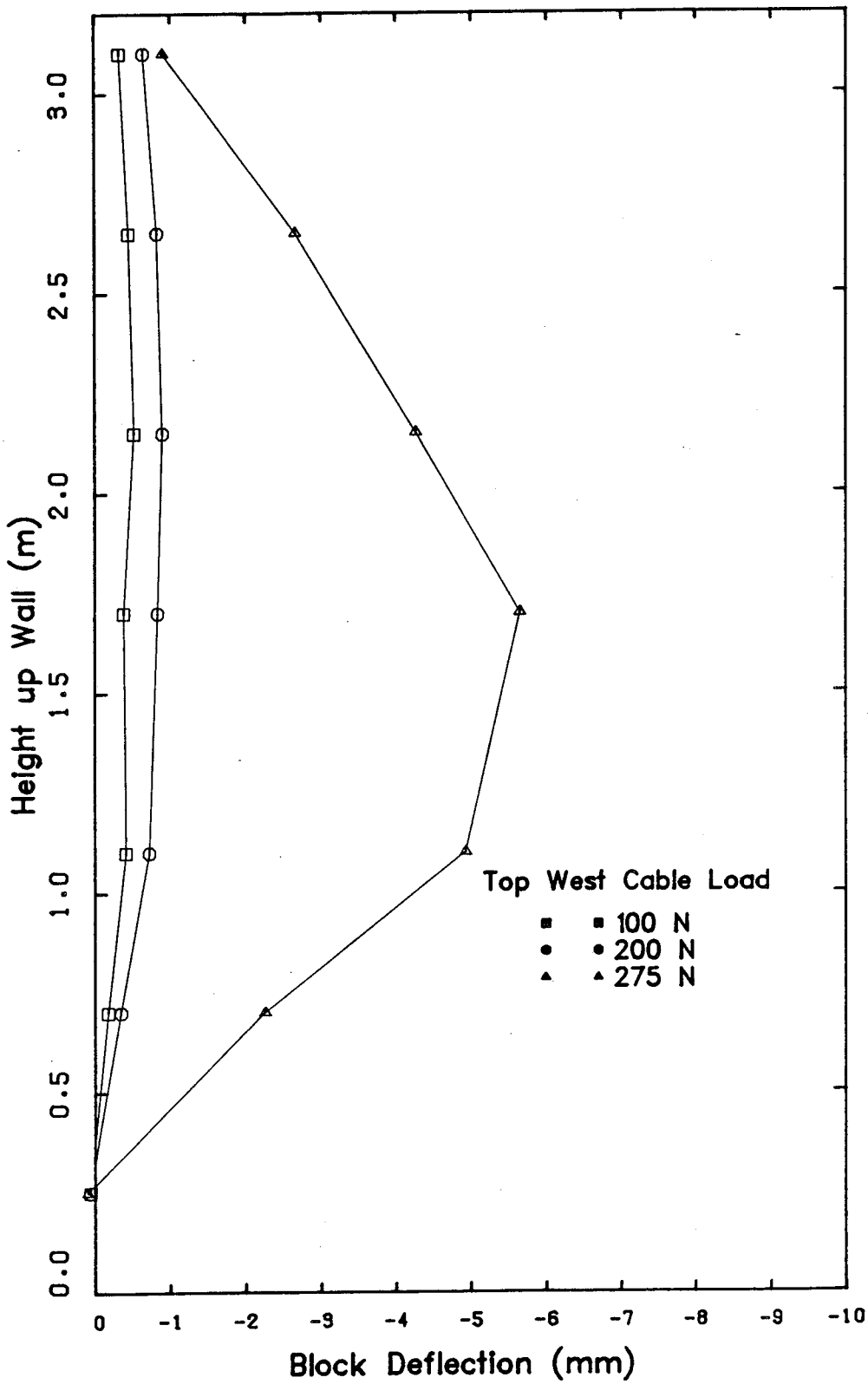

Figure C-24 Block Wall Deflections - Series No.2 Wall No.6

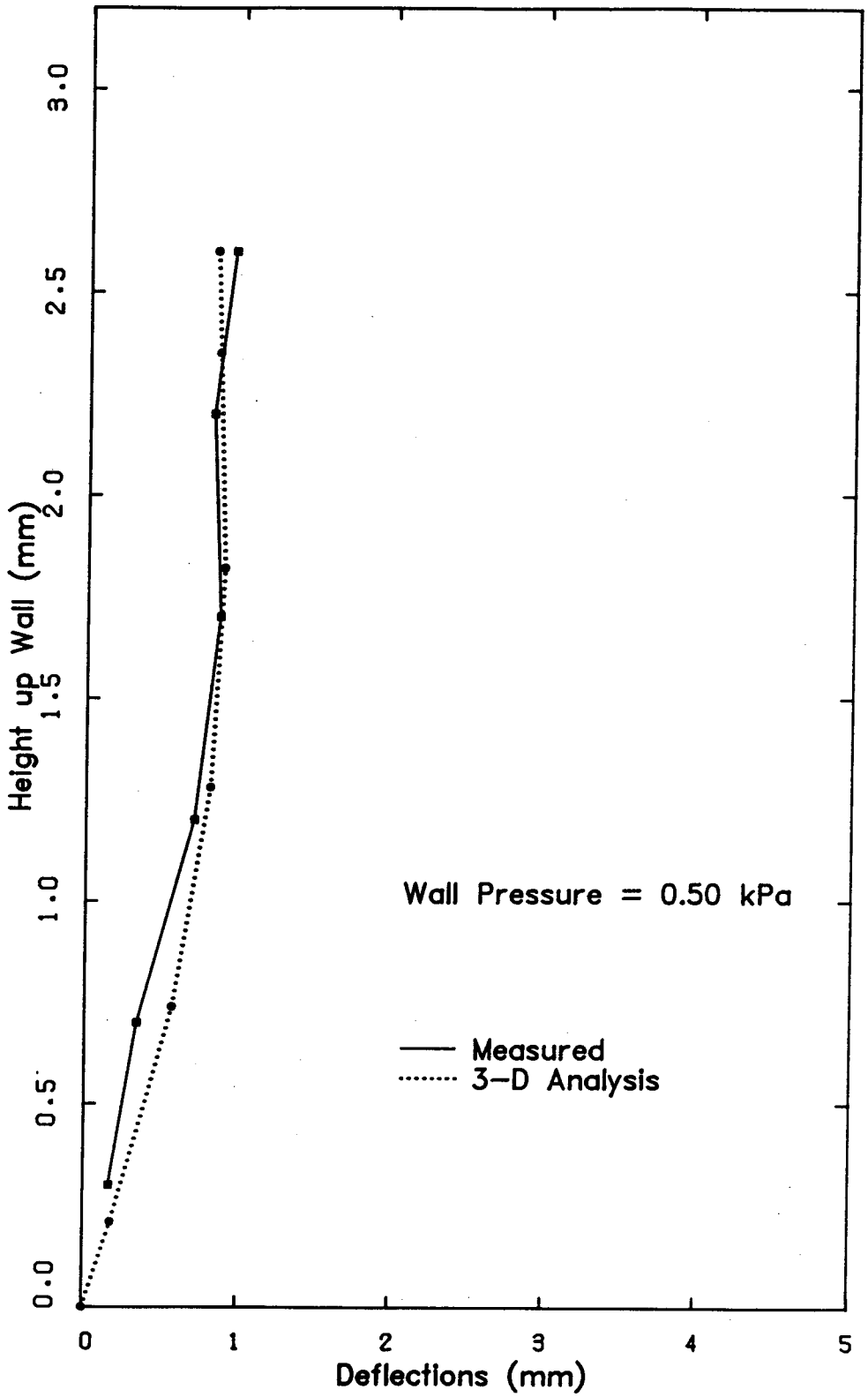

Figure C-25 Brick Veneer Deflections - Series No.1 Wall No.2 - Measured and Predicted

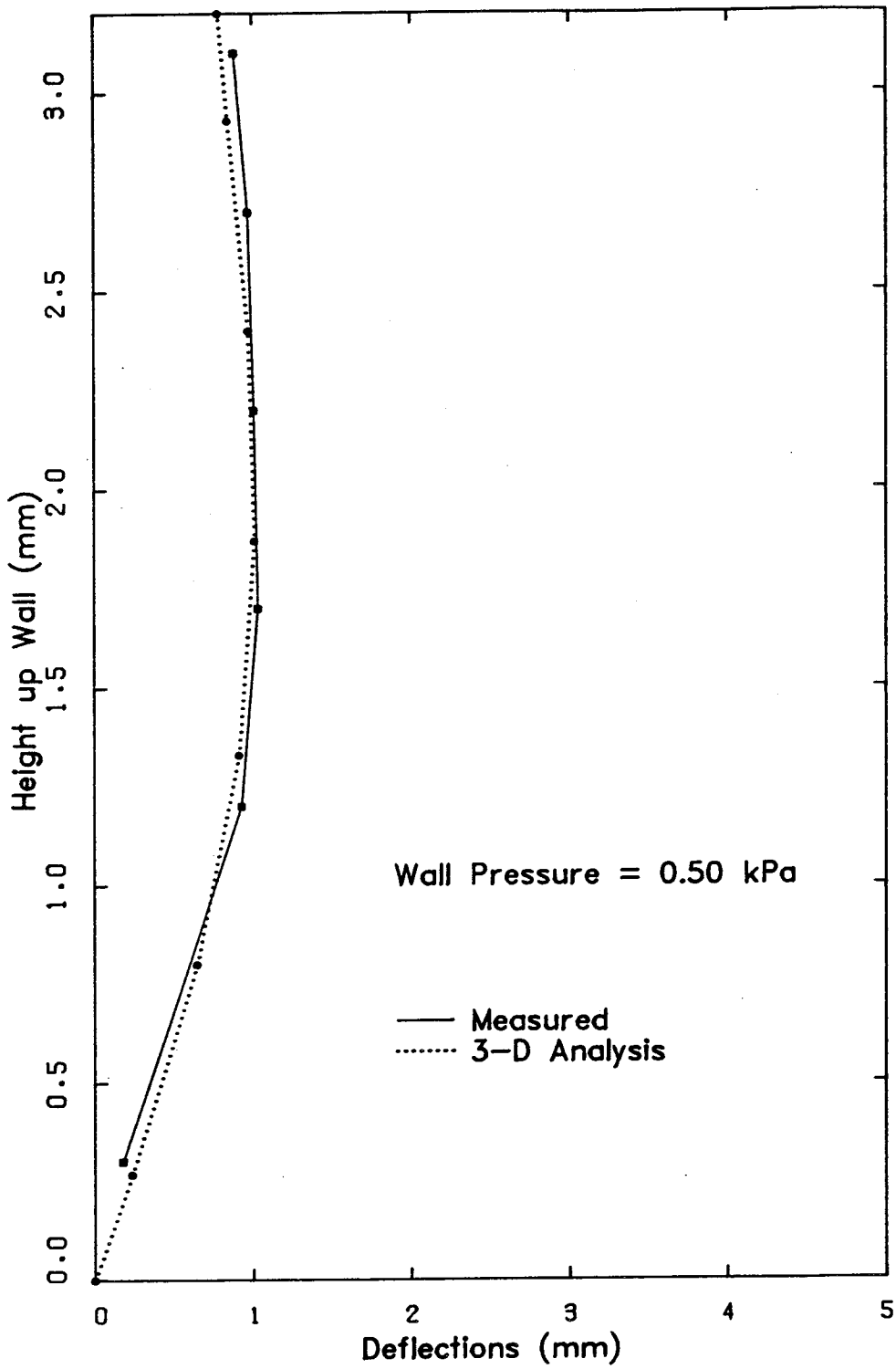

Figure C-26 Brick Veneer Deflections - Series No.1 Wall No.3 - Measured and Predicted

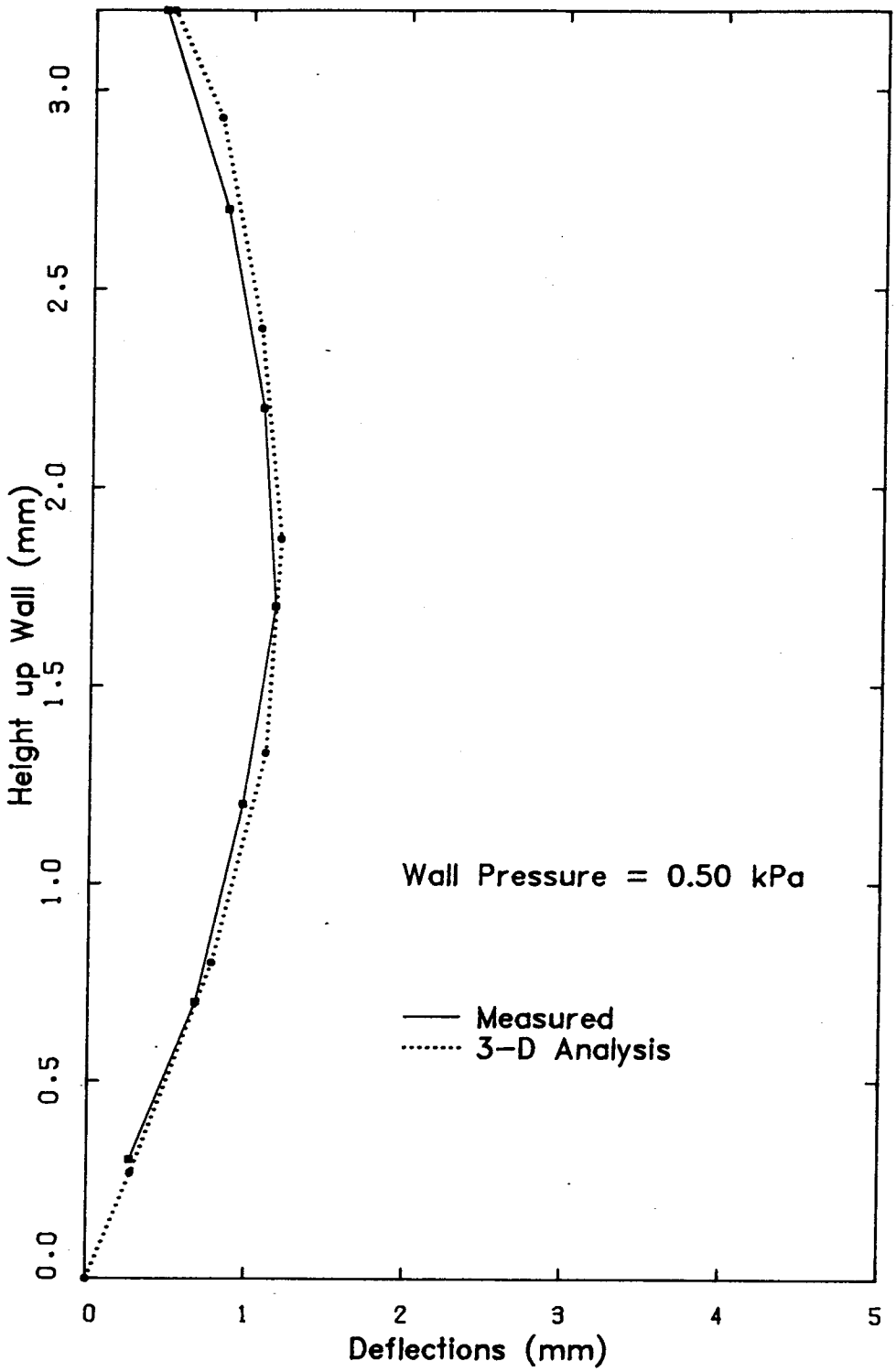

Figure C-27 Brick Veneer Deflections - Series No.1 Wall No.5 - Measured and Predicted

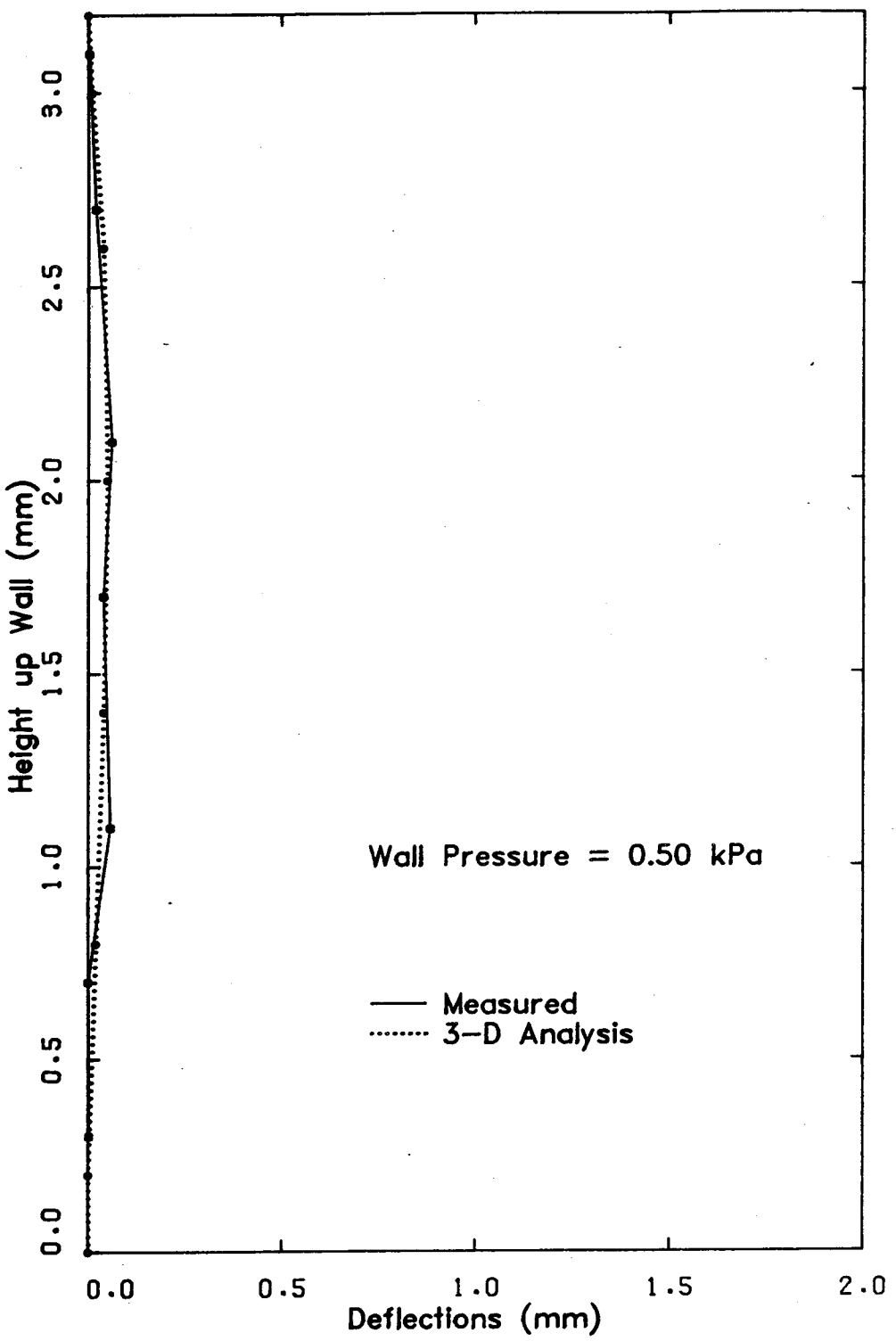

Figure C-28 Brick Veneer Deflections - Series No.1 Wall No.6 - Measured and Predicted

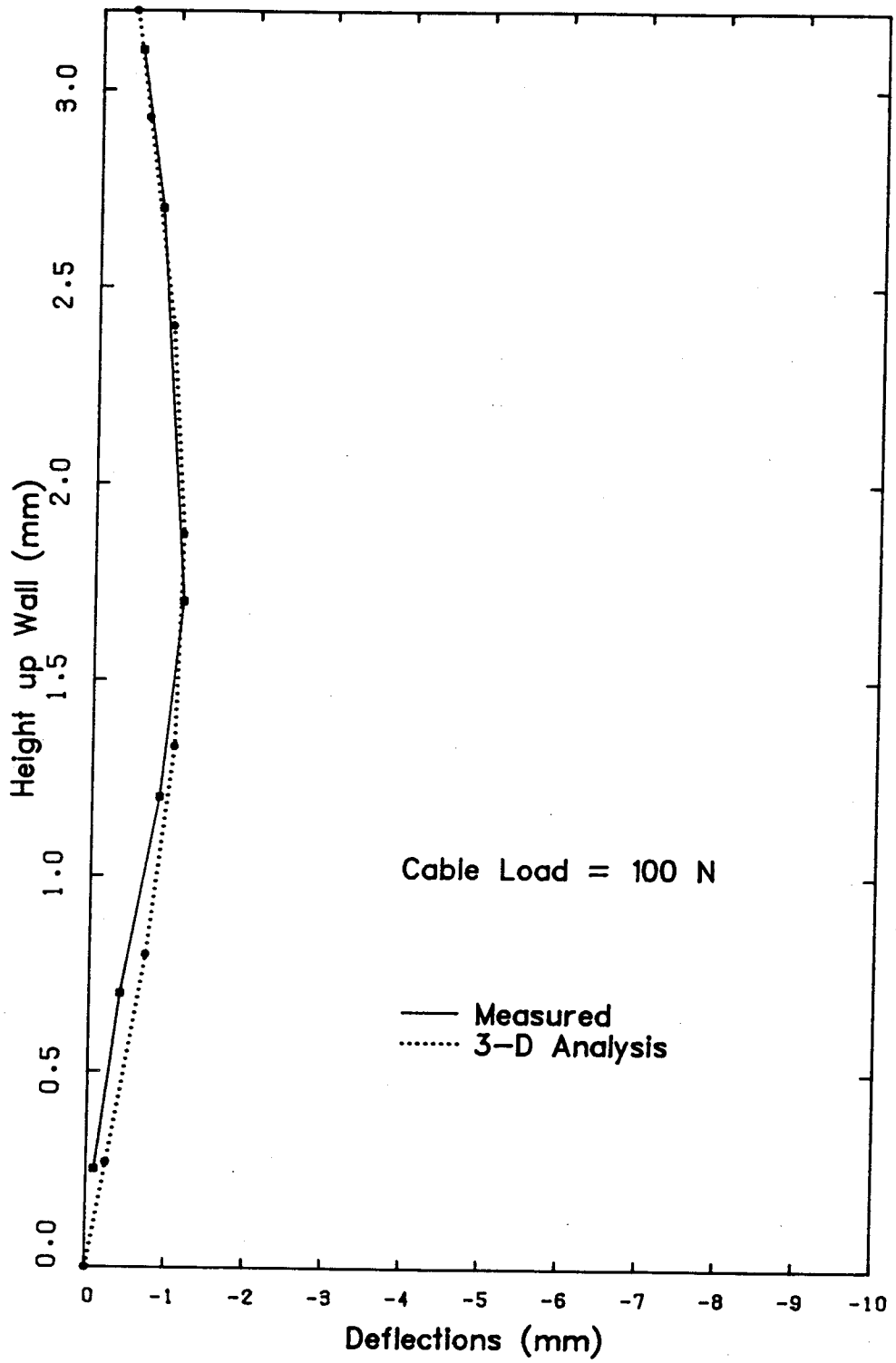

Figure C-29 Brick Veneer Deflections - Series No.2 Wall No.1 - Measured and Predicted

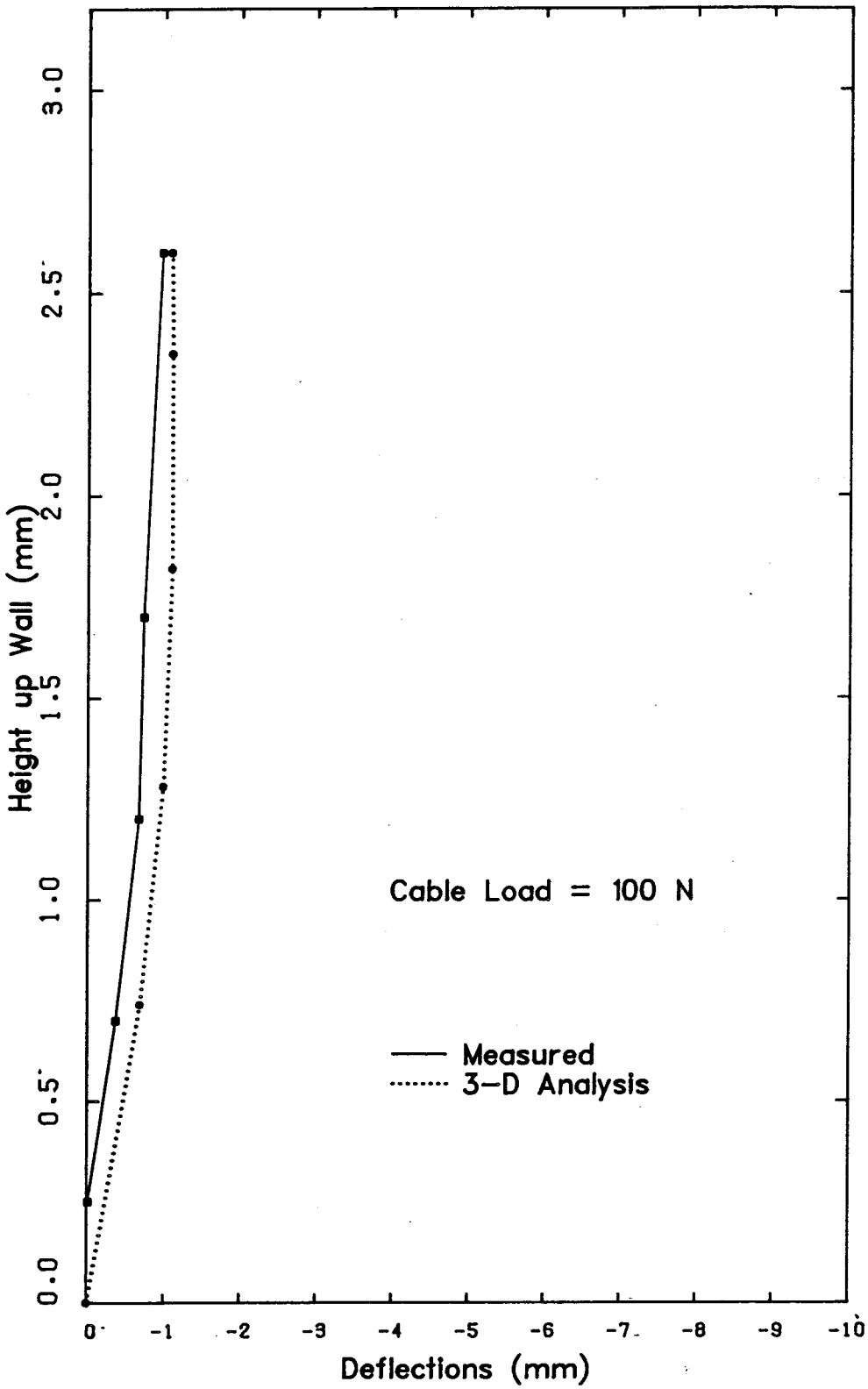

Figure C-30 Brick Veneer Deflections - Series No.2 Wall No.2 - Measured and Predicted

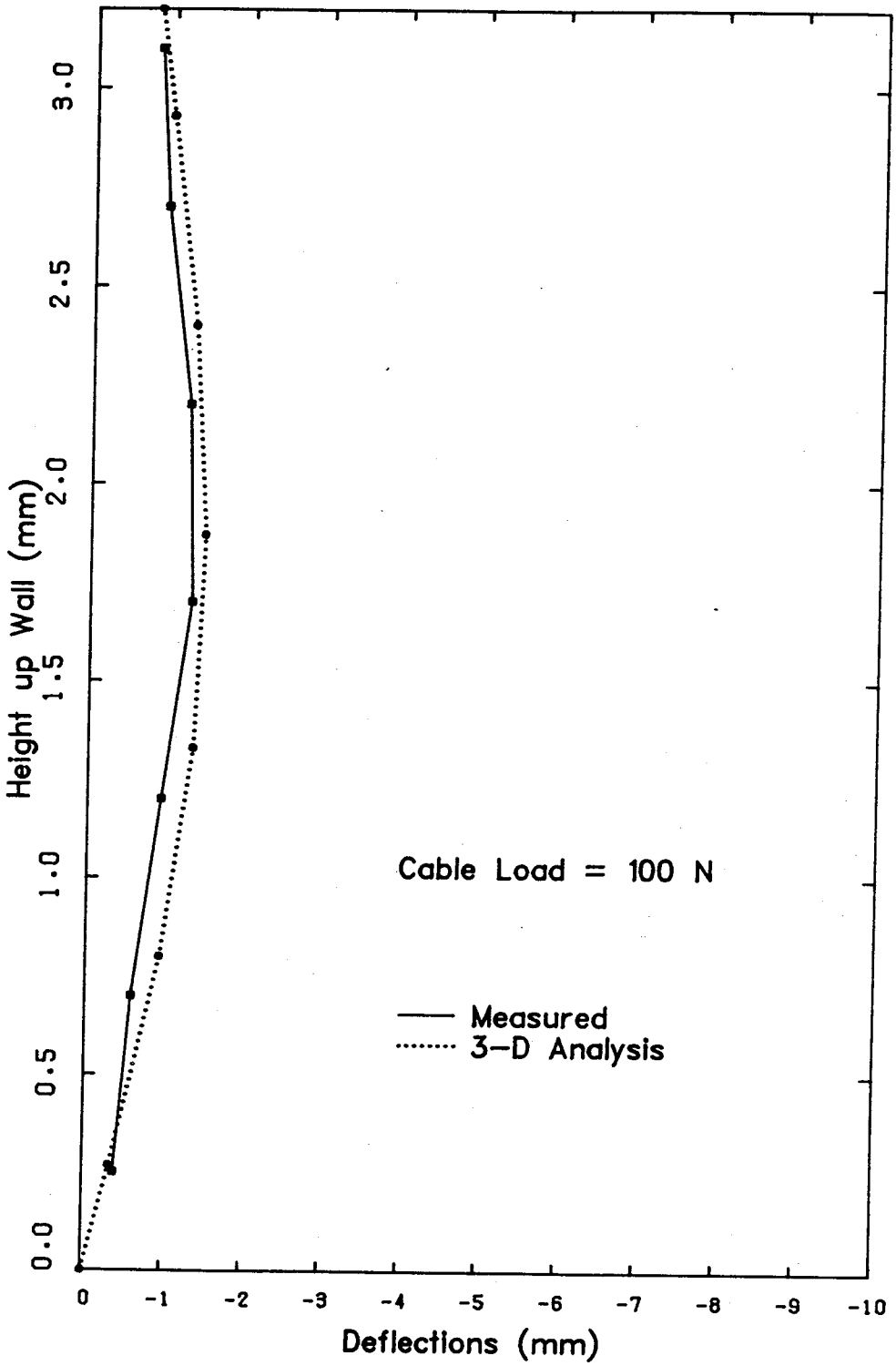

Figure C-31 Brick Veneer Deflections - Series No.2 Wall No.3 - Measured and Predicted

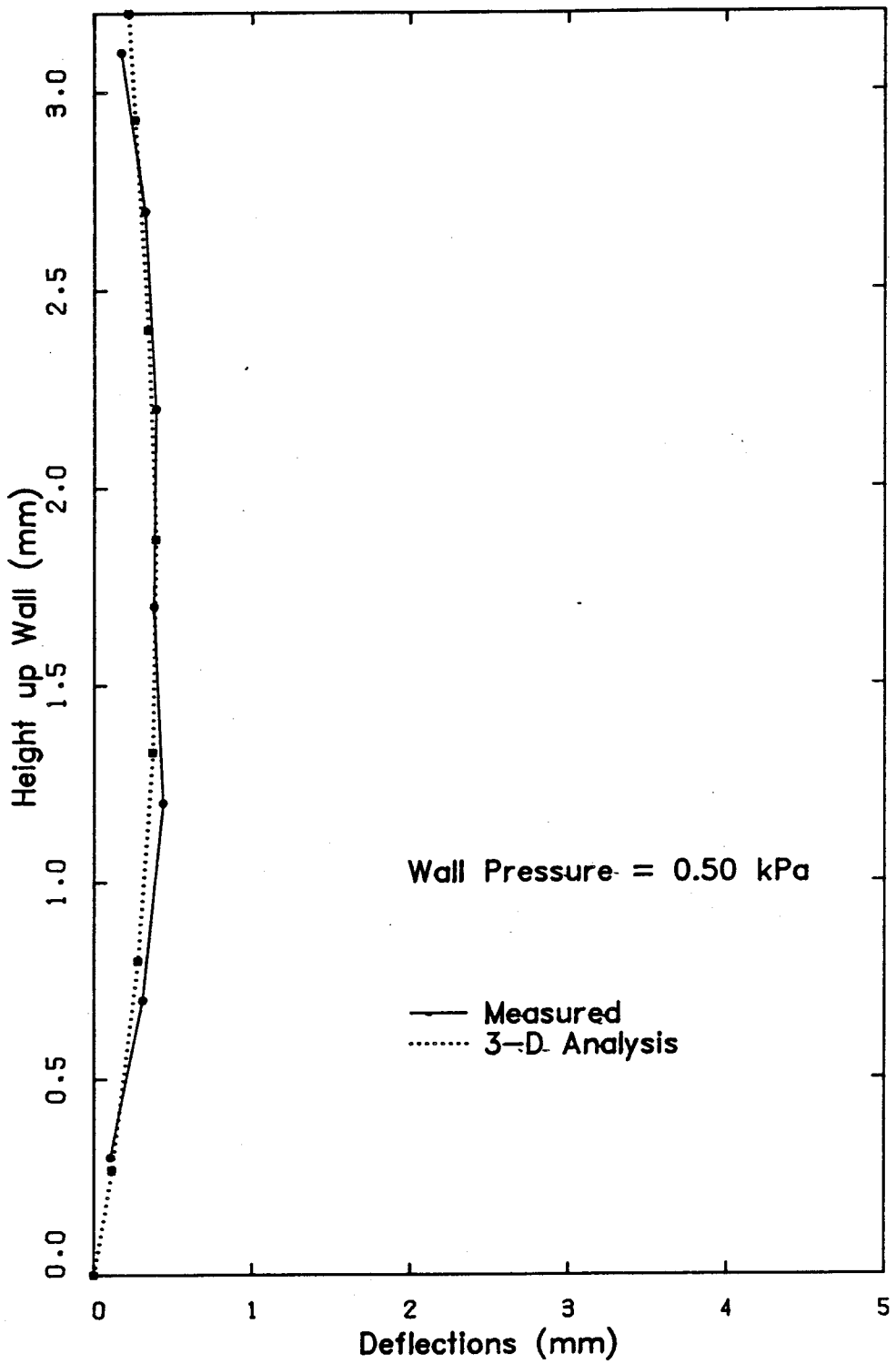

Figure C-32 Brick Veneer Deflections - Series No.2 Wall No.4 - Measured and Predicted

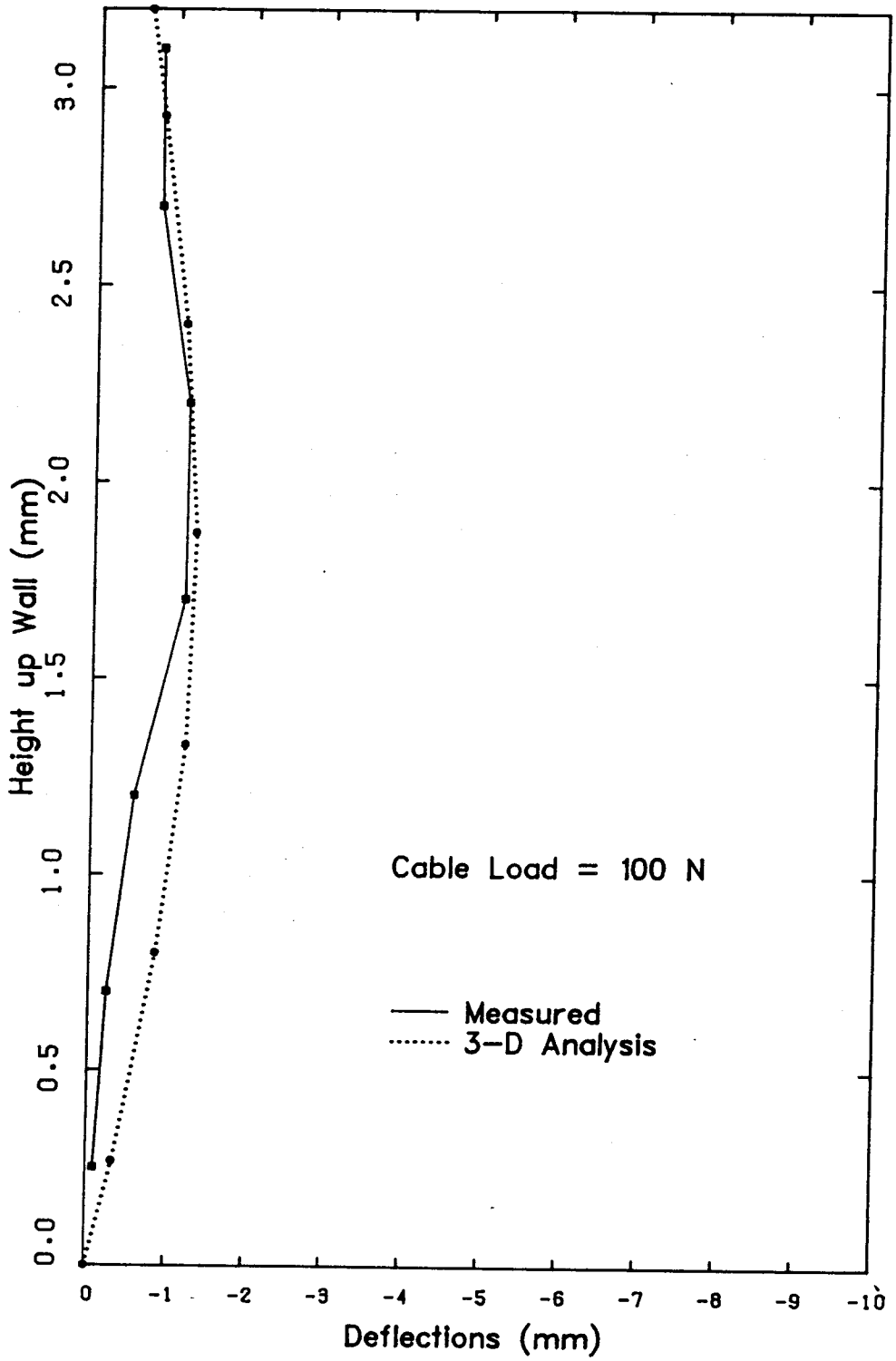

Figure C-33 Brick Veneer Deflections - Series No.2 Wall No.5 - Measured and Predicted

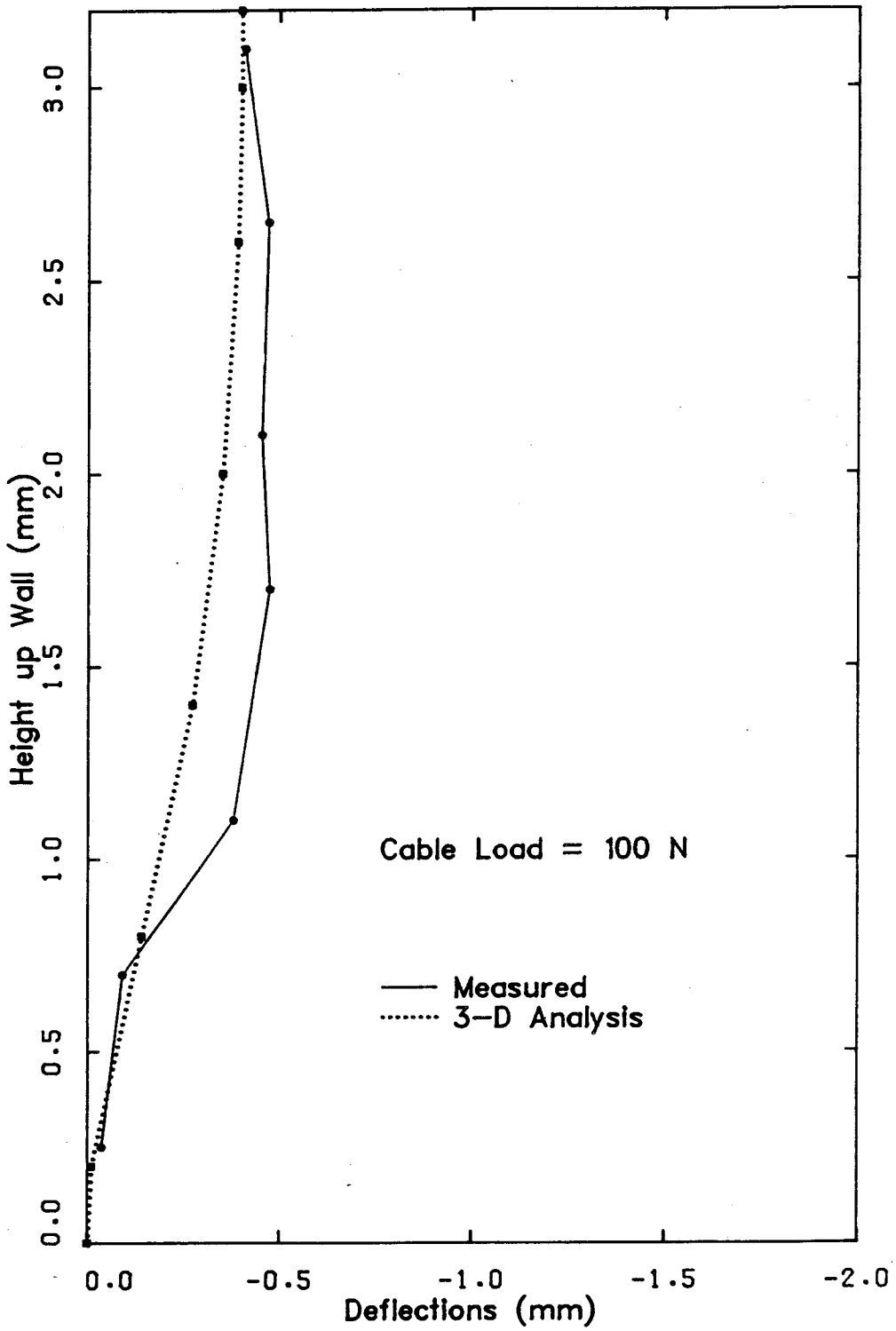

Figure C-34 Brick Veneer Deflections - Series No.2 Wall No.6 - Measured and Predicted

APPENDIX D - DESIGN EXAMPLE

A typical veneer wall system is shown in Figure D-1. This wall is assumed to be located on the upper floor of a four storey office building and the building is assumed to have a steel frame. It was also assumed that adequate expansion joints were located in both the veneer and the backing wall.

The NBC of Canada[24] recommends the use of the 1/10 year wind for the design of cladding systems. Using the simplified calculation procedures for cladding systems outlined in this code, the design wind pressures (p) were calculated as shown below. It was assumed that this building had an exposure factor (C_e) of 1.1 and had uniform openings on all sides. The design pressures were calculated based on the 1/10 year wind for Edmonton, Alberta.

$$p_{ext} = q\ C_e\ C_g\ C_p$$

$$= 0.32 \times 1.0 \times 1.8 = 0.634 \text{ kPa}$$

or

$$= 0.40 \times 1.0 \times -2.1 = -0.739 \text{ kPa}$$

$$p_{int} = q\ C_e\ C_{pi}$$

$$= 0.32 \times 1.0 \times -0.30 = -0.096 \text{ kPa}$$

For these wind pressures and a tributary width of 400 mm, maximum factored uniform wind loads were calculated. The two critical configurations of these loads are shown in Figures D-2 and D-3. Also shown in these figures are the

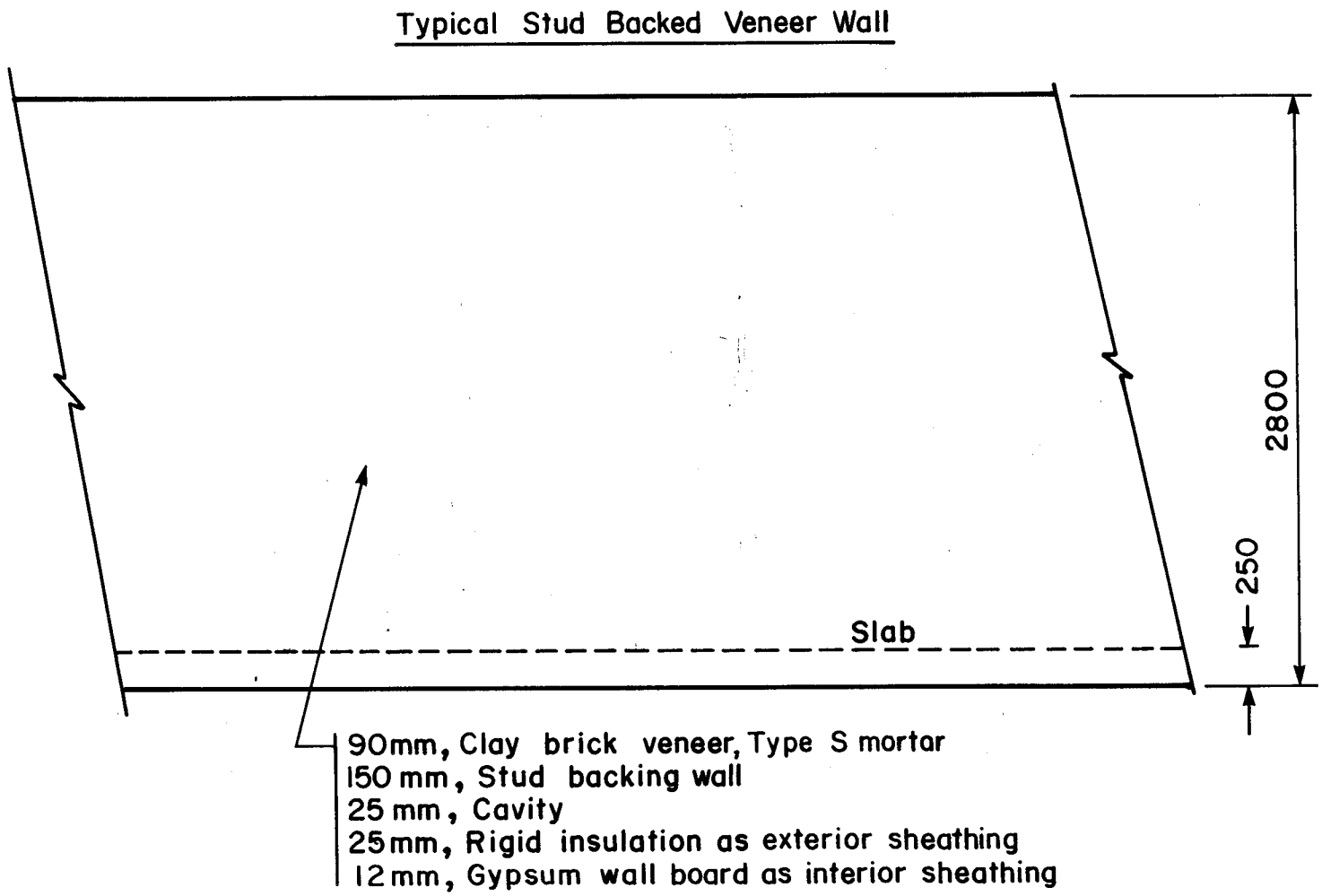

Figure D-1 Proposed Veneer Wall System

plane frames formed by each of the two configurations of the stud, ties and veneer. The nominal spacing the ties was assumed to be 400 mm by 520 mm.

For both load cases, the maximum veneer moments, tie loads, stud moments and stud reactions were obtained from an elastic analysis performed on the two plane-frames. These analyses used the nominal properties listed for the 150 mm deep 20 gauge steel studs, the average effective area of flange mounted ties on 20 gauge studs, and the properties of the veneer, listed in Tables 6.1 and 6.2.

The maximum veneer moment obtained from these analyses was 0.170 kNm (Configuration 2 - Load Case 2). The maximum compressive tie load was 585 N (Configuration 2 - Load Case 1) and the maximum tensile tie load was 575 N (Configuration 2 - Load Case 2). The maximum stud moment and reactions were calculated as 0.281 kNm (Configuration 1 - Load Case 2) and 575 N (Configuration 2 - Load Case 2), respectively. At the location of the maximum stud moment, the tie load was 187 N.

Veneer Moment

In order to calculate a veneer moment resistance, a value of the nominal modulus of rupture of the veneer must be chosen. CSA CAN3-S304-M78[11] specifies an allowable flexural tensile stress of 0.25 MPa for walls constructed of type S mortar and clay brick. This allowable value is based on a safety factor of greater than 3. It can be assumed that the tensile strength of this type of masonry is equal to 0.75 MPa (3 x 0.25 MPa). However, for this type of mortar

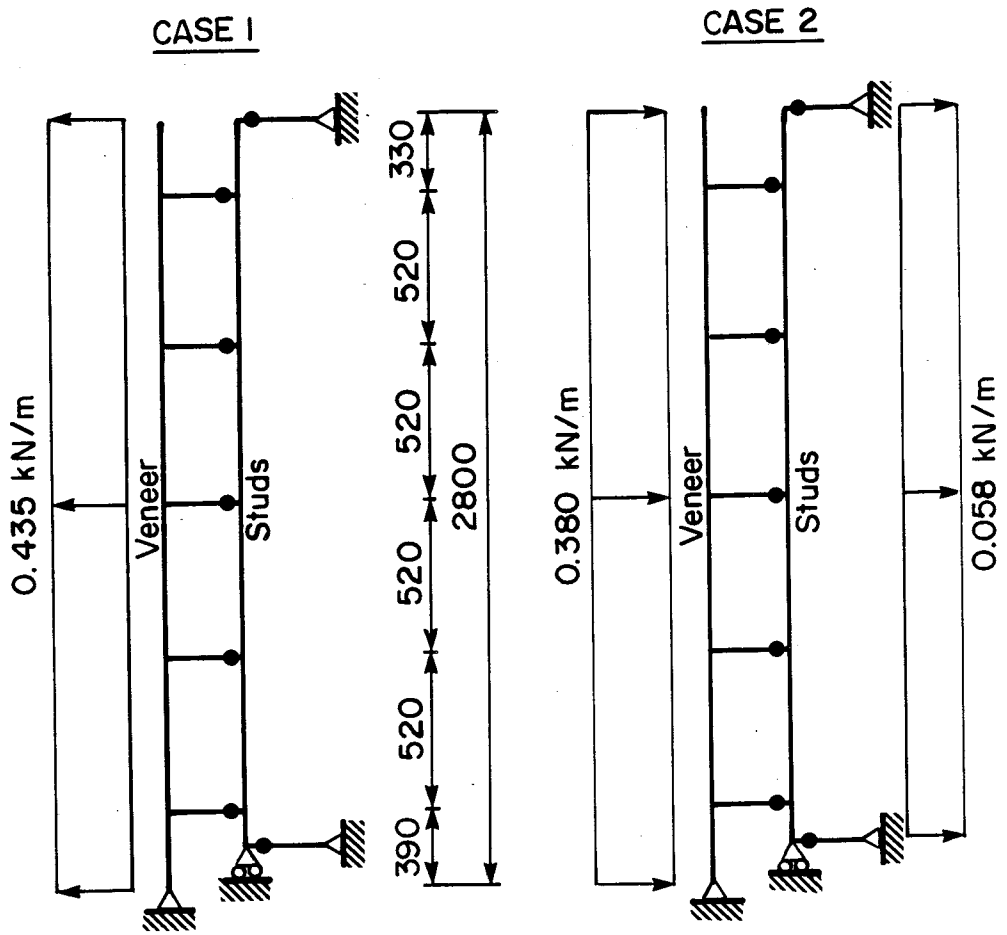

Figure D-2 The Assumed 2 Dimensional Frame and Loading - Stud Line Configuration 1

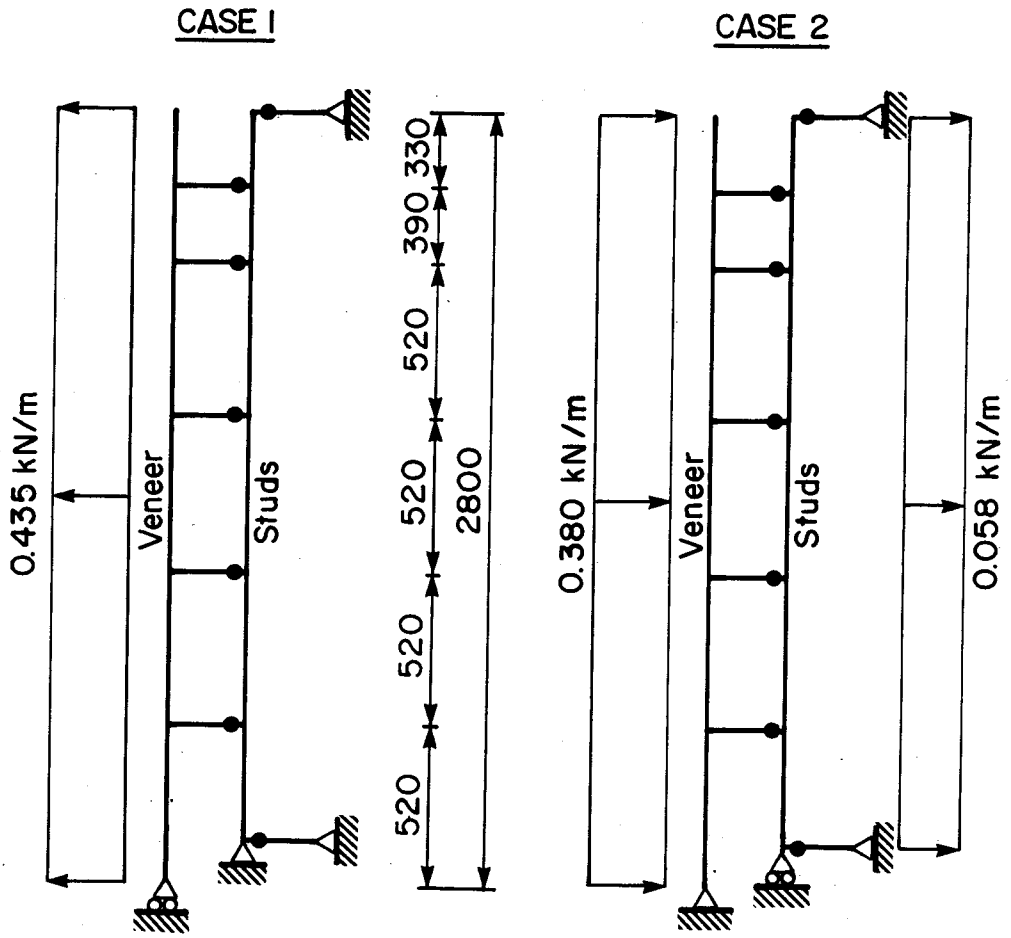

Figure D-3 The Assumed 2 Dimensional Frame and Loading - Stud Line Configuration 2

and brick, the British Standard BS 5628[34] specifies a "characteristic tensile strength" of 0.500 MPa. It was assumed that the nominal modulus of the veneer was between these values and a value of 0.600 MPa was chosen.

Since the environment in Edmonton is very dry it was assumed that tie corrosion was not a critical design consideration. For this reason, a ϕ_m of 0.8 is used in the resistance calculation. Based on the above assumptions, the moment resistance of the veneer (M_r) is:

$$M_r = \phi_m \frac{\sigma_r I}{y}$$

$$= 0.8 \frac{0.600 \times 1.56 \times 10^7}{42}$$

$$= 0.178 \text{ kNm} > 0.170 \text{ kNm}$$

Clearly, the factored veneer moment resistance is greater than the factored applied moment. Thus, the veneer has adequate moment resistance for the applied load effects.

Tie Loads

It is assumed that 18 gauge corrugated tie and platform systems are to be used in this wall system (see Figure 4.1). From tests, the nominal ultimate strength of this tie system is 1180 N (compression) and 910 N (tension). These values were based on the average linear load limits listed in Table 5.1. Since these tie systems exhibited significant reserve strength, this average value was not reduced as specified in CSA-CAN3-A370.

Insufficient data was availiable for the derivation of statistically significant tie resistance performance

factors. However, if ϕ_t is assumed to have a value of 0.7, the following resistances can be calculated:

$$T = \phi_t \, T_r$$

$$= 0.7 \times 1180 = 826 \text{ N (compression)}$$

and

$$= 0.7 \times 910 = 637 \text{ N (tension)}$$

Because the factored tie resistances are greater than the maximum factored tie loads this tie type and spacing is satisfactory.

Stud Flexural-Cripping

To check the resistance of the stud it is assumed that the procedures outlined in CAN3-CSA-S136-M84 can be used to design the steel studs.

The studs were assumed to fully braced and the bearing length of the ties were assumed to be 30 mm. Using the precedures fom the code the flexural resistance of the stud is:

$$M_r = \phi \, S_x \, Fy$$

$$= 0.9 \times 9600. \times 320 = 2.76 \text{ kNm}$$

The interior web crippling resistance is:

$$P_r = \phi_s \, 16 \, t^2 \, Fy \, A \, B \, C \, D$$

$$A = (1.22 - 0.22k)$$

$$B = (1.06 - 0.06R_c)$$

$$C = (1.00 - 0.07N)$$

$$D = (1.00 - 0.0014H)$$

therefore

$$P_r = (0.80)\ 16\ (0.91)^2\ 320\ A\ B\ C\ D$$

$$A = (1.22 - 0.22 \times 320/230)$$

$$B = (1.06 - 0.06 \times 3.0/0.91)$$

$$C = (1.00 - 0.07 \times 30/0.91)$$

$$D = (1.00 - 0.0014 \times 150/0.91)$$

$$P_r = 2.50\ kN$$

Checking the combined bending and crippling resistance of the stud.

$$\frac{M_f}{M_r} + \frac{P_f}{P_r} \leq 1.3$$

$$\frac{0.281}{2.76} + \frac{0.187}{2.50} \leq 1.3$$

$$0.177 \leq 0.78$$

These ratios indicate that the bending and crippling resistances of the stud are much greater than the applied moment or concentrated load. Thus, the studs have have more than adequate resistance.

Stud Support Failure

There is the possibility that the stud might fail by crippling at the supports. The nominal crippling resistance of the stud at the supports is given by Equation 6.5 and the following calculation indicates that the studs have adequate strength at this location.

$$P_r = \phi_s\ 10\ t^2\ Fy\ A\ B\ C\ D \qquad [6.5]$$

$$A = (1.33 - 0.33k)$$

$$B = (1.15 - 0.15R_c)$$

$$C = (1.00 - 0.01N)$$

$$D = (1.00 - 0.0018H)$$

Therefore

$$P_r = (0.80)\ 10\ (0.91)^2\ 320\ A\ B\ C\ D$$

$$A = (1.33 - 0.33 \times 320/230)$$

$$B = (1.15 - 0.15 \times 3.0/0.91)$$

$$C = (1.00 - 0.01 \times 30/0.91)$$

$$D = (1.00 - 0.0018 \times 150/0.91)$$

$$= 1.12\ kN > 0.575$$

Maximum Deflections

For the factored wind loads, the maximum deflection of the veneer was 2.62 mm. This value was less than the deflection limit of L/480 (5.83mm). Thus, under service load levels, the wall system deflections will be well below this limit.

In summary, the proposed masonry veneer wall system was found to be adequate for the 1/10 wind loadings in Edmonton, Alberta. The reader is reminded that the performance factors used in this design example are based upon a limited number of tests and have, therefore, a limited statistical significance.

RECENT STRUCTURAL ENGINEERING REPORTS

Department of Civil Engineering

University of Alberta

125. *Analysis of Field Measured Deflections Scotia Place Office Tower* by A. Scanlon and E. Ho, December 1984.

126. *Ultimate Behaviour of Continuous Deep Reinforced Concrete Beams* by D.R. Ricketts and J.G. MacGregor, January 1985.

127. *The Interaction of Masonry Veneer and Steel Studs in Curtain Wall Construction* by W.M. McGinley, J. Warwaruk, J. Longworth and M. Hatzinikolas, May 1985.

128. *Evaluation of Existing Bridge Structure by Nondestructive Test Methods* by L. Mikhailovsky and A. Scanlon, May 1985.

129. *Finite Element Modelling of Buried Structures* by D.K. Playdon and S.H. Simmonds, October 1985.

130. *Behaviour and Ultimate Strength of Transversely Loaded Continuous Steel Plates* by K.P. Ratzlaff and D.J.L. Kennedy, November 1985.

131. *Inelastic Lateral Buckling of Steel Beam-Columns* by P.E. Cuk, M.A. Bradford and N.S. Trahair, December 1985.

132. *Design Strengths of Steel Beam-Columns* by N.S. Trahair, December 1985.

133. *Behaviour of Fillet Welds as a Function of the Angle of Loading* by G.S. Miazga and D.J.L. Kennedy, March 1986.

134. *Inelastic Seismic Response of Precast Concrete Large Panel Coupled Shear Wall Systems* by M.R. Kianoush and A. Scanlon, March 1986.

135. *Finite Element Prediction of Bin Loads* by A.H. Askari and A.E. Elwi, June 1986.

136. *Shear Behavior of Large Diameter Fabricated Steel Cylinders* by J. Mok and A.E. Elwi, June 1986.

137. *Local Buckling Rules for Structural Steel Members* by S. Bild and G.L. Kulak, May 1986.

138. *Finite Element Prediction of Reinforced Concrete Behavior* by S. Balakrishnan and D.W. Murray, July 1986.

139. *Behavior and Strength of Masonry Wall/Slab Joints* by T.M. Olatunji and J. Warwaruk, July 1986.

140. *Bayesian Analysis of In-Situ Test Data for Estimating the Compressive Strength of Concrete in Existing Structures* by G.J. Kriviak and A. Scanlon, July 1986.

141. *Shear-Moment Transfer in Slab-Column Connections* by S.D.B. Alexander and S.H. Simmonds, July 1986.

142. *Minimum Thickness Requirements for Deflection Control of Two-Way Slab Systems* by D.P. Thompson and A. Scanlon, November 1986.

143. *Shrinkage and Flexural Tests of Two Full-Scale Composite Trusses* by A. Brattland and D.J.L. Kennedy, December 1986.

144. *Combined Flexure and Torsion of I-Shaped Steel Beams* by R.G. Driver and D.J.L. Kennedy, March 1987.

145. *Cyclic and Static Behaviour of Thin Panel Steel Plate Shear Walls* by E.W. Tromposch and G.L. Kulak, April 1987.

146. *Postbuckling Behavior of Thin Steel Cylinders Under Transverse Shear* by V.G. Roman and A.E. Elwi, May 1987.

147. *Incipient Flow in Silos - A Numerical Approach* by R.A. Link and A.E. Elwi, May 1987.

148. *Design of Web-Flange Beam or Girder Splices* by D. Green and G.L. Kulak, May 1987.

149. *Spreadsheet Solution of Elastic Plate Bending Problems* by G.E. Small and S.H. Simmonds, July 1987.

150. *Behaviour of Transversely Loaded Continuous Steel-Concrete Composite Plates* by S.J. Kennedy and J.J. Cheng, July 1987.

151. *Behaviour and Ultimate Strength of Partial Joint Penetration Groove Welds* by D.P. Gagnon and D.J.L. Kennedy, July 1987.

152. *KBES for Design of Reinforced Concrete Columns* by A. Bezzina and S.H. Simmonds, July 1987.

153. *Compressive Behavior of Gusset Plate Connections* by S.Z. Hu and J.J. Cheng, July 1987.

154. *Development of Structural Steel Design Standards* by P.J. Marek and D.J.L. Kennedy, October 1987.

155. *Behaviour of Bolted Joints of Corrugated Steel Plates* by R.W.S. Lee and D.J.L. Kennedy, January 1988.

156. *Masonry Veneer Wall Systems* by W.M. McGinley, J. Warwaruk, J. Longworth and M. Hatzinikolas, January 1988.